


University of South Wales



2059345

 *Bound by*
Abbey
Bookbinding Co.
116 Cathays Terrace, Cardiff CF24 4HY
South Wales, U.K. Tel: (029) 20395882

THE MONITORING AND CONTROL OF STOKER-FIRED BOILER PLANT BY NEURAL NETWORKS

ALEX ZYH SIONG CHONG

A thesis presented in partial fulfilment of the requirements of the University of Glamorgan/Prifysgol Morgannwg for the award of the degree of
Doctor of Philosophy

This research programme was carried out in collaboration with the British Coal Utilisation Research Association (B.C.U.R.A.), the UK Department of Trade & Industry (DTI), The British High Commissioner's Chevening Awards Scheme of Malaysia, Coal Technology Development Division (CTDD) and
James Proctor Limited

August 1999

The University of Glamorgan

*~My Parents,
Wife and Child,
Brothers,
Sister and unborn Niece~*

Certificate of Research

This is to certify that, except where specific reference is made, the work described in this thesis is the result of the candidate. Neither this thesis, nor any part of it, has been presented, or is currently submitted, in candidature for any degree at any other University.

Signed:



Mr. Alex Zyh Siong CHONG (Candidate)

Signed:



Dr. Steven WILCOX (Director of Studies)

Date:



Abstract

This thesis is concerned with the implementation of Artificial Neural Networks (ANNs) to monitor and control chain grate stoker-fired coal boilers with a view to improving the combustion efficiency whilst minimising pollutant emissions. A novel Neural Network Based Controller (NNBC) was developed following a comprehensive set of experiments carried out on a stoker test facility at the Coal Research Establishment (CRE) Ltd., before being evaluated on an industrial chain grate stoker at Her Majesty's Prison Garth, Leyland. The NNBC mimicked the actions of an expert boiler operator, by providing 'near optimum' settings of coal feed and air flow, as well as taking into account the correct 'staging' sequence of these parameters during load following conditions, before subsequently fine tuning the combustion air under quasi-steady-state conditions. Test results from the on-line implementation of the NNBC on both chain grate stoker plants have demonstrated that improved *transient* and *steady-state* combustion conditions were attained without having any adverse effect on the pollutant emissions nor the integrity of the appliances.

A novel combustion monitoring system was also developed during the course of the work that can be used to infer the stability of combustion on the fire bed, following a pilot study of the 'flame front' movement during boiler load changes on the stoker test facility at CRE. This novel low-cost flame front monitor was rigorously tested on the industrial stoker plant, and long hours of successful on-line operation were achieved. It was also demonstrated with the use of ANNs, that the data gathered from the novel flame front monitor can be processed to yield evidence concerning movement of the ignition plane over a short period of time (several minutes). The prototype controller and flame front monitor would thus provide both stoker manufacturers and users with a means of meeting future legislative limits on pollutant emissions as indicated by the European Commission, as well as improving the combustion efficiency of this type of coal firing equipment.

Finally, ANNs were also used as a *simplistic* means to represent the complex coal combustion process on the bed of the stoker test facility whilst burning a particular type of coal. The resultant ‘black-box’ models of the combustion derivatives were able to represent the dynamics of the process and delivered accurate one-step ahead predictions over a wide range of unseen data. The work demonstrated the complex functional mapping capability of ANNs and also addressed the deficiencies in mathematical modelling of the coal combustion process on fixed grate, as indicated in the literature.

Acknowledgements

First and foremost I would like to express my sincere gratitude to Professor John Ward, one of my supervisors, for the opportunity of a lifetime and guidance, which have changed not only my life but the life of my loved ones for the better. Heartfelt thanks to my Director of Studies, Dr. Steven Wilcox for his patience and constant supervision over the last four years, especially in brushing up my presentation and writing up skills. Thanks are also due to Mr. Keith Baker and Mr. Mike Crouch for playing a part in realising this small ambition of mine. My wife, who deserves my eternal gratitude, for her love, patience and endurance which has made this possible and for giving me a beautiful son who has been an immense source of inspiration.

In addition, there are a number of people with whom I have both the privilege and pleasure to work with and also friends who have offered their friendship and encouragement in difficult times. I have great pleasure in mentioning the names of these individuals and their contribution towards my family and myself.

Professor William G. Kaye of B.C.U.R.A. for his enthusiasm and commitment both to the project and the team which has taken the research into an exciting new horizon. His constructive comments and ‘difficult’ questions have made the numerous meetings over the last few years a memorable experience.

Dr. Andy Butt of what used to be the Coal Technology Development Division (CTDD) of British Coal for his inspiring ideas and guidance. Much of the early work on the test facility at Stoke Orchard would not have been possible without his participation in the project. Thanks are also due to the staff of CTDD, in particular Mr. Mark Kirby and Mr. Wayne Green for the countless number of early mornings and late nights when carrying out the ‘never-ending’ experiments on PB29.

Mr. Andrew Proctor of James Proctor Limited, Burnley, Lancashire, for his collaboration in the case study on the industrial stoker plant which has given so much more flavour to the project. Many thanks also to Mr. Wayne Jessop, Proctor’s senior

commissioning engineer, for his assistance in operating the plant and also the countless number of spell-bounding ‘private lectures’ on efficient chain grate stoker operation.

Mr. Neil Whatley and Mr. Adrian Candle of Control System Services Limited, Newport, for their professionalism and interest in my work. The success of the earlier control trials on the test facility at Coal Research Establishment was only possible because of their intimate knowledge of the Tactician process controller which enabled the communication link between the different operating platforms to be established.

Mr. Bill Gayler and Mr. Dave Dawson of Bristol Babcock UK Limited, Kidderminster, for being extremely helpful despite their busy schedule in making the one Bristol-Babcock RTU a workable piece of equipment. Without the Accol code for the RTU and their expert advice, none of the control experiments on the industrial stoker would have been possible.

Mr. Dave Bradshaw, the Chief Boilerman at Her Majesty’s Prison Garth for looking after me during my stay in Leyland, and for his ingenious ‘Blue Peter’ technology which has accelerated the setting up of the equipment, particularly the flame front monitor, for the many hours of test runs on the industrial chain grate. My sincere thanks also to the rest of the mob, Brian, Rob and Barry.

Mr. Gulianno Premier, my former lecturer at the University and now a colleague, for his expert advice on the system identification work and for having me as part of his team in the final year undergraduate control engineering module. The modelling work on the combustion derivatives in Chapter 5 using the Neural Network Based System Identification Toolbox would have been very difficult without his pointers.

Mr. Gareth Betteney, Senior Technical Officer at the School of Design and Advanced Technology, who was my field work mentor during the final year of my undergraduate study. I was fortunate enough to still have his guiding light through the dark and winding journey of this research project. The success of the combustion monitoring

prototype and the data logging facility for work at Garth was due much to his guidance and support.

Friends and Colleagues at the Lodge, in particular Russ, Monica, Sara, Olli, Claire, Kirsty, Steven, Sarah, Toja and Alan for their friendship and support, and also for making the office such a pleasant environment to work in. I wish them all the very best of luck with their quest for the holy grail.

My Malaysian friends, in particular Jackie, Eddy, Priscilla, Shee Ming, Teck Hin, Ooi Hong and David, for their warm friendship and support which they have offered and the home-like atmosphere which they have fostered.

Lastly but most certainly not the least, Pastor Paul Kim and family for their thoughts, encouragement and constant prayers.

Table of Contents

CERTIFICATE OF RESEARCH	I
ABSTRACT	II
ACKNOWLEDGEMENTS	IV
TABLE OF CONTENTS	VII
LIST OF FIGURES	XII
LIST OF TABLES	XVII
NOMENCLATURE	XIX
1. INTRODUCTION	1
<i>1.1 Structure of the Thesis</i>	5
2. LITERATURE REVIEW	8
<i>2.1 Coal as a Possible Primary Source of Energy for the Future</i>	8
2.1.1 What is Coal?	8
2.1.2 Background	11
2.1.3 The Importance of Coal	12
2.1.4 Environmental Impacts from Coal Combustion	13
2.1.4.1 Sulphur Oxides	15
2.1.4.2 Nitrogen Oxides	16
2.1.4.3 Carbon Dioxide	16
2.1.4.4 Smoke and Particulate Matter	17
2.1.5 Conclusions	18
<i>2.2 Conventional Coal Firing Appliances</i>	18
2.2.1 Background	18
2.2.2 Combustion Principles on Grates and the Stokers	20
2.2.2.1 Overfeed Combustion	20
2.2.2.2 Underfeed Combustion	22
2.2.3 Combustion Process on a Chain Grate Stoker	24
2.2.4 Requisites to Efficient Coal Combustion on Chain Grates	28
2.2.5 Conclusions	29
<i>2.3 Condition Monitoring and Control of Lump Coal Combustion on Chain Grates</i>	29
2.3.1 Background	29
2.3.1.1 Case Study - Possible Savings from an Efficiently Operated Stoker Fired Boiler	31
2.3.2 Previous Research in Lump Coal Combustion	32
2.3.3 Conclusions	46
<i>2.4 Artificial Intelligence (AI) Using Artificial Neural Networks (ANNs)</i>	46

2.4.1 Background on Artificial Neural Networks (ANNs)	49
2.4.2 Principles of Artificial Neural Networks	50
2.4.2.1 Supervised Learning - Feed-Forward Multi-Layered Perceptron (MLP) Network	53
2.4.2.2 Unsupervised Learning – Competitive Learning Network	55
2.4.3 Literature on Related Artificial Neural Networks Applications	57
2.4.4 Conclusions	64
3. CHAIN GRATE STOKER BOILER TEST FACILITY, STOKER BOILER OPERATION & TEST PROCEDURES	65
3.1 <i>Plant Description</i>	65
3.1.1 Coal Feed Mechanism	66
3.1.2 Combustion Air Supply	71
3.1.3 Chain Grate Stoker	72
3.1.4 The Two Pass Shell Boiler & Cooling Water Circuit	73
3.2 <i>The Plant Control System and Instrumentation</i>	73
3.2.1 Gas Analysis	77
3.2.2 Flue Gas Temperatures	78
3.2.3 Refractory Arch Temperatures	78
3.2.4 Other Measurements	80
3.3 <i>Coal Combustion on Chain Grate Stoker</i>	80
3.3.1 Combustion Calculation for Daw Mill Type Coal	82
3.3.1.1 Combustion Air Calculation for Singles Grade Coal	85
3.3.1.2 Combustion Air Calculation for Smalls Grade Coal	87
3.3.1.3 Calibration Setting of the Grate Speed for Singles and Smalls	88
3.3.2 Combustion Air Distribution on the Grate	90
3.4 <i>Experimental Procedures</i>	93
3.4.1 Experiments with Gradual Load Changes	94
3.4.2 Experiments with Large Load Changes Following Two Different Coal and Air Staging Profiles	96
3.4.3 Experiments with the Neural Network Based Controller	98
3.4.3.1 NNBC Implementation on the Stoker Test Facility Burning Singles	98
3.4.3.2 NNBC Implementation on the Stoker Test Facility Burning Smalls	99
3.4.3.3 NNBC Implementation on an Industrial Chain Grate Stoker Fired Plant	100
4. EXPERIMENTAL RESULTS & DISCUSSION – A STUDY INTO THE BEHAVIOUR OF THE STOKER TEST FACILITY	102
4.1 <i>Boiler Response to Gradual Load Changes</i>	103
4.1.1 Test 1 - Gradual Load Changes at Near Optimum Air	104
4.1.2 Test 2 - Gradual Load Changes at Lower Excess Air	107
4.1.3 Test 3 - Gradual Load Changes at Higher Excess Air	110
4.1.4 Test 4 - Gradual Load Changes at Faster Grate Speed	113
4.1.5 Test 5 - Gradual Load Changes with a Uniform Air Distribution	116
4.1.6 Summary of Section 4.1	119
4.2 <i>Boiler Response to Large Load Changes</i>	120

4.2.1 Test 6 - Large Load Changes with Staging Profile 1	121
4.2.2 Test 7 - Large Load Changes with Staging Profile 2	125
4.2.3 Conclusions of Section 4.2	130
5. DEVELOPMENT & TESTING OF THE NEURAL NETWORK BASED CONTROLLER & BLACK BOX MODELS	131
5.1 <i>The Concept of the Control Strategy - Minimising Boiler Losses</i>	132
5.1.1 Background	132
5.1.2 Minimising Boiler Losses	133
5.1.3 The Control Approach	135
5.2 <i>The Development of the Neural Network Based Controller (NNBC)</i>	138
5.2.1 Background - The Overall Controller Strategy	139
5.2.2 Setting Network	140
5.2.3 The Corrective Network	142
5.3 <i>Testing & Tuning of the Neural Network Based Controller (NNBC)</i>	144
5.3.1 Control Experiments with Singles Grade Coal	147
5.3.1.1 Control Experiment (Test 8) with Unsuitable Controller Parameter Settings Burning Singles	147
5.3.1.2 Control Experiment (Test 11) with Suitable Controller Parameter Settings Burning Singles	150
5.3.2 Control Experiment (Test 12) with Burning Smalls Using NNBC Derived from Burning Singles	154
5.4 <i>Case Study – Implementation of the NNBC to an Industrial Chain Grate Stoker Fired Shell Boiler</i>	157
5.4.1 Description of the 3.7MW Industrial Scale Chain Grate Stoker Fired Shell Boiler & Plant Instrumentation	157
5.4.2 Preliminary Test on the 3.7MW Chain Grate Stoker Fired Shell Boiler (Test 13)	159
5.4.3 Plant Response Following Automatic Operation of the Boiler under Conventional PID Control (Test 14 & 15)	162
5.4.3.1 Plant Response Under Automatic Conventional PID Controller Mode Tracking Hot Water Temperature Set Point (Test 14)	162
5.4.3.2 Plant Response Under Automatic Conventional PID Controller Mode Following Temperature Set Point Change (Test 15)	166
5.4.4 Plant Response Following Neural Network Based Controller (NNBC) Operation (Test 16, 17a & 17b)	167
5.4.4.1 Plant Response Under Automatic NNBC Mode Tracking Hot Water Temperature Set Point (Test 16)	169
5.4.4.2 Plant Response Under Automatic NNBC Mode Following Temperature Set Point Change (Test 17a & 17b)	171
5.5 <i>Neural Network Based System Identification – Black Box Modelling Using ANNs</i>	175
5.5.1 System Identification Procedure	175
5.5.2 Feed-Forward Multi-Layered Perceptron (MLP) Neural Network – Architecture of the Neural Network ARX Models	179

5.5.2.1 Non-linear (Neural Network) ARX Model for Oxygen in the Flue Gas	183
5.5.2.2 Non-linear (Neural Network) ARX Model for Nitrogen Oxides (NO _x) Emission	190
5.5.2.3 Non-linear (Neural Network) ARX Model for Carbon Monoxide Emission	198
6. DEVELOPMENT & TESTING OF A PROTOTYPE FLAME FRONT MONITORING DEVICE	206
6.1 <i>Flame Front Detector - Pilot Study to Investigate the Feasibility of Using Optical Means as An Alternative to Thermocouples</i>	207
6.1.1 The Use of Thermocouples to Infer the Movement of the Ignition Plane	209
6.1.2 Classification of the Flame Front through the Inspection Porthole	211
6.1.3 Flame Front Movement Following Gradual Load Changes at Optimum Air – Test 1	212
6.1.4 Flame Front Movement Following Gradual Load Changes at Lower Excess Air – Test 2	214
6.1.5 Flame Front Movement Following Gradual Load Changes at Higher Excess Air – Test 3	215
6.1.6 Flame Front Movement Following Large Load Changes with an Undesirable Staging Profile – Test 6	216
6.1.7 Flame Front Movement Following Large Step Changes with a Desirable Staging Profile – Test 7	217
6.2 <i>The Development & Testing of the Flame Front Monitor</i>	219
6.2.1 Flame Front Monitor Results & the Hybrid Neural Network Classifier	222
6.2.1.1 Industrial Plant Response Under Automatic NNBC Mode in Tracking the Hot Water Temperature Set Point (Test 16)	224
6.2.1.2 Industrial Plant Response Under Automatic NNBC Mode to a Step Change in the Hot Water Temperature Set Point (Test 17a)	225
6.2.1.3 Industrial Plant Response Under Automatic NNBC Mode to a Step Change in the Hot Water Temperature Set Point (Test 17b)	226
6.3 <i>Conclusions</i>	227
7. CONCLUSIONS & RECOMMENDATION FOR FURTHER WORK	228
7.1 <i>Performance of the Neural Network Based Controller (NNBC)</i>	229
7.2 <i>Identified Models of Combustion Derivatives by Using the 'Black-Box' Modelling Technique of ANNs</i>	230
7.3 <i>Novel Flame Front Monitoring System</i>	231
7.4 <i>Recommendation for Further Work</i>	232
REFERENCES	235
APPENDIX A – FUEL SPECIFICATION FOR EXPERIMENTS ON THE STOKER TEST FACILITY	247
APPENDIX B – FUEL SPECIFICATION FOR THE EXPERIMENTS ON THE INDUSTRIAL STOKER PLANT	250
APPENDIX C – GRATE ASH ANALYSIS TO BS1016: PART 104 FOR LOSS ON IGNITION	252
APPENDIX D – THE NNBC MATLAB™ FILE FOR THE STOKER TEST FACILITY	256

APPENDIX E – THE SETTING NETWORK MATLAB™ FILE FOR SINGLES AND SMALLS GRADE COAL	259
APPENDIX F – THE CORRECTIVE NETWORK MATLAB™ FILE	262
APPENDIX G – THE NNBC MATLAB™ FILE FOR THE INDUSTRIAL STOKER PLANT	265
PUBLICATIONS	270

List of Figures

FIGURE 2.1 STAGES OF COMBUSTION PROCESS ON A CHAIN GRATE STOKER [GOOD PRACTICE GUIDE 88, 1993]	27
FIGURE 2.2 MCCULLOCH AND PITTS NEURON MODEL	51
FIGURE 2.3 A GENERALISED DIAGRAM OF A 3-LAYER FEED-FORWARD MLP NETWORK [DEMUTH AND BEALE, 1995]	55
FIGURE 2.4 LEARNING VECTOR QUANTISATION NETWORK STRUCTURE [DEMUTH AND BEALE, 1995]	56
FIGURE 3.1 BLOCK DIAGRAM OF THE 0.75MW CHAIN GRATE STOKER BOILER TEST FACILITY	67
FIGURE 3.2 THE GUILLOTINE & FIRE BREAK ASSEMBLY [GOOD PRACTICE GUIDE 88, 1993]	69
FIGURE 3.3 PLAN VIEW OF LINK GEOMETRY, LINK SET ARRANGEMENT & CHAIN MAT ASSEMBLY [CTDD, 1995]	69
FIGURE 3.4 STOKER TEST FACILITY GRATE & BED DIMENSIONS [CTDD, 1995]	70
FIGURE 3.5 SENSORS LOCATION ON THE STOKER TEST FACILITY	75
FIGURE 3.6 THE BLOCK DIAGRAM OF MEASURED AND CONTROLLED PARAMETERS WITH THE DIGITAL CONTROLLERS, SENSORS, AND PLANT COMPUTERS	76
FIGURE 3.7 THERMOCOUPLES ARRANGEMENT IN THE REFRACTORY ARCH OF THE STOKER TEST FACILITY	79
FIGURE 3.8 INDICATED ROTARY VALVE SPEED ON THE FRONT END CONTROLLER VS. ACTUAL COAL FEED RATE FOR SINGLES GRADE COAL [CTDD, 1995]	86
FIGURE 3.9 INDICATED ROTARY VALVE SPEED ON THE FRONT END CONTROLLER VS. ACTUAL COAL FEED RATE FOR SMALLS GRADE COAL [CTDD, 1995]	87
FIGURE 3.10 INDICATED GRATE SPEED OF THE FRONT END CONTROLLER VS. ACTUAL GRATE SPEED & BED REPLACEMENT TIME FOR SINGLES & SMALLS GRADE COAL [CTDD, 1995]	89
FIGURE 3.11 INDICATED AIR SETTINGS ON THE FRONT END CONTROLLER VS. ACTUAL AIR FLOW RATES ON DUCT 1, 2, 3 & 4 FOR SINGLES & SMALLS GRADE COAL [CTDD, 1995]	90
FIGURE 3.12 RELATIONSHIP BETWEEN O ₂ , CO ₂ AND EXCESS AIR LEVEL FOR BITUMINOUS COAL	96
FIGURE 4.1 FLAME FRONT INDICATION THROUGH THE INSPECTION PORTHOLE	102
FIGURE 4.2 FLUE GAS TEMPERATURE AT THE STACK INLET & OXYGEN CONCENTRATION IN THE SMOKE TUBE FROM TEST 1	105
FIGURE 4.3 NO _x & CO EMISSIONS IN THE EXHAUST DUCT FROM TEST 1	105
FIGURE 4.4 FLUE GAS TEMPERATURE AT THE STACK INLET & OXYGEN CONCENTRATION IN THE SMOKE TUBE FROM TEST 2	108
FIGURE 4.5 NO _x & CO EMISSIONS IN THE EXHAUST DUCT FROM TEST 2	108
FIGURE 4.6 FLUE GAS TEMPERATURE AT THE STACK INLET & OXYGEN CONCENTRATION IN THE SMOKE TUBE FROM TEST 3	111

FIGURE 4.7 NO _x & CO EMISSIONS IN THE EXHAUST DUCT FROM TEST 3	111
FIGURE 4.8 FLUE GAS TEMPERATURE AT THE STACK INLET & OXYGEN CONCENTRATION IN THE SMOKE TUBE FROM TEST 4	114
FIGURE 4.9 NO _x & CO EMISSIONS IN THE EXHAUST DUCT FROM TEST 4	114
FIGURE 4.10 FLUE GAS TEMPERATURE AT THE STACK INLET & OXYGEN CONCENTRATION IN THE SMOKE TUBE FROM TEST 5	117
FIGURE 4.11 NO _x & CO EMISSIONS IN THE EXHAUST DUCT FROM TEST 5	118
FIGURE 4.12 COAL FEED & AIR FLOW STAGING SEQUENCE FOLLOWING LARGE LOAD CHANGES IN TEST 6 WITH STAGING PROFILE 1	121
FIGURE 4.13 FLUE GAS TEMPERATURE AT THE STACK INLET & OXYGEN CONCENTRATION IN THE SMOKE TUBE FROM TEST 6 - STAGING PROFILE 1	122
FIGURE 4.14 NO _x & CO EMISSIONS IN THE EXHAUST DUCT FROM TEST 6 - STAGING PROFILE 1	122
FIGURE 4.15 COAL FEED & AIR FLOW STAGING SEQUENCE FOLLOWING LARGE LOAD CHANGES IN TEST 7 WITH STAGING PROFILE 2	125
FIGURE 4.16 FLUE GAS TEMPERATURE AT THE STACK INLET & OXYGEN CONCENTRATION IN THE SMOKE TUBE FROM TEST 7 - STAGING PROFILE 2	126
FIGURE 4.17 NO _x & CO EMISSIONS IN THE EXHAUST DUCT FROM TEST 7 - STAGING PROFILE 2	127
FIGURE 5.1 FIRE BED PROFILE DURING TRANSIENTS FOLLOWING LARGE LOAD CHANGES	137
FIGURE 5.2 OVERALL NEURAL NETWORK BASED CONTROLLER STRATEGY	140
FIGURE 5.3 OXYGEN RESPONSE TO UNDESIRABLE CONTROLLER GAIN & SAMPLING PERIOD WITH BURNING SINGLES - TEST 8	148
FIGURE 5.4 FLUE GAS TEMPERATURE RESPONSE TO UNDESIRABLE CONTROLLER GAIN & SAMPLING PERIOD WITH BURNING SINGLES – TEST 8	149
FIGURE 5.5 NO _x & CO EMISSIONS TO UNDESIRABLE CONTROLLER GAIN & SAMPLING PERIOD WITH BURNING SINGLES – TEST 8	150
FIGURE 5.6 OXYGEN RESPONSE TO DESIRABLE CONTROLLER GAIN & SAMPLING PERIOD WITH BURNING SINGLES – TEST 11	151
FIGURE 5.7 FLUE GAS TEMPERATURE RESPONSE TO DESIRABLE CONTROLLER GAIN & SAMPLING PERIOD WHILST BURNING SINGLES – TEST 11	153
FIGURE 5.8 ARCH TEMPERATURE PATTERN TO DESIRABLE GAIN & SAMPLING PERIOD WHILST BURNING SINGLES – TEST 11	153
FIGURE 5.9 OXYGEN RESPONSE WITH BURNING SMALLS – NNBC DERIVED FROM BURNING SINGLES (TEST 12)	155
FIGURE 5.10 FLUE GAS TEMPERATURE WITH BURNING SMALLS – NNBC DERIVED FROM BURNING SINGLES (TEST 12)	156
FIGURE 5.11 NO _x & CO EMISSIONS FROM BURNING SMALLS – NNBC DERIVED FROM BURNING SINGLES (TEST 12)	156

FIGURE 5.12 OXYGEN CONCENTRATION & FLUE GAS TEMPERATURE UNDER OPERATOR'S BEST PRACTICE FOLLOWING GRADUAL LOAD CHANGES FOR THE INDUSTRIAL STOKER	160
FIGURE 5.13 POLLUTANT EMISSIONS UNDER OPERATOR'S BEST PRACTICE FOLLOWING GRADUAL LOAD CHANGES FOR THE INDUSTRIAL STOKER	161
FIGURE 5.14 OXYGEN CONCENTRATION & WATER TEMPERATURE UNDER PID CONTROLLER EFFORT TO TRACKING THE SET POINT TEMPERATURE	162
FIGURE 5.15 OXYGEN CONCENTRATION & CO EMISSION UNDER PID CONTROLLER EFFORT TO TRACKING THE SET POINT TEMPERATURE	164
FIGURE 5.16 SO ₂ & NO _x EMISSIONS UNDER PID CONTROLLER EFFORT TO TRACKING THE SET POINT TEMPERATURE	165
FIGURE 5.17 REFRACTORY ARCH TEMPERATURE PATTERN UNDER PID CONTROLLER EFFORT TO TRACKING THE SET POINT TEMPERATURE	165
FIGURE 5.18 OXYGEN CONCENTRATION & WATER TEMPERATURE FOLLOWING A STEP CHANGE IN THE HOT WATER TEMPERATURE SET POINT UNDER CONVENTIONAL PID CONTROL	166
FIGURE 5.19 POLLUTANT EMISSIONS FOLLOWING A STEP CHANGE IN THE HOT WATER TEMPERATURE SET POINT UNDER CONVENTIONAL PID CONTROL	167
FIGURE 5.20 MODIFIED NNBC STRUCTURE FOR THE CONTROL OF THE INDUSTRIAL CHAIN GRATE STOKER PLANT	168
FIGURE 5.21 OXYGEN CONCENTRATION & WATER TEMPERATURE UNDER NNBC EFFORT TO TRACKING THE SET POINT TEMPERATURE	170
FIGURE 5.22 POLLUTANT EMISSIONS UNDER UNDER NNBC EFFORT TO TRACKING THE SET POINT TEMPERATURE	170
FIGURE 5.23 OXYGEN CONCENTRATION & WATER TEMPERATURE FOLLOWING A STEP CHANGE IN THE HOT WATER TEMPERATURE SET POINT WITH THE NNBC (TEST 17A)	172
FIGURE 5.24 POLLUTANT EMISSIONS FOLLOWING A STEP CHANGE IN THE HOT WATER TEMPERATURE SET POINT WITH THE NNBC (TEST 17A)	172
FIGURE 5.25 OXYGEN CONCENTRATION & WATER TEMPERATURE FOLLOWING A STEP CHANGE IN THE HOT WATER TEMPERATURE SET POINT WITH THE NNBC (TEST 17B)	173
FIGURE 5.26 POLLUTANT EMISSIONS FOLLOWING A STEP CHANGE IN THE HOT WATER TEMPERATURE SET POINT WITH THE NNBC (TEST 17B)	174
FIGURE 5.27 THE FOUR BASIC STEPS TOWARDS SYSTEM IDENTIFICATION	178
FIGURE 5.28 THE FEED-FORWARD MLP NETWORK ARCHITECTURE FOR THE ARX NEURAL MODEL STRUCTURE	181
FIGURE 5.29 THE NEURAL NETWORK ARX MODEL FOR OXYGEN IN THE FLUE GAS	184
FIGURE 5.30 TRAINING ERROR VS NUMBER OF ITERATIONS FOR THE OXYGEN MODEL	185
FIGURE 5.31 TARGETS VS. ONE STEP AHEAD MODEL PREDICTIONS FOR THE OXYGEN MODEL	186
FIGURE 5.32 ONE-STEP AHEAD PREDICTION BY THE NEURAL NETWORK ARX MODEL FOR OXYGEN IN THE FLUE GAS WITH VALIDATION DATA SET 1 (TEST 1)	186
FIGURE 5.33 ONE STEP AHEAD PREDICTION BY THE NEURAL NETWORK ARX MODEL FOR	

OXYGEN IN THE FLUE GAS WITH VALIDATION DATA SET 2 (TEST 6)	187
FIGURE 5.34 ONE STEP AHEAD PREDICTION BY THE NEURAL NETWORK ARX MODEL FOR OXYGEN IN THE FLUE GAS WITH VALIDATION DATA SET 3 (TEST 8)	187
FIGURE 5.35 ONE STEP AHEAD PREDICTION BY THE NEURAL NETWORK ARX MODEL FOR OXYGEN IN THE FLUE GAS WITH VALIDATION DATA SET 4 (TEST 9)	188
FIGURE 5.36 ONE STEP AHEAD PREDICTION BY THE NEURAL NETWORK ARX MODEL FOR OXYGEN IN FLUE GAS WITH FLUE GAS TEMPERATURE AS ONE OF THE INPUT TO THE MODEL WITH VALIDATION SET 2 (TEST 6)	189
FIGURE 5.37 ONE STEP AHEAD PREDICTION BY THE NEURAL NETWORK ARX MODEL FOR OXYGEN IN FLUE GAS WITH FLUE GAS TEMPERATURE AS ONE OF THE INPUT TO THE MODEL WITH VALIDATION SET 4 (TEST 9)	190
FIGURE 5.38 THE NEURAL NETWORK ARX MODEL FOR NITROGEN OXIDES EMISSION	192
FIGURE 5.39 TRAINING ERROR VS. NUMBER OF ITERATIONS FOR THE NITROGEN OXIDES EMISSION MODEL	193
FIGURE 5.40 TARGETS VS. ONE STEP AHEAD MODEL PREDICTIONS FOR THE NITROGEN OXIDES MODEL	193
FIGURE 5.41 ONE STEP AHEAD PREDICTION BY THE NEURAL NETWORK ARX MODEL FOR NITROGEN OXIDES EMISSION WITH VALIDATION DATA SET 1 (TEST 1)	194
FIGURE 5.42 ONE STEP AHEAD PREDICTION BY THE NEURAL NETWORK ARX MODEL FOR NITROGEN OXIDES EMISSION WITH VALIDATION DATA SET 2 (TEST 6)	195
FIGURE 5.43 ONE STEP AHEAD PREDICTION BY THE PRUNED NEURAL NETWORK ARX MODEL FOR NITROGEN OXIDES EMISSION WITH VALIDATION DATA SET 1 (TEST 1)	196
FIGURE 5.44 ONE STEP AHEAD PREDICTION BY THE PRUNED NEURAL NETWORK ARX MODEL FOR NITROGEN OXIDES EMISSION WITH VALIDATION DATA SET 2 (TEST 6)	196
FIGURE 5.45 ONE STEP AHEAD PREDICTION BY THE PRUNED NEURAL NETWORK ARX MODEL FOR NITROGEN OXIDES EMISSION WITH VALIDATION DATA SET 3 (TEST 8)	197
FIGURE 5.46 ONE STEP AHEAD PREDICTION BY THE PRUNED NEURAL NETWORK ARX MODEL FOR NITROGEN OXIDES EMISSION WITH VALIDATION DATA SET 4 (TEST 9)	197
FIGURE 5.47 THE NEURAL NETWORK ARX MODEL FOR CARBON MONOXIDE EMISSION	199
FIGURE 5.48 TRAINING ERROR VS. NUMBER OF ITERATIONS FOR THE CARBON MONOXIDE EMISSION MODEL	200
FIGURE 5.49 TRAINING TARGETS VS. ONE STEP AHEAD MODEL PREDICTIONS FOR THE CARBON MONOXIDE MODEL	200
FIGURE 5.50 ONE STEP AHEAD PREDICTION BY THE NEURAL NETWORK ARX MODEL FOR CARBON MONOXIDE EMISSION WITH VALIDATION DATA SET 1 (TEST 1)	201
FIGURE 5.51 ONE STEP AHEAD PREDICTION BY THE NEURAL NETWORK ARX MODEL FOR CARBON MONOXIDE EMISSION WITH VALIDATION DATA SET 4 (TEST 9)	202
FIGURE 5.52 ONE STEP AHEAD PREDICTION BY THE PRUNED NEURAL NETWORK ARX MODEL FOR CARBON MONOXIDE EMISSION WITH VALIDATION DATA SET 1 (TEST 1)	202

FIGURE 5.53 ONE STEP AHEAD PREDICTION BY THE PRUNED NEURAL NETWORK ARX MODEL FOR CARBON MONOXIDE EMISSION WITH VALIDATION DATA SET 2 (TEST 6)	203
FIGURE 5.54 ONE STEP AHEAD PREDICTION BY THE PRUNED NEURAL NETWORK ARX MODEL FOR CARBON MONOXIDE EMISSION WITH VALIDATION DATA SET 3 (TEST 8)	203
FIGURE 5.55 ONE STEP AHEAD PREDICTION BY THE PRUNED NEURAL NETWORK ARX MODEL FOR CARBON MONOXIDE EMISSION WITH VALIDATION DATA SET 4 (TEST 9)	204
FIGURE 6.1 PLAN VIEW OF THE REFRACTORY ARCH WITH THE THERMOCOUPLES	209
FIGURE 6.2 ARCH TEMPERATURE DISTRIBUTIONS FOLLOWING GRADUAL LOAD CHANGES AT OPTIMUM OPERATING CONDITIONS – TEST 1	210
FIGURE 6.3 REFERENCE FLAME FRONT ZONES THROUGH THE ARCH INSPECTION PORTHOLE	212
FIGURE 6.4 FLAME FRONT MOVEMENT FOLLOWING GRADUAL LOAD CHANGES AT OPTIMUM AIR (TEST 1)	213
FIGURE 6.5 FLAME FRONT MOVEMENT FOLLOWING GRADUAL LOAD CHANGES AT LOWER EXCESS AIR (TEST 2)	214
FIGURE 6.6 FLAME FRONT MOVEMENT FOLLOWING GRADUAL LOAD CHANGES AT HIGHER EXCESS AIR (TEST 3)	215
FIGURE 6.7 FLAME FRONT MOVEMENT FOLLOWING LARGE STEP CHANGES WITH AN UNDESIRABLE STAGING PROFILE (TEST 6)	217
FIGURE 6.8 FLAME FRONT MOVEMENT FOLLOWING LARGE STEP CHANGES WITH A DESIRABLE STAGING PROFILE (TEST 7)	219
FIGURE 6.9 BLOCK DIAGRAM OF FLAME FRONT MONITOR AND DATA LOGGER	220
FIGURE 6.10 TYPICAL FLAME FRONT MONITOR RESPONSE TO THE IMAGE OF THE FIRE BED	221
FIGURE 6.11 FLAME FRONT MOVEMENT FOLLOWING LOAD CHANGES TO MAINTAIN THE HOT WATER TEMPERATURE SET POINT OF THE INDUSTRIAL STOKER PLANT (TEST 16)	225
FIGURE 6.12 FLAME FRONT MOVEMENT FOLLOWING A STEP CHANGE IN THE HOT WATER TEMPERATURE SET POINT OF THE INDUSTRIAL STOKER PLANT (TEST 17A)	226
FIGURE 6.13 FLAME FRONT MOVEMENT FOLLOWING A STEP CHANGE IN THE HOT WATER TEMPERATURE SET POINT OF THE INDUSTRIAL STOKER PLANT (TEST 17B)	227
FIGURE 7.1 THE INCLUSION OF FLAME FRONT MONITORING NETWORK INTO THE NNBC STRATEGY	233

List of Tables

TABLE 3.1 BITUMINOUS COAL CONSTITUENTS AND IGNITION TEMPERATURES [GOOD PRACTICE GUIDE 88, 1993]	81
TABLE 3.2 PROXIMATE ANALYSIS OF A TYPICAL COAL (% BY WEIGHT) [GUNN AND HORTON, 1989]	83
TABLE 3.3 ULTIMATE ANALYSIS OF LOW ASH DAW MILL COAL (PERCENTAGE BY MASS) - FREE BURNING BITUMINOUS COAL (NCB RANK CODE 802)	84
TABLE 3.4 ANALYSIS OF DAW MILL COAL COMBUSTION BY MASS	85
TABLE 3.5 ESTIMATED COMBUSTION AIR WITH THE CORRESPONDING THERMAL OUTPUT FOR SINGLES GRADE DAW MILL TYPE COAL	86
TABLE 3.6 ESTIMATED COMBUSTION AIR WITH THE CORRESPONDING THERMAL OUTPUT FOR SMALLS GRADE DAW MILL TYPE COAL	88
TABLE 3.7 INDICATED ROTARY VALVE & GRATE SPEED SETTINGS WITH THE REQUIRED COAL FEED RATE FOR SINGLES & SMALLS [CTDD, 1995]	89
TABLE 3.8 PRIMARY AIR DISTRIBUTION PROFILE ALONG THE FIRE BED	91
TABLE 3.9 OPERATOR'S OPTIMUM AIR SETTINGS ON THE FOUR AIR DUCTS FOR SINGLES AND SMALLS GRADE COAL [CTDD, 1995]	92
TABLE 4.1 GRATE SURFACE TEMPERATURE AT THE STOKER FRONT, CARBON IN ASH LOSSES & AVERAGE FLAME FRONT LOCATION AT STEADY-STATE COMBUSTION FROM TEST 1	106
TABLE 4.2 GRATE SURFACE TEMPERATURE AT THE STOKER FRONT, CARBON IN ASH LOSSES & AVERAGE FLAME FRONT LOCATION AT STEADY-STATE COMBUSTION FROM TEST 2	109
TABLE 4.3 GRATE SURFACE TEMPERATURE AT THE STOKER FRONT, CARBON IN ASH LOSSES & AVERAGE FLAME FRONT LOCATION AT STEADY-STATE COMBUSTION FROM TEST 3	112
TABLE 4.4 GRATE SURFACE TEMPERATURE AT THE STOKER FRONT, CARBON IN ASH LOSSES & AVERAGE FLAME FRONT LOCATION AT STEADY-STATE COMBUSTION FROM TEST 4	115
TABLE 4.5 GRATE SURFACE TEMPERATURE AT THE STOKER FRONT, CARBON IN ASH LOSSES & AVERAGE FLAME FRONT LOCATION AT STEADY-STATE COMBUSTION FROM TEST 5	118
TABLE 4.6 AVERAGE FLAME FRONT MOVEMENT FROM TEST 6 WITH STAGING PROFILE (SP) 1	124
TABLE 4.7 AVERAGE FLAME FRONT MOVEMENT FROM TEST 7 WITH STAGING PROFILE (SP) 2	129
TABLE 5.1 TARGET AREAS FOR MINIMISING BOILER LOSSES, IMPLICATIONS ON THE PLANT & PRACTICAL REMEDIES [GOOD PRACTICE GUIDE 30, 1992]	134
TABLE 5.2 NEAR OPTIMUM SETTINGS OF COAL FEED & AIRFLOW FOR THE FOUR BOILER LOADS FOR SINGLES GRADE COAL	141
TABLE 5.3 NEAR OPTIMUM SETTINGS OF COAL FEED & AIRFLOW FOR THE FOUR BOILER LOADS FOR SMALLS GRADE COAL	141
TABLE 5.4 TOTAL PRIMARY AIR SUPPLIED WITH THE ACTUAL OXYGEN IN FLUE GAS BAND	143

TABLE 5.5 RELATIONSHIP BETWEEN THE RANGES OF OXYGEN READING WITH THE BAND OF PRIMARY AIR	143
TABLE 5.6 SUMMARY OF RESULTS OF THE CONTROL EXPERIMENTS WITH SINGLES	145
TABLE 5.7 OXYGEN TARGET BAND WITH THE CORRESPONDING RANGE OF FIRING RATE	168
TABLE 6.1 FLAME FRONT ZONES AND THEIR DISCRETE LOCATION RELATIVE TO THE CENTRE OF THE INSPECTION PORTHOLE	212
TABLE 6.2 EXAMPLE DATA SET FOR THE HYBRID NEURAL NETWORK TRAINING	223
TABLE 6.3 HYBRID NEURAL NETWORK CLASSIFIER OUTPUT ON UNSEEN DATA	223

Nomenclature

ζ	Combustion efficiency	
cv	Fuel calorific value	kJ/kg
X_s	Excess air as a percentage from the stoichiometric	
MCR	Maximum continuous boiler output rating	
MW_{th}	Thermal output from a boiler	MW
FR	Boiler firing rate as a percentage of the MCR	
K_p	Proportional gain factor	
PV	Hot water temperature	°C
n, m	Number of element(s) in the input and output vectors	
f	Theoretical function governing the relationship between input and output data	
f	Functional mapping approximated by a neural network	
$\varphi(t)$	Regressor vector function of the ARX structure	
θ	Weight and bias vectors of a neural network architecture	
n_a	Number of past output data	
n_k	Number of delay(s) associated with an input	
n_b	Number of past input data	
$g(\varphi(t), \theta)$	Predictor function of the neural network	
t	Time expressed in terms of the sampling period	
ASSE	Average sum squared error	
y_i	Actual plant response for input vector i	
Y_i	Model Prediction for input vector i	
N	Number of input/output samples in the data set	
w, W	Weights of a neural network	
b, B	Biases of a neural network	
$u(t), y(t)$	Input and output of a neural network	
f, F	Activation function of the neurons in each network layer	
U, Y	Input and output space in the mathematical context	
T	Threshold limit of an artificial neuron	
η	Learning rate in the context of neural network learning	

1. Introduction

Boilers were mostly coal-fired until the 1950's when oil became an affordable alternative. Despite the relatively old technology the essential principles of these coal fired appliances remain the same and are still widely used in many industries, hospitals and schools throughout the UK for hot water and steam [DTI Case Study 004, 1998]. Although new methods of coal firing have been developed over the years such as pulverised fuel (pf) firing and fluidised bed combustion, there is a strong indication that for the small to medium size range, conventional coal firing appliances will remain for some time to come [Gunn, 1982]. One incentive for the continuing use of these conventional coal firing appliances stems from the prospect of coal being used as the primary energy source in the future due to an inevitable decline in the supply of oil and gas [Schobert, 1987]. Furthermore, with the advent of modern handling equipment in the 1980's for coal and the disposal of ash, fully automatic operation of such conventional coal firing appliances has become more common nowadays making them more attractive in the market place [Robson *et al.*, 1988; Proctor, 1999].

Despite the higher costs of handling and maintenance, conventional coal fired equipment produces very low levels of nitrogen oxides due to the lower peak temperature (as compared to pulverised fuel firing) and the fuel costs are lower than oil or gas [Cooke, 1991; IEA Statistics, 1997]. Fossil fuels account for about 80% of the primary energy used on earth with coal being the most abundant source of all despite having the smallest share in its consumption. Many countries, including Germany, USA, Australia, Russia, India and China, have enormous coal reserves which will last for a long time at today's rate of consumption [IEA Statistics, 1997]. With the relatively higher prices of crude oil and the prospect for possible increases in the future, a considerable number of oil importing countries have undertaken research into better ways to burn coal [IEA Coal Research, 1993; Good Practice Guide 30, 1992].

However, whilst it can provide much of the valuable energy needed for power generation and heating, the products of combustion can also cause pollution. An important global issue that has received much attention over the past few decades is the

emission of greenhouse gases (GHGs) from the burning of fossil fuel. With respect to stationary combustion plants, carbon dioxide and nitrous oxide are the principal GHGs influenced by human activities. The United Nation's Intergovernmental Panel on Climate Change (IPCC) has recently concluded that:

“emissions resulting from human activities are substantially increasing the atmospheric concentrations of greenhouse gases”

[Houghton et al., 1990, Executive Summary].

If part of that human influence on the climate was to be the warming of the surface of the earth, then it is *vital* to find ways in which the emissions of these GHGs can be reduced. Therefore, increasing pressure has been placed on combustion engineers to develop methods that are able to quantify and enhance the performance of industrial boilers. In particular, the need to comply with more stringent environmental requirements, by lowering the emission of nitrogen oxides without having to jeopardise efficiency [Clarke and Williams, 1992]. Although there are no current legislative limits on the emission of nitrogen oxides for smaller combustion plants below 20MW, these plants are subjected to the Clean Air Act of 1956 and 1968. It is also likely that the European Commission will introduce directives to cover the emission of nitrogen oxides from such burners in the near future. The current emphasis on carbon dioxide emission is to improve the overall combustion efficiency which in turn reduces the production of carbon dioxide, as less fuel is burnt for any given thermal output [Good Practice Guide 30, 1992].

Most industrial and commercial coal-fired boilers employ moving or static grate combustion systems. These have evolved over more than a century so that current designs are robust and reliable. A recent case study published by the Department of Trade and Industry (DTI) has reported that a large proportion of the 3.2 million tonnes of coal consumed annually in the UK is being used in stoker fired systems with chain grate systems dominating as the primary stokers [DTI Case Study 004, 1998]. However it is still difficult to optimise the combustion efficiency of these boilers particularly under fluctuating load-following conditions, whilst simultaneously

maintaining rigorous control of pollutant emissions. Moreover, the problem is exacerbated during extended periods of operation when changes in the fuel and subsequently boiler characteristics can lead to further deviation from the optimal air/fuel ratio. The resultant reductions in operating efficiency may be accompanied by significantly increased emissions of particulate and gaseous pollutants, higher carbon in ash losses, as well as enhanced rates of boiler fouling. Thus the overall thermal efficiency of the boiler can fall by 10% or more from an initial typical value of approximately 80% at maximum continuous rating (MCR). Similarly the emission of the oxides of nitrogen can more than double to over 350 ppm (normalised to a 6% oxygen concentration) during an operating campaign [Grainger and Gibson, 1981]. Therefore, a control system should be able to deliver the optimum coal and air feed required for a certain load demand regardless of the magnitude and direction of the load change and, in addition, be able to fine tune the air to yield an optimum air/fuel ratio without jeopardising production. This will result in improved combustion efficiency of these boilers and can offer considerable savings (demonstrated in a case study in Section 2.3.1), in the fuel and maintenance costs over an extended period of time, with prolonged boiler availability.

Classical linear control methods such as closed-loop PID control, have limited application in controlling the combustion process since mathematical models based on the fundamentals of combustion and heat transfer do not adequately describe the operation of the boiler for practical implementation [Smoot, 1984; Hobbs *et al.*, 1992, 1993]. Even if a simplified model (transfer functions) of the process can be devised for a limited range of operating conditions, it will be difficult to deal with the variations in fuel characteristics (coal type, size and moisture content) over extended periods of operation [Chong *et al.*, 1999]. Moreover, the ‘coupling’ effects between the various input parameters (coal feed and air flow) on the process parameters such as water temperature, excess air level and stability of combustion is extremely difficult to quantify in the ‘mathematical’ sense therefore making the tasks of delivering the appropriate control decisions extremely difficult from a conventional control strategy perspective. Also with the underfeed lump coal combustion process, the requirement of a smooth transition from one load to the other is vital to ensure satisfactory

combustion, Gunn (1982), and such a transition can only be addressed from the experience and know-how of the field expert [Butt and Pulley, 1996; Neuffer *et al.*, 1997; DTI Case Study 004, 1998].

A more promising alternative to control this type of boiler plant is to use the non-linear 'black-box' model approach to *represent* the expert operator's *knowledge* based on artificial neural networks. Artificial neural networks, with their massively parallel structure are able to map the complex non-linear relationships that exist between the input and output data. These knowledge representation block(s) can then be integrated within a framework of rules formulated from the logical decision making process of the field expert to control the combustion process. In order to successfully use a neural network, representative data over a suitable range of operating conditions *must* be made available. This data base is then used to train the neural network to represent the relationship between the desired input and output data [Jain *et al.*, 1996; Esteves *et al.*, 1998; Pal and Srimani, 1996; Boger, 1997]. The main objective of this work was thus to develop such a neural network based controller which is able to maximise the combustion efficiency whilst maintaining the pollutant emissions to acceptable levels on a pilot scale (0.75MW) chain grate stoker test facility. In addition, the research was also concerned with the development of a combustion monitoring system to infer the movement of the ignition plane on the bed, i.e. stability of combustion.

At present it is common practice for plant operators to provide high levels of excess air to ensure complete burn out of the coal. Using the minimum amount of excess air, consistent with satisfactory coal burn out will help to maximise boiler efficiency and minimise nitrous oxide formation. Thus a systematic series of experiments has been conducted over a range of load following conditions to gather information on the boiler operation at both optimum and sub-optimum conditions. During each test various combustion derivatives, such as, pollutant emissions (nitrogen oxides and carbon monoxide), the oxygen content in the flue gas, carbon in ash losses, grate surface temperature at the stoker front and a series of refractory arch temperatures were all monitored. Chapter 4 provides a detailed description of the results obtained from these experiments. The gathered data were selected and then used for the training of

individual neural network components within a suitable control strategy that mimicked the decision making process of an expert human operator off line, so that the controller can detect undesirable boiler behaviour and, based on past learning experience, decide on the necessary remedial actions. Chapter 5 provides a detailed treatment of the development and testing of the controller structure.

1.1 Structure of the Thesis

The outline of the ensuing Chapters in this thesis are as follows:

Chapter 2 – Introduces the reader to the subject of coal in general before discussing the topic of coal combustion from the perspective of conventional firing appliances. Issues that are discussed include the impact of their operation on the environment, the current legislation on emissions and the possibility of increasing use of these systems in the near future as the key motivation behind this work. This is followed by a comprehensive review of chain and travelling grate stoker development over the last half a century, reported in chronological order and highlighting the improvements that can be attained with the aid of modern equipment. The final main Section is geared towards justifying the adopted Artificial Intelligence (AI) technique to address the non-linear multi-variable control problems and also as a convenient classification means for the novel combustion monitoring device developed during the course of the work. Relevant literature in the application of AI to similar and related processes is also laid out to further supplement the discussion regarding the use of ANNs in this work.

Chapter 3 – Provides an overall description of the chain grate stoker test facility used in this work and the extensive plant instrumentation and control system employed in the experimental programme. This is followed by a description of the calibration of the coal and air feed for the entire load range of the test facility, along with the ‘near optimum’ air distribution profiles which were empirically derived for the two types of coal used in the experiments. Finally, an outline of the test procedures carried out on the pilot scale test facility and also on an industrial stoker plant is laid out in the last Section.

Chapter 4 – Discusses the results gathered from the experiments designed to investigate the behaviour of the test facility with reference to a comprehensive range of combustion derivatives. These tests had the primary objective of generating the necessary data required for the neural network training. Two distinctive sets of experiments were carried out, namely boiler response to gradual load changes at various operating conditions for ‘steady-state’ patterns and also to large load changes with two different staging profiles for transient investigation. The boiler response to the operator’s best practice was taken as the bench mark for comparison against the other test runs involving gradual load changes. The test facility’s response to large load changes was evaluated for different staging profiles, with particularly reference to flame front movement and transient carbon monoxide emission.

Chapter 5 – Describes the development of the neural network based controller and also the models of the derivatives of combustion via the use of Artificial Neural Networks (ANNs). The former involves introducing the reader to the conceptual design of the controller to minimise boiler losses before progressing into the work with feed-forward Multi-Layered Perceptron (MLP) network to construct the required modules within the proposed control strategy. This is followed by a detailed account of the on-line implementation of the developed neural network based controller on the test facility to burn two different coals and also onto an industrial scale chain grate stoker boiler. The Neural Network Based Controller (NNBC) performance is compared with the operator’s best practice and, in the case of the industrial stoker tests, with the plant PID control system. The modelling work on the combustion derivatives is appended in the final main Section concerning the development of oxygen, carbon monoxide and nitrogen oxides models using ANN as a black-box modelling tool for the stoker test facility burning Singles grade coal.

Chapter 6 - Describes the development of a novel optical monitoring device for the monitoring of the flame front movement through the inspection porthole as a means of inferring the stability of combustion. This Chapter first introduces the reader to the concept of the ignition plane prior to describing a pilot study conducted on the pilot test facility in order to evaluate the feasibility of the approach. The following Section

details the development of the sensor and its subsequent implementation onto the test facility to monitor flame front movement. A neural network classification technique was employed to analyse the data gathered from the sensor off line before its final evaluation onto the industrial stoker plant. Conclusions from the work on the combustion monitoring system are drawn in the final Section of this Chapter.

Chapter 7 – Draws the overall conclusions from the work with respect to the performance of the neural network based controller, on both pilot and industrial scale chain grate stoker fired boilers. In addition, conclusions are drawn concerning the use of the models to predict the derivatives of combustion and on the performance of the novel flame front monitoring system. Recommendations for further work are laid out in the last Section of this Chapter.

2. Literature Review

As this work spans several disciplines, this Chapter reviews the use of coal particularly its continuing role in the future, conventional coal firing appliances as a popular means of combusting lump coal, emphasising their combustion principles and requirements. This is followed by a review of the chain and travelling grate stoker development over the last half a century and the use of Artificial Neural Networks (ANNs) as a modern tool to address the monitoring and control problem of such a process in order to enhance its performance.

2.1 Coal as a Possible Primary Source of Energy for the Future

This section first introduces the reader to the subject of coal in general, what is coal, how coal was formed and its analysis and classification for commercial purposes. This is followed by a description of the evolution of coal combustion to the modern ways in which coal is utilised namely for the generation of electricity, usage in iron production and heat generation. Although currently supplying less than one third of the world's electricity supply, the enormous reserves of coal raises the question of coal possibly becoming the primary source of fuel in the future. Finally a global concern has been raised regarding the burning of fossil fuel and with respect to stationary combustion plants, the emission of green house gases. The impact in which the pollutants, namely oxides of sulphur, oxides of nitrogen and carbon dioxide, have on our environment is laid out in this Section together with the current legislative limits and ways in which these pollutants can be minimised or retained from being released to the atmosphere. Conclusions are drawn in the end of this section.

2.1.1 What is Coal?

Coal is a fossil (organic sedimentary rock) formed by the action of temperature and pressure on fallen plant debris over millions of years which has always been associated

with moisture and various amounts of minerals. Coal is composed of a complex mixture of organic chemical substances containing carbon, hydrogen and oxygen, along with lesser amounts of nitrogen, sulphur and some trace elements. It is closely linked to peat, which is considered to be its precursor, and also to natural gas and petroleum, thought to be formed by a similar process. These fossil fuels are vital natural resources for energy and within this group, coal represents by far the largest fraction of the resources and reserves.

Coal formation occurred in two distinct stages, one biochemical and the other geochemical. Variations in the plant material and the extent of its decomposition during the first stage largely account for the different petrographic components known as macerals, by analogy with the minerals in rocks. The subsequent action of differing degrees of pressure and heat over a long period of time during the geochemical stage, (much commercial valued coal was first deposited in the Carboniferous Period - 225 to 300 million years) acting on the peat like deposits, contributed to the differences in the maturity or 'rank' of the coal. In addition to the normal pressure of the overburden, pressure arising from tectonic movements can accelerate the transformation. Such additional pressures, and not merely time, are probably essential for progression to anthracite.

The 'rank' increases from lignite (less than 60 million years) through low rank coal and high rank coal to anthracite. The carbon content increases with increase in coal rank, while the oxygen and hydrogen content decreases, along with the reactivity of the coal [Grainger and Gibson, 1981]. The calorific value also increases with increasing rank accompanied by the subsequent decrease in volatile matter which is driven off by the action of heat, and the coal generally becomes stronger and harder from the effect of pressure. Occasionally the areas where coal was being formed were inundated by sea water, resulting in contamination by various salts, of which sodium, potassium, calcium, chlorine, fluorine and sulphur may be the most significant elements. Coal analysis is carried out to BS1016 on a mass basis and the results can be either 'proximate' or 'ultimate'. The results of these analysis may be presented on 'as-received', 'as-fired', 'dry-basis' or 'dry-mineral-matter-free' basis. Both methods give

the moisture and ash content of the fuel, as well as the *gross calorific value*¹ from the given sample. The difference between the two methods is that the ‘proximate’ analysis gives the combustible content of the fuel in terms of fixed carbon and volatile, whilst the ‘ultimate’ analysis further breaks down the combustible content of the fuel to its constituents, namely carbon, sulphur and hydrogen. Some form of classification is a prime necessity commercially owing to the great diversity of coal. The Seyler chart enables coal to be classified by two pairs of parameters, either by carbon and hydrogen or by volatile matter and calorific value. This system has been of great value in codifying and classifying coal properties; it is however too complex for commercial use. In simplifying coal classification, volatile matter and calorific value have generally been accepted as the basis for differentiating rank in the main coal classification system currently in use. In the classification of bituminous coals for use in coke making, it has proved necessary to introduce a second classification parameter to segregate coals for carbonisation in order to address the swelling and caking properties.

In the UK the measure of the caking properties is determined by the BS Swelling Number and the Gray-King coke type, with similar systems of greater or lesser complexity being employed in other countries [Good Practice Guide 88, 1993; Grainger and Gibson, 1981]. The methodology used to classify a coal in this system is relatively easy and cheap to perform and the parameters measured are clearly related to the main commercial use of coals [Grainger and Gibson, 1981]. Currently bituminous coal supplies most of the energy that comes from coal and over recent years, sulphur in particular, has become an increasingly important aspect of coal quality [Schobert, 1987].

¹ *The calorific value (cv) of a fuel is the quantity of heat released by the combustion of a unit mass of the fuel under specified conditions of temperature and pressure. It is important to note that the difference between the gross and net cv of a fuel, is that the gross cv is the total heat released whilst the net cv discounts the latent heat of the water vapour as being not available for useful heat transfer [Gunn and Horton, 1989].*

2.1.2 Background

Coal seams appear on the earth's surface in many places in the world and owing to its unusual appearance and combustibility, archaeologists believe that it could have been used as ornaments and possibly for heat in prehistoric times. It is not known for certain when or where coal was first used as a fuel, but some evidence suggests that it could have been in either India or China some two thousand years ago. Theophrastus, a pupil of the Greek philosopher, Aristotle, wrote in his publication *De Lapidus* around 300 B.C., described a black stone that was sometimes used by blacksmiths instead of charcoal. In fact, the term anthracite originated from the ancient Greek word, *anthrax*, used by Theophrastus to describe the so-called black stone. Marco Polo reported the Chinese burning a black stone for heating and cooking upon his return to Venice in 1295.

The first major record of coal usage in Britain dates back to the 13th century where an internal and export coal trade was established. By the 14th century, the use of coal became widespread enough that mining in Great Britain had spread through many counties in England, and into Wales and Scotland. However it wasn't until the 16th and early 17th century, that a vast increase in coal production was seen not only in Great Britain, but also across Continental Europe due to severe depletion of wood (owing to the increased demand for wood and iron). The conversion from wood to coal as the predominant energy source during the next century lead to two major discoveries, firstly the steam engine, an invention born out of the need to keep deep coal mines dry and secondly cheap iron production on a large scale by the use of coke [Schobert, 1987]. The industrial revolution was fuelled on coal, both through the invention of the steam engine and by the development of iron production by coke smelting instead of charcoal [The Open University, 1973]. During the early colonisation period of North America coal was also heavily used and coal mining played an important role in the industrialisation of the USA from the early 18th century.

The use of coal was unprecedented until the 1950's when cheap oil and gas became available, particularly in the domestic and power generation sectors. Coal consumption

switched to the utility industry for small scale process heat and steam generation which was concurrent with the industrial expansion during that period of time [Schobert, 1987]. Then in the 1970's, the Organisation of Petroleum Exporting Countries (OPEC) imposed an oil embargo. Drastic increases in oil prices dramatically illustrated to the world, the economic and political hazards of relying on an energy source for which sizeable fraction must be imported. Coal usage, which had been dormant during the 1960's suddenly revived and became an increasingly attractive energy option. In Japan for instance an increase of 25% in coal imports was registered over a 3 year period.

This also led to the formation of bodies such as the International Energy Agency (IEA) under the Organisation for Economic Co-operation and Development (OECD) in 1974 with the objective to engage in research into more effective and less polluting coal combustion devices. Today the OECD countries include some of the world's most developed nations such as USA, Japan, Canada, Australia and numerous members of the European Union, such as the UK, Germany and France [IEA Coal Research, 1993]. However the decline in oil prices during the mid 1980's again attracted global attention which resulted in a decline in coal usage. Nevertheless oil and gas supplies will one day inevitably be scarce. Today, the production of electricity by coal dominates with the production of iron coming second [IEA Statistics, 1997].

2.1.3 The Importance of Coal

The importance of fossil fuel cannot be over emphasised as the primary energy source to sustain global economic progress and improve the standard of living. Since the continuing increase of the world population is inevitable at least in the near future, it seems certain that the world energy demand will grow at least a few percent per year. The International Energy Agency (IEA) in 1997 has projected a steady growth (annual average of 2.2%) of world primary energy demand until 2010, with heavy reliance on fossil fuel (90%) to satisfy the increase of such a demand and has accepted an estimate of a 1.5 fold increase in energy consumption in 2010, using the base year of 1993 for the analysis [IEA Statistics, 1997]. Although coal is the most abundant and cheapest form of fossil fuel, natural oil and gas are currently supplying the majority of the

world's energy needs [IEA Statistics, 1997]. However, this scenario cannot last and the energy market will have to be replaced by an energy source that is abundant and can easily be extracted and utilised. Coal satisfies these requirements especially with the aid of new coal combustion technology [Grainger and Gibson, 1981]. Furthermore coal prices tend to be relatively more stable (steam coal price in 1997 was slightly lower than at 1990) than the prices of other fossil fuels, together with only a moderate rate of increase on long term contracts (periods exceeding 1 year) have the potential to motivate more use of coal [Good Practice Guide 30, 1992; IEA Statistics, 1997]. It is thought that the growth in the use of coal is inevitable in the near future for several reasons:

1. Supplies of oil and natural gas sooner or later will become increasingly scarce;
2. New processes for more efficient coal burning and conversion to synthetic fuels or chemicals will offer new options for using coal;
3. Concerns over the reliance on energy imported from politically unstable regions of the world remains;
4. The increasing development of the Third World has opened new markets for coal and has changed the focus of world coal use;

2.1.4 Environmental Impacts from Coal Combustion

Coal has always been regarded as a dirty fuel in comparison to other fossil fuels, and indeed in earlier days to wood. Although burning coal could generate valuable heat and power, the process of combusting coal can also pollute. The first noticeable irritant particularly in association with open fire combustion is smoke production which consists mainly of soot and condensed tar vapours as a result of incomplete combustion of the volatile matter [Schobert, 1987]. Until the early 1950's, smoking chimneys were usual, particularly in urban areas where coal was the primary source of fuel for both domestic and industrial use. Boilers were operated on crude grates and even then, many were hand fired with poor efficiency and dense 'pea-soup' fogs occurred in the due season [Gunn, 1989]. London holds the dubious honour of being the first to experience severe air pollution. First public complaints were raised in 1285 and again in 1288 about the deterioration of air quality resulting from the excessive use

of coal for firing lime kilns. The complaints eventually resulted in the issue of a royal proclamation forbidding the use of 'sea coal' in London. However, despite the early royal effort to reduce coal usage no real attention was seriously taken. In 1578, Elizabeth 1 complained of the smoke from coal fires used in breweries. The London Company of Brewers agreed, apparently voluntarily, to use wood as the fuel in breweries near Westminster for the comfort of the Queen [Schobert, 1987].

A large proportion of the problem originated from low level emission from domestic fires in densely populated areas and also significant contribution from industries. By around 1910, London had an annual soot fallout of 426 tons per square mile, although this appalling statistic was only one third of the annual soot fall in Pittsburgh, America, which in 1911 boasted the highest death rate in the world from pneumonia [Schobert, 1987]. The inefficient burning of coal largely contributed to the smoky, foggy atmosphere in London, as portrayed in the Sherlock Holmes fiction by Sir Arthur Conan Doyle. In December 1952 a disastrous fog settled over London, which resulted in about 4,000 deaths over a period of four days. Public outcry resulted in the Clean Air Act being passed in 1956, which was significantly redrafted in 1968 to extend control over emissions from burning liquid fuels [Gunn, 1989].

As a consequence of these acts, smoke or emission control zones were designated where dark smoke could only be emitted for limited periods, restricted emissions of grit and dust, and maximum ground level concentrations of sulphur compounds from the flue gases were set. Some areas were designated 'smokeless' zones which basically limited boiler operators to clean fuels [Good Practice Guide 30, 1992]. Having addressed the problem of smoke and dust emissions, it has since been recognised that sulphur compounds in the flue gas although dispersed with high chimneys, were being transported elsewhere subsequently producing acid rain. In addition other products of combustion have also been recognised to have adverse affects on the climate on a global scale and this has led to many countries imposing 'green policies' to address this issue.

The three major derivatives of combustion which are potentially harmful to the environment are the oxides of sulphur (SO_x), oxides of nitrogen (NO_x) and carbon dioxide (CO₂) [Good Practice Guide 30, 1992]. With respect to stationary combustion plants, carbon dioxide and nitrous oxide are the principal GHGs influenced by human activities.

The United Nation's Intergovernmental Panel on Climate Change (IPCC) has recently concluded that there is a *discernible human influence* on global climate [Houghton *et al.*, 1990]. Currently the 1990 Environmental Protection Act (EPA 1990) only deals with single or multiple boilers and furnaces with an aggregated² total net rated thermal input of 50MW or more, although a related part of the act deals with *individual* boilers and furnaces of 20 to 50MW net thermal input. However, the European Union is moving towards including small combustion plants of 1 to 50MW thermal input in its directive, in which many of the conventional stokers are within this range, but no final decision has yet been reached. The following Sub Sections describe the effects that each one has on the environment, the current legislative limits for coal fired boilers and ways of minimising the emission of these pollutants.

2.1.4.1 Sulphur Oxides

Sulphur oxides (SO_x) emission resulting from coal combustion (oxidation) is thought to contribute to one fourth of the sulphur oxides in the atmosphere. Its emission is a major concern due to its negative effect on human health (sulphuric acid coated ash particles taken into the lung can cause severe breathing problems), corrosive effects on many materials and is responsible for the formation of sulphurous acid in rain causing grievous environmental issues [Schobert, 1987]. The current legislative limits for coal fired boiler plant of net thermal input between 20 to 50MW_{th} (closest range to conventional stoker firing appliances) is 2000mg/Nm³ (milligram per Normal meter cube) or 700ppm normalised to 6% oxygen in the flue gas [IEA Statistics, 1997]. The amount of sulphur oxides emitted is dependent primarily on the amount of sulphur

² Term referring to a group of boilers or furnaces on a site where the emissions can be sent through a common stack [Good Practice Guide 88, 1993].

contained in the fuel. In general about 10% of the sulphur will be retained in the ash and the rest if not captured will be released to the atmosphere [Cooke, 1991]. The current commercial remedies includes flue gas ‘scrubbing’ using limestone to capture the emitted sulphur dioxide as calcium sulphate for larger plants ($> 50\text{MW}_{\text{th}}$) and/or using coal that has a lower sulphur content. The average British coal sold into the industrial market has a sulphur content of around 1.3% and is less polluting than heavier fuel oils. Further details on sulphur capture can be found in Section 2.3.2.

2.1.4.2 Nitrogen Oxides

Nitrogen oxides emission does not pose so much of an immediate threat as compared to sulphur oxides. It is thought that nitrogen oxides emission from coal combustion represents a fractional 5% of the total nitrogen oxides in the air. It is a contributory element towards the generic ‘greenhouse’ effect which is thought to be responsible for the global warming of the earth’s surface and also the formation of nitric acid in rain. However, the most notorious role of nitrogen oxides is perhaps in the aspect of air pollution, where NO_x causes smog formation through reactions with oxygen and hydrocarbon in the presence of light [Schobert, 1987]. The current legislative limit for stoker fired plant of net thermal input between 20 to 50MW_{th} is $500\text{mg}/\text{Nm}^3$ (milligram per Normal meter cube) or 245ppm normalised to 6% oxygen in the flue gas [IEA Statistics, 1997]. However, nitrogen oxides emission does not raise much concern in chain grates (the most popular form of stoker) owing to its natural form of primary air staging along the fire bed and in some circumstances the secondary air, although by lowering the excess air level consistent with good burnout can minimise nitrogen oxides emission [Clarke and Williams, 1992; Livingston *et al.*, 1995].

2.1.4.3 Carbon Dioxide

Carbon dioxide is not a pollutant, however concerns have been expressed that further increases of the CO_2 content in the atmosphere, resulting from additional fossil fuel combustion, might impose significant threats on the climate due to the so-called ‘greenhouse’ effect. CO_2 is more transparent to solar radiation than to the balancing outward radiation from the earth, so that increases in the CO_2 content of the atmosphere can result in a warming of the earth’s surface. Other materials, including

water vapour and dust, can also affect this radiative balance although the relative importance of these substances is not known [Grainger and Gibson, 1981]. It is believed that coal combustion accounts for 3Gt of carbon injected into the atmosphere out of the total 5Gt from fossil fuel combustion and the CO₂ concentration is undoubtedly rising slowly [Houghton *et al.*, 1990]. However this amount should be viewed against the fact that the total amount of CO₂ in the atmosphere is about 700Gt of carbon and other reservoirs (the biosphere, oceans and sediments) are thought to accommodate far more with annual reversible exchange rates between the atmosphere and these reservoirs in the order of 100Gt of carbon. In addition to fossil fuel combustion for energy, deforestation is believed to have had a large effect recently. CO₂ is an inevitable product of complete combustion, it could be removed by wet scrubbing or by absorption but this would mean a substantial cost along with loss of energy and having the problem of disposing the retained carbon dioxide. The current emphasis is on improving overall thermal efficiency by burning less fuel for the same output thereby reducing the total CO₂ produced [Good Practice Guide 30, 1992].

2.1.4.4 Smoke and Particulate Matter

Smoke primarily consists of soot and tar vapours as a result of incomplete combustion of the volatile matters. In addition to causing environmental nuisance, it is a clear indication of reduced plant performance which is more apparent in conventional stoker firing owing to the lower turbulence in the furnace chamber as compared to the pulverised fuel (pf) burner. The length of time allowed (in a basis of 8 hours operation) for 'dark smoke' emission via the use of the British Standard Ringlemann Chart (BS 2742C), is dependent on the number of furnaces associated with the stack. However, continuous emission of 'dark smoke' for more than 4 minutes or 'black smoke' for more than 2 minutes in any 30 minutes of operation is considered to be a violation [Good Practice Guide 88, 1993]. In many cases, the problems can be rectified by adjusting the plant operational parameters to suit the coal used.

Particulate matter (grit and dust) is not so much of a problem with conventional stoker firing owing to the bigger particles which can be retained with the use of a high efficiency cyclone and also to the lower combustion intensity. The most apparent threat

to health is due to the respirable size of the particles. The current legislative limit for stoker fired plant with an individual net thermal input of between 20 to 50MW_{th} is 300mg/Nm³ (milligram per Normal meter cube) normalised to 6% oxygen in the flue gas [IEA Statistics, 1997]. Practical remedies in some extreme cases would include the retrofitting of an electrostatic precipitator, although in many cases a high efficiency cyclone would be sufficient.

2.1.5 Conclusions

There are indications that coal could be used for a long period of time in the future, until the development of alternative energy source(s) that are abundant and less polluting. In order to make coal competitive in the energy market place, the process of coal utilisation must be carried out in such a way that efficiency is maximised whilst minimising the pollutant emissions. Concerns over the negative influence of human activities on the global climate has further raised the issue of improving the standards of coal and other fossil fuel combustion sources.

2.2 Conventional Coal Firing Appliances

This Section provides a little background on conventional stoker development, followed by a brief description of the various types of stoking devices available to date with emphasis on chain/travelling grate stokers since they are the most popular form of conventional firing appliances for industrial coal fired boilers. The remaining two Sub-Sections are dedicated to describing the combustion process on the grate prior to highlighting the criteria for efficient combustion on the bed. Conclusions are drawn in the final Section.

2.2.1 Background

Until about 150 years ago, coal fired boilers were fitted with large non moving grates onto which coal was shovelled directly by hand. The person responsible for feeding the

coal and trimming the fire was known as the stoker. Inevitably the coal and air distributions were poor resulting in considerable smoke emission and boiler efficiency was low [Good Practice Guide 88, 1993]. Over the years significant effort has been applied to minimise the inherent disadvantages of fixed bed stokers which were low efficiency, smoke production, ash and coal handling without having to involve excessive complication. The main improvements which have taken place were the provision of a controlled air supply to the fire bed and the development of mechanical means for feeding coal to the bed and removal of ash.

As a consequence, more efficient and controllable combustion devices resulted which reduced labour requirements. The mechanical stokers was perhaps the key feature of the evolution process and a number of basic types have emerged [Grainger and Gibson, 1981]. They were first used in water tube boilers until the 1950's (pulverised fuel firing replaced mechanical grates) and thereafter became more popular in smaller boiler types, especially shell boilers. Cheap oil and gas in the 1950's and 1960's temporarily removed the incentive for further developments in mechanical stoker firing equipment. In recent years owing to renewed interest in coal utilisation along with the availability of modern materials and equipment, more work has been devoted onto these systems.

Despite the limitations associated with mechanical stokers such as the rate of heat release per unit area and higher maintenance requirements, they possess some important advantages. Mechanical stokers are robust and simple compared to pf firing without requiring grinding (a heavy cost item in capital and maintenance), particulate emissions are relatively simple to control, modern stokers can offer high turn down ratios, with the aid of modern link materials these boilers can generally be 'banked' overnight and started the following day with ease [Grainger and Gibson, 1981]. Therefore it is not surprising that despite their long history, mechanical stokers are still widely used throughout the UK mainly for the production of process heat (below 20MW_{th}) and a few in larger water tube boilers for steam production (between 20 to 50MW_{th}) in the process and utility sectors. Currently boilers rated up to 12MW_{th} are supplied with a single stoker and between 12MW_{th} to 20MW_{th} with two stokers (each accommodating a separate furnace chamber) with multi-tubular shell boilers

dominating the market for outputs between 3MW_{th} and 20MW_{th} . However, travelling grate stokers have been fitted onto larger water tube boiler installations with individual boiler steam outputs of more than 20MW_{th} [Good Practice Guide 30, 1992].

2.2.2 Combustion Principles on Grates and the Stokers

It is vital to initiate and maintain stable combustion conditions on the bed in order to achieve high efficiency. In addition, adequate time must be allowed for a high degree of carbon burn out and also to ensure near complete combustion of the volatile matters. The latter requirement is usually met by providing extra air and turbulence at the appropriate point and by maintaining an adequate temperature. However there is an optimum level of excess air, since the sensible heat loss in the flue gas increases with the excess air. The design of different stokers vary mainly in the way fresh coal is applied to the bed, and other factors such as coal rank, size, moisture content and ash properties are also important criteria for good stoker design. Essentially there are two main principles of combustion associated with conventional coal firing devices, and almost all of the stokers that are still in use today can be classified as having overfeed or underfeed combustion principle. The sections that follow illustrates the two combustion principles and lists the main type of stokers that can still be found in considerable numbers throughout the UK [DTI Case Study 004, 1998].

2.2.2.1 Overfeed Combustion

Fresh coal is charged onto an already burning bed, a similar scene to the burning of coal briquettes or charcoal in the barbecue stove on a nice summer afternoon. The characteristics of this combustion principle are as follows:

1. The fresh charge is heated by convection from the hot gases leaving the fuel bed beneath it and also by radiation, hence resulting in rapid ignition;
2. The charge is initially heated in an oxygen depleted atmosphere, resulting in the release of volatile matter without burning which appears as smoke;
3. Coal is heated without burning hence enhancing its coking properties. Such coke may be in relatively large masses and therefore can be difficult to burn, therefore resulting in the tendency towards larger unburned material loss.

In modern stokers employing such a principle, the fire bed is usually kept thin to allow some unconsumed air to pass through the bed to burn the green coal and also the emitted volatile matter. In addition, overfire air is necessary to provide the additional oxygen needed to completely burn off the volatile. The drawback of such a system is with its coal feed facility which involves dropping of the fuel onto the grate. Any fine material present will be entrained by the gases leaving the fuel bed, and be carried forward without complete combustion. This could cause a significant thermal loss if the fuel sizing and moisture content are not properly selected. It follows therefore that such systems are only suitable for graded fuels such as Singles. Other mechanical feed systems push the coal onto the fuel bed by means of a ram. This avoids the suspension of fines in the over fire gases but has the effect of developing any coking properties of the coal due to the reciprocating action of the grate. Therefore high rank coals are not very suitable on these stoking systems [Gunn, 1982].

The most popular form of mechanical stoker, employing the principle of overfeed is the 'spreader stoker'. In this system, the feeding and distributing mechanisms continuously project coal into the furnace above a bed of either the stationary horizontal grate, dumping grate, or travelling grate, depending on the duty required from the boiler and frequency of de-ashing. Manual ash removal is a requisite for the stationary and dumping grate design, and hence is only suitable for smaller units. Fines are partly burned in suspension, while larger particles are intensely burned on the grate without agitation. The air openings in the grate surface are usually restricted to less than 5% of the total grate area to minimise the effect of relatively wide variations in the fuel bed (size distribution). In addition, the small openings help to increase the air velocity which promotes the creation of turbulence [Johnson and Auth, 1951].

There are a few advantages with the spreader stoker, namely rapid ignition of fresh charge, better response to load changes than the underfeed type (to be discussed later on). They are more capable of burning a large variety of coal at high rates (between 1.9 to 2.37 MW m⁻² hr⁻¹) Uniformity of sizing is not a vital requirement due to the rapid ignition, which also means that the fuel type can easily be changed, and the ash formed contains less clinker [Gunn and Horton, 1989; Johnson and Auth, 1951].

The main disadvantages of spreader stokers are the relatively higher particles and grit carry over into the flue gas passage due to the coal feeding nature. This is particularly true when ungraded coal is burnt, as further degradation can occur during handling, giving rise to a higher proportion of fines. This can cause a reduction in boiler efficiency due to the higher unburned fuel loss along with an increased boiler fouling rate. However this can be compensated for, to some extent, by re-firing the entrained grit from the arrestor, although such an additional measure poses additional costs. Smoke formation is more of a problem if the coal is being fed too quickly into the furnace chamber. The fuel bed distribution is not as uniform as with the underfeed travelling grate type, as the larger pieces will fall in a different spot than the smaller pieces [Johnson and Auth, 1951, Gunn and Horton, 1989].

2.2.2.2 Underfeed Combustion

This is the direct opposite of overfeed combustion, where coal is fed from beneath a burning bed. Air passes through the unignited fuel at the bottom of the bed, with which it does not react until the ignition plane is reached. The ignition process is assisted by radiation from the burning fuel above and provided if sufficient air is supplied, the volatile matters burn almost completely above the overlying fire bed. However there is no convected heat to aid the preheat of fresh charge hence resulting in a slower ignition rate as compared to overfeed combustion. Since coal is gently fed from beneath the burning fuel bed, there is no suspension of fines, and grit carry over is considerably less than with spreader stokers. Furthermore the initial burning of the coal in an oxidising atmosphere tends to inhibit coke formation [Gunn and Horton, 1989]. The characteristics of underfeed combustion are:

1. Less tendency to form smoke than with overfeed, the quantity and pattern of over-fire admission is therefore less critical;
2. It is less sensitive to fines content than overfeed stokers;
3. Less tendency to form coke than with overfeed methods using a ram feed.

Chain and travelling grate stokers have the widest application in the combustion of solid fuel for both water tube and fire tube boilers. In principle, both stokers consist of a moving grate of the endless mat type. Spacing between the assembled links of the

mat is regular and fine allowing a uniform passage of air for combustion and also to provide cooling with the high air velocity through these interstices. The travelling grate stoker is similar to the chain grate with the distinctive difference of having individual cast iron flap type louvers that are mounted freely on a rod to form the endless mat instead of small links. As the mat passes over the rear roller, the ash is discharged from the grate, providing a self cleaning feature. Large travelling grates (up to 70MW), normally have a rear arch in addition to the front arch in order to maintain a sufficiently high temperature in the rear region of the grate to ensure satisfactory char combustion.

In the case of the chain grate stokers (mainly fitted onto fire tube boilers), the actual combustion flame passes over the rear end of the grate hence performing this task. With the case of water tube boilers (mainly fired by travelling grate stokers) being larger in size, there is less constraint on the depth of the stoker windbox hence enabling a better air distribution facility, such as dampered air compartments, to be installed for improved combustion on the bed [Johnson and Auth, 1951; Gunn and Horton, 1989].

In both cases, chain and travelling grate stokers, coal is gravity fed onto the front of the stoker from a hopper. The fuel bed depth is regulated by manually adjusting the height of a guillotine door under which the coal passes on the grate. In modern chain grates, the fuel bed height (around 120mm for Smalls grade bituminous coal) is set by regulating the speed of a rotary feeder (that delivers coal from the hopper onto the grate) and the grate speed to yield a uniform bed height regardless of the load required. The correct fuel bed is then carried underneath a hot ignition arch which radiates heat on top of the freshly charged coal to release its volatile matter and subsequently to combust the char. The primary air is fed from beneath the grate, and as with the principle of underfeed combustion, smoke formation is minimal, with burning rates of up to $1.4\text{MW m}^{-2}\text{ hr}^{-1}$. Turn down ratio as high as 8:1 can be achieved, and the response to load change is fairly rapid. The stoker can also be banked on a standby basis with due care so as not to overheat the grate mat [Proctor, 1999].

In order to harvest the virtues of underfeed stokers, careful attention must be paid to the selection of fuel type, size and moisture content. The coal size distribution must be uniform, as large lumps will not burnout completely by the time it reaches the end of the grate. Correct moisture content is essential to ensure the proper combustion of fines and finally, ash content of the fuel type must exceed 5% in general (depending on the material of the link), with chrome alloy link being most tolerant (minimum of 4% ash content), to avoid any premature link breakage. In addition the ash fusion temperature must be high to avoid the formation of clinker, which would block the air passage and making ash disposal difficult. The best type of coals for underfeed travelling grate stokers are high volatile (free burning) bituminous and sub-bituminous coals that are non or weakly caking with high ash fusion temperatures. High rank coal such as anthracite is not suitable [Good Practice Guide 88, 1993].

One advantage of these appliances is that it produces very little NO_x due to its distributed under grate air [Cooke, 1991]. The simplest form of air distribution in the smaller fire tube chain grates is by the use of graded baffles. This in effect stages the air along the fire bed. Overfire air is only necessary in the case of large travelling grate stokers. Smoke formation is minimal and because the fresh coal is gently fed onto the grate, there is minimal suspension of fines, and therefore can provide a better carbon burnout than the spreaders. They are well suited to burn ungraded fuels, such as Smalls, but the type of coal used must be properly selected. These stokers are robust and well suited for fully automatic operation with the availability of automatic ash removal, coal feeding apparatus, water cooled side cheeks and in some cases automatic ignition with hot air ignitor [Butt and Pulley, 1996; Robson *et al.*, 1988]. Underfeed travelling grate stokers have been built for sizes up to 78MW (water tube boilers) but future application will probably be mainly in fire tube boilers [Grainger and Gibson, 1981; Good Practice Guide 30, 1992].

2.2.3 Combustion Process on a Chain Grate Stoker

The manner in which lump coal is burnt on most types of chain grate stoker is very similar. This section is aimed at providing the reader with an overview of the various

stages of combustion that take place on the grate in the furnace chamber of a chain grate stoker fired boiler before progressing further into the next section, which deals with the requisites for efficient combustion on the grate. It is necessary for the reader to be familiar with the concept of the ignition plane, which is one of the key parameters to monitor in order to achieve a stable and optimum combustion of coal on the grate. Details of the development of a novel ignition plane monitor is provided in Chapter 6.

A bed of burning coal with an adequate supply of primary air can be divided into three zones for illustrative purposes as shown in Figure 2.1, although in reality the boundaries between each zone are quite difficult to define as combustion takes place gradually along the length of the grate.

Stage 1 - The freshly supplied coal is passed beneath the ignition arch, the moisture content is firstly driven off as vapour by the radiant heat of the arch. As the temperature of the bed reaches 350°C or higher, the volatile matter in the coal is distilled off in the form of methane, hydrogen, carbon monoxide, carbon dioxide and other hydrocarbon gases. This volatile matter will then burn and if the primary air in this main combustion region is not sufficient, smoke will be produced. Ignition occurs on the top surface of the 'green coal' and travels downwards to the grate, reaching the grate, ideally, at about half the grate length.

Stage 2 - As the bed of coal travels further into the furnace tube, at between 1/3 to 2/3 of the grate length, combustion of both the volatile and fixed carbon takes place. The rate at which the coal burns is dependent on the rate at which it can be ignited. Stability of both the ignition arch and therefore the main combustion zone is maintained by back radiation from the burning embers beneath the arch.

Stage 3 - The remaining char is burned off and the combustion process should have ideally been completed before the end of the grate, with the ash and clinker being discharged off the rear end of the grate as the chain mat travels round the roller.

It is important to note that different types of coal will have a different bed profile on the grate. For instance, a high rank (high fixed carbon) low volatile anthracite will take longer to ignite resulting in a much longer fire bed, and since most of the heat is liberated from the bed, care must be exercised to avoid the chain mat from overheating by providing sufficient cooling air and choosing the correct type of alloy links. Conversely, if a low rank high volatile bituminous coal is used, then the bed will be relatively shorter and the primary air supply towards the end of the grate will have to be reduced to prevent heat dilution.

The ash content of the fuel burnt is also an important factor as the ash forms an insulating layer that helps to protect the grate from the intense heat in the furnace tube. Coals with ash content of between 7 to 15% are the most recommended although very often the lower limit can be extended to as low as 4% by using the correct material for the links. In fact the construction material of the links for a chain grate stoker is solely dependent on the ash content of the coal to be used [Good Practice Guide 88, 1993].

Finally, as with any combustion process the ignition factor must also be carefully taken into account to ensure stable and satisfactory combustion, and therefore the design of the ignition arch plays an important role in deciding which types of coal that can be combusted on a particular chain grate, as high rank coal will need a longer ignition arch than a high volatile low rank coal. In large travelling grate stokers for water tube boiler installations, there may be an additional rear refractory arch at the end of the grate in order to assist the combustion process due to the larger size and mass of coal on the mat [Gunn and Horton, 1989].

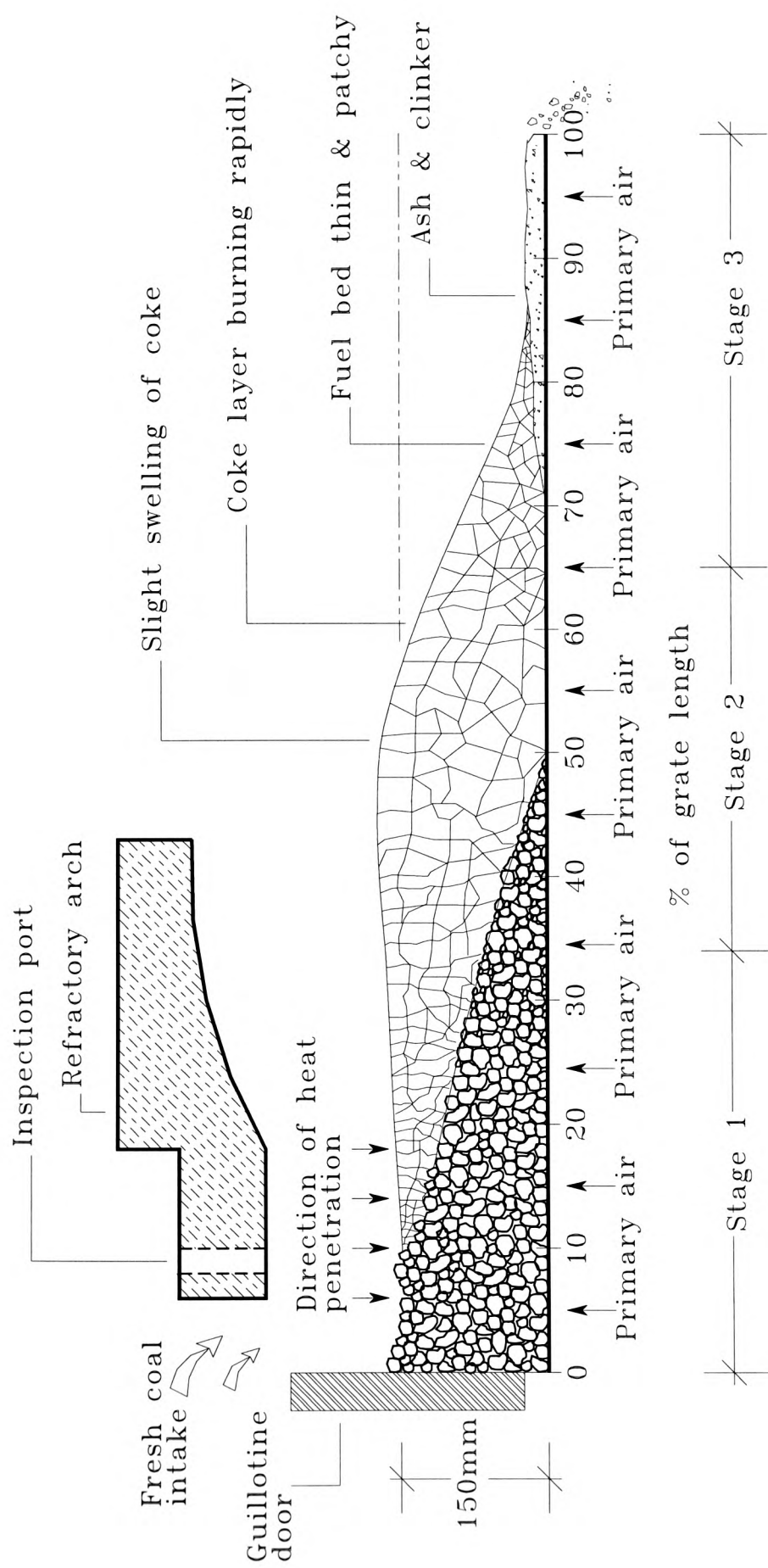


Figure 2.1 Stages of Combustion Process on a Chain Grate Stoker [Good Practice Guide 88, 1993]

2.2.4 Requisites to Efficient Coal Combustion on Chain Grates

From section 2.2.3, it can be seen that there are several conditions that must be met, in order to operate a chain grate stoker efficiently. Assuming that the stoker is in good working order and that the correct type of coal is being used (size distribution and rank) with the appropriate moisture content, particularly when burning Smalls. The remaining criteria are the correct regulation of coal and air feed in order to meet the load demand. It is vital to ensure that the rate at which the coal is being fed into the furnace chamber matches the rate at which it can be ignited, so as to obtain a bed profile similar to that shown in Figure 2.1. This in turn will ensure good carbon burnout and stable self-supporting combustion conditions.

Optimum excess air must then be provided to ensure the minimum sensible heat loss in the flue gas whilst maintaining satisfactory combustion. For bituminous coal firing, the optimum range of excess air is between 35% to 50% from the stoichiometric to give an oxygen reading in the flue gas of between 5 to 7%. Careful attention must also be given to the primary air distribution along the length of the bed to ensure proper cooling of the chain mat in addition to having good combustion [Good Practice Guide 88, 1993]. This can be achieved by the creation of baffles in the windbox or with the provision of damper(s). In the case of this project, individual air compartments to exercise more control over the air distribution. A typical breakdown of the total primary air supplied along the length of the grates (four compartments in total) can be found in Section 3.3.3.

In addition to the forced draught supply, adequate suction must also be provided via the use of an induced draught fan to ensure clean boiler operation. In situations where large load changes are frequent, it is important to alter the coal and air feed in such a way that the ignition plane movement and also the transient CO emission is minimised. Gunn (1982) asserted that on load increase the air should lead the coal feed in small steps over a period of a few minutes and vice versa on load decrease, in order to improve the combustion process following large load changes. This has been experimentally verified in this work. Further details on the staging of coal feed and air flow in response to large load changes can be found in Section 4.2.

2.2.5 Conclusions

Chain/travelling grate stokers are still the preferred means for coal fired boilers in commerce and industry. Many of its features, such as self-cleaning, robustness and safety with the aid of modern handling equipment such as pneumatic system have made them very suitable for full automation. However, the proper control of chain/travelling grates to maximise combustion whilst minimising pollutant emissions, require scrupulous set-up of the plant followed by careful manipulation of the many input variables.

2.3 Condition Monitoring and Control of Lump Coal Combustion on Chain Grates

The purpose of this Section is to highlight the possible cost savings that can be achieved by a marginal improvement in combustion efficiency on chain grate stoker fired plant where a case study is presented as an example. This is followed by a comprehensive discussion on the previous work carried out with respect to lump coal combustion on conventional firing appliances and aspects that could still be improved are identified. Conclusions are made at the end of this Section.

2.3.1 Background

Simple as it may seem to a layman, the combustion of lump coal on a travelling grate is actually a highly complex process that can be subjected to various disturbances and uncertainties if the governing parameters are not properly set up and maintained. Uniformity of the coal size distribution and the quality of the coal burnt, the fuel bed distribution over the grate and the moisture content are just a few of the major concerns of chain grate stoker users. It is normal practice for the user to rely on a commissioning engineer, who is usually external, to set up the boiler plant i.e. calibrating the fuel feed and air flow for the entire turndown range, for the particular coal type (most commercial chain grates burn Smalls grade bituminous coal, NCB rank between 709-

902) [Good Practice Guide 88, 1993; Proctor, 1999]. The fuel used will then be negotiated with the supplier to ensure reliable long term supply and consistency in both the coal quality and size distribution.

If all these criteria are satisfied then the plant is expected to perform according to specification, which would be smoke free operation with an oxygen concentration in the flue gas (those boilers fitted with long term Zirconia oxygen analyser) of between 7 to 9% at high fire, 9 to 11% at medium fire and 11 to 13% at low fire (in order to create the necessary turbulence) with satisfactory coal burnout by visual inspection of the grate ash (losses usually about 3% including riddling losses). The corresponding excess air level from the stoichiometric are between 45 and 65%, 65 and 100%, 100 and 160%, respectively for bituminous coal firing. This is usually the case for a fairly modern chain grate stoker that has been designed for automatic or semi-automatic operation, equipped with an industrial control system (in the range of £1200 including installation and commissioning) for the regulation of coal feed and air flow (with the aid of variable speed drives (VSD) or frequency inverters) to achieve the desired hot water set point temperature [Good Practice Guide 2, 1998; Good Practice Case Study 35, 1991].

However this is not the case for the vast majority of stokers, and even with modern ones, it is difficult to consistently maintain a minimum amount of excess air for good combustion whilst maintaining good carbon burnout. The usual practice is to set a high excess air level, to ensure a short fire bed to avoid live fire from passing over the grate during frequent large load changes, i.e. changing the grate speed from low to high and vice versa over a short period of time [Proctor, 1999]. In doing so, one will obviously have little carbon in ash losses, but the penalty in dry flue gas losses can be very significant, especially when the boiler plant is operated in such a manner over an extended period of time. The next Section presents the reader with the possible savings in a real case study, in terms of coal costs, if some sort of a control system could be provided to maintain the excess air level to a minimum whilst keeping the pollutant emissions at an acceptable level and also preserving the stability of combustion, particularly during frequent large load fluctuations.

2.3.1.1 Case Study - Possible Savings from an Efficiently Operated Stoker Fired Boiler

A case study in collaboration with James Proctor Limited (Lancashire based stoker manufacturer) and Her Majesty's Prison (HMP) Garth (at Leyland, Lancashire), featuring a pressurised hot water shell boiler has been investigated here for the purpose of illustration. The boiler is a 3.7MWth chain grate stoker fired boiler, supplying pressurised hot water for space heating and hot water at a set point of 120°C and a working pressure of 4 bar. The average output from the boiler during the winter months is about 70% of its maximum continuous rating (MCR) with a corresponding average oxygen concentration in the flue gas of 11%, which corresponded to a carbon dioxide concentration of 8.5%.

The following steps show the fuel savings that can be obtained by comparing the efficiency of the boiler working as it is with the boiler being controlled by some sort of a control system that is able to maintain a minimum excess air level. The procedure for calculating the thermal efficiency of the boiler is based on BS845, which considers four aspects of combustion: the heat content in the dry-flue gas; heat content in the water vapour; unburned combustibles and radiation losses [BS845 - Part 1, 1987]. The following criteria can be established for comparison: boiler loading of 5 months (at least) in a year (about 150 days); gross calorific value of coal used of 28,000 kJ/kg and fuel costs of £55/tonne [Adapted from Good Practice Guide 88, 1993].

First Case - Boiler operating at 11% oxygen (or 8.5% carbon dioxide) with a dry flue gas loss³ of 15%. Other losses have been assumed to be 8% (heat content in the water vapour, unburned combustibles and radiation losses).

Plant thermal efficiency = 100% – (15% + 8%) = 77%.

Fuel consumption/yr. = $(0.7 \times 3700) / (0.77 \times 28000) \times 3600 \times 24 \times 150 = 1557$ tonnes.

Fuel costs/yr. = $1557 \times £55 = £85,635$.

³ The dry flue gas loss can be calculated from the Siegert formula as described in BS845, Pt.1, 1987.

Second Case - Boiler operating at 8% oxygen (or 11.5% carbon dioxide) with a dry flue gas loss² of 11.5%. As with the first case, the other losses have been assumed to be 8%.

Plant thermal efficiency = $100\% - (11.5\% + 8\%) = 80.5\%$.

Fuel consumption/yr. = $(0.7 \times 3700)/(0.805 \times 28000) \times 3600 \times 24 \times 150 = 1489$ tonnes.

Fuel costs/yr. = $1489 \times £55 = £81,895$.

Hence the possible annual savings that could be achieved in this medium size stoker boiler by maintaining a minimum excess air level whilst satisfying other operating constraints such as grate temperature at stoker front and pollutant emissions is £3,740. HMP Garth has three chain grate stoker fired shell boilers (two in operation with one on standby) of the same thermal capacity, therefore the total potential annual savings are approximately £7,480.

2.3.2 Previous Research in Lump Coal Combustion

It has recently been reported in a case study published by the Department of Trade and Industry (DTI) of the UK, that a large portion of the approximately 3.2 million tonnes of coal used up annually in the industrial market sector is burned on moving grate stokers [DTI Case Study 004, 1998]. A few percent increase in operating efficiency pro-rata whilst minimising pollutant emissions would translate into huge savings both in coal costs and carbon dioxide emission. This section discusses the work that has been carried out to control such or similar processes reported in the literature and to use this work to point to areas where further improvements could be attained.

One of the very first pieces of work reported in the literature to control and regulate steam pressure production from a chain grate fired boiler was carried out by BCURA in the 1950's. The vast majority of chain and travelling grate stokers at that time were used in water tube boilers for steam production and found extensive use in power station boilers. Prior to the research into automatic control of stoker fired boilers, considerable effort was initially made into the investigation of the performance of the

stoker fired plant with respect to the property of the fuel burnt (rank, coking behaviour, clinkering properties, etc.), fines content, moisture and ash property. It was mainly due to this characterisation work that it was possible to formulate the standard practice that is still used today [Hayward, 1951; MacDonald and Murray, 1955; MacDonald and Murray, 1953; Gunn, 1952; Rawlings *et al.*, 1962]. Most of the early work involving the control of chain grate stokers were carried out by BCURA and the National Coal Board (NCB), which included, building automatic handling systems for coal and ash, which is one of the pre-requisites for an automatic combustion plant. Other major design features included water-cooled side cheeks, which removed the need for manual slicing, [Thurlow, 1962; Harris *et al.*, 1962].

The main improvement in the control of the combustion process on the grate was perhaps the way in which the primary air can be uniformly distributed over the length of the grate despite the varying bed resistance to air flow. An excellent example of such work was reported by Rolfe (1961) of BCURA, which involved the creation of baffles in the windbox under the grate for the even distribution of primary air, to avoid high excess air escaping through the back of the grate and thereby improving the efficiency. These baffle systems are still used in many stokers in operation today with the aid of modern link design to ensure uniformity of the air distribution despite the varying fuel bed resistance along its length [Rolfe, 1961; Good Practice Guide 88, 1993].

However, there were no mechanisms by which to regulate the amount of primary air supplied to meet the varying characteristics of the fuel bed, in particular fluctuation in the fuel's calorific value in order to consistently maintain a low excess air level. That is, the air/fuel ratio is fixed and changes in the air flow to meet the changes in steam pressure will be followed accordingly by the grate speed according to pre-set values for the specific type of coal burnt. The success of these systems relied heavily on the relatively small turndown range (3:1 ratio) to meet the load demand and consistency of the fuel used (quality and size). Steam pressure regulation was carried out via the use of a proportional controller which regulated the firing rate in direct proportion to changes in the steam pressure [Rolfe, 1962].

With the advancement of modern linear control theory in the late 50's, effort was seen in applying frequency response techniques to study and develop a model (transfer function) of these systems in line with the theory but was not successful [Ogata, 1990]. An interesting paper written by Baker and Loveridge (1965), describes this very effort that had been conducted on a chain grate stoker test facility. Numerous assumptions, such as constant feed-water inlet temperature and small amplitude of the waveform, etc.) were made and the authors selected the most linear working range of the boiler. Heat input to the system (coal and air feed) was varied sinusoidally over a range of frequencies (period varying from 2 minutes to 127 minutes) and the response (heat output) was continuously measured. Their conclusions were that the dynamic nature of the stoker fired shell boiler (lump coal combustion stage) was imperfectly understood and unclear, despite the numerous assumptions that were made. However the results obtained that characterised the steam generation stage (heat input to the steam drum and steam output) was more promising with a response curve resembling that of a first order system (within operational limits). This led to the work published by Marks (1987) which described the principles for regulating the steam pressure from a chain grate fired shell boiler by the introduction of the so-called 'make up' pressure in order to keep a constant steam pressure in the vessel following step or ramp changes in the steam demand. This work was primarily based on the knowledge of the dynamics of the steam generation stage but with little description of the combustion stage. No experimental data was provided to verify his simulation results [Baker and Loveridge, 1965; Marks, 1987]. Despite the claims of success, no report or case studies have been made during that era on the application of these appliances in fully automated operation.

Further research into coal combustion on these small to medium size plants involving conventional combustion devices then laid dormant for more than a decade before the oil embargo, imposed by OPEC in the 1970's sparked new interests in lump coal combustion. This was due to the availability of cheap oil and gas during that time and also the escalating interest in using pf burners in power station boilers owing to its rapid response and the relatively more uniform nature of combustion. Thus the market for conventional stokers shifted from mainly large water tube boilers to small and

medium size installations, primarily shell boilers, and found extensive use in process industries [Schobert, 1987]. During the 1960's until the end of the 1970's, the research effort into coal combustion was mainly focused on pulverised fuel firing, where the earliest flue gas oxygen monitoring work was reported. This was attributed to the sheer operating costs involved in these power station burners and the growing concerns on nitrogen oxides emission from stationary fossil fuel combustion sources, particularly coal, due to the inherently high nitrogen content in the fuel [Luxl, 1962; Ounstead, 1969; Sarofim and Flagan, 1976].

Other work involving the inclusion of carbon monoxide readings via the use of an infra-red carbon monoxide sensor, into the overall control strategy/advisory panel was reported to optimise the combustion efficiency in these large water tube boilers by maintaining a suitable excess air level without jeopardising emissions [Anson *et al.*, 1971; Birkby *et al.*, 1973; Ormerod and Read, 1979; Ormerod, 1981]. At this time the work on the fluidised bed combustor was intensified and the first commercial installations established, therefore dominating the attention for cleaner coal combustion technology [Grainger and Gibson, 1981]. This reduction in work on stoker firing was also reflected elsewhere. For instance, in the U.S. the last major research conducted on stoker development technologies was carried out in the late 70's, with the main objective of minimising pollutant emissions whilst optimising thermal efficiency [Langsjoen, 1981; Langsjoen *et al.*, 1981].

The revival of interest in coal combustion in the late 1970's, accompanied by increasing pressure from environmental groups and subsequently the government calling for reduced emissions of the so-called 'green house' gasses (carbon dioxide and nitrogen oxides) inevitably motivated more work into ways to minimise these emissions whilst satisfying production. An early example of such an investigation can be seen in work published by Giammar *et al.* (1979), where the nitrogen oxides emission characteristics were studied by burning a range of coals on a pilot scale underfeed stoker. The experimental results showed that the fuel nitrogen conversion to NO for a travelling grate stoker was exceptionally low (8-15%), compared to spreader stokers (12-20%) and pf firing systems (30-50%), under excess air firing conditions

[Giammar *et al.*, 1979]. These results were in agreement with an earlier survey on NO_x emission control technology from stationary combustion sources published by the Massachusetts Institute of Technology, where Sarofim and Flagan (1976), found the lowest emissions from coal fired units were from underfeed stokers, although the cause was not clearly understood and the fundamental parameters that influence the formation of NO_x were not well defined.

Pollutant formation from fossil fuel combustion, in particular, NO_x emission from coal combustion sources was identified as one of the key areas for future research, as quoted by Smoot and Hill (1983). It was not until the mid 1980's when thorough investigations of the parameters that influence nitrogen oxide (the main constituent of the general term NO_x) formation in underfeed stokers was conducted. One piece of work in this area was by Starley *et al.* (1985), where empirical studies were conducted on a pot furnace test facility (to simulate the combustion process on travelling grate stokers) burning bituminous coal with a typical burning rate of 1.3MW/m². In this work, the amount of primary air was varied from fuel rich (34% below stoichiometric air) to fuel lean (40% above stoichiometric air) conditions on the fire bed but maintaining a constant overall stoichiometry of 1.45 (primary and secondary air, which is typical in bituminous coal firing). It was found that the bed region stoichiometry is the governing parameter that influences exhaust NO emission. By decreasing the bed region stoichiometry to 44% below stoichiometric air, a 67% reduction in NO emission was achieved. This was due to the favoured formation of nitrogenous intermediates, ammonia (NH₃) and hydrogen cyanide (HCN), in the fuel rich zone rather than NO, which are not as easily oxidised to NO when the secondary air was added [Starley *et al.*, 1985]. Although in a practical system the overfire air is only about 10 to 15% of the total air flow supplied, if used, the nature of the primary air distribution in the windbox essentially stages the combustion along the length of the bed, (Section 2.2.3).

Another interesting report on the effort to minimise pollutant emission in order to comply with tightening legislation, in this case particulate emissions, was the one reported by Prizzi (1985) on large travelling grate stokers used in power station boilers. The report described the author's effort to improve the combustion process of the

travelling grate stoker by addressing the key issues of underfeed stoker firing in tackling the problem with excessive grit emission. This paper highlighted the importance of understanding the fundamental requirements in stoker firing before considering optimising or improving the performance of such burners. Many of the improved aspects which were initially overlooked by the author were in fact fundamental issues, such as the size distribution of the coal used (coal with a highly inconsistent size distribution giving rise to the problem of excessive grit carry over) with the correct bed height (about 150cm), good working condition of the stoker, regulation for the correct coal feed rate with near optimal excess air level and uniform air distribution on the bed. Many of the issues brought up by Prizzi (1985) have since been well documented in a good practice guide published by the Energy Efficiency Office under the Best Practice Programme for the use of chain/travelling grate stokers [Good Practice Guide 88, 1993].

In the field of applied combustion, Smoot and Hill (1983) stressed the need for more research into clean and efficient combustion of low grade liquid and solid fuels with reductions in pollutant emissions through combustion control. With respect to underfeed mass burn stokers, the key area that can still be improved is the primary air distribution along the grate, as this is the main parameter that controls the rate of combustion, and hence the pollutant formation. Changes in coal and primary air feed (firing rate) to meet the load demand should be carried out in a such a manner that will help to ensure stable combustion, as described in Section 2.2.4 [Gunn, 1982].

This was also recognised by other authors such as Hadvig (1989) who described a customised gas sampling system installed on a 12.5MW_{th} travelling grate stoker with a view to optimising the combustion process in the various zones along the bed length by regulating the amount of air flow to these zones (5 individual zones). In this work both the oxygen and carbon monoxide level of each of the zones (just above the bed) were continuously measured, and the primary air regulated to maintain a desired level of oxygen and carbon monoxide. However, the general applicability of this is difficult as these probes need to be situated low enough to sample the gaseous species before being mixed with gases from adjacent zones and are therefore subjected to high

working temperatures and contamination from particles ejected from the fuel bed. This would inevitably incur high maintenance costs, in addition to the high costs of installing a reliable long term CO sensor. However, it does prove from an academic perspective the advantages and benefits that could be gained if the excess air level could be regulated to meet the combustion need of the various sections of the bed, without jeopardising emissions and would certainly improve the combustion efficiency (as illustrated in the case study of Section 2.3.1.1).

In addition to the task of achieving good control over the combustion process, the aspect of complete automation of the stoker plant is also vital to ensure competitiveness of these devices in the market with oil and gas burners [McHale, 1988]. Since coal is a relatively more difficult fuel to deal with, there are a few prerequisites that must be made available before any automation can take place. These issues were addressed by Robson *et al.* (1988) of NEI International Combustion Ltd. who highlighted the growing effort by manufacturers to automate such devices. The main criteria quoted by the authors for automation were automatic ignition, burnback control, self-cleaning and an ignition plane control system. The chain grate stoker was nominated to be the most suitable candidate in this study to meet these criteria. Self-cleaning feature, relatively higher flexibility with various coal types and robustness were just a few of the virtues of the chain grate stoker that attracted the authors attention. Water cooled side cheeks were utilised for the automatic clearing of slag formation at the base of the stoker arch (indeed they are widely used in modern chain grate stokers today) [Good Practice Guide 88, 1993; Butt and Pulley, 1996; Proctor, 1999]. Hot air from an electrical fan was used as an automatic ignitor to initiate the combustion process on the stoker. This hot air ignitor was activated by a timer to ignite the freshly supplied coal before commencement of normal operation when a suitable arch temperature was reached (700°C).

In the aspect of burn-back sensing and prevention, the authors used thermocouple sensors and a burner management system or set point controller to deal with possible burn-back. A better solution now available would perhaps be the Proctor's fire break unit. This utilises a gap between the hopper and the grate to ensure that no possible

burnback can occur [Good Practice Guide 88, 1993; Proctor, 1999]. Robson *et al.* (1988) did not control the primary air to maintain an adequate excess air level for the coal feed, except to assist with the proper set-up of the fuel and air throughout the turndown range via the use of a long term Zirconia oxygen analyser [CODEL, 1998; Land Combustion, 1998]. For the control of the ignition plane, Robson *et al.* (1988) suggested the use of a 'dead plate' as a means to control the ignition plane but no mention of automatic control was given. Depending on the type of coal burnt, the dead plate (an adjustable plate to ensure that the air in the front section is just enough to maintain the desired location of the ignition plane) was adjusted accordingly to achieve the desired result.

However, this will not be able to deal with fluctuations in the fuel bed distribution that could occur during normal operation. This could result in poor combustion on the bed but not being reflected in the overall oxygen concentration in the flue gas unless a boiler operator is present to do make further adjustments. Gunn and Horton (1989) identified that oxygen trimming has yet to be fully developed for lump coal combustion due to the possibility of uneven burning on the bed. In fact no published work up to the early 1990's has been found on the application of oxygen trim control to a stoker fired boiler. A monitoring and control device that could ensure ignition at the correct location would provide greater confidence in an on-line control system (both to the regulation of the firing rate and fine tuning of the combustion air). The other possible alternative is to use a long term carbon monoxide sensor, but for small to medium size installations, the capital costs of installing such analyser is difficult to justify. The cost of a long term infra-red carbon monoxide sensor is around £7,500 as compared to a long term Zirconium cell oxygen analyser which is about £2,500 [CODEL, 1998; Land Combustion, 1998]. No literature on the use of carbon monoxide in an overall control strategy for optimising the air/fuel ratio for lump coal stoker firing is available to date, highlighting the reluctance of users to make such an investment.

The 1980's was also an era when much combustion modelling work was undertaken. These modelling studies resulted in a better understanding of the coal combustion process and gave researchers the opportunity to demonstrate their ideas in computer

simulation packages. However despite all the effort on the mathematical modelling of coal combustion processes, much work is still required before they could be used in a control system and so far no successful practical application of such a model has been reported for lump coal combustion on chain grates. An excellent review report on coal combustion modelling, presented by Smoot (1984) listed the deficiencies of the models at that time and quoted:

“model development has not reached the point where significant use is made in process development for coal utilisation”

[Smoot, 1984, pg. 229].

This review of fossil fuel combustion modelling included fixed or slowly moving beds, fluidised and suspended beds, always with an emphasis on the gasification aspect of combustion [Smoot, 1984]. Many authors, according to Smoot (1984) focused their modelling effort on the radiative heat transfer in the furnace but did little to describe the reaction and flow processes. When in fact the accuracy of the radiative heat transfer analysis hinges on the ability to predict the complex chemical and physical processes that govern the concentration and size of particulate [Sarofim and Hottel, 1978]. Smoot (1984) further concluded that no model specifically for the direct combustion of coal on stokers could be identified. Even for the modelling of fixed beds (gasifiers), the processes were complicated by the fact that:

“the possibility of layers accumulating around the large, slow moving particles, by gaseous flow in porous media of changing particle size and shape, by changing oxidisers (oxygen, carbon dioxide, water vapour), by inter particle effects such as pore diffusion, by larger particle sizes and particle temperature gradients, and by changes in the rate controlling processes for char consumption”

[Smoot, 1984, pg. 236].

Finally Smoot (1984) identified the following areas that still require attention:

1. Modelling of direct combustion processes, such as moving grate systems;
2. Modelling of pollutant formation processes;
3. Comparison of model predictions with detailed real experimental data;
4. Incorporation of more governing process parameters into a well documented and evaluated code for further evaluation.

Recently Hobbs *et al.* (1992, 1993) published another review of fixed bed coal gasification and showed that improvements have been obtained with respect to the modelling of such processes, but require numerous measurements (such as the pressure profile along the length of the bed in order to have a better bed void fraction/factor for the model calculation) from the plant, therefore rendering the whole process, particularly for the small to medium size stoker combustion plants, unjustifiable. Other authors such as Gupta and Lilley (1987), emphasised the need for more complicated fluid dynamics and turbulence flow studies with the aid of new and more powerful computing facilities, in order to increase model accuracy and reliability. In addition, both experimental and theoretical studies are required as the turbulent flow through a bed of lump coal is less predictable than the relatively more uniform combustion of a pf burner. In addition, long term effects on the heat transfer surfaces in the plant (boiler/combustor) due to corrosion, erosion and also slagging are even more difficult to model and predict. This is due to the fact that the rate of attack is dependent not only on the chemical composition and temperature of the process fluids and materials of construction but also on parameters such as velocity, flow aerodynamics and geometry of the system [Gupta and Lilley, 1987].

Field work investigating the slagging properties of various fuel properties has been investigated by authors such as Sanyal and Williamson (1981) and Kautz *et al.* (1983) in order to provide guidelines and the right type of coal to be used in order to minimise the fouling and corrosive effect. In this respect, the standard industrial practice is to operate the boiler as efficiently as possible with the recommended grade of coal and should the flue gas temperature throughout the turndown range have increased significantly over a long operating period, soot blowers would be used to clean the

smoke tubes. This cleaning exercise is generally carried out as part of the boiler house maintenance work every year [Gunn and Horton, 1989].

The 1990's have seen more effort being expended to improve combustion on chain grate stokers and the majority of it has been dedicated to the reduction of pollutant emissions in particular nitrogen oxides and sulphur dioxide. This research effort was primarily due to the tightening of legislation on pollutant emissions from stationary combustion sources imposed by the European Commission under its 'Large Combustion Plants' Directive in 1988 [EEC Directive 88/609, 1988; Clarke and Williams, 1992]. As described in Sub-Section 2.1.4, although there are no single chain grates with a duty greater than 20MW, a few chain grate stokers can be combined to obtain a net thermal input greater than the 50MW limit, therefore placing such modular systems under Her Majesty's Inspectorate of Pollution's (HMIP) approval. In addition, possible legislation could be imposed in the near future by the European Commission on small to medium size installations (1 to 50MW_{th}) and this has also prompted more attention on improving the firing method of these relatively conventional coal firing devices [Clarke and Williams, 1992; Good Practice Guide 88, 1993].

Many of the techniques used to control pollutant emissions, were in fact derived from commercial remedies for pf fired and fluidised bed burners. These include modification of the combustion conditions in the furnace and/or post combustion flue gas treatment. Since the emission of nitrogen oxides is inherently low in underfeed stokers, it poses very little concern and so far only a few practical examples (in large travelling grate stokers) have been reported which involve flue gas recirculation into the furnace by mixing with the incoming air. This effectively dilutes the oxygen concentration and lowers the peak temperature, although care must be taken to determine the optimum amount of recirculation without losing valuable efficiency. Nitrogen oxides reduction of up to 20% using this technique have been claimed [Cooke and Pragnell, 1989; Cooke, 1991].

The general practice however, is to consistently provide a low excess air level without having to lose efficiency in incomplete combustion therefore reducing both thermal

and fuel NO_x formation [Clarke and Williams, 1992; Coal R&D Project Summary 057, 1996]. An air supply regime that provides relatively lower nitrogen oxides emissions has been suggested by Livingston *et al.* (1995) for chain/travelling grate stokers. This work involved staging of the primary air with low excess air level in an underfeed pot furnace test facility [Livingston *et al.*, 1995; Babcock International, 1995]. Livingston *et al.* (1995) also emphasised the need for a better air distribution facility along the bed, and for conditions similar to those of industrial underfeed stokers (burning rate of 1.4MW/m², 40% excess air with 15% of the total combustion air as secondary air), nitrogen oxides emissions of 400-450mg/Nm³ or 195-220ppm, dry at 6% oxygen, have been claimed. This level of nitrogen oxides emissions can be considered low, as the most applicable legislative limit (boiler plant of net thermal input between 20 to 50MW_m) is 245ppm, dry at 6% oxygen for stoker boilers [Livingston *et al.*, 1995].

Sulphur dioxide emission poses more of a problem than nitrogen oxides in stoker firing since 90% of the sulphur content in the fuel is emitted as sulphur dioxide during combustion, with the rest being retained in the ash [Cooke and Pragnell, 1989]. The standard commercial practice for large travelling grate stokers, is to use fine sorbent such as limestone (<100µm), injected into the flue gas stream to capture the emitted sulphur dioxide as calcium sulphate [Ekman and Wang, 1990]. The sorbent can be either injected directly above the fuel bed in the furnace zone, where the gas temperature is around 1100°C (suitable conditions for sulphur dioxide capture), or in the exhaust flue gas duct in humidified conditions (mixing the sorbent with water) in order to maximise sulphur dioxide retention [Cooke, 1991; Toole-O'Neil, 1990]. These techniques may yield fairly good results (40-60% with the in furnace sorbent injection, and 40-80% with the flue gas treatment) but there are also many associated problems with it. On top of the high costs involved in retrofitting the necessary equipment (e.g. ducts, pumps, fans, higher duty dust collector, sorbent preparation and injection equipment), the fine size of the sorbent significantly increases the dust burden, can cause fouling and undesired deposition within the boiler. Furthermore, fine sorbent injection technique can have implications on the ash handling equipment and its subsequent disposal [Cooke, 1991].

Following the need to develop a cheaper solution for sulphur dioxide capture, other alternatives have also been investigated by authors such as Ford *et al.* (1991). These authors demonstrated the addition of grate sorbent to a fixed grate furnace simulator and also to a commercial underfeed stoker-fired unit. This work involved using fine limestone ($<0.5\text{mm}$), coarse limestone (1-3mm) and pelletised coal/limestone mixture (calcium to sulphur ratio of about 2:1 with 2% cement as binder and 10% of limestone sized below $100\mu\text{m}$), together with bed cooling using flue gas recirculation and the addition of water to empirically study the effect of these parameters in sulphur dioxide abatement. They have claimed that 31% of sulphur dioxide reduction was attained in the commercial stoker unit when burning a pelletised coal/limestone mixture without excessive ash melting (limestone reduces the ash melting temperature) [Ford *et al.*, 1991; Ford *et al.*, 1992]. Such work could provide a modest amount of sulphur dioxide abatement with minimal modification to the plant and therefore could help small to medium size chain/travelling grate stokers to comply with future legislation.

As the key parameter that influences sulphur dioxide emission is the sulphur content in the fuel, it was not the purpose of this research to study sulphur dioxide emissions. But rather the correct regulation of the firing rate to meet the required load demand with good combustion efficiency, whilst keeping nitrogen oxides and carbon monoxide to acceptable levels. The most recent work in sulphur dioxide abatement in lump coal combustion, is currently underway involving the Coal Research Establishment (CRE) in Cheltenham, and also various academic institutions across Europe with financial support from the European Coal and Steel Community (ECSC) on the addition of petroleum coke (a highly reactive fuel with little ash content) in solid fuel briquettes with anthracite and limestone/dolomite as a cost effective means of sulphur dioxide abatement [CRE, 1994; ECSC, 1996]. Sulphur retention of 42% has been claimed by the CRE (1994) when burning briquettes of petroleum coke, anthracite and dolomite.

As the increase in energy demand is inevitable in the near future, with coal being the most abundant source of raw fuel, emphasis has been strongly placed upon combustion engineers to enhance the performance of coal burners without adversely affecting the environment [Zimmermeyer, 1992]. With respect to small and medium size boilers (1

to 50MW_{th}) emphasis has been on improving the overall combustion efficiency by addressing the fundamental aspects of underfeed stoker combustion and increasing the awareness of users to the available technology and expertise to enhance the performance of these plants. These include the selection of the right type and size of coal, having suitable wetness, correct operation of the stokers, the use of portable sensors (long term Zirconia analyser for the larger installations) to provide an indication of the excess air level, retrofitting of variable speed drives (VSD) for better air control and the use of modern digital controller(s) [Fuel Efficiency Booklet 17, 1994; Good Practice Case Study 35, 1991; Good Practice Guide 2, 1998].

The effort to increase awareness in the UK is clearly reflected in the strings of publications by the Department of the Environment to address the efficient use of coal fired boilers [Good Practice Guide 88, 1993; Good Practice Guide 30, 1992; Fuel Efficiency Booklet 17, 1994; Good Practice Case Study 35, 1991; Good Practice Case Study 352, 1997; Good Practice Guide 2, 1998]. Full automation of a chain grate stoker boiler is much more common nowadays with the aid of pneumatic coal and ash handling devices, the use of Proctor's fire break unit and also the availability of long term oxygen sensors to enable the commissioning engineer to quantify the performance of the plant [Proctor, 1999]. Long term Zirconia oxygen analysers are available with moderate prices (approximately £2,500, 1998 price) and could motivate prospective users to install such a device to assist the plant operator in maintaining a good combustion efficiency with a short payback period.

With respect to further research and development into the control of industrial coal fired boilers, the Department of Trade and Industry (DTI) of the UK has engaged in various joint research programme with the British Coal Utilisation Research Association (BCURA) and Coal Research Establishment Limited (CRE) with financial support from the European Coal and Steel Community (ECSC), and in applying artificial intelligence techniques to the on-line condition monitoring and control of chain/travelling grate stoker fired boilers [Neuffer *et al.*, 1995; Neuffer *et al.*, 1996; Coal R&D Project Summary 051, 1997]. One such piece of novel work was carried out by Butt and Pulley (1997) in processing digitised images of the fire bed with an

Artificial Intelligence (AI) technique (using an artificial neural network) to classify the combustion behaviour on the fire bed. It was found that the developed on-line classification Artificial Neural Network (ANN) was able to recognise the various digital images of varying light intensity, to deliver an accurate judgement as to the combustion conditions on the bed.

Other authors such as Neuffer *et al.* (1995, 1996) opted for a hybrid rule based system in which the conventional Proportional and Integral (PI) process variable control loops, such as the flue gas temperature, refractory arch temperature and excess air level, were integrated to function within a rule based framework devised from experienced plant personnel. Much of this work was focused on the modelling of the combustion process on the grate for the purpose of formulating the appropriate control strategies in a simulation environment [Neuffer *et al.*, 1996]. The hybrid controller was implemented on-line and claimed to be able to maintain the near optimum level of excess air even in the presence of disturbances [DTI Case Study 004, 1998].

2.3.3 Conclusions

The continuing development of chain/travelling grate stokers particularly over the last half a century has yielded the robust machine in use today. However, the aspect of combustion air control has been identified as a prime area for improvement. In addition, various aspects of combustion modelling are still in need of attention.

2.4 Artificial Intelligence (AI) Using Artificial Neural Networks (ANNs)

Over the last decade or so there has been a staggering surge in applying AI and Knowledge-Based (KB) control techniques to real life problems with encouraging success and showed promise for the future with the development of new AI tools along with the growth in computing power. Work in this respect is spread across many disciplines and includes the fossil fuel combustion process (DTI Case Study 004, 1998;

Lu, 1997), wastewater treatment (Esteves *et al.*, 1998; Boger, 1997; Wilcox *et al.*, 1995), metal cutting (Silva *et al.*, 1997), medical diagnosis (DeClariss and Su, 1993), financial stock forecasting (Yoon *et al.*, 1994) and manufacturing (Huang and Zhang, 1994; Noguchi *et al.*, 1993), to name only a handful.

It is in general, an empirical approach with little theoretical support and the potential for generalisation from one application to the other is almost non-existent [Neuffer *et al.*, 1997]. The success of its use stems from the tailoring of available techniques to a particular application or task with the aid of the human expert(s) in co-ordinating the flow of information to and from modules (knowledge bases) by formulating the correct set of rules. Some of the key areas in the broad AI issues cover the use of ANNs, application of knowledge expertise, machine learned control and the aspect of condition monitoring [McGhee *et al.*, 1990]. Currently these areas are rapidly being grouped together at the conceptual level into what is known as 'intelligent control' [Harris *et al.*, 1993].

The main thrust of intelligent control is attempting to incorporate the positive aspects of human experts whilst avoiding the elements of fatigue, inconsistency and unreliability associated with its human counterparts [Harris *et al.*, 1993]. However, it must be stressed here that the work carried out in this research (parallel to those in the relevant literature) involved using the AI tools to address an engineering problem that carried more emphasis on the practicality, simplicity and reliability aspects of the solution rather than the more academic nature of AI application as reported by many mathematicians, non-linear control theorists (in itself a broad and diversified area with a narrow window of applications) and researchers alike.

The use of AI techniques in this work can be very well justified from the complex non-linear lump coal combustion process on the grate with the added practical difficulties involved in manipulating the many parameters involved in controlling such a process, as described in the earlier Sections of this Chapter. Moreover the problem of 'smoothing' the transient during fluctuating load following conditions (one of the main

objective of the investigation) can *only* be addressed empirically based on intuition, past experience and field knowledge [Chong *et al.*, 1997; Neuffer *et al.*, 1997].

Many of such ‘intelligent control’ techniques involve the use of ANNs, which in itself has gained much popularity and attention over the last decade. In fact it is the major contributor to the crude term ‘intelligence’ in the broad context of AI control. The term ‘intelligence’ refers to the neural networks ability to *learn* from examples and *store* the experience which can be used to deduce/infer the outcome of new or incomplete information presented to the network through parallel distributed computation. The ANNs computation mechanisms differ from conventional computer programming which are typically stochastic, heuristic and associative. Connectionist models as sometimes referred to, represent input/output mappings $f:U \rightarrow Y$, where U is the input space and Y is the output space, which can be multi-dimensional. This is in agreement with other definitions of an intelligent system, whereby the estimation of mappings f , are based on experiential evidence [Harris *et al.*, 1993]. Therefore, ANNs are well suited to situations where sufficient information/data can be gathered (for the ANNs training) and where the use of linguistic rules to interpret the outcome of the complex non-linear process is almost impossible.

The main use of ANNs currently are in the area of data classification, system identification and discrete time decision making with strong indications that it will play an increasingly important role in the future of intelligent control systems [Pham, 1994; Huang and Zhang, 1994; Harris *et al.*, 1993]. It is a promising field of many ideas and in practice, is best approached by an applications orientated method based on plant knowledge and experience.

The Sub-Sections that follow provide the reader with a general background to ANNs, including a brief historical review before progressing to describe the principles of ANNs operation with emphasis on two of the most popular types of neural networks also employed in this work, namely the feed-forward Multi-Layered Perceptron (MLP) and the Learning Vector Quantisation (LVQ) network. A survey on the application of ANNs to complex industrial plant/processes is provided in the following Section, that

serves as an overview of the current status of ANNs design and utilisation focusing on the subject of coal combustion. Finally conclusions are drawn in the last Section.

2.4.1 Background on Artificial Neural Networks (ANNs)

Significant advances have been made in developing new ‘intelligent’ systems able to deal with the imprecision and uncertainty in the real-world, and ANNs are one of the key component of this approach [Pal and Srimani, 1996]. Inspired by biological neural systems, ANN technology attempts to mimic some of the core features of its biological counterparts namely fault tolerance, inferencing capability and learning ability. It is a massively parallel system (processing of vast amount of information) consisting of large numbers of simple processing elements (neurons) that imitates some of the organisational principles believed to be used in the animal brain [Jain *et al.*, 1996]. Recently, it has provided researchers from many scientific disciplines with an impetus in the form of exciting new tools and techniques that have taken the realm of possibility into a new horizon.

This exciting new field has experienced three periods of extensive activities. The first peak in the 1940’s was due to the pioneering work by McCulloch and Pitts (1943) in modelling the function of a biological neuron followed by Hebb (1949) who postulated the learning technique that made a profound impact towards the future development of the field. The second phase took place in the 1960’s, very much attributed to the concept of the ‘Perceptron’ (predecessor of the modern MLP network) and the learning algorithm of Rosenblatt (1962) followed by the work by Minsky and Papert (1969) revealing the limitation of the single layer ‘Perceptron’ network. The learning scheme of Rosenblatt (1962) could not solve problems which require the construction of *multi-layered* ‘Perceptron’ networks in order to deal with complex non-linear problems. As a result ANN research lapsed into stagnation for almost 2 decades. Since the 1980’s renewed interest motivated more work into the development of neural network architecture and the associated learning scheme. Among the many who contributed to this resurgence include:

1. Hopfield (1984) who introduced the recurrent neural network architectures;
2. Rumelhart and McClelland (1986) on the popular back-propagation learning algorithm for feed-forward Multi-Layered Perceptron (MLP) network or more commonly known as the back-propagation network;
3. Kohonen (1989) for work on associative memory for unsupervised learning network for feature mapping.

In the recent years, ANNs have been applied to address real life problems where new corporations dedicated towards the commercialisation of such technology have emerged [Bailey and Thompson, 1990]. In the UK, the Department of Trade and Industry (DTI) has created a web-site (DTI NeuroComputing Web, 1998) in their effort to encourage ANNs implementation to industry. It covers practical issues concerning the application of ANNs, highlighting many useful aspects such as the feasibility, costs, design, planning and provide pointers as to commercial consulting entities, as well as the range of available software and hardware currently available. However it is believed that the field is still in its infancy despite the colourful history and the much celebrated success, and much more work will have to be done before this field can realise its full potential [Zurada, 1992].

2.4.2 Principles of Artificial Neural Networks

Artificial Neurons - A fundamental aspect of ANNs is the simple non-linear processing elements which are essentially simplistic models of neurons in the biological brain. An excellent example of a single artificial neuron is the one which was first modelled by McCulloch and Pitts in 1943 and even today, many of the underlying principles are still employed [Demuth and Beale, 1995]. An engineering interpretation of the McCulloch and Pitts neuron is shown in Figure 2.2.

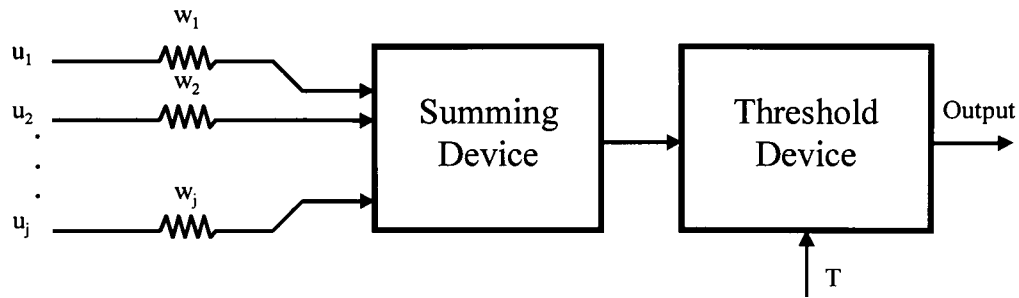


Figure 2.2 McCulloch and Pitts Neuron Model

The model of the artificial neuron computes the weighted sum of its input signal (u_1, u_2, \dots, u_j are voltages and w_1, w_2, \dots, w_j are the resistances set by the variable resistors) and if the sum is greater than the threshold T (voltage comparator), the model would generate an output of 1, otherwise an output of 0. Mathematically this can be represented as;

$y = f\left(\sum_{j=1}^n w_j u_j - T\right)$, where f is the unity step function at 0, w_j is the weight associated with the input u_j (j from 1 to n), T is the threshold limit and y is the final output of the neuron model.

The authors have proven that, in principle, if the weights (connection strength) of a group of the neuron models are suitably chosen, it is able to perform universal computations. This idea was subsequently pursued by Rosenblatt (1962) who formulated the first automatic weight adjustment mechanism for a collection of such neuron models. In fact the direct descendent of the early McCulloch and Pitts neuron model is the 'Perceptron' element used in the back-propagation network where the activation curve can take the form of linear, sigmoid or Gaussian distribution functions [Demuth and Beale, 1995].

Learning Rule - Hebb (1949) postulated that if two neurons are activated synchronously then the connection strength between the two neurons is increased. Mathematically the Hebbian rule can be expressed as;

$w_{ij}(t+1) = w_{ij}(t) + \eta y_j(t) u_i(t)$, where $w_{ij}(t+1)$ is the connection strength between two neurons at the next time step, y_j and u_i are the output of neurons j and i respectively, and η is the learning rate.

An important feature of the Hebbian rule, is that the learning mechanism is performed locally i.e. changes in the connection strength is solely dependent on the activities of the two parent neurons. This is a universal concept adopted by many types of neural network architectures in use today, despite their differences in network topology, computational element (neuron) characteristics and learning rules (ways in which the connection strength is modified in response to an objective function).

Network Architectures – ANNs can be grouped into two categories based on the network connection architecture, namely feed-forward networks and recurrent networks. In the feed-forward network, neurons are organised into layers where information is passed from the input to the final output layer in a unidirectional manner whereas in recurrent networks, feed-back connections within the network either between layers and/or between neurons can be found [Jain *et al.*, 1996]. In general, feed-forward networks are *static*, they are capable of mapping the given set of inputs to the corresponding outputs i.e. the output is independent of the previous input and output of the network. Recurrent networks on the other hand are *dynamic*, meaning the output at time instant t , is dependent on the previous output or state of the neurons within the network as a result of the feed-back paths. An excellent introductory material on artificial neural networks, particularly the various neural network architectures, can be found in the publication by Jain *et al.* (1996).

Learning – In general the learning process in an ANN involves updating of the network weights and/or architecture in order to efficiently perform a particular function. Very often the network must learn from the given examples by iteratively adjusting the connection strength in the network so that its performance is enhanced with training. ANNs learning can be broadly classified into *supervised* and *unsupervised*. Supervised learning as the name implies, requires a teacher to pair each

input vector to the network with a target vector representing the desired output. When an input vector is introduced, the network proceeds to calculate the output, and the error (between the target and the output) is often used to modify the weights according to an adopted learning algorithm that tends to minimise the prediction error. The training input vectors are passed sequentially through the network and errors are calculated followed by weight adjustments for each training iteration, until the error for the entire set of training vectors reaches an acceptable level (as specified by the designer) [Demuth and Beale, 1995; Jain *et al.*, 1996; Pal and Srimani, 1996].

Unsupervised training requires no target vector for the training input vectors presented to the network, hence, no comparisons are done to predetermine the ideal responses. The training set consists solely of input vectors. The training algorithm modifies the network weights to recognise vectors that are consistent. Hence the training algorithm essentially extracts regularities and correlations in the input data patterns and adopt the network's future responses to the recognised patterns accordingly. In this way, often used paths in the network connecting both the source (input features) and destination neuron are strengthened [Hebb, 1949]. Upon the completion of network training, it can also be used to recognise unseen data patterns by virtue of the ANNs generalisation ability (to a certain extent). It is these special features of learning and generalisation that contributed to the robustness of ANNs and also its effectiveness through inherent parallel operations. The following two subsections introduce the reader to the two types of ANNs employed in this research work, namely the feed-forward Multi-Layered Perceptron (MLP) network and Learning Vector Quantisation (LVQ) network.

2.4.2.1 Supervised Learning - Feed-Forward Multi-Layered Perceptron (MLP) Network

The most popular type of neural network comes from the family of feed-forward networks, known as the Multi-Layered Perceptron. The feed-forward MLP network can be trained with the popular error back-propagation learning rule [Rumelhart and McClelland, 1986]. The learning paradigm utilises a gradient descent method which adjusts the initial weights assigned to the network, by an amount proportional to the partial derivative of the error function with respect to the given weight. In the interests

of brevity, the detailed mathematical analysis of the back-propagation algorithm is omitted here. More information on this can be found in Jain *et al.* (1996), Demuth and Beale (1995) and Zurada (1992). The number of elements in the input and output layer are solely dependent of the number of features/attributes associated with the input and output vectors, whilst the neurons in the middle layer(s) are generally subjected to empirical evaluation. The back-propagation learning rule is a typical supervised learning procedure and is as follows:

1. Initialise the weights of the network (usually up to three layers), at random values between 0 and 1;
2. Present input vectors together with the desired target to the network;
3. The network then proceeds to calculate the output based on the input vectors presented, and then compares this output with the target, to evaluate the error;
4. Adjust the weights of the network using the error back propagation algorithm to improve the overall network performance so as to achieve the desired target;
5. Repeat step 2, 3 and 4, and calculate the sum square error of the network;
6. If the sum square error of the network is within an acceptable range, then terminate the training process, if not, go back to step 2 [Jain *et al.*, 1996].

The feed-forward MLP network can be applied to most real-life problems [Demuth and Beale, 1995]. This can be attributed to the simplicity of its use in addition to incorporating the virtues of ANNs, being robustness and the fast computational speed. Figure 2.3 shows a typical network topology, which consists of an input layer, a hidden layer (for internal representation of the relationship between input and output data), and finally an output layer. As the complexity in the functional relationship between the input and output data increases, more neurons in the hidden layer(s) will be required.

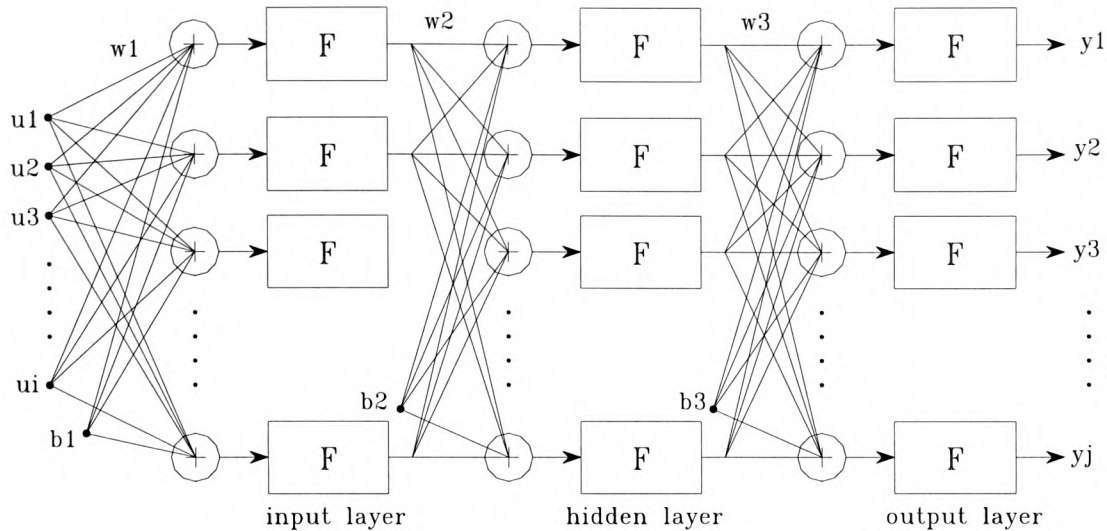


Figure 2.3 A Generalised Diagram of a 3-Layer Feed-Forward MLP Network [Demuth and Beale, 1995]

Where u and y are the input and output vectors of the network architecture, F is the transfer function of the processing elements (neurons), w and b are the weight and bias matrix for the three layers (denoted by 1, 2 & 3) associated with the network.

2.4.2.2 Unsupervised Learning – Competitive Learning Network

Unlike the feed-forward MLP network (in which multiple output neurons can be activated simultaneously), ‘Competitive’ neurons compete with each other for activation. As a result, only a single output neuron in the competitive layer is active at any particular instant. This phenomenon is known as ‘winner-take-all’ learning and such learning has been found in biological neural networks [Zurada, 1992]. Competitive learning is often employed to cluster input data, where similar patterns are collectively grouped together based on data correlation and represented by a single winning neuron. During the competitive learning process, only the weight vectors associated with the winning neuron are updated. Such learning is unsupervised, and the learning procedure can be summarised as follows:

1. Initialise weights to small random values and set the initial learning rate;
2. Present input vectors with a pattern β , and evaluate the network outputs;
3. Select the neurons which weight best match the input vectors;

4. Update the weights of the winning neuron, with the Kohonen (1989) learning rule;
5. Decrease the learning rate by a fractional amount;
6. Repeat steps 2 to 5 until the change in weight values is less than a specified threshold or a maximum number of iterations is reached [Jain *et al.*, 1996].

The most popular form of Competitive learning is Learning Vector Quantisation (LVQ) employed for data compression, speech and image processing [Jain *et al.*, 1996]. The structure of the LVQ network bears close resemblance to the standard feed-forward MLP network and consists of two layers. The first layer is a competitive layer, which learns to classify input vectors as described above where training is performed in an unsupervised mode. The second layer transforms the competitive layer's classes into target classifications defined by the user in binary form [Demuth and Beale, 1994]. The structure of the LVQ network is as shown in Figure 2.4. A rule of thumb is to use more competitive neurons than the possible input patterns to enable the competitive layer to create sub-classes for the desired target through the use of the linear layer.

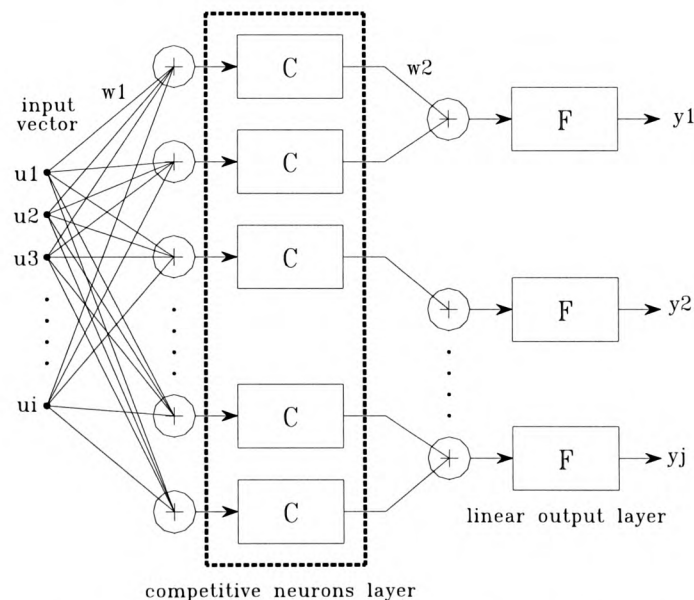


Figure 2.4 Learning Vector Quantisation Network Structure [Demuth and Beale, 1995]

Where u and y are the input and output vectors of the LVQ network, F is the linear transfer function which translate the competitive layer's output to the user specified

binary targets, w_1 and w_2 are the weight matrices associated with the two layers and C denotes the competitive neuron in the first layer.

2.4.3 Literature on Related Artificial Neural Networks Applications

As the discipline in which ANNs have been applied to is immensely diverse, the cited literature here focuses on the application of ANNs to areas more closely related to the research aims. This comprised of identification of non-linear processes (the modelling work on combustion derivatives), data pattern classification (the novel flame front monitoring system and LVQ network classification) and the use of ANN models within a rule-based framework for empirical process control (development of the neural network based controller). It is worth mentioning here that the use of ANNs in lump coal combustion on grates reported in the literature is extremely limited, therefore in this Section references were made on other types of complex industrial processes (large pf, oil and gas fired systems, wastewater treatment and chemical processes) which have received a similar application of ANNs in order to provide a more comprehensive review.

One of the early use of ANNs was in pattern recognition as reported by Venkatasubramanian and Chan (1989), who used the classification ability of ANNs for *multiple* process fault diagnosis (difficult to address using the traditional fault-tree diagnosis) for a chemical process in a petroleum refinery plant. The authors highlighted the advantages of the hybrid ANNs in a rule based framework over a pure Rule Based Expert System (RBES) when dealing with numerous possibilities of faults (symptoms) and the associated diagnosis (equipment malfunctions) which included the ANNs salient classification ability in high dimensional space and their generalisation capability even on partially corrupted information. They have also found that the standard feed-forward MLP network with more than one hidden layer did not significantly assist in improving the prediction accuracy of ANNs whilst counterproductively increased the computing time. An important conclusion from their

work which was parallel to the findings in this research was that ANNs performed reasonably well in generalising unseen data that are similar to the training set, whereas they fail for novel scenarios which were significantly different from what the neural networks were trained upon. This was an example of early work in combining ANNs and a knowledge-based system to form a hybrid intelligent structure for complex real-life industrial problem. The ability of ANNs in recognising complex non-linear patterns from the given examples with fast computational speed was also exploited by many other workers such as Sinnasamy *et al.* (1990) and Shaw (1990) for the on-line detection of multiple sensor failure and multi-variable alarming respectively, in a process control system.

Gutmark *et al.* (1990) reported the use of feed-forward MLP networks to model the behaviour of a propane gas burner in an effort to derive a control strategy for the closed-loop control of the burner by investigating the chemiluminescent emission of CH as an indicator of good combustion and black-body emission from soot particles as the reverse. Standard three layer MLP networks were used as the 'black-box' model structures with the backpropagation learning algorithm to represent the static (non-time varying) characteristics of the burner when subjected to varying frequencies and amplitude of the fuel flow with respect to the derivatives of combustion (the average chemiluminescent emission of CH, OH radicals and black body emission from soot particles). Therefore the two inputs to the networks (the author used the term 'emulator') which were the frequency and amplitude the fuel flow and the single output was each of the combustion derivatives respectively. Gutmark *et al.* (1990) also quoted that a sufficiently large envelope of accurate training data must be made available for the networks training in order to obtain a satisfactory representation of the actual system. This statement demonstrated that although ANNs are claimed to be able to see through noisy and incomplete data, the only means to exercise confidence over the predictive capability of the ANN models, is to carefully select data (to suitable accuracy) from a sufficiently large operating envelope gathered using the correct sampling frequency.

The use of an optical imaging sensor in conjunction with ANNs was also demonstrated by Allen *et al.* (1993) on a laboratory scale liquid fuel burner (heptane-air) test facility. A standard three layer MLP network trained with data gathered from the process and was found to be able to classify partial data from the imaging sensor and deliver an accurate prediction of the discrete level of energy release rate (reflected by the OH emission pattern in the primary flame zone). The output from the neural network classifier was used to maximise the combustion process by manipulating the fuel feed depending on the error between the actual rate of energy release to the desired target. The ideal output from the neural network classifier according to Allen *et al.* (1996) was either 0 or 1, but since the MLP network does not provide such a clear classification boundary, an interrogation module was required. The authors opted for a time averaged maximum over 4 sampling period (100 seconds) to determine the exact level of heat release. In this respect, a supervised classification neural network (such as the LVQ network) could be more appropriate for the task of discretely classifying the digitised images which would eliminate the need for a rule based interrogation module [Demuth and Beale, 1994].

Ribeiro *et al.* (1993) described their computer simulation work using two feed-forward MLP networks for the modelling of an industrial gas fired kiln and proposed a control strategy by utilising the inverse model of the plant in a simulation environment which they claimed to be successful. The inputs and outputs of the plant model were fuel/air flow rate and flue gas/product surface temperature respectively in an effort to stabilise the temperature profile within the kiln to a set point in the presence of disturbances (by adding a noise signal to the output of the mathematical model, which was adopted as the 'actual' process in their simulation script). Their approach hinged on the use of the 'inverse' model (feeding the output of the process to the network as input and vice versa) of the simulated kiln to function as the forward loop controller which was developed using data (for both training and testing purposes) gathered from a heavily simplified mathematical model of the actual plant. No real data was provided to supplement the claim of success due to the high running costs of the plant, and is one example that highlights the limited applicability of the relatively more academic control strategies in dealing with complex industrial control situations.

It is also the author's conviction that since no real data can be generated from the 'difficult process', then their approach should not be based upon the use of ANNs since one of the main pre-requisites for such an approach is the availability of such information. Nevertheless, in parallel with the findings of this research project and the remarks by Gutmark *et al.* (1990), Ribeiro *et al.* (1993) emphasised the need to train the ANN modules to a wide enough span of the system's operating conditions gathered using an appropriate sampling time in order to enhance the generalisation capability of the ANNs.

With respect to industrial scale coal combustion plant, Reinschmidt and Ling (1994) described a simulation study with the standard feed-forward MLP networks where the authors constructed a NO_x model and a feed-forward controller for the 'near optimum' settings of the input variables using real data gathered from a pulverised fuel (pf) burner for power plant boilers. As only steady-state NO_x emission was considered, these two networks were essentially static models, performing a mapping tasks based on the given inputs (parameters associated with the operation of the burner, such as air/fuel damper positions and feed rates and oxygen in flue gas) to the desired output (NO_x) and vice versa for the forward loop controller. In the simulation environment the two networks were cascaded in order to maintain the desired NO_x set point under representative operating scenarios, namely faulty equipment such as the absence of one of the overfire air and fuel dampers (due to maintenance work) or *interpolating* the emission of NO_x (at 80MW_{th}) from the training load ranges (from 50 to 106MW_{th}). Computer simulation results demonstrated that the cascaded ANN models were able to represent the underlying relationship between the input and output data and the authors claimed that it could be used as an on-line advisor to more inexperienced plant personnel.

The work reported by Reinschmidt and Ling (1994), demonstrated the feasibility of using a static ANN model trained to represent the 'near optimum' settings of the input parameters to function as a 'forward loop' controller that can be used to interpolate unseen intermediate loads, as a simple open loop controller for a complex industrial plant. Given that a feedback loop can be made available to supply the controller with

information as to the behaviour of the combustion process in the burner (such as using the oxygen concentration in the flue gas), then adjustments on the input parameters can be performed to enhance the integrity of the control strategy. However it is the author's conviction that open loop stability of the pf burner system should not be an issue when implementing such an empirical control approach.

A more recent study adopting the open-loop control strategy was reported by Saha *et al.* (1998) who described the use of a feed-forward MLP network to model the 'inverse' dynamics of a gas fired boiler for steam production. The 'inverse model' was constructed by using the plant output (steam pressure, drum water level and steam flow) as inputs to the MLP network and employing the plant input (gas flow rate, air flow rate and feed water flow rate) as the output from the neural network. The training data was gathered from the 'near optimum' operation of the plant PID controller in tracking the steam flow following changes in the steam header pressure and drum water level as requested by the plant personnel over a suitable working range (steam pressure from 80 to 110 bar) and conditions. The developed neural network was used as a simple feed-forward controller (taking the plant response and delivering the appropriate input settings), and off-line test results with unseen data (also from the plant) have shown that the neural network was able to represent the underlying relationship between the input and output data.

Another report on the application of ANNs to the control of large power plant was by Eki *et al.* (1997) who reported a computer simulation of a fossil-fuel fired power plant (due to the stability criteria and running costs of the plant). A 3-layer MLP network was used to map the non-linear relationship between the possible load patterns and the corresponding optimal fuel input setting (taking into account the 'dead' time of the process). Simulation results have indicated that the derived neural network controller was able to minimise the boiler temperature fluctuation (less than $\pm 5^{\circ}\text{C}$) which in turn helped to maintain a better steam production for the turbine generator.

By virtue of the ability of ANNs to represent complex input/output relationships, it has also been successfully used in identifying the complex dynamical behaviour of

numerous industrial processes. One recent report of the application of ANNs to dynamically model a non-linear process was reported by Berger *et al.* (1996), where the authors used a standard 3-layer MLP network to model the hydrodesulphurisation process of atmospheric gas oil as a function of the variables associated with the bench-reactor that they used. Their work addressed the need for more robust models of such processes which was hindered by the complexity of the process and lack of experimental data. In this respect, the field share a similar fate with modelling of coal combustion on grates particularly in the gasification aspects where mathematical modelling of the process is hindered by the complex kinetics of the combustion process as reported by Hobbs *et al.* (1992, 1993). Berger *et al.* (1996) stressed the need to gather a sufficiently large and accurate data-base regarding the process to be modelled in order to ensure a better representation of the theoretical function.

An interesting paper by Boger (1997) reports the author's field experience in applying ANNs to model industrial processes. Three case studies were provided to illustrate the success stories with the use of ANNs and emphasised that the developed models were better at interpolating than extrapolating. It must be stressed here that although ANNs can be successfully applied to model complex non-linear processes, the parameters of the developed model have *no physical* meaning and hence makes the 'black-box' model *very* application specific. Also in many industrial cases the required data-bases are not so readily available due to costs and the available measurements. These two are the major inhibiting factors of the ANNs approach, which according to Boger (1997) need to be strongly emphasised, as the success or failure of a neural network application essentially hinges on them.

A similar view was also expressed by Guo *et al.* (1997) who used standard 3-layer MLP networks to estimate the parameters required by a mathematical model of a batch feed atmospheric fluidised bed reactor, using steam as the fluidising medium to predict the production of methane (CH_4), carbon monoxide (CO), hydrogen (H_2) and carbon dioxide (CO_2). The authors claimed that the neural network estimators (a group for the pyrolysis model and the other for the char gasification model) can *only* deliver a similar estimation to the training data gathered from the atmospheric fluidised bed

reactor (using lignite and anthracite). The combination of the 'first principles model' and the neural network estimator have been claimed to be satisfactory compared to the actual plant data for two sets of operating conditions (one for lignite and the other for anthracite) in which the neural network estimators have been trained upon. Further details on the identification/modelling of non-linear processes using ANNs can be found in Section 5.4.

In the aspect of 'intelligent control' of real-life processes using ANNs, Esteves *et al.* (1998) have shown that standard MLP network was found to be the most suitable candidate from a range of ANNs for the control of a laboratory scale anaerobic digester to digest textile wastewater. The back-propagation networks were trained off-line using actual plant data gathered over a range of operating conditions namely steady-state, changes in feed (load) and sensor failures (a frequently encountered problem in large scale wastewater treatment plant). Test results have concluded that the developed neural networks were able to suggest sensible changes in the control variables such as load dilution and bicarbonate alkalinity to maintain optimum reactor operation. A standard MLP network has also been used for the on-line control of the level of bicarbonate alkalinity (to counter the acid production by the micro-bacterial population) in a fluidised bed reactor in the presence of disturbances (such as a sudden increase in the organic feed strength) [Wilcox *et al.*, 1995].

More recently the use of AI techniques particularly through the use of ANNs have also been extended to include the control of the coal combustion process in recognition of the increasingly tightening legislative limits on pollutant emissions whilst increasing combustion efficiency [Radl, 1999; DTI Case Study 004, 1998]. One such recent study involved the use of an ANN classifier to determine the impurities and ash forming species in coal burnt in a pf power station boiler. Due to the inherent parallel distributed computation of ANNs, the neural network classifier was able to quickly and efficiently determine the unwanted vital elements in the fuel burnt [Salehfar and Benson, 1998]. The authors claimed that the approach was promising and has the potential to save coal-fired boilers considerable costs in dealing with ash problems. Another parallel approach was adopted by Yin *et al.* (1998) who used a feed-forward

back-propagation neural network to predict the ash fusion or softening temperature of coal ash based on the ash composition data. The motivation behind the authors work, was to reduce the effect of boiler fouling by minimising the effect of clinker formation in large coal-fired power plant boilers. The authors claimed that the AI approach using a backpropagation neural network was easier to implement and utilised with better accuracy than the conventional techniques after training [Yin *et al.*, 1998].

Other workers such as Reifman and Feldman (1998) opted to use the recurrent network (having feed-back paths within the network to enable internal representation of time-dependent information) to model the dynamic behaviour of NO_x formation from a pf fired boiler, using the control variables (burner tilt position in the superheat and reheat furnace and excess air level) and employed a feed-forward MLP network to map the target NO_x level, load and current NO_x level to the setting of the control variables. The two MLP networks were trained with data gathered from a purposely designed experiment and simulation results involving a cascaded arrangement of the two networks have shown that the approach could be feasible for on-line implementation.

2.4.4 Conclusions

From the relevant literature, it appears that Artificial Intelligence (AI), particularly through the use of Artificial Neural Networks (ANNs) has been widely applied to a variety of industrial processes. The popularity of its use stemmed from the ability of ANNs to extract the relationship from a priori knowledge, its potential to generalise on unseen or partially corrupted information and robustness. In general, this technique involves the careful selection of meaningful examples gathered from sufficiently large operating conditions by the field expert, in order to enable the ANN to perform a specific function. On-line learning of these modules (continuous adaptation) in general was avoided in order to prevent the neural networks learning about ‘undesirable’ behaviour of the process. Very often these neural network ‘modules’ are embedded within a framework of rules also formulated by the field expert in order to enable the ‘intelligent controller’ to enhance the performance of complex industrial processes.

3. Chain Grate Stoker Boiler Test Facility, Stoker Boiler Operation & Test Procedures

The Chapter begins by outlining the main features of the stoker test facility and also the comprehensive range of plant instrumentation and control system employed for the purpose of the experimental procedures. An overview of the requirements for good operation of the chain grate stoker boiler is then provided before a detailed account of the combustion calculation for the stoker test facility for the two grades of coal burnt along with the air distribution profile is laid out. The last main section of this Chapter lists and briefly describes all the experiments carried out on the test facility to first, gather information regarding the boiler response to both gradual and large load changes under various operating conditions and subsequently to test the developed neural network based controller on the test facility and also onto an industrial stoker plant.

3.1 Plant Description

The principal features of the two pass chain grate stoker fired shell boiler were a furnace tube, a reversal chamber and a smoke tube heat exchanger. The stoker was designed as a scaled down version of a commercially available chain grate and can be operated at combustion intensities of up to 1.4 MW/m^2 which was similar to those found on larger chain grate stokers. Since the aim was to automate the operation of the plant, some modern features were also included into the stoker test facility. These were:

1. Water cooling facility was fitted at the base of the stoker refractory arch, more widely known as water cooled side cheeks, in order to prevent slag formation;
2. Coal delivery was achieved by regulating the rotational speed of a rotary valve and the grate speed, hence eliminating the need for the use of a guillotine door to maintain the fuel bed height, also known as the fire break unit;
3. Automatic de-ashing was carried out by the use of a screw feeder that transferred the wet ash through mixing with water prior to disposal, from the ash chute to an

ash collection bin situated outside the plant house. The ash was immediately mixed with water to prevent any unburned carbon in the ash from being further combusted (ash samples were used to determine the actual loss in combustion efficiency in terms of unburned combustibles in the ash at steady-state) and also to make the task of removing the ash easier.

These three new features can now be found in many modern stokers, which are aimed at semi or fully automatic operation after plant start up. The primary combustion air was supplied via a variable speed forced draught fan and an induced draught fan was provided to maintain a slight suction in the furnace chamber. Figure 3.1 illustrates the stoker test facility, the cooling water circuit for the extraction of heat contained in the hot flue gas in the furnace tube, reversal chamber and smoke tube. The ensuing Sub-Sections provide further details of the test facility which can be divided broadly into the coal feeding mechanism, combustion air supply, chain grate stoker and the two pass shell boiler and cooling water circuit.

3.1.1 Coal Feed Mechanism

Fresh coal was transferred on demand, from an external storage bunker of two tonne capacity, located outside the boiler house, into the mini hopper via a screw feeder. The amount of coal in the hopper was automatically maintained by the use of an electrical switch that activated the screw feeder whenever the coal level fell below a pre-set level. When running the test facility at its MCR of 0.75MW, the amount of coal consumed within a 10 operating hours day was roughly 1200kg. Therefore the external storage bunker was replenished of its coal supply once every one and a half working days. Inside the boiler house, coal was gravity fed onto the grate by regulating the speed of a rotary valve, whilst the fuel bed height was maintained to a constant level by manipulating the grate speed. The two motors speed were monitored by using an electronic tachometer mounted directly onto the motors drive shaft controlled by a dual loop industrial digital controller.

Such a coal feeding feature can be found in modern chain grate stokers, and is known as the Proctor 'fire break unit' [Proctor, 1999]. This feature eliminates the risk of 'burn back' which can occur in conventional stokers that employ a guillotine door to maintain the fuel bed height. Undesirable movement of the ignition plane towards the stoker front was further prevented by a dead plate fitted underneath the grate near the stoker front, which stops any primary air from leaking towards the front. Burn back occurs when the ignition plane moves toward the stoker front faster than the rate at which fresh coal is being transported into the furnace chamber.

The stoker test facility was commissioned to burn Smalls grade coal (National Coal Board rank code 802 - 12.5 to 25mm in length) but in order to overcome the problem of handling Smalls, which could easily be further degraded in the screw feeder, Singles grade coal (National Coal Board rank code 802 - 25 to 38mm in length) was fired in all the test runs except one [Francis and Peters, 1980]. This occurred in the final stage of the work where Smalls was used to test the capability of the neural network based controller to cope with burning a different grade coal. When operating at MCR of 0.75MW with Singles, the coal feed rate was 120kg per hour with a rotary valve and grate speed combination to give a bed height of roughly 150mm. Following the rule of thumb which dictates that the bed height should be six times the diameter of the top size particles [Gunn, 1982]. It follows therefore, that the bed height for Smalls was roughly 100mm. The bed height was maintained to the respective levels for Singles and Smalls, for the entire range of operating loads tested in the stoker boiler operation (0.3, 0.4, 0.5 and 0.6MW).

The rotary valve, which sat at the bottom of the hopper, consisted of a cylindrical drum on which metal chains were strapped and when the drum rotated, coal carried on the chains was allowed to fall and at the same time the chains were free to swing and clear themselves of any attached pieces of coal. Figure 3.2 below provides an illustration of both the usage of a guillotine door on conventional stokers, and also the 'fire break' system on modern stokers.

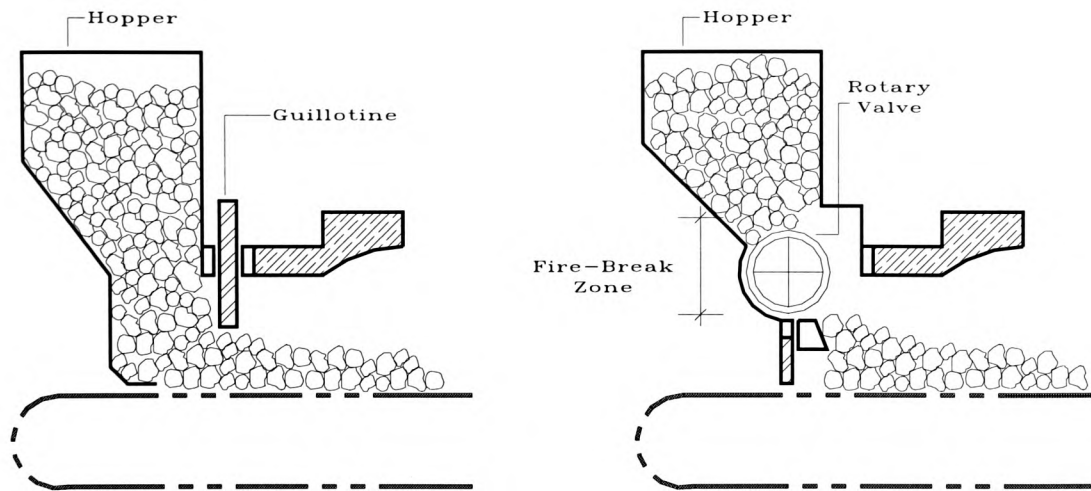
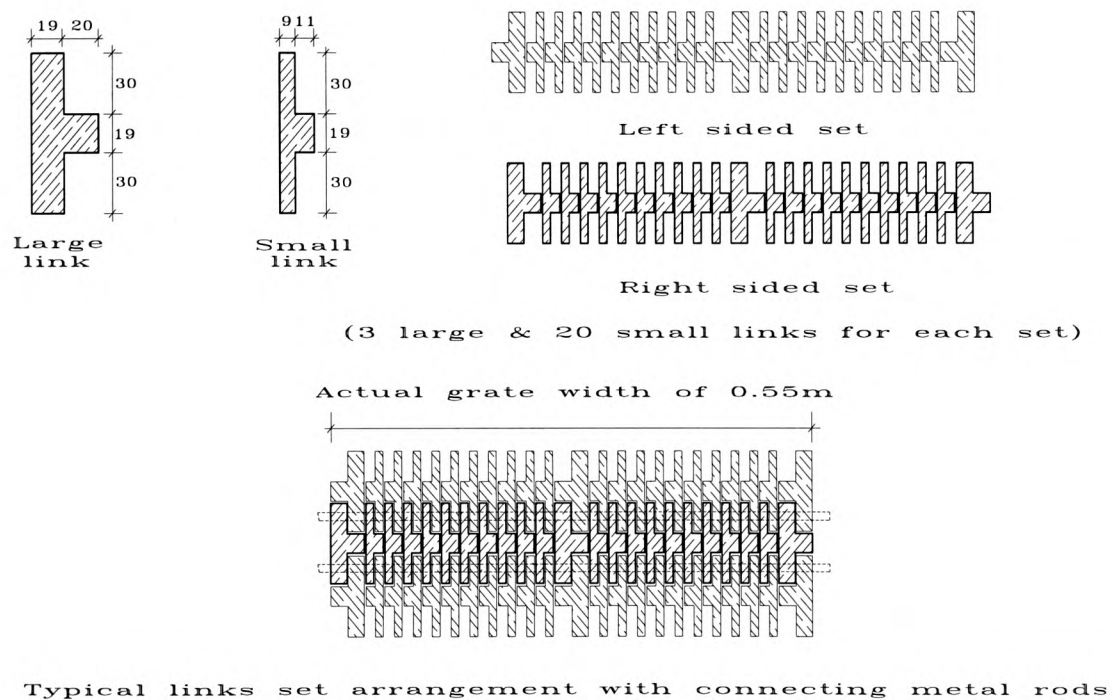


Figure 3.2 The Guillotine & Fire Break Assembly [Good Practice Guide 88, 1993]



Note: The chain mat consisted of 33 left sided sets & 33 right sided sets

Link geometry dimension in mm

Figure 3.3 Plan View of Link Geometry, Link Set Arrangement & Chain Mat Assembly [CTDD, 1995]

The grate was constructed from small chrome alloy cast iron links, which were assembled together with metal rods to form an endless mat as shown in Figure 3.3. The geometry of the grate was designed to dissipate heat absorbed from the hot surface (exposed to the burning embers) efficiently by the primary air provided from underneath the grate. In addition, the geometry also minimised the quantity of small pieces of coal (riddling) that would otherwise escape through the grate. The aim of a regular and fine spacing between links was to create a high air velocity for better penetration into the fuel bed so as to promote better air distribution along the entire length of the grate.

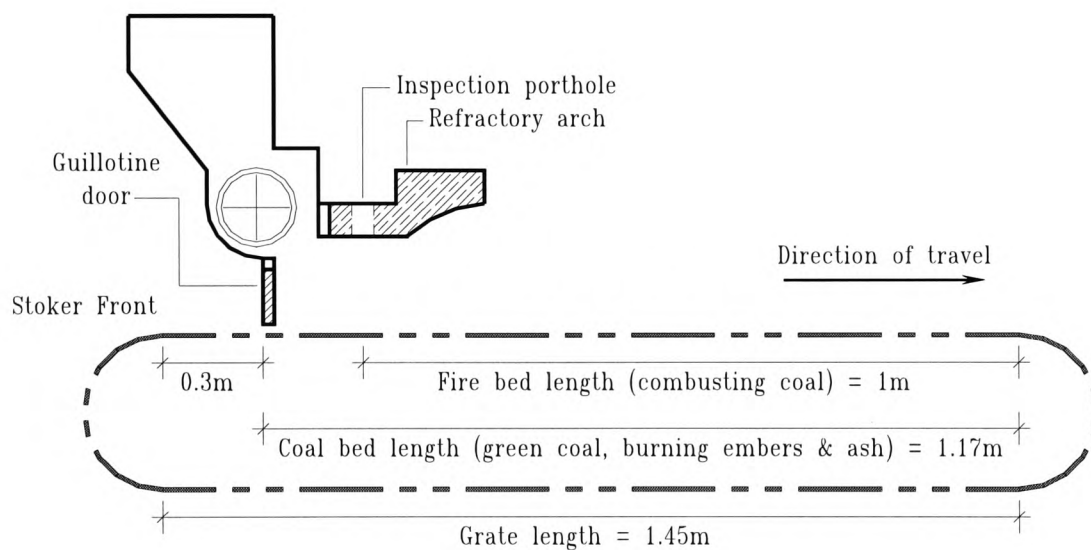


Figure 3.4 Stoker Test Facility Grate & Bed Dimensions [CTDD, 1995]

When operating at a maximum combustion intensity of approximately 1.4MW/m^2 , burning low ranking Bituminous coal, the expected maximum thermal output from the boiler was roughly 0.75MW (assuming a thermal efficiency of 80%). Therefore with a grate width of 0.55m , the effective length on the grate to allow for the burning of coal was approximately 1m , in order to deliver the expected maximum output as depicted in Figure 3.4 [Butt and Pulley, 1996]. The inspection porthole was located at the start of the combusting fuel bed also shown in Figure 3.4, with a diameter of 60mm which enabled the plant operator to check that ignition was taking place at the correct location on the grate. Regardless of the boiler operating load, the positioning of the ‘flame

front' in-line with the porthole was one of the key operating criteria to be satisfied. This was attained by regulating the grate speed to deliver both the required bed height and the desired location of the flame front for every coal feed rate.

3.1.2 Combustion Air Supply

Combustion air was supplied to the stoker air chamber by a forced draught fan operating at a constant discharge pressure of 660mm WG. The total air flow (with a turndown range of 7:1) was regulated by a variable speed forced draught fan motor. This was divided into four separate streams, which supplied each individual air chamber underneath the grate. The air flow rate to each of these four air ducts was regulated by a modulating valve and the flow rate to each air duct was measured using a 'vortex shedder' flow meter. The air flow rate in each duct was continuously monitored and controlled by a single closed loop controller. The stoker air chamber located underneath the grate consisted of 4 sections with two adjacent compartments in each section with air being supplied to each of them individually. This enabled the air distribution along the length of the grate to be altered in order to regulate the position of the ignition plane and also to meet the requirements of different coals.

Two grades of coal were burnt on the grate, namely Daw Mill Singles (25 to 38mm in length) and Smalls (12.5 to 25mm in length), and the air distribution profile was adjusted accordingly depending on the grade of coal used. For instance when burning Singles, the fire-bed profile was longer than when burning Smalls, due to larger coal particles, which required more air in the last section of the air plenum on the grate to provide adequate cooling of the grate. With Smalls, particularly at low load (0.3, 0.4MW), very little air was required in the last section as only ash was left. Suitable pressure drops across the boiler were also maintained according to the load demanded, by the use of an induced draught fan. This slight suction (1.25 to 2.5mm WG) was maintained via a closed loop set point controller, was vital for clean boiler plant operation and also to prevent the front of the stoker from overheating.

3.1.3 Chain Grate Stoker

Green coal was ignited from the top solely by radiation provided by the hot refractory arch as it entered the furnace tube. During manual operation of the plant, the operator ensured that the coal fed under the stoker arch could be ignited and that the flame could be seen through the inspection port hole. This was vital to ensure that ignition occurred at the right location on the grate in order to obtain satisfactory coal burnout. The ignition plane travelled downward through the bed, reaching the grate at approximately half of its total length. Residual ash and unburnt coal was deposited at the rear end of the grate into a water filled ash chute, and the wet ash was further transported to an ash collection bin situated outside the plant house via a screw feeder.

The level of water inside the ash chute was automatically maintained and formed part of the boiler safety system, i.e. a low level of water triggered an emergency shutdown sequence. During operation, the ash produced during combustion formed an insulating layer of inert material that provided some protection to the downstream part of the grate from the high temperatures prevailing in the furnace tube. Further cooling air was provided in the last section of the grate, due to the relatively low ash content in the Daw Mill type coal (5%) used in all the experiments, to avoid the chain mat from overheating.

In order to prevent slag formation on the base of the refractory arch, water cooled side cheeks were incorporated at the base of the ignition arch. Most coals fired in this type of stoker form slag on the hot surface of the ignition arch, which consequently flows down by gravity in a molten state. Molten ash froze when it came into contact with the cooled side cheeks, which then broke away and was transported down the grate to the ash disposal system. This helped to ensure that more consistent and efficient burning of the fire bed could take place and was required for full automation.

3.1.4 The Two Pass Shell Boiler & Cooling Water Circuit

Hot flue gases produced during combustion were cooled by passage through the water cooled furnace tube, reversal chamber and the smoke tube heat exchanger before being cleaned by passage through a high efficiency cyclone and subsequent discharge into the atmosphere via the stack. The exhaust flue gas temperature in the stack inlet was kept to a value above 140°C to avoid deposition of sulphuric acid, which can cause stack corrosion. Flue gas passage through the boiler were assisted by a slight suction provided by the induced draught fan installed after the cyclone. With the two pass test facility, it was assumed that the majority of the heat was transferred to the furnace tube wall via radiation with the rest being transferred via convection in the reversal chamber and the smoke tube. In general the time taken for the temperature of the flue gas to settle after a step change in the load was approximately 15 to 20 minutes [Good Practice Guide 88, 1993].

The cooling water facility for the plant comprised of an evaporative cooling tower, an indirect plate heat exchanger and two centrifugal pumps. As depicted in Figure 3.1, the plant cooling water circuit consisted of the boiler circuit which removed heat from the hot sections of the boiler (furnace tube, reversal chamber and smoke tube) and transferred the heat across to the cooling tower circuit via the plate heat exchanger. Circulation of water both in the boiler and cooling tower was achieved by using a centrifugal pump. In all the experiments carried out the cooling water flow rate in the boiler was maintained at a constant value of 6.5kg/s. Both the flow and temperature of the cooling water in the boiler circuit was continuously monitored, and any flow or pump failure or the temperature of cooling water exceeding a pre-set limit of 82°C, triggered an emergency shutdown sequence.

3.2 The Plant Control System and Instrumentation

The original plant control system comprised of a supervisory computer hosting seven front end PID industrial controllers. These front end controllers could be configured to operate in manual (providing facilities to raise or lower the desired set point of the

actuators via the front panel push buttons), or in automatic modes. In addition to managing the operator's setting of input parameters to the boiler (coal, primary air feed rate and induced fan suction), it also had a utility to log measurements obtained from various plant sensors, which included a Zirconia probe for measurement of the oxygen concentration in the flue gas and K-type thermocouples for temperature measurement. The sensor information was then transferred to the host computer running a commercial software package called 'Tactician', via an internal communication interface. The software provided an on-line visual display of all process and control variables every 30 seconds on the computer screen, hence providing an easy reference for the plant operator. The 'Tactician' supervisory computer was also capable of two way communication with a separate Personal Computer that could be running an intelligent controller by accepting instructions from the intelligent controller and remotely adjusting the settings of the front end controllers, and providing feedback information from the host computer's database via the 'Tactician' data transfer utility.

In addition to the plant sensors, a portable gas analyser (Testo 350) was used to measure the NO_x and CO emissions in the flue gas, and the readings were continuously logged to a separate Personal Computer via a serial link. Finally a portable digital thermocouple meter was used to measure the surface temperature of the grate at the stoker front during a series of experiments designed to investigate the behaviour of the boiler. Measurement of grate surface temperature was carried out manually. The subsections that follow, further describe the plant instrumentation used to measure the derivatives of combustion and are divided into gas analysis, flue gas temperatures, refractory arch temperatures and other measurements. Figure 3.5 illustrates the location of the sensors described in this section.

Figure 3.6 is a block diagram to represent the structure of the plant's distributed control system and also the additional sensors that were used to quantify the behaviour of the stoker test facility. Both the control and process variables are appended at the lowest hierarchy, followed by the respective actuators and sensors at the next level, subsequently with the dedicated controller panels and loggers and finally the host plant computer and the intelligent controller sitting at the highest level. Solid lines with two

arrow heads indicate two way communication, a solid line with a single arrow head for one way communication and hidden line to denote the variables that are associated with their respective actuators or sensors.

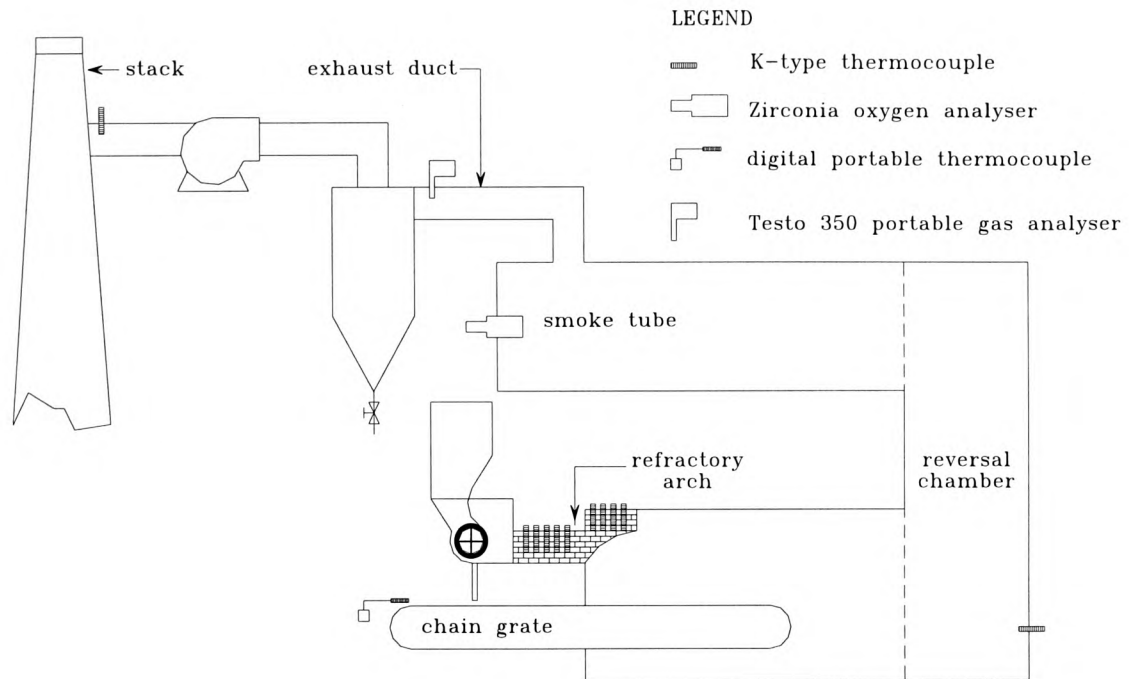


Figure 3.5 Sensors Location on the Stoker Test Facility

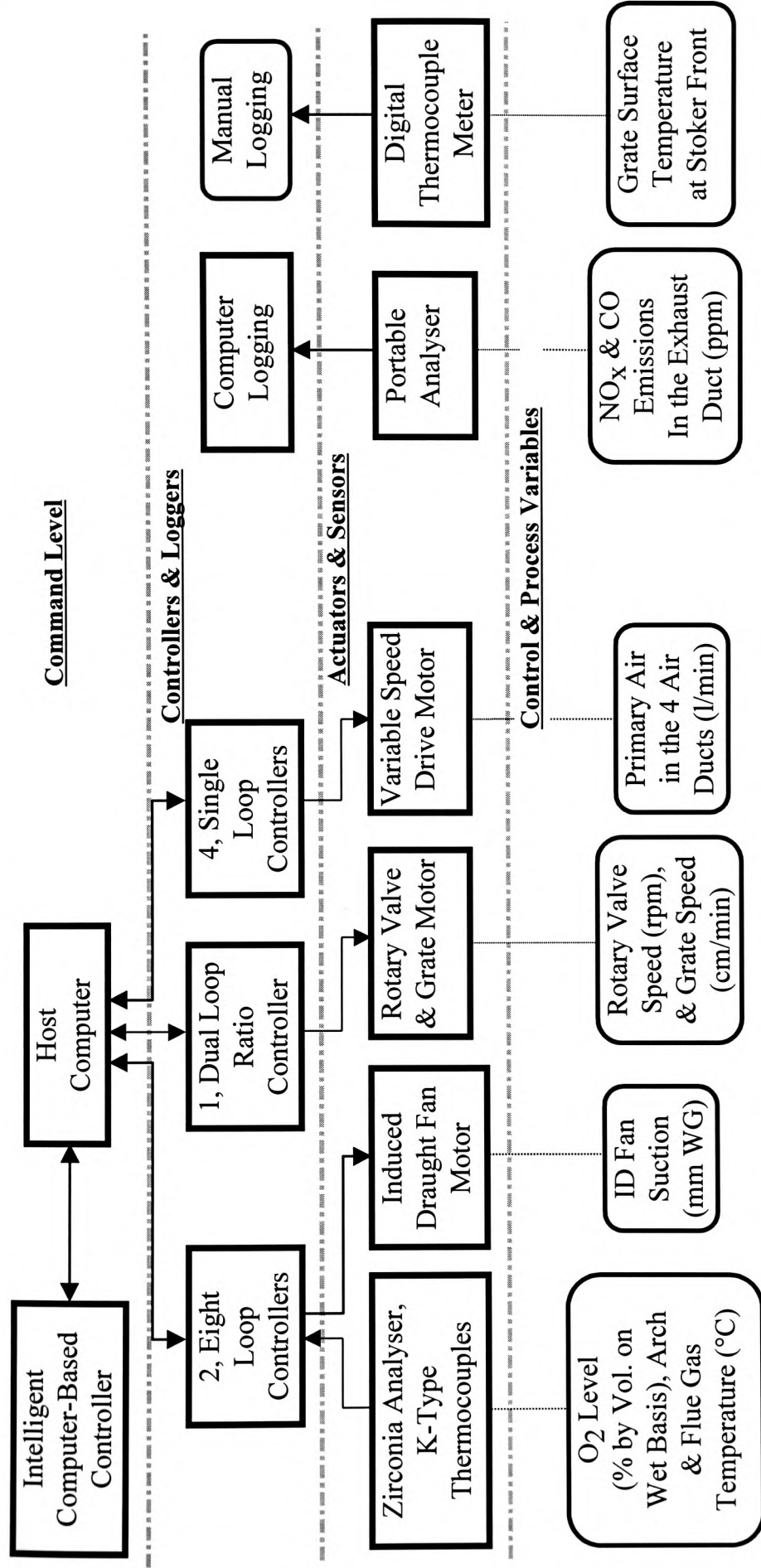


Figure 3.6 The Block Diagram of Measured and Controlled Parameters with the Digital Controllers, Sensors, and Plant Computers

3.2.1 Gas Analysis

A Zirconia probe based oxygen analyser was installed at the end of the smoke tube to measure the oxygen concentration in the flue gas. By examining the oxygen concentration in the flue gas, the operator can adjust the primary air in order to provide the correct level of excess air to suit the particular coal feed rate, for coal combustion the oxygen target was between 5 to 7% for good manual operation. The technique of monitoring the oxygen concentration in the flue gas and subsequently adjusting the combustion air is called 'oxygen trimming'. Such a technique can be very successful on oil and gas fired burners to maintain a minimum level of excess air without adversely affecting the emissions, and has been applied in practice [Gunn and Horton, 1989]. However with lump coal combustion on the grate the task of maintaining a good operating efficiency is more difficult as there are other factors such as the longer ignition time, incomplete mixing between air and fuel as compared to oil and gas (hence the high level of excess air). In addition, combustion hysteresis, particularly during frequent fluctuating load changes coupled with various other disturbances such as the coal size spread and distribution on the grate, moisture content and coal quality inevitably demands more attention from the plant operator [Good Practice Guide 88, 1993]. Nevertheless it is expected that the oxygen reading will form a major input to the neural network based control system along with other complimentary information which will be treated in detail in Chapter 5. The position of the analyser was such that the flue gas can be assumed to be completely mixed before any reading was taken. The oxygen reading was then logged continuously and stored in the host computer's database.

In addition to the Zirconia oxygen analyser, a portable flue gas analyser, 'Testo 350', was installed at the exhaust duct before the cyclone to measure the carbon monoxide and nitrogen oxides emission. The readings were continuously logged by a separate personal computer with a Windows based 'Testo-ComLight' software that came with the analyser. The CO reading is a very good indicator of the combustion process, and in most large coal fired plants, such as in the electricity generation sector, long term CO sensors have been widely installed along with flue gas oxygen measurements, to ensure good combustion efficiency and to comply with legislation. Small to medium

size coal fired plants, less than 20MW, could find the cost of a long term CO sensor difficult to justify, around £6,500 including installation and commissioning [Land Combustion, 1998; CODEL, 1998], and moreover at such scale, there is no legislative limit on NO_x or CO emission. Nonetheless, for the purpose of this work, both CO and NO_x measurements are presented along with various other sensor measurements for a comprehensive investigation of the performance of the test facility under various test conditions.

3.2.2 Flue Gas Temperatures

The temperature of the flue gas was measured in two locations, these were, at the base of the reversal chamber facing the furnace tube and also at the stack inlet, as indicated by the thermocouple legend in Figure 3.5. Temperature measurements were taken by the use of K-type thermocouples (temperature range of 0-1100°C) and as with the oxygen measurement, these temperature measurements were also continuously logged via the same eight loop controller panel and subsequently stored in the 'Tactician' data base of the host computer. The flue gas temperature reading at the reversal cell was the most sensitive to load changes as it was closest to the fire bed, which could provide a good indication of flue gas temperature changes following any load change or perturbation to the system, such as moisture content, change in the coal quality or distribution. Particular attention was paid to the flue gas temperature at the stack during boiler operation as the temperature must not be allowed to fall below 140°C, as it can promote chimney or stack corrosion by deposition of sulphuric acid. This is especially true when coal with a high sulphur content, greater than 2.5% (ultimate analysis), is being used [Grainger and Gibson, 1981]. Therefore justifying the need for the thermocouple installation.

3.2.3 Refractory Arch Temperatures

As one of the key issues to address in lump coal combustion on the grate was movement of the ignition plane (detailed treatment of the concept of ignition plane will

be provided in Section 3.3.1) an array of seven K-type thermocouples was installed in the refractory arch. This enabled a temperature distribution profile to be drawn and subsequently the stability of combustion or the rate of the ignition plane movement to be inferred from the arch temperature readings following load changes. As would be expected the location of the ignition plane was strongly dependent on the working temperature of the arch and grate speed. In fact the remedial action to bring the ignition plane back to a satisfactory position was by slowing or increasing the speed of the moving grate depending whether the ignition plane was moving further towards the furnace tube or back to the stoker front respectively. All the thermocouple tips were located 6mm from the inner surface of the refractory arch and a schematic of the thermocouple arrangement is shown in Figure 3.7.

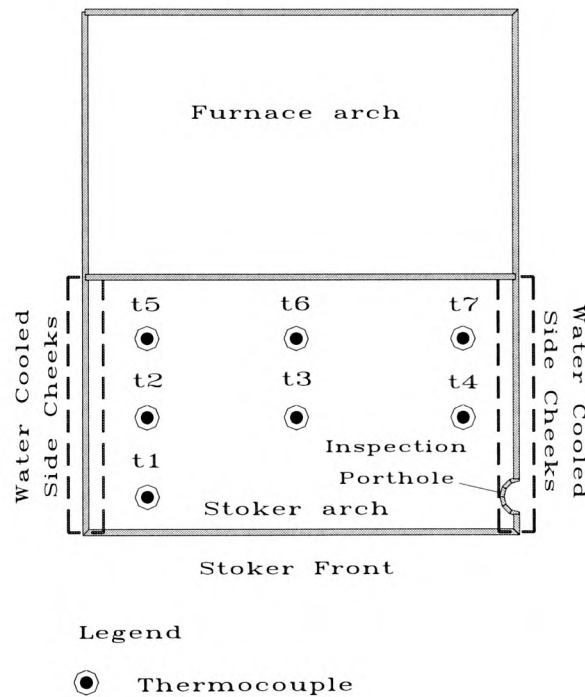


Figure 3.7 Thermocouples Arrangement in the Refractory Arch of the Stoker Test Facility

3.2.4 Other Measurements

In addition to the measurements described in the earlier sections, grate surface temperature was also recorded manually by the use of a portable digital thermocouple. The grate surface temperature reading was important to ensure that enough cooling air was being provided to avoid the mat from overheating. With the grate surface temperature measurement, three readings were taken across the width of the grate every 15 minutes past the hour of a load change. The highest acceptable grate surface temperature was between 70 to 80°C for the chrome alloy links, and in normal practice, the operator would touch the grate on the stoker front from time to time to ensure that the grate was not too hot. Further discussion of the grate surface temperature following load changes during manual operation is made in Chapter 4.

Finally, ash samples collected from experiments carried out with gradual load changes at near optimum and sub optimum operating conditions, together with one sample from the neural network control experiment were submitted to commercial laboratories for carbon in ash analysis [Appendix C]. These ash samples were analysed according to the following British Standards for the amount of unburned fuel in the ash:

1. BS1016 - Part 104.2 (1991) for the determination of moisture content in the ash sample;
2. BS1016 - Part 104.4 (1991) for unburned carbon residues in the dry ash sample.

This enabled the subsequent calculation of the efficiency losses to be made, hence providing a good basis for comparison between the performance of the boiler at various loads and operating conditions. Detailed treatment of this can be found in Chapter 4.

3.3 Coal Combustion on Chain Grate Stoker

Combustion of lump coal supported on a mechanical grate involves bringing coal and air together at a temperature high enough to decompose the content of the fuel to its combustible substances, namely fixed carbon and volatile matter, and subsequently

igniting the fixed carbon. The combustion then becomes self supporting if the conditions on the fire bed are properly maintained, such as the rate at which fresh coal is fed does not exceed the rate at which it can be ignited, sufficient air is provided, good air turbulence for mixing and the refractory arch is hot enough to maintain ignition of fresh coal. For the test facility, only when the inner arch surface temperature was higher than 800°C would the plant operator begin normal operation. The ignition temperature of various combustible substances within bituminous coal, the type used in this work, is provided in Table 3.1.

Table 3.1 Bituminous Coal Constituents and Ignition Temperatures [Good Practice Guide 88, 1993]

Combustible Substance	Molecular Symbol	Approximate Ignition Temp (°C)
Sulphur	S	243
Fixed Carbon	C	407
Acetylene	C ₂ H ₂	482
Ethane	C ₂ H ₆	538
Hydrogen	H ₂	610
Methane	CH ₄	650
Carbon Monoxide	CO	654

Note: The approximate ignition temperature of 'fixed carbon' for semi-bituminous and anthracite coal is 466 °C and 496 °C respectively as they are higher ranking coal.

Adequate combustion air must be provided to enable satisfactory burnout of all combustible matter and fixed carbon without having too much excess air, as the efficiency reduces in proportion to the excess air level [Good Practice Guide 88, 1993]. The air flow distribution along the length of the grate is also an important factor to suit the type of coal being used in order to ensure adequate cooling of the grate and also to completely combust the volatile matter. Since Daw Mill bituminous coal is a relatively low rank free burning coal (NCB rank code 802) secondary combustion air was not necessary [Good Practice Guide 88, 1993].

The following Section describes the chemistry of lump coal combustion for the calculation of combustion air required for the coal feed rates encountered in the test procedure for both types of coal used in the stoker test facility, the calibration graphs of the input parameters that relate the front end controller setting to the actual feed rate. Finally the empirically derived near optimum air distribution profile along the length of the grate for every load stages for both Singles and Smalls grade coal is also provided.

3.3.1 Combustion Calculation for Daw Mill Type Coal

Carbon, hydrogen and sulphur are the combustible elements present in coal which are very often conglomerated between themselves in addition to other substances. Analysis of coal is performed on a mass basis and it can either be ‘proximate’ or ‘ultimate’, carried out to BS1016 (1991). Both methods give the moisture and ash content of the fuel, as well as the gross calorific value from the given sample, and the difference between the two methods is that the ‘proximate’ analysis gives the combustible content of the fuel in terms of fixed carbon and volatile, whilst the ‘ultimate’ analysis further breaks down the combustible content of the fuel into its elemental constituents. Therefore the ‘proximate’ analysis provides a limited indication of the combustion properties of the fuel as compared to the ‘ultimate’ analysis. Hence for the purpose of calculating the required air and products of combustion, the results from ‘ultimate’ analysis are used [Gunn and Horton, 1989]. It must be mentioned here that the results obtained from the analysis, either ‘proximate’ or ‘ultimate’ can be presented on a number of bases and the typical ones are ‘as received’, ‘as fired’, ‘dry’ and ‘dry-ash-free’ (daf), or ‘dry-mineral matter-free’ (dmmf). Table 3.2 illustrates the ‘proximate’ analysis of a typical coal presented in three bases, ‘as fired’, ‘dry’ and ‘dry-ash-free’.

Table 3.2 Proximate Analysis of a Typical Coal (% by weight) [Gunn and Horton, 1989]

Constituent	'As Fired'	'Dry'	'Dry-Ash-Free'
Fixed Carbon	50.2	57.0	62.5
Volatiles	30.1	34.2	37.5
Ash	7.7	8.8	-
Moisture	12.0	-	-
Total	100.0	100.0	100.0
Gross Calorific Value (kJ/kg)	27000	30682	33624

The difference between the results obtained from the 'as fired' and 'as received' bases, both 'proximate' and 'ultimate' analysis, is usually down to the moisture content in the coal due to storage, handling of the coal, and also climatic condition [Gunn and Horton, 1989]. The 'dry' analysis provides the constituents of the sample (% by weight) with no moisture, whilst the 'dry-ash-free' discounted both the moisture and ash content. These values can be obtained by multiplying the 'as received' or 'as fired' by the following expressions:

1. 'dry basis' = 'as received' or 'as fired' constituents $\times \frac{100}{(100 - \text{percentage moisture})}$;
2. 'dry-ash-free basis' = 'as received' or 'as fired' constituents $\times \frac{100}{(100 - \text{percentage moisture} + \text{ash})}$.

The 'ultimate' analysis of Daw Mill type coal is used here to determine the amount of combustion air required and also the products of combustion [Gunn and Horton, 1989]. Table 3.3 provides the ultimate analysis of the low ash Daw Mill type coal on the 'as received basis', and these values have been used in the combustion calculation. In other words, the 'ultimate' analysis of the coal when it was received from the supplier, was assumed to be the same when the coal was being fired, hence the term 'as fired'. Details of the fuel specification for the two types of coal burned on the test facility can be found in Appendix A.

Table 3.3 Ultimate Analysis of Low Ash Daw Mill Coal (percentage by mass) - Free Burning Bituminous Coal (NCB Rank Code 802)

Element	% by mass
Carbon	72.8
Hydrogen	5.1
Sulphur	1.5
Oxygen	4.7
Nitrogen	1.4
Moisture	10.0
Ash	4.5
Gross Calorific Value (kJ/kg)	28573

The combustion calculation that follows will be considered with 40% of excess air (which is the typical figure used in medium sized boilers), and making due allowances for the oxygen that is already present in the fuel, therefore is deducted from the total oxygen demand for stoichiometric combustion [Gunn and Horton, 1989]. Since the ultimate analysis of the fuel was mass based, the combustion calculations will follow the same route. The basic combustion equations are as follows:

1. $C + O_2 = CO_2$, 12 unit mass of carbon requires 32 unit mass of oxygen to deliver 44 unit mass of carbon dioxide. Since there is 72.8% of carbon present in 1kg of coal being fired (0.728kg of carbon in 1kg of coal supplied), shown in Table 3.3, the amount of stoichiometric oxygen required for complete combustion is $0.728/12 \times 32 = 1.93\text{kg}$, to produce $0.728/12 \times 44 = 2.67\text{kg}$ of carbon dioxide. The equation thus becomes $0.728C + 1.93O_2 = 2.67CO_2$;
2. $2H_2 + O_2 = 2H_2O$, 5.1% of hydrogen content in 1kg of coal being fired, hence similarly the equation turns to $0.051H_2 + 0.408O_2 = 0.459H_2O$;
3. $S + O_2 = SO_2$, 1.5% of sulphur content in 1kg of coal being fired, hence with the same analysis, the equation becomes $0.015S + 0.015O_2 = 0.03SO_2$. The results obtained from these equations are tabulated in Table 3.4 for illustration.

Table 3.4 Analysis of Daw Mill Coal Combustion by Mass

Fuel constituent	Mass per kg of coal	O ₂ required for stoichiometric combustion, kg/kg of coal	Products of combustion with stoichiometric O ₂ , kg of gas/kg of coal			
			CO ₂	H ₂ O	SO ₂	N ₂
C	0.728	1.930	2.67	-	-	-
H	0.051	0.408	-	0.459	-	-
S	0.015	0.015	-	-	0.03	-
O ₂	0.047	-0.047	-	-	-	-
N ₂	0.014	nil	-	-	-	0.014
H ₂ O	0.100	nil	-	0.100	-	-
Ash	0.045	nil	-	-	-	-
Total	1	2.306	2.67	0.559	0.03	0.014

Therefore the stoichiometric *air* required to deliver 2.306kg of oxygen for every 1 kg of coal fired is $(2.306/0.23) \times 1\text{kg} = 10\text{kg}$, since 23% by weight of air consists of oxygen and 77% of nitrogen [Gunn and Horton, 1989].

However, the combustion air requirement in *practice* includes 40% of excess air, in order to promote turbulence for the mixing of coal and air, therefore the amount of air required is $= 10\text{kg} \times 1.4 = 14\text{kg/ kg of coal fired}$.

3.3.1.1 Combustion Air Calculation for Singles Grade Coal

Figure 3.8 shows the linear relationship between the indicated rotary valve speed (setting on the front panel controller) with the actual coal delivery rate for Singles grade coal. It is worth stating that the grate speed has been calibrated to match the rotary valve speed to give a constant bed height of approximately 150mm for all loads (0.3, 0.4, 0.5 and 0.6MW).

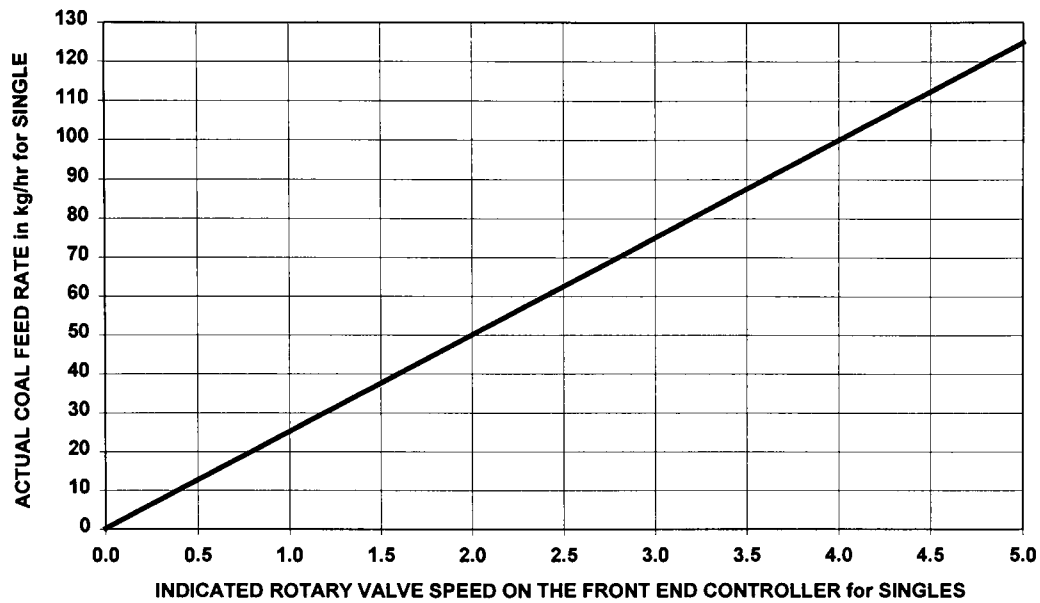


Figure 3.8 Indicated Rotary Valve Speed on the Front End Controller vs. Actual Coal Feed Rate for Singles Grade Coal [CTDD, 1995]

Table 3.5 shows the estimated amount of air flow required based on the calculation described in Section 3.3.1. The density of air was assumed to be 1.29kg/m^3 , and the thermal output from the boiler was calculated by assuming an overall thermal efficiency (ζ) of 75%, which is common in this type of boiler. The gross calorific value of the coal was used in the calculation of the thermal output [Gunn and Horton, 1989].

Table 3.5 Estimated Combustion Air with the Corresponding Thermal Output for Singles Grade Daw Mill Type Coal

Indicated rotary valve setting	Actual coal feed rate in kg/hr	Estimated thermal output (MW) with 75% working ζ based on gross cv of 28573 kJ/kg	Estimated air flow at 40% Xs air in kg of air/hr	Estimated air flow rate in litres/min
2.15	53	0.315	742	9587
2.65	67	0.400	938	12120
3.30	84	0.500	1176	15194
3.90	99	0.600	1386	17907

Note: 1000 litres = 1m^3

3.3.1.2 Combustion Air Calculation for Smalls Grade Coal

Similarly with Singles, the calibration graph of the actual coal feed rate and the indicated rotary valve speed setting on the front panel controller is provided in Figure 3.9. Please note that when using Smalls, the grate speed has been calibrated to match the rotary valve speed to give a constant bed height of about 100mm for all four load stages. Table 3.6 shows the estimated amount of combustion air required for the range of coal feed rates. The density of air was again assumed to be 1.29kg/m^3 , and the thermal output from the boiler was calculated using the gross calorific value and by assuming an overall thermal efficiency (ζ) of 75%. The estimated amount of combustion air for the four load stages with Smalls was similar to those of Singles. This was attributed to the fact that the only difference between Singles and Smalls was the physical size and that the fuel feed rates required to delivered the expected thermal output were identical. However the air distribution profile along the length of the grate was adjusted according to the type of coal burned as the Singles had a longer fire bed compared to the Smalls due to their larger size and thicker bed height. More details are provided in Section 3.3.2.

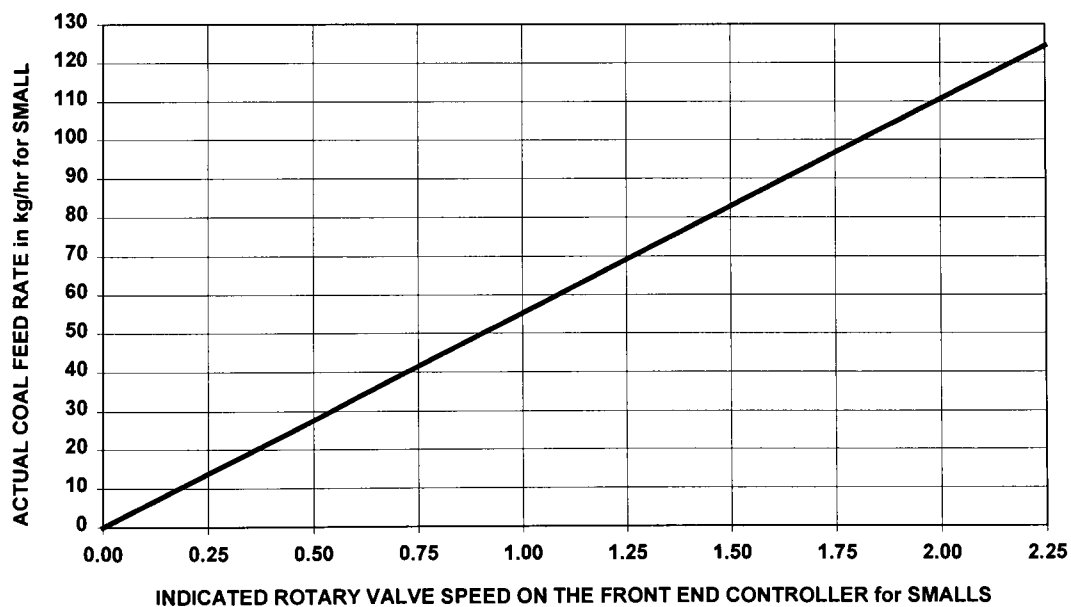


Figure 3.9 Indicated Rotary Valve Speed on the Front End Controller vs. Actual Coal Feed Rate for Smalls Grade Coal [CTDD, 1995]

Table 3.6 Estimated Combustion Air with the Corresponding Thermal Output for
Smalls Grade Daw Mill Type Coal

Indicated rotary valve setting	Actual coal feed rate in kg/hr	Estimated thermal output (MW) with 75% working ζ based on gross cv-28573 kJ/kg	Estimated air flow at 40% xs air in kg of air/hr	Estimated air flow rate in litres/min
0.93	53	0.32	742	9587
1.18	65	0.39	910	11757
1.54	85	0.51	1190	15375
1.81	100	0.60	1400	18088

Note: 1000 litres = 1m³

3.3.1.3 Calibration Setting of the Grate Speed for Singles and Smalls

An important factor associated with the grate speed was the time taken to re-establish the bed for a particular coal feed rate. As shown in Figure 3.4, the effective length of the fire bed was 1m, therefore the bed replacement time was essentially the time taken by the grate to travel 1m from the point of the inspection porthole until the end of the grate. This measure provided the operator with an indication of the duration of transient time following a load change. For instance, as depicted in Figure 3.10, the time taken to replace the coal bed at a grate speed of 3.6cm/min (controller panel setting of 11.25) which corresponded to 0.6MW thermal output, was 30 minutes. Similarly, at 0.3MW thermal output, with a grate speed of 1.6 cm/min (controller panel setting of 6.2), the time required was 50 minutes, when burning Singles. The transient time of the plant when subjected to a step change in load was approximately half the bed replacement time [CTDD, 1995]. This can be attributed to the fact that the ignition plane reached the grate at about half the fire bed length at steady-state combustion, and therefore the transient condition was when the grate moved the first half of the coal bed forward. An average transient period after a step change in load was approximately 20 minutes for the entire load range. It was due to this reason that the ash collection bin was positioned after 20 minutes past the hour of a load change in order to obtain the steady-state ash sample for the operating load. Details on grate ash sample results can be found in Appendix C and are discussed in Chapter 4.

Table 3.7 shows the rotary valve and grate speed settings that were used on the stoker test facility to deliver the required coal feed rate whilst keeping a constant bed height for both Singles and Smalls. The coal feed rates corresponded to the four thermal loads of the test facility namely, 0.3, 0.4, 0.5 and 0.6MW. These settings were used to train a neural network to function as a look-up table within the proposed control strategy, in order to control the plant after start-up and details can be found in Chapter 5.

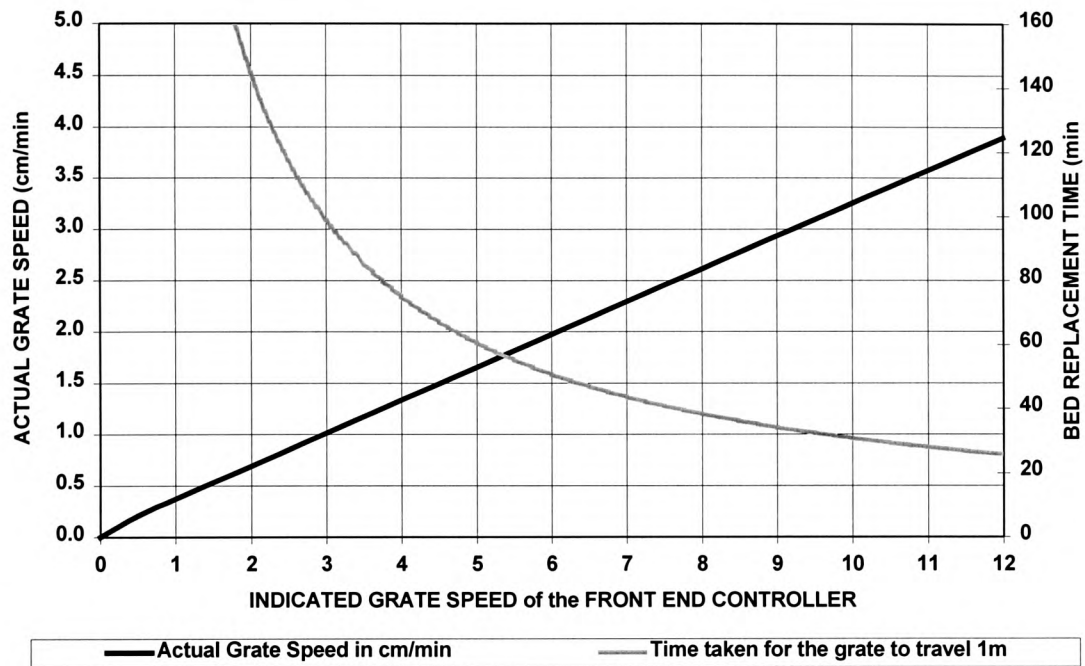


Figure 3.10 Indicated Grate Speed of the Front End Controller vs. Actual Grate Speed & Bed Replacement Time for Singles & Smalls Grade Coal [CTDD, 1995]

Table 3.7 Indicated Rotary Valve & Grate Speed Settings with the Required Coal Feed Rate for Singles & Smalls [CTDD, 1995]

Singles (constant bed height of 150mm)			Smalls (constant bed height of 100mm)		
Actual Coal Feed Rate (kg/hr)	Indicated Rotary Valve Setting	Indicated Grate Speed	Actual Coal Feed Rate (kg/hr)	Indicated Rotary Valve Setting	Indicated Grate Speed
	2.15	6.20	53	0.93	6.20
67	2.65	7.60	65	1.18	7.60
84	3.30	9.52	85	1.54	9.52
99	3.90	11.25	100	1.81	11.25

3.3.2 Combustion Air Distribution on the Grate

The linear relationship between the indicated setting on the front end controllers with the actual flow rate of the four primary air flows is as shown in Figure 3.11.

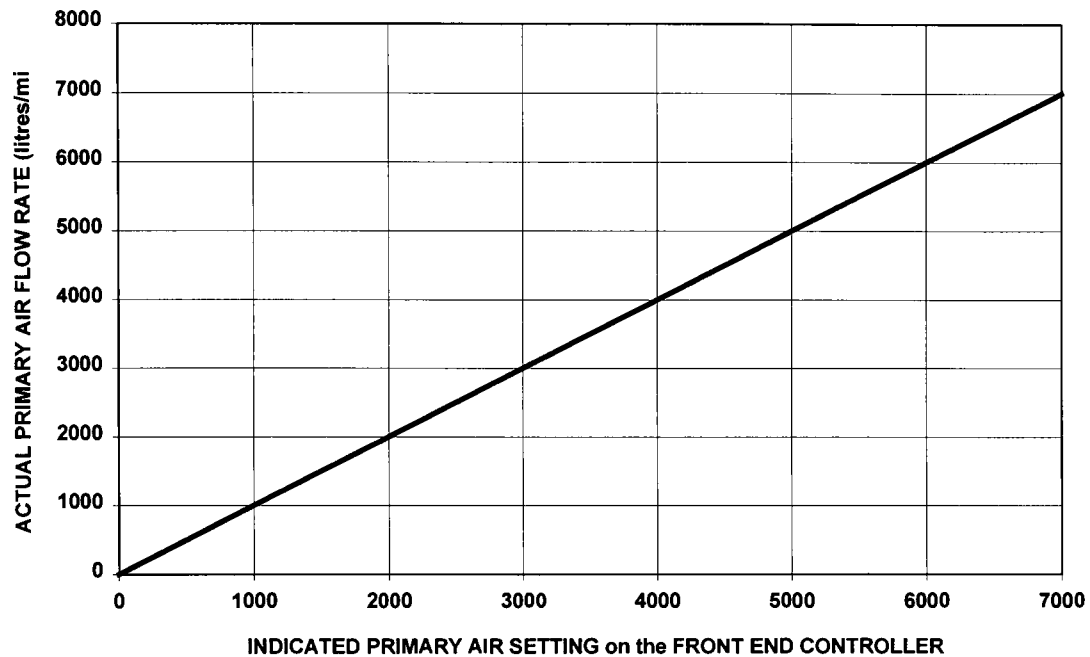


Figure 3.11 Indicated Air Settings on the Front End Controller vs. Actual Air Flow Rates on Duct 1, 2, 3 & 4 for Singles & Smalls Grade Coal [CTDD, 1995]

Very few modern chain grates have the air distribution facility that was available on the chain grate stoker employed in this work, where primary air was individually supplied to four separate sections of the grate. Instead, a motorised damper and graded baffles are more widely employed in industrial stokers, to divide the primary air into lesser regions on the bed (usually two, on the front and back) [Good Practice Guide 88, 1993]. The information on the air distribution profile on the test facility was empirically obtained through experience by taking into consideration factors such as the grate surface temperature, pollutant emissions, grate ash losses and oxygen concentration in the flue gas.

This Section presents the actual air distribution profile that was employed in the test procedure carried out at operator's best practice after having estimated the primary air feed rate of the four load stages for both Singles and Smalls. Before proceeding further

into the description of the air distribution, it is worth noting that all but one experiment was conducted whilst burning Singles. This was to ensure consistency of the test data for the purpose of neural network training and the only experiment carried out with Smalls was to evaluate the performance of the neural network based controller at dealing with burning a different coal. Thus no prior experiment was carried out in this work to evaluate the response of the plant to the optimal air settings of Smalls, but nonetheless the air distribution profile obtained from previous experiments (carried out by the Coal Research Establishment Ltd.) is presented in Table 3.9. The illustration that follows applies only to Singles grade coal.

A typical arrangement of the primary air flow distribution profile in the four air sections of the grate is shown in Table 3.8, where the front and rear sections (1 and 4) constituted about 20% of the total primary air supply, whilst 80% of the remaining air was targeted at the two middle sections (2 and 3) where the main combustion zone resided. Such an air distribution can help to ensure more efficient burning on the grate, as pointed out by Livingston *et al.* (1995) and Starley *et al.* (1985). Chain grate stokers are inherently low NO_x burners due to the lower peak temperature (lower burning rates) and also to the natural form of air staging along the bed [Clarke and Williams, 1992].

Table 3.8 Primary Air Distribution Profile Along the Fire Bed

Air Plenum Section	Function
1st (front)	The air flow to the front section was to maintain a desirable location of the ignition plane.
2nd (middle)	To provide sufficient air to burn off the distilled volatile and residual char.
3rd (middle)	To provide sufficient air to burn off the distilled volatile and residual char.
4th (rear)	To ensure complete burn out of the remaining char and to provide cooling air to the rear end of the grate.

The estimated combustion air for every load stage was implemented on the stoker plant according to the distribution described in Table 3.8 with 20% of the total being allocated to section 1 and 4, whilst the remainder was evenly divided between section 2 and 3. However depending on the fire bed profile, fine adjustments on the air distribution were necessary in order to satisfy the plant operating constraints. These were maintaining a minimum excess air level (oxygen concentration of between 5 to 7%) without adversely affecting the pollutant emissions, ensuring good coal burn out by visual inspection of the grate ash and finally to ensure that sufficient cooling was being provided in the rear section of the grate. The operator's near optimum setting of the primary air for Singles in the four air ducts is shown in Table 3.9.

The results obtained from implementing these settings on the test facility when burning Singles, can be found in Section 4.1.1 of Chapter 4 to demonstrate the desirable boiler response which satisfied all the operating constraints (oxygen concentration in the flue gas of between 5 to 7%, satisfactory coal burn out and grate surface temperature).

Table 3.9 Operator's Optimum Air Settings on the Four Air Ducts for Singles and Smalls Grade Coal [CTDD, 1995]

Indicated Primary Air Setting	Singles Grade Coal				Smalls Grade Coal			
	Boiler Load in MW				Boiler Load in MW			
	0.3	0.4	0.5	0.6	0.3	0.4	0.5	0.6
Duct 1	1200	1200	1300	3000	1400	1500	1600	2000
Duct 2	4200	5200	6000	7000	4300	5400	6000	6500
Duct 3	3200	4200	5000	7000	3300	4400	5000	6000
Duct 4	600	800	1000	1500	900	1000	1200	1700
Total	9200	11400	13300	18500	9900	12300	13800	16200

The reason for including these settings is because they were used to train a neural network to function as a look-up table (delivering the optimum air settings for the load required) and was subsequently used by the NNBC to deliver the initial air settings before fine tuning of the air to the main combustion zone under steady-state conditions.

3.4 Experimental Procedures

This Section provides an overview of the experimental procedures conducted in order to investigate the behaviour of the stoker test facility and to evaluate the performance of the Neural Network Based Controller (NNBC) on the stoker test facility and also on an industrial chain grate stoker.

The first series of *manual* experiments were aimed at investigating the stoker test facility's response to gradual load changes at optimal and sub-optimal working conditions. In addition, the effect of staging the coal feed and air flow in a series of small steps in response to a large load change was also studied. Boiler load change was simulated by manually adjusting the coal feed and primary air flow via the front end controllers. Since the results from these experiments were required for the neural network training whereby consistency in the training data was of paramount importance, only Daw Mill Singles grade coal was used throughout this first series of experiments.

From the gathered information regarding the stoker test facility, a NNBC was developed, and the second series of *control* experiments were carried out to evaluate its performance against operator's best practice. Also in this series of experiments, the NNBC was implemented on-line to control an industrial chain grate stoker boiler in a case study carried out in conjunction with James Proctor Limited, a Lancashire based stoker manufacturer.

The highest load attainable on the stoker test facility was 0.6MW due to plate heat exchanger fouling (MCR of test facility was 0.75MW) and this constraint was carefully taken into account when operating the boiler in order to avoid any two phase flow in the cooling water pipes. The lowest operating load was 0.3MW (at full turndown) and hence the limits of the operating load was between these two figures. A comprehensive range of combustion derivatives were continuously monitored and these were:

1. A series of refractory arch temperature readings;
2. Grate surface temperature at stoker front;

3. Oxygen concentration in the flue gas (at the end of smoke tube);
4. Carbon monoxide emission in the flue gas;
5. Nitrogen oxides emission in the flue gas;
6. Flue gas temperature at the reversal chamber and stack inlet.

In addition to the above list, grate ash samples were collected for every load stage (0.3, 0.4, 0.5 and 0.6MW) at *steady-state combustion* for the *manual* experiments. One ash sample (from steady-state combustion at 0.6MW) was obtained when the test facility was operated by the NNBC burning Singles grade coal. No ash sample was collected when burning Smalls because a fair portion at the rear end of the grate was blown away from the ash collection chute in addition to the difficulties of these light particles sinking into the ash removal system. These ash samples were sent to commercial laboratories for the analysis of unburned carbon and the results were used to calculate the combustion efficiency loss in the ash at steady-state condition according to BS845: Part 1 (1987).

Finally, a CCD (Charged Coupled Device) camera was used to record the image of the fire bed through the inspection porthole in the *manual* experiments. The concept of monitoring the flame front movement to infer the stability of combustion was taken further and an alternative sensor using a linear array of photodiodes installed in a 35mm Single Lens Reflex camera was developed. The results obtained from the video camera and the construction of the flame front monitoring device are presented in Chapter 6. Whereas a detailed treatment of the results obtained from the *manual* experiments is given in Chapter 4, and the implementation of the NNBC in Chapter 5.

3.4.1 Experiments with Gradual Load Changes

These experiments were aimed at providing the neural networks with information about the response of the stoker test facility at both optimal and sub-optimal operating conditions. As mentioned earlier, Dawmill Singles was used in all the experiments, in order to obtain consistency in the test data. The ultimate aim would be to operate the plant efficiently whilst maintaining acceptable NO_x and CO emissions, with minimum

intervention from the plant operator. The results gathered from operating the test facility to the 'operator's best practice' was treated as a bench mark for near optimal combustion. The bench mark for a near optimal combustion were, an oxygen concentration in the exhaust flue gas of between 5 to 7% by volume, CO level in the flue gas of less than 400ppm and a stable flame front location. A stable flame front location⁴ meant that the plant operator can see flickering of the flame through the inspection port during both transient and steady-state conditions regardless of the magnitude of the load change.

Sub-optimal regions of the test facility response were aimed at a 3-5% (lower excess air level) and a 7-9% (higher excess air level) oxygen concentration in the flue gas. The primary air was varied accordingly with a view to generate this envelope of sub-optimal data. The former was achieved by *lowering* the total 'near optimum' air flow by an average of 15% for the 4 operating loads, and similarly the latter was attained by *increasing* the total 'near optimum' air flow by an average of 15%. Figure 3.12 shows the relationship between the amount of excess air level from the stoichiometric with the expected oxygen and carbon dioxide content in the flue gas when burning bituminous coal such as the 'Dawmill'. As illustrated in Figure 3.12, the entire span of the boiler response in terms of the excess air level ranged from 15 to 80% from stoichiometric, which in a practical sense, was sufficiently large to account for any possible deviations from the near optimal air/fuel ratio during a normal operating campaign. Other variations from the operator's best practice included operating the stoker test facility at a higher grate speed and having equal distributions of the near optimal primary air between the four air sections on the grate.

The load of the stoker test facility was varied from 0.3MW to 0.6MW in 0.1MW step increments and back to 0.3MW in five operating conditions. These five conditions were:

⁴ *The flame front movement can provide an indication of the ignition plane movement i.e. the stability of combustion on the grate. This idea was one of the key objectives of the research work.*

Test 1: At near optimum primary air with the corresponding flue gas O₂ concentration of between 5 to 7% (30 - 50% excess air);

Test 2: At a lower level of excess air with the corresponding flue gas O₂ concentration of between 3 to 5% (15 - 30% excess air);

Test 3: At a higher level of excess air with the corresponding flue gas O₂ concentration of between 7 to 9% (50 - 80% excess air);

Test 4: Running the grate faster to simulate the condition of a thinner fire bed with less residence time on the grate (providing the optimal amount of air but increasing the grate speed by 20%);

Test 5: Simulating the set up of most industrial chain grate stokers which distributes the total primary air equally along the grate.

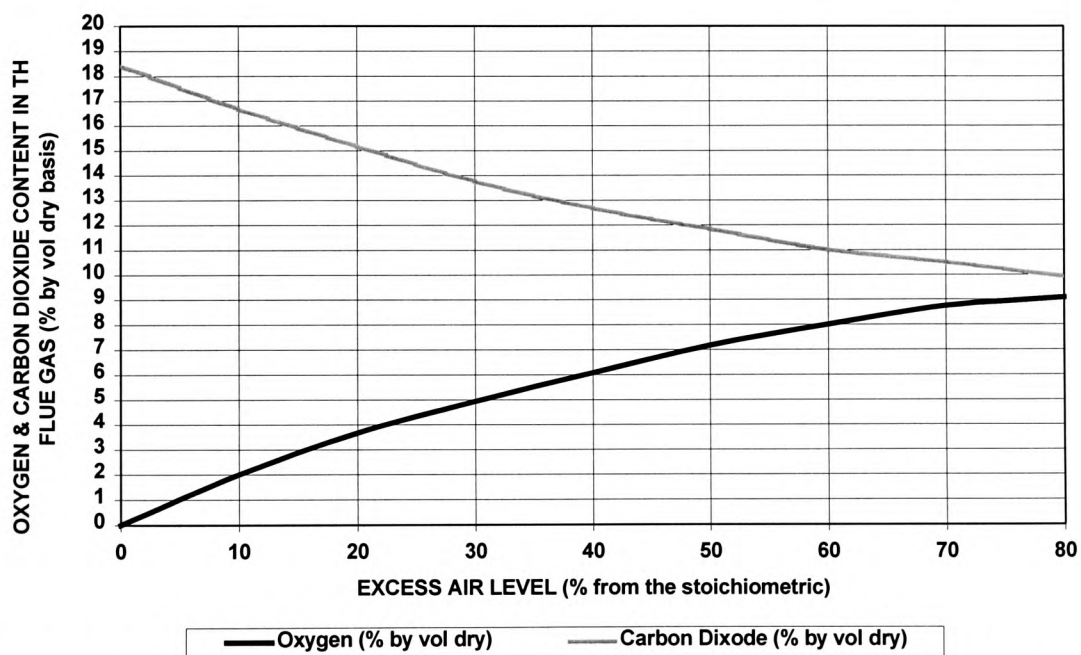


Figure 3.12 Relationship Between O₂, CO₂ and Excess Air Level for Bituminous Coal

3.4.2 Experiments with Large Load Changes Following Two Different Coal and Air Staging Profiles

The objective of these experiments was to determine the fastest and most stable way to operate the boiler in large load following conditions without excessive movement of

the ignition plane whilst maintaining acceptable transient CO emission. Hence the load demanded from the boiler was altered from 0.3MW to 0.6MW and vice versa, over a relatively short period of time (in the range of 2 to 3 minutes). It should be noted that the average transient behaviour of the stoker test facility from the point of load change to steady-state condition was about 20 minutes. Therefore the time taken to complete the staging process can be seen as relatively short.

Instead of having almost an instantaneous change in the input parameters, the coal and air settings were gradually introduced over a series of smaller steps with a view to minimise the movement of the ignition plane. This would help to ensure a stable combustion of coal on the fire bed. However the sequence in which these input parameters were delivered was altered in both magnitude and direction, in two distinct ways for load increase and decrease, as noted by Gunn (1982) as a means to reduce smoke emission and to promote better transient combustion. According to Gunn (1982), on load increase, the primary air should be allowed to change first in order to provide a higher combustion intensity on the fire bed, before introducing more fresh coal. However, the quantity of primary air introduced must be carefully controlled, i.e. the total increment of air being spread over a period of time. This staging sequence can be referred to as '*air leading the coal feed*'.

On load decrease, the coal feed should be brought down first before reducing the primary air, in order to provide sufficient air to cater for a higher combustion intensity, initially prevailing in the furnace tube. As with load increase, the amount of primary air must be brought down gradually over a period of time following the reduction in coal feed. This staging sequence can be referred to as '*coal leading the air feed*'. Two tests were carried out to investigate the effect of coal and air staging, and these were:

Test 6: Increase the coal feed first before the air on load step up (0.3 to 0.6MW) and on load step down (0.6 to 0.3MW), decrease the air feed before the coal;

Test 7: Increase the air feed first before the coal on load step up (0.3 to 0.6MW) and on load step down (0.6 to 0.3MW), decrease the coal feed before the air.

3.4.3 Experiments with the Neural Network Based Controller

The performance of the developed NNBC was evaluated on the test facility and also on an industrial chain grate stoker fired boiler. The former was concerned with carrying out an initial set of experiments to determine the appropriate NNBC control parameters with Singles prior to testing the NNBC whilst burning a 'different' coal where Smalls was used. The latter was concerned with the implementation of the NNBC onto an industrial chain grate where its performance was assessed against the plant original PID control system.

The NNBC essentially seeks to provide the minimum amount of air flow required for optimum combustion, without having to sacrifice CO emission and carbon in ash losses. Feed forward Multi-Layered Perceptron (MLP) networks were used to construct the neural network components, namely the corrective network (for the oxygen trimming loop) and the 'look-up table' (to deliver a good initial estimate of coal feed and air flow) using gathered plant data and were subsequently integrated into an overall control strategy which was formulated by the field expert based on past experience. In addition, a desirable staging profile was taken into account when executing large load changes and such knowledge was also built into the overall controller strategy. The bench mark of the NNBC was to achieve the lowest possible excess air level in light of other operating constraints.

3.4.3.1 NNBC Implementation on the Stoker Test Facility Burning Singles

Initial work with the NNBC included experimenting with different controller parameters on the stoker test facility and these were the corrective gain factor and the controller sampling period. The corrective gain factor determined the amount of air flow tuning required in the two middle sections of the grate, based on the oxygen error reading (deviation from the target of 6%) and the sampling period was the length of time between each successive control decision made by the NNBC. Two values of the corrective gain factor, 5 and 10, which were empirically derived from the results of the earlier tests (Test 1 to 5, as illustrated in Section 5.2.3 of Chapter 5), were

implemented. As for the controller sampling period, an initial value of 10 seconds was employed and gradually increased until a suitable value was found. Four control experiments (Test 8 to 11) were first conducted when burning Singles and these were:

Test 8: Control experiment with Singles, load change from 0.3MW to 0.6MW and back to 0.3MW with corrective gain of 10 and sampling period of 10 seconds;

Test 9: Control experiment with Singles, load change from 0.3MW to 0.6MW and back to 0.3MW with corrective gain of 10 and sampling period of 30 seconds;

Test 10: Control experiment with Singles, load change from 0.5MW to 0.6MW to 0.3MW to 0.4MW to 0.5MW with corrective gain of 5 and sampling period of 60 seconds;

Test 11: Control experiment with Singles, load change from 0.3MW to 0.6MW in 0.1MW steps, followed by 0.6MW to 0.3MW and back to 0.6MW with corrective gain of 5 and sampling period of 120 seconds.

3.4.3.2 NNBC Implementation on the Stoker Test Facility Burning Smalls

The next experiment on the test facility was conducted with burning Smalls to examine the NNBC ability to deal with the use of a different type of coal. The experiment conducted was:

Test 12: Control experiment with Smalls, load change from 0.6MW to 0.4MW in 0.1MW steps, followed by 0.4MW to 0.6MW and 0.6MW to 0.3MW with two corrective gains (5 and 2.5) and two sampling periods (120 and 240 seconds).

The reader is reminded here that the NNBC was only trained with data relating to burning Singles on the stoker test facility. Also, it must be mentioned here that the calibration of the front panel distributed controller for the coal feed rate (rotary valve and grate speed) was *altered* prior to the experiment which rendered the given information on the coal and air settings ‘inaccurate’. This resulted in a much thicker fire bed than what would otherwise be obtained with the previous input parameter

settings. Nonetheless, this was viewed as a ‘disturbance’ to the combustion process and the NNBC response to such variation is presented in Section 5.3.2 of Chapter 5.

3.4.3.3 NNBC Implementation on an Industrial Chain Grate Stoker Fired Plant

The final set of control experiments were the most challenging since the on-board instrumentation and control system of the industrial chain grate weren’t as extravagant as the test facility at CRE and furthermore there were other operational issues that were not found during earlier work with the test facility. These differences included a varying band of ‘optimum’ excess air level depending on the operating load, due to the simplistic air distribution facility employing an under-grate damper system, necessitating a significantly higher excess air level at low loads (oxygen in flue gas of >11%) as compared to medium (oxygen of between 9 to 11%) and high loads (oxygen of between 7 to 9%). In addition, since the boiler demand was reflected in terms of the process variable (hot water temperature), the NNBC first priority was to satisfy the hot water production prior to trimming the excess air. Details of this work can be found in Section 5.4 of Chapter 5. The first experiment carried out on the industrial chain grate was to characterise the behaviour of the plant before evaluating the on-board PID controller performance, followed by the implementation of the NNBC to control the plant. The experiments conducted on the 3.7MW_{th} chain grate stoker fired plant were:

Test 13: Firing rate of the boiler was altered manually from full turn down at 17% of MCR to 83% of MCR and back down to 17% of MCR, in 17% MCR steps at plant operator’s best practice;

Test 14: Plant response under the influence of the conventional PID controller in tracking the process variable set point of 120°C;

Test 15: Plant response under the influence of the conventional PID controller, following a process variable set point change from 105°C to 120°C;

Test 16: Plant response under the influence of the NNBC in tracking the process variable set point of 120°C;

Test 17a: Plant response under the influence of the NNBC, following a process variable set point change from 88°C to 105°C;

Test 17b: Plant response under the influence of the NNBC, following a process variable set point change from 105°C to 120°C.

4. Experimental Results & Discussion – A Study into the Behaviour of the Stoker Test Facility

This Chapter describes the data gathered from a series of experiments carried out to investigate the behaviour of the stoker boiler when subjected to gradual load changes at optimal and various sub-optimal operating conditions and also the effect of varying the staging sequence of coal and air feed in smaller steps following a large change in the load required. Please note that all the experiments described in this Chapter were carried out when burning *Singles* and that the load change was simulated by *manually* adjusting the coal and air feed from the front end controllers.

Data is presented and discussed with reference to the oxygen concentration in the flue gas, nitrogen oxides and carbon monoxide emissions, flue gas temperature at the stack inlet and flame front location through the inspection porthole. The flame front refers to the location where the fuel bed starts to ignite and it is an important factor in stoker firing as it ultimately dictates the efficiency and stability of the combustion process. Late ignition results in higher carbon in ash losses as the burning coal will not have sufficient time to burn off along with possible grate overheating from exposure to burning coal with little or no ash layer to protect the grate. On the other hand, early ignition can cause heavy smoking at the stoker front which could result in overheating of the stoker front and live fire passing into the hopper (for stokers without a fire break unit) if the problem is not rectified soon enough. In this Chapter, the flame front position as seen by the operator through the inspection porthole during the course of the experiment, is provided by the use of Figure 4.1 for further illustration:

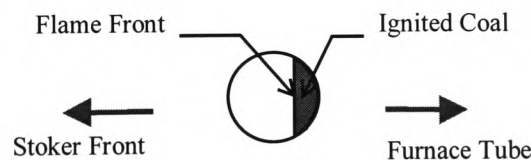


Figure 4.1 Flame Front Indication Through the Inspection Porthole

For experiments with gradual load changes, only the average flame front position at steady-state combustion is provided and as for the experiments with large load changes, one average diagram is given every 5 minutes over the entire duration of the test. This information together with the other sensor measurements will help to characterise the combustion process on the grate. A detailed discussion of the relationship between the flame front movement and the arch temperature distribution pattern in order to characterise the ignition plane movement following load changes is given in Chapter 6.

For the experiments with gradual load changes, grate surface temperature at the stoker front and carbon in ash (CIA) losses are also included. The CIA losses were later converted to the actual loss in combustion efficiency according to BS845:Part1 (1987).

4.1 Boiler Response to Gradual Load Changes

The objective of this series of experiments was to investigate the response of the test facility to gradual load changes at both optimal and sub-optimal operating conditions. Both the coal feed and air flow were changed simultaneously to vary the desired boiler output from 0.3 to 0.6MW and back to 0.3MW in 0.1MW steps, at five operating conditions, namely Test 1 to Test 5. Test 1 to Test 4 were carried out using the empirical air distribution along the grate which was described in Section 3.3.3 (20% of the total combustion air to the front and rear sections with the remainder equally divided between the two middle sections). In Test 5 the total near optimum air flow was distributed equally at each air section, i.e. 25% of the total air flow in each air section of the grate. Full description of the experimental procedures can be found in Section 3.4.1 of Chapter 3.

The results obtained from Test 1 are used in the following sub-sections as a benchmark for ‘optimum’ combustion, since it was derived from the plant operator’s best practice. As described in Section 3.4.1, in order to categorise the combustion process as optimal there was a set of criteria that needed to be satisfied and these would be an oxygen concentration in the flue gas of between 5 to 7% (which corresponded to an

excess air level of between 30 to 50% from stoichiometric), CO level of less than 400ppm, grate surface temperature at the stoker front of no more than 80°C and a visible flame front through the inspection porthole.

4.1.1 Test 1 - Gradual Load Changes at Near Optimum Air

The results presented here serve as a bench-mark for what the plant operator would call optimum operation of the stoker boiler and will therefore be used as the standard against which to compare the response of the boiler to various other operating conditions.

As expected with a near optimum excess air, distributed along the grate according to the operator's best practice (Section 3.3.2), the oxygen level remained mostly within the 5 to 7% optimal band following the gradual load changes shown in Figure 4.2. This confirms the range of excess air level that was provided for the four loads to be within 30 to 50%, (refer to Figure 3.12). The NO_x emission trend shown in Figure 4.3 is similar to the oxygen profile which can be explained by the fact that both the fuel and thermal NO_x were heavily influenced by the amount of combustion air available [Clarke and Williams, 1992]. The average NO_x level recorded from this experiment was approximately 120ppm, normalised to 6% oxygen, which is low even for stoker fired boilers which are inherently low NO_x producers.

Such virtue comes from the fact that the peak temperature in the fire bed is relatively low, about 1600°C (thermal NO_x formation being minimal at temperatures below 1500°C) compared to pulverised fuel (pf) firing. As for the CO emission, the average level was 50ppm which is highly acceptable as the maximum arbitrary limit was set to 400ppm. It is worth stating at this point that the stack would only smoke if the CO level was higher than 2500ppm, hence the average figure in this test was negligible by comparison. This suggests that there was sufficient air available for the entire range of loads for the satisfactory combustion of the volatile matter.

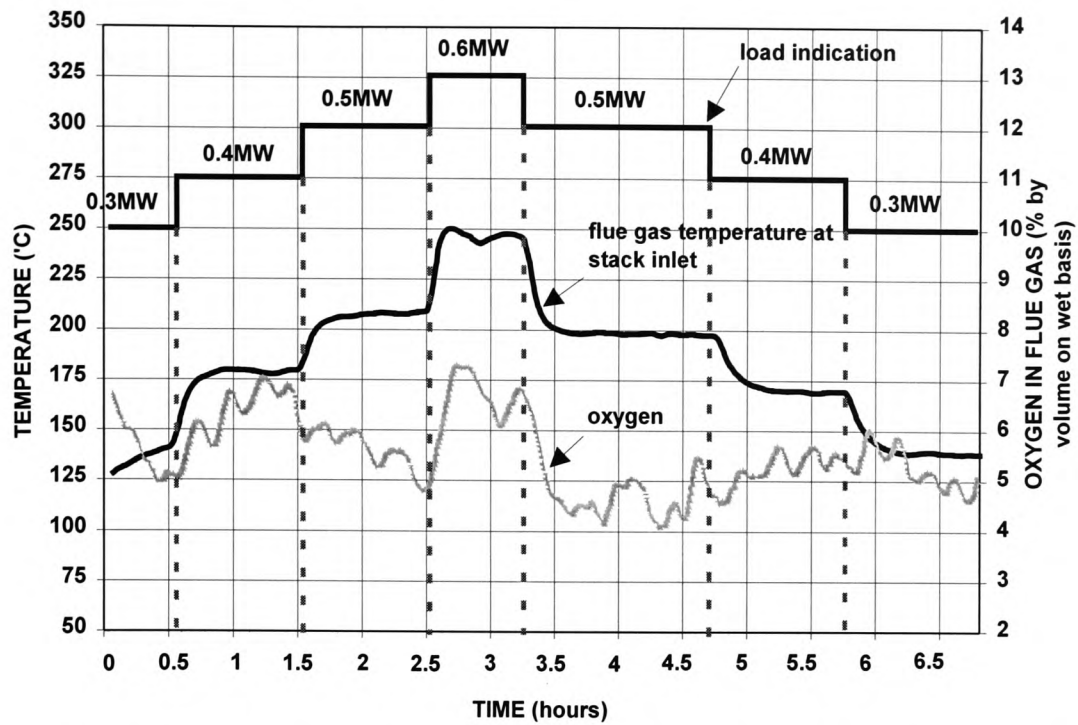


Figure 4.2 Flue Gas Temperature at the Stack Inlet & Oxygen Concentration in the Smoke Tube from Test 1

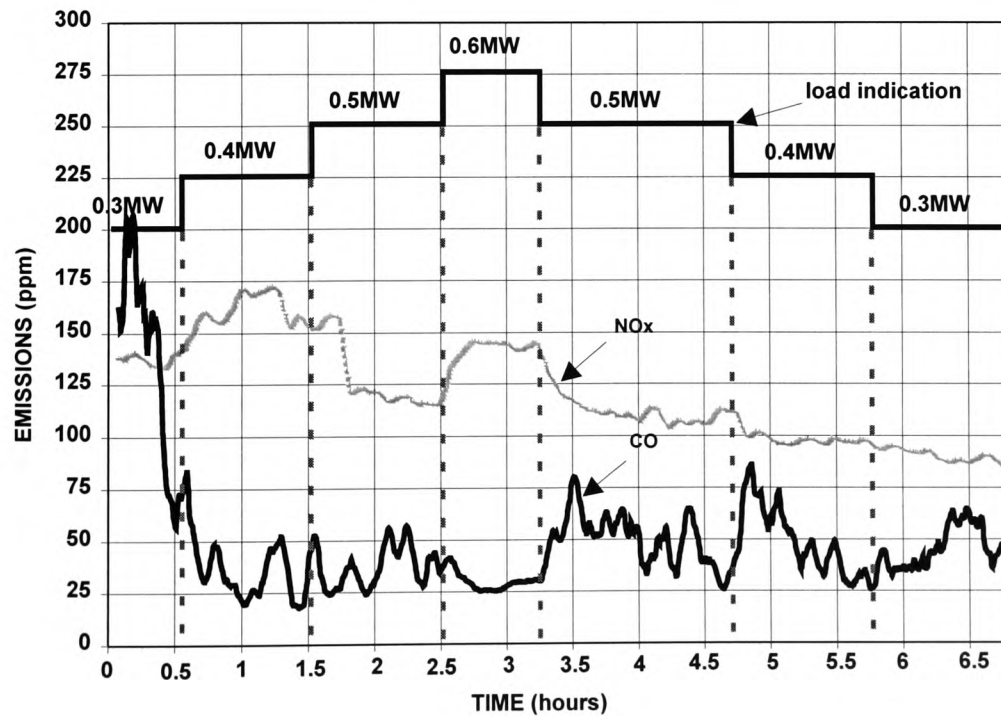




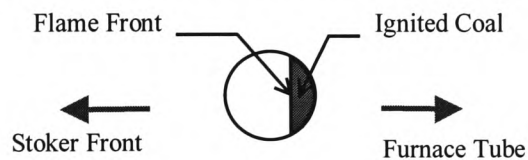


Figure 4.3 NO_x & CO Emissions in the Exhaust Duct from Test 1

Table 4.1 Grate Surface Temperature at the Stoker Front, Carbon in Ash Losses & Average Flame Front Location at Steady-State Combustion from Test 1

Boiler Load in MW	0.3	0.4	0.5	0.6
Grate Surface Temperature in °C	72	75	77	75
Unburned Carbon in Ash (%) in weight of dry sample)	41.2	38.5	31.9	39.8
Loss in Combustion Efficiency in %	1.87	1.47	1.50	1.69
Average Flame Front Location at Steady-State Combustion				

Legend: Flame Front Location Through the Inspection Porthole



At the same time adequate cooling air was also available to the grate as the average grate temperature for every load stage was between 72 and 77°C (the grate surface temperature constraint being not higher than 80°C). As for the losses in the grate ash, an acceptable figure for losses of unburned material (which includes riddling, small pieces of coal dropping through the spacing between chain links, and grit trapped in the cyclone), in a well-commissioned chain grate stoker is 2.5% [Good Practice Guide 88, 1993]. In this work, riddling and grit losses were negligible as Singles was used (compared to Smalls in industrial practice which constitutes a higher proportion of fines) and the material collected in the cyclone was of the order of 200 grams, which was very small in comparison to the grate ash losses. The actual efficiency loss in the grate ash was between 1.47 to 1.87%, as shown in Table 4.1, giving an average efficiency loss in the ash of 1.63%, and can therefore be considered satisfactory as it was lower than 2.5%. The average flame front location was noted to be within the visible range of the inspection porthole, hence suggesting that ignition occurred at the appropriate location. The amount of combustion air provided for each boiler load, 0.3,

0.4, 0.5 and 0.6MW (assuming a 75% combustion efficiency) was adequate to yield satisfactory coal burnout whilst satisfying the other constraints of an oxygen concentration of between 5 to 7%, an acceptable grate surface temperature and low gaseous pollutant emissions. The flame front was also noted to be within the visible range of the inspection porthole suggesting that the fresh charge of coal was ignited at the desired location at all four loads to give sufficient time for satisfactory burn out.

4.1.2 Test 2 - Gradual Load Changes at Lower Excess Air

The objective of this experiment was to gather information regarding the response of the stoker test facility to a reduced amount of combustion air from the near 'optimum' level. The total combustion air for the four load stages was reduced by an average of 15% from the operator's optimum with the same air distribution profile on the grate as in Test 1. Data presented in this section is compared to the near optimum response obtained from Test 1.

Following Test 1, the total amount of combustion air was reduced by 20% at 0.6MW and 10% at 0.3, 0.4 and 0.5MW, from the near optimum requirement in order to obtain the target oxygen concentration of between 3 to 5%. A smaller reduction in the combustion air for 0.3, 0.4 and 0.5MW was necessary as a 20% reduction resulted in oxygen concentration falling below 2% with very high CO levels (peak of 6000ppm). This can be seen in the first 3 load stages in Figure 4.4 and 4.5. However, at 0.6MW a 20% reduction from the optimum total satisfied the target oxygen band and this can be attributed to the relatively higher combustion intensity that prevailed at this load. The average CO level for this test run following gradual load changes with an O₂ concentration within the 3 to 5% range (after 2.5 hours into the test) was 65ppm. This represents an increase of 30% in the average CO production at a lower excess air level compared to those attainable at a near optimum air flow. However, this reduction in the total air flow did not have any significant effect on the average NO_x emission level which was 118ppm and again followed a similar profile to the oxygen trend.

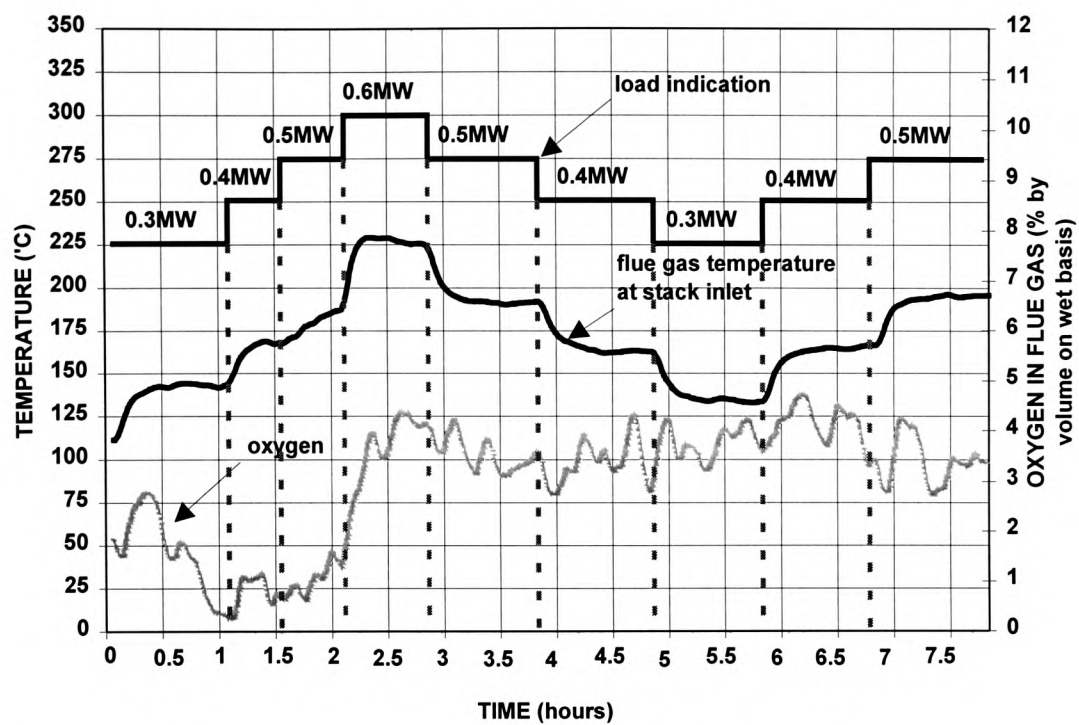


Figure 4.4 Flue Gas Temperature at the Stack Inlet & Oxygen Concentration in the Smoke Tube from Test 2

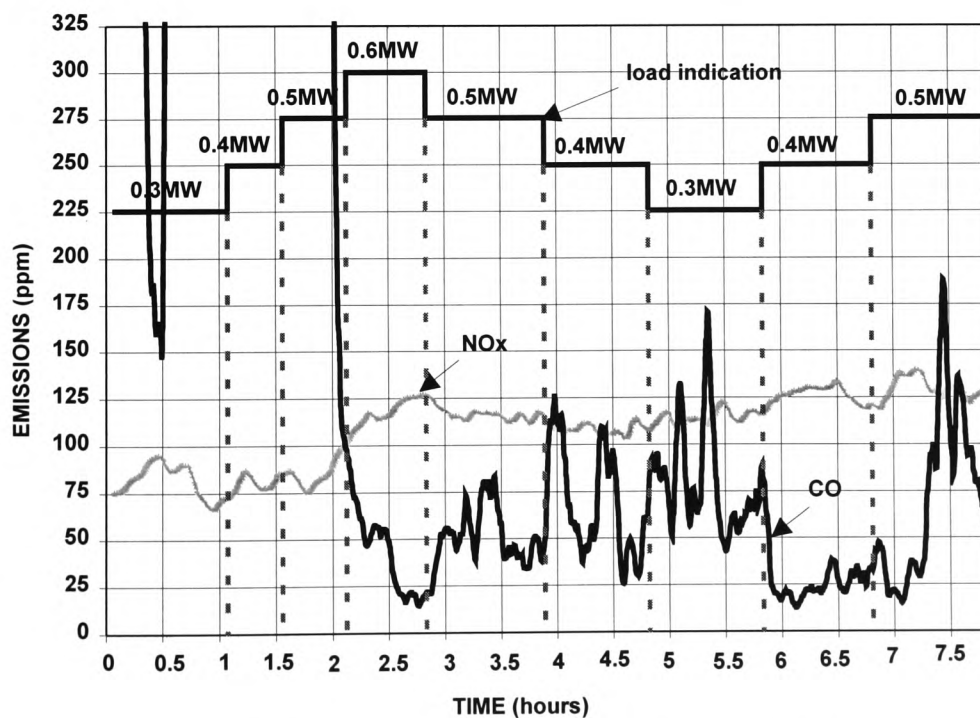

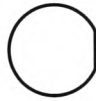
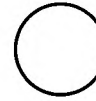
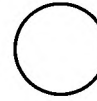


Figure 4.5 NO_x & CO Emissions in the Exhaust Duct from Test 2

Table 4.2 Grate Surface Temperature at the Stoker Front, Carbon in Ash Losses & Average Flame Front Location at Steady-State Combustion from Test 2

Boiler Load in MW	0.3	0.4	0.5	0.6
Grate Surface Temperature in °C	82	95	105	105
Unburned Carbon in Ash (% in weight of dry sample)	66.2	55.8	56.0	not available
Loss in Combustion Efficiency in %	4.90	3.50	4.15	not available
Average Flame Front Location at Steady-State Combustion				

Legend: Flame Front Location Through the Inspection Porthole (Figure 4.1)

Note: No ash sample was taken at 0.6MW because of the short test duration due to plate heat exchanger fouling.

Although the average CO level rose to 65ppm (an increase of 30% compared to Test 1), the increase in the grate surface temperature and the loss of unburned carbon in the grate ash were much more significant. As shown in Table 4.2, the average grate surface temperature was between 82 and 105°C suggesting that there was insufficient cooling air particularly at loads higher than 0.3MW. This can be attributed to the lower bed combustion intensity which hindered the formation of an adequate ash layer, in addition to an increase in unburned carbon. The average efficiency loss was 4.18% compared to 1.63% in Test 1, which represents an increase of 156% from those attainable at near optimum combustion. As in Test 1, the efficiency loss at 0.3MW was the highest suggesting that the air flow could be increased slightly to reduce the loss. The flame front was noted to be only occasionally visible at the right edge of the porthole (towards the furnace tube) and for loads greater than 0.4MW it was hardly visible (Table 4.2). This suggests that ignition of the fuel bed occurred later due to a less intense fire bed, resulting in a cooler refractory arch.

The excess air provided in this experiment resulted in an oxygen concentration of between 3 to 5%, which represented an excess air level of between 15 to 30% in bituminous coal firing. This reduction of excess air from the near optimum increased the CO emission although the penalty in the ash losses and the grate surface temperature were much more significant. The increase in efficiency loss in the grate ash can also be linked to the flame front location which occurred later due to non-optimal combustion on the fire bed. Data gathered from this experiment represents the non-optimal response of the stoker test facility to a lower excess air level.

4.1.3 Test 3 - Gradual Load Changes at Higher Excess Air

The objective of this experiment was to gather data regarding the response of the stoker test facility to a higher excess air level. The total combustion air for the four load stages was increased by an average of 15% from the operator's optimum with the same air distribution profile on the grate as in Test 1. Data reported in this section is compared to the standard obtained from Test 1.

Following Test 1 and 2, the total combustion air was raised by 10% at 0.6MW and 20% at 0.3, 0.4 and 0.5MW from the near optimum requirement to deliver the upper target oxygen band in the exhaust flue gas of between 7 to 9%. As the excess air requirement at high fire is less than at low fire in chain grate stokers, it follows therefore that in order to push the oxygen concentration higher than the near optimum band, more air will be required at lower [Livingston *et al.*, 1995]. This is shown in Figure 4.6, where the oxygen concentration fluctuated between 7 and 9% throughout the entire duration of the experiment.

With a higher excess air level, the CO emission dropped to an average of 25ppm (a 50% reduction from Test 1), which would be expected since the combustion intensity was elevated with more turbulence that better promoted the combustion of the volatile and char. The average NO_x level rose to approximately 140ppm, although such an increase from Test 1 (17%) was still far from causing any sort of concern over its emission (see Section 4.1.1 for limits on NO_x emission from stokers).

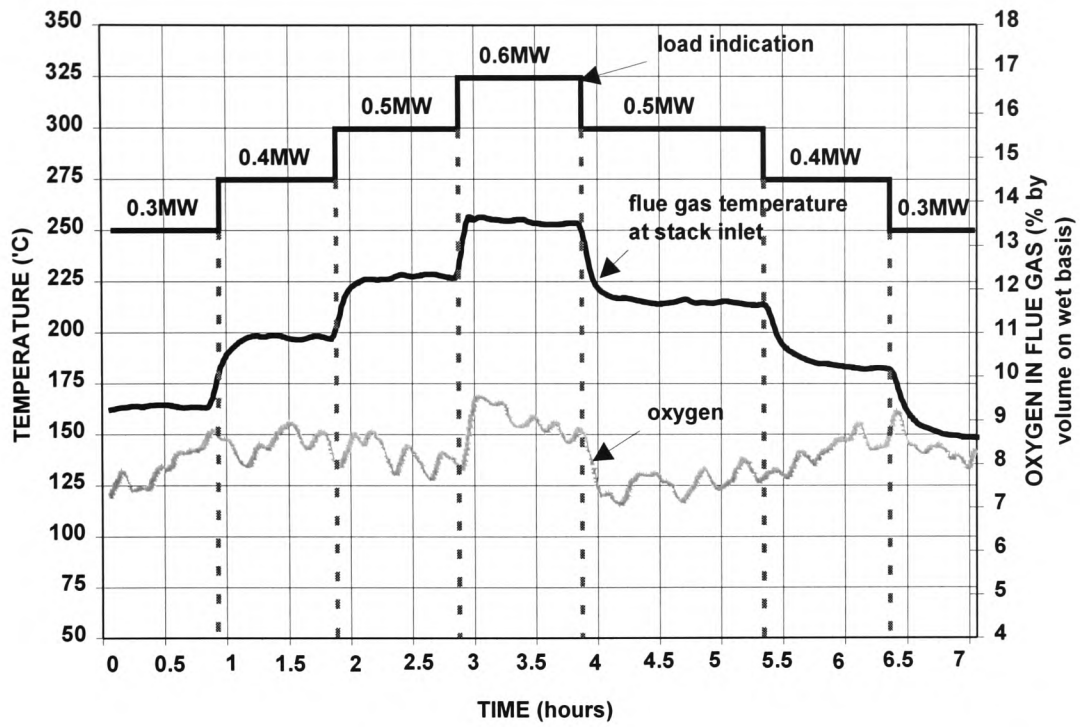


Figure 4.6 Flue Gas Temperature at the Stack Inlet & Oxygen Concentration in the Smoke Tube from Test 3

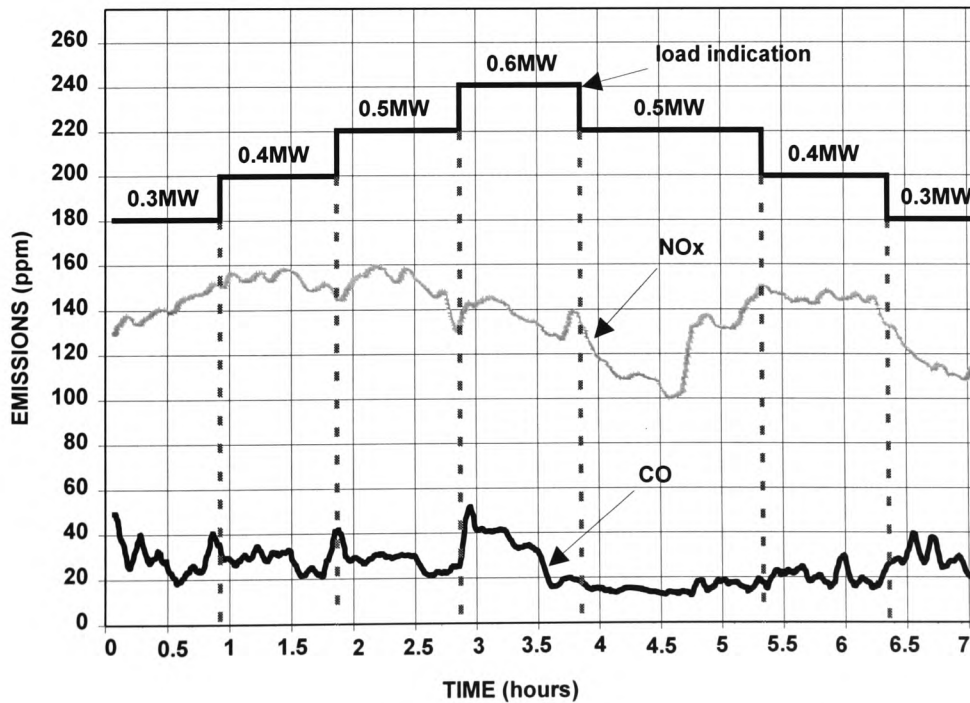


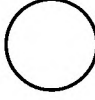
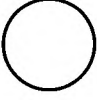


Figure 4.7 NO_x & CO Emissions in the Exhaust Duct from Test 3

Table 4.3 Grate Surface Temperature at the Stoker Front, Carbon in Ash Losses & Average Flame Front Location at Steady-State Combustion from Test 3

Boiler Load in MW	0.3	0.4	0.5	0.6
Grate Surface Temperature in °C	48	52	52	48
Unburned Carbon in Ash (% in weight of dry sample)	not available	29.6	23.6	26.8
Loss in Combustion Efficiency in %	not available	1.27	1.24	1.53
Average Flame Front Location at Steady-State Combustion				

Legend: Flame Front Location Through the Inspection Porthole (Figure 4.1)

Note: No ash sample was taken at 0.3MW due to fault in the ash removal system.

An increase in the combustion air provided more cooling to the grate which resulted in the grate surface temperature at the stoker front attaining an average of only 50°C (Table 4.3). By having more combustion air, a further reduction in the grate ash loss can be expected and an average efficiency loss in the ash of 1.34% was obtained in this experiment. However, this marginal reduction in the grate ash loss as compared to Test 1 (1.63%) following an increase in the excess air level, was attained at the expense of losing the overall combustion efficiency. The corresponding flue gas loss in this experiment was approximately 2% with the higher excess air level [Good Practice Guide 88, 1993]. This suggests that the increase in the air flow had raised the combustion intensity on the fire bed by a marginal amount only. Instead the additional air played a more significant role in cooling the flue gas and therefore the refractory arch. This is further supported by the flame front location of the four operating loads, which occurred towards the furnace tube, i.e. the arch wasn't warm enough to properly ignite the freshly supplied coal at the correct location.

The amount of excess air provided in this experiment resulted in an oxygen concentration in the flue gas of between 7 and 9%, which represented an excess air level of between 50 and 70% for bituminous coal firing. This resulted in a 50% reduction in the CO emission from the near optimum mark accompanied by a much cooler grate surface temperature. This however resulted in a small improvement in the carbon in ash losses. The increase in combustion air had a large negative effect on the stability of combustion as the additional air imposed a cooling effect on the arch, which resulted in the ignition of freshly charged coal occurring further into the furnace tube. This increase in excess air could easily have resulted in an additional 2% loss of combustion efficiency in the dry flue gas [Good Practice Guide 88, 1993; Good Practice Guide 30, 1992]. Data gathered from this experiment represent the non-optimal response of the stoker test facility to a higher excess air level.

4.1.4 Test 4 - Gradual Load Changes at Faster Grate Speed

After having investigated the variation in excess air levels to the combustion behaviour of the stoker test facility, this experiment was aimed at studying the boiler response to a variation in the coal feed rate. The rate of coal delivery onto the grate by the rotary valve remained unchanged, therefore the coal feed rate to the boiler was the same as in the previous tests. However the grate speed was increased by 20% from the setting in Test 1 which demonstrated non-optimal combustion on the grate due to less residence time for combustion and a thinner fire bed. As with the previous Sections, data gathered from this experiment is compared to the standard obtained from the operator's best practice (Test 1).

Although the oxygen concentration in the exhaust flue gas remained mostly within the 5 to 7% optimum band suggesting that the combustion intensity was comparable to Test 1, a closer analysis revealed that the overall oxygen concentration in this experiment was higher by 1% than that achieved in Test 1. This was derived by comparing the average oxygen concentration of the two experiments (5.3% from Test 1 and 6.2 from Test 4). Therefore the amount of oxygen consumed was less in this case than for optimum grate speed settings.

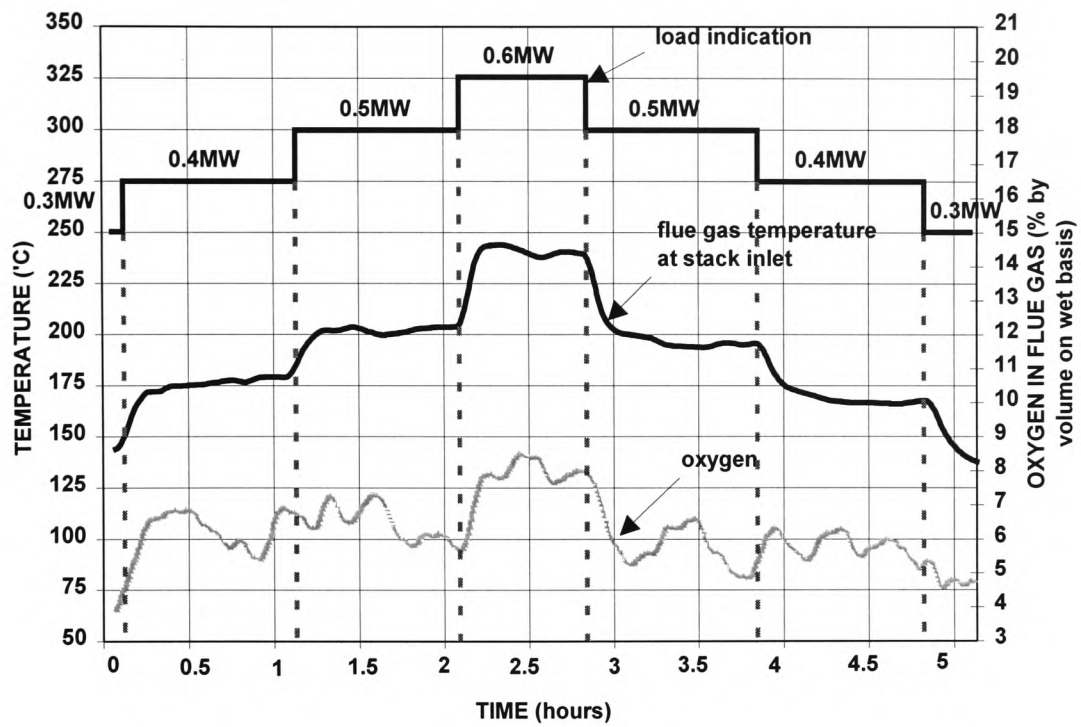


Figure 4.8 Flue Gas Temperature at the Stack Inlet & Oxygen Concentration in the Smoke Tube from Test 4

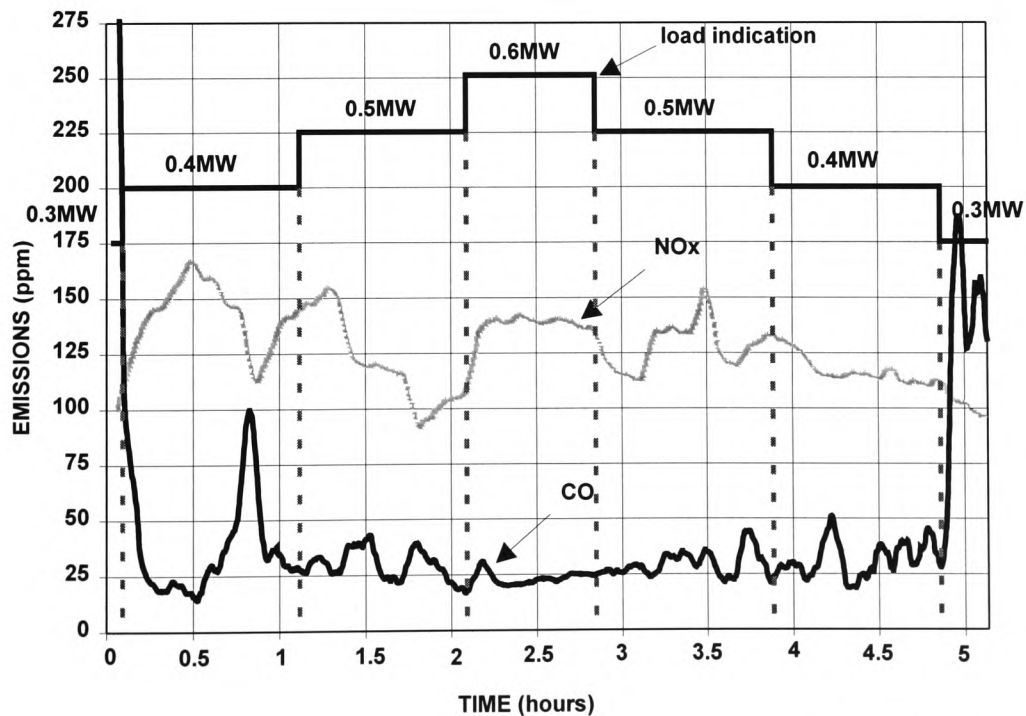

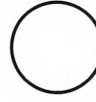
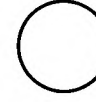
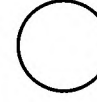


Figure 4.9 NO_x & CO Emissions in the Exhaust Duct from Test 4

This confirms the statement made earlier in this Section, that when coal being transported into the combustion chamber had a shorter residence time it will lead to a poorer burn out. The average CO level remained very low (40ppm), suggesting that there was sufficient air available for the mixing and combustion of volatile matter, particularly in this experiment as the fuel bed was thinner which allowed better air penetration. As with Tests 2 and 3 there was hardly any change in the average NO_x level (126ppm) recorded in this experiment as compared to Test 1 (120ppm).

Table 4.4 Grate Surface Temperature at the Stoker Front, Carbon in Ash Losses & Average Flame Front Location at Steady-State Combustion from Test 4

Boiler Load in MW	0.3	0.4	0.5	0.6
Grate Surface Temperature in °C	80	92	87	90
Unburned Carbon in Ash (%) in weight of dry sample)	41.5	62.6	43.7	51.3
Loss in Combustion Efficiency in %	5.40	3.93	3.76	4.23
Average Flame Front Location at Steady-State Combustion				

Legend: Flame Front Location Through the Inspection Porthole (Figure 4.1)

The grate surface temperature rose to between 80 and 90°C, indicating that the fire bed was longer since the same amount of air was provided here as in Test 1, i.e. burning coal was transported to the rear end of the grate having a thinner ash layer. This was accompanied by an increase in the average grate ash loss to 4.33% (Table 4.4), which is 165% higher than the average attainable with the optimal grate speed setting. As with Test 1, the loss at 0.3MW was the highest, suggesting that the combustion intensity was the lowest at this load. Finally the higher grate speed also resulted in a shift in the ignition plane towards the furnace tube and as shown in Table 4.4, the flame front was just visible at 0.3 and 0.4MW, whilst at higher loads it was not within

the visible range, i.e. the speed at which coal can be ignited was slower than the rate at which fresh coal was being fed to the stoker.

In this test the increase in grate speed resulted in higher grate ash losses and increased grate surface temperature despite having the 'optimum' combustion air (as in Test 1). The oxygen concentration in the flue gas remained mostly within 5 to 7% suggesting that the combustion intensity was comparable to Test 1, although the overall oxygen concentration was higher by 1%. This can be attributed to the shorter time on the fire bed for satisfactory coal burnout. The CO level was low (average of 40ppm) as the thinner bed allowed better air penetration for the mixing and combustion of the volatile. As with the previous tests, the average NO_x level remained low.

4.1.5 Test 5 - Gradual Load Changes with a Uniform Air Distribution

The aim of this experiment was to simulate the scenario of many industrial chain grate stokers having only a simplistic air distribution facility. The simplest case was adopted by considering no under-grate damper, with the total combustion air flow being equally divided between the four air plenums on the grate. For the purpose of comparison with the optimum bench mark, the coal feed and air flow settings employed in Test 1 were adopted for the four load stages in this experiment.

The first observation that can be made is the lower 'settling band' of the flue gas oxygen concentration for all four load stages (with an average oxygen concentration of 3.1% compared to 5.5% in Test 1), despite having the supposedly 'near optimum' combustion air as in Test 1. In this Test, the air supplied to the 1st section was considerably higher (25% of the total air flow) than in Test 1 and the stoker was noticed to be 'smoking' at the front. This meant that a fair portion of the airflow supplied to the first section escaped without playing any significant role in combustion. It follows therefore that the total amount of combustion air supplied to the 3 remaining sections on the grate was in fact lower in this experiment than in Test 1. The deficit in

combustion air was accompanied by an overall fall in the flue gas temperature by 10°C and also a lower average NO_x production of 78 ppm (35% lower than at operator's optimum). This clearly suggests that the combustion intensity on the bed in this test was lower, which can be expected since 50% of the total airflow was supplied to the two middle sections as compared to 80% at operator's best practice. Further evidence to point to a reduced boiler performance can be found in the higher efficiency losses in the ash, with an average of 3.04% compared to 1.63% in Test 1. This is also reflected in the higher grate surface temperature as less ash was formed, which further confirms that the combustion process was in fact *less optimal* than the operator's best practice. There was no concern over the CO emission (average of 43 ppm) since the airflow to the last section on the grate was higher (25% of the total compared to about 10% in Test 1), hence supplying the additional air required for the combustion of the volatile matters. Despite a relatively less intense fire in the furnace tube, the average flame front locations were highly comparable to Test 1 owing to the plentiful supply of oxygen for the ignition of fresh charge in the first section on the grate.

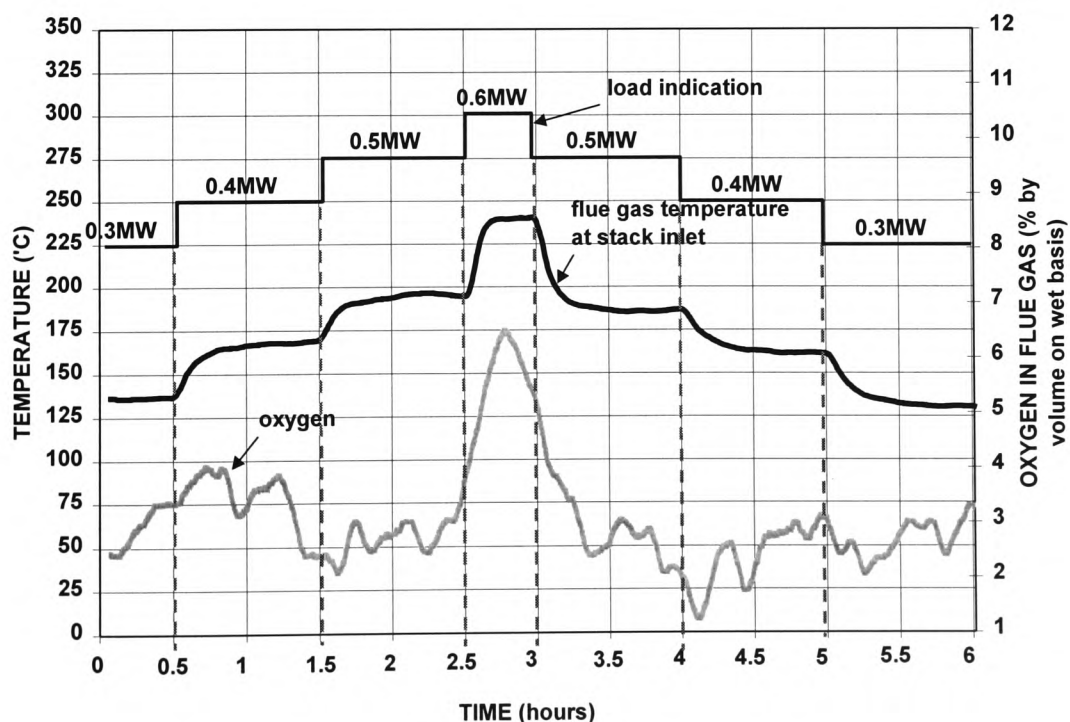


Figure 4.10 Flue Gas Temperature at the Stack Inlet & Oxygen Concentration in the Smoke Tube from Test 5

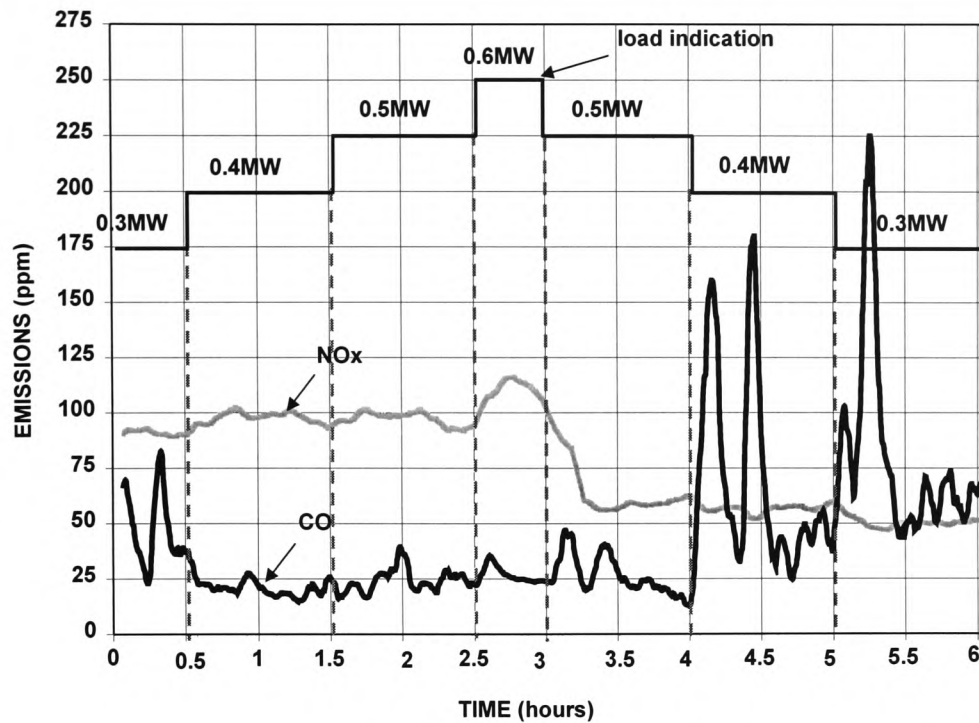






Figure 4.11 NO_x & CO Emissions in the Exhaust Duct from Test 5

Table 4.5 Grate Surface Temperature at the Stoker Front, Carbon in Ash Losses & Average Flame Front Location at Steady-State Combustion from Test 5

Boiler Load in MW	0.3	0.4	0.5	0.6
Grate Surface Temperature in °C	86	90	92	88
Unburned Carbon in Ash (% in weight of dry sample)	43.7	43.5	49.2	not available
Loss in Combustion Efficiency in %	2.45	2.35	4.31	not available
Average Flame Front Location at Steady-State Combustion				

Legend: Flame Front Location Through the Inspection Porthole (Figure 4.1)

Note: No ash sample was taken at 0.6MW because of the short test duration due to plate heat exchanger fouling.

In this scenario of stoker fired boiler operation, the plant operator would *increase* the total air flow to raise the flue gas temperature in order to avoid problems associated with sulphuric acid deposition on the surface of the stack (temperature lower than 140°C), and to provide a higher degree of cooling to the grate. This will inevitably result in a further loss in combustion efficiency since satisfactory plant operation would otherwise have been obtained by having the correct air distribution profile. Moreover, higher suction would be required by the ID fan (hence increased power consumption) in order to maintain clean plant operation therefore further contributing to this flue gas loss. The NO_x level remained lower than Test 1, as the amount of combustion air supplied to the combustion zone has been decreased.

4.1.6 Summary of Section 4.1

The main objective of the experiments carried out in this Section were to generate the necessary data bases required for the training of the neural networks, to be used in a control strategy formulated from the experience of the field expert. An experiment based on the expert operator's best practice was carried out to serve as the bench mark for 'optimum' boiler operation before a range of variations from this optimum mark were investigated. These variations included lower and higher excess air level, higher grate speed and a simplistic air distribution profile on the grate. Results gathered from a wide spectrum of sensors have confirmed the criteria for optimum stoker operation and have demonstrated the improvements that can be obtained. These criteria were the provision of a 'near optimum' setting of the input parameters coupled with a suitable air distribution profile on the grate.

4.2 Boiler Response to Large Load Changes

The objective of the experiments was to find a rapid way to run the boiler from turn down to full load and vice versa whilst maintaining stable combustion and acceptable transient CO emissions. Stable combustion here refers to a visible flame front through the inspection porthole, as illustrated in the introduction to this Chapter. It was for this reason that an average flame front location has been provided every 5 minutes of the entire test duration to provide the reader with an indication of its movement following changes in the input parameters (coal feed and air flow). Two experiments, Tests 6 and 7, were conducted by varying the staging sequence of coal feed and air flow in both magnitude and direction following large load changes. In this Section, the staging sequence in Tests 6 and 7 are more conveniently referred to as 'Staging Profile' (SP) 1 and 2 respectively.

The coal feed and air flow settings at 0.3 and 0.6MW were at the operator's best practice and that the air distribution profile on the grate was as in Test 1. The staging of coal feed and air flow was completed within 2 to 3 minutes in both tests. This time period was necessary as sudden large changes in the combustion air can disrupt the safe operation of the boiler. In particular when operating from 0.3 to 0.6MW, increasing the air flow rapidly could cause the flue gas in the furnace chamber to escape through the stoker front. This would happen when the slight suction provided by the induced draught fan was not able to overcome the sudden increase in furnace pressure.

The average time taken to reach steady-state combustion, with reference to the flue gas temperature, from the point of load change was about 20 minutes. This shows that the time allowed for staging to complete is relatively short. The main criteria for a satisfactory transient boiler response were low CO emissions, minimum deviation in the oxygen concentration from the optimal band and a visible flame front through the porthole. The transient boiler response following the two staging profiles is compared and discussed in the following two sub-sections and the improvements attained with a desirable staging profile have been highlighted in the conclusion to this section.

4.2.1 Test 6 - Large Load Changes with Staging Profile 1

The boiler load was changed from 0.3 to 0.6MW and back down to 0.3MW with the staging sequence as illustrated in Figure 4.12 shown below.

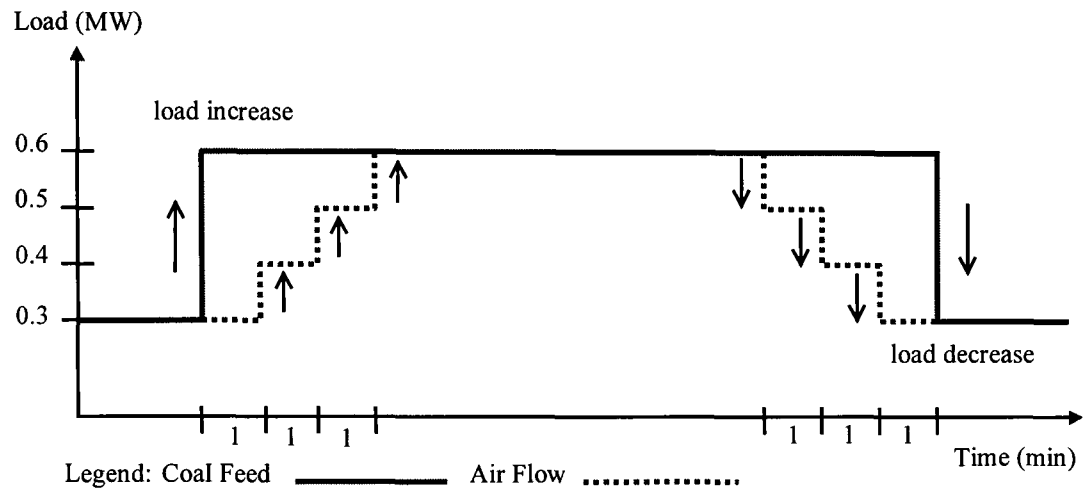


Figure 4.12 Coal Feed & Air Flow Staging Sequence Following Large Load Changes in Test 6 with Staging Profile 1

On load increase, the coal feed (rotary valve and grate speed) was brought up to the setting required for 0.6MW in a single step, followed by increasing the air feed 1 minute after, in three 0.1MW steps over a period of 2 minutes, i.e. the total time for the staging of coal feed and air flow was 3 minutes. This staging sequence is referred to as coal leading the air flow on load increase.

Upon load decrease, the air flow was brought down first in 0.1MW steps over a period of 2 minutes to the setting of 0.3MW before reducing the coal feed rate one minute after in a single step. Therefore this staging sequence is referred to as air leading the coal feed on load decrease. The boiler response particularly during transients is discussed with reference to the CO and NO_x emissions, oxygen fluctuation in the flue gas and flame front movement.

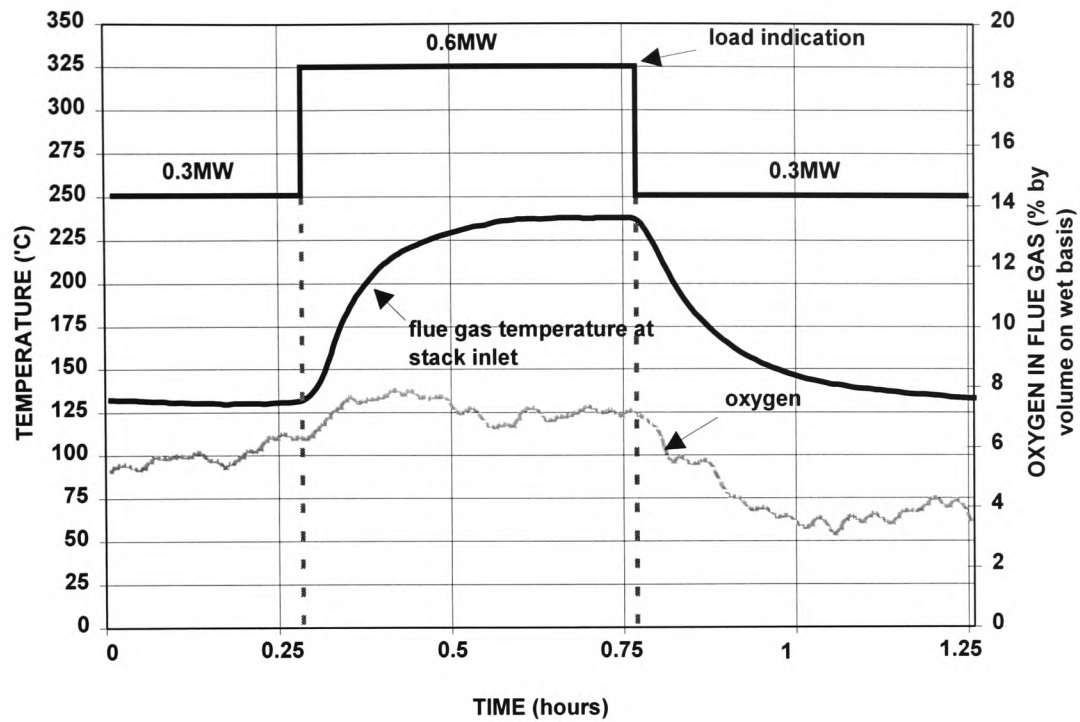


Figure 4.13 Flue Gas Temperature at the Stack Inlet & Oxygen Concentration in the Smoke Tube from Test 6 - Staging Profile 1

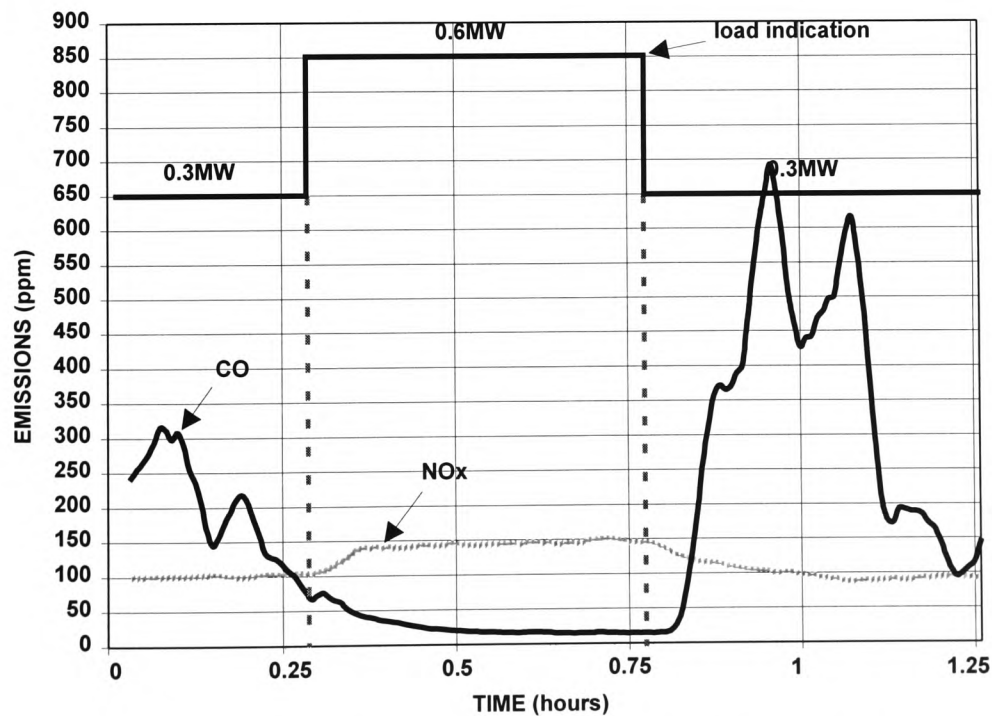


Figure 4.14 NO_x & CO Emissions in the Exhaust Duct from Test 6 - Staging Profile 1






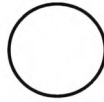

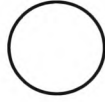
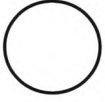
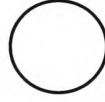
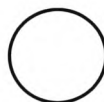

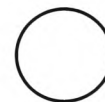


On load increase - Since the boiler required a much longer time to respond to any changes in the coal feed (between 15 and 20 minutes to reach steady-state, depending on the load) as opposed to the combustion air (in the order of 15 seconds), leading the coal first on load increase did not have much effect on the transient CO emissions as shown in Figure 4.14. The higher values of CO (peak of 310ppm), before the load change from 0.3MW to 0.6MW was a result from a change in the depth of the fire bed that occurred in Test 4. The oxygen concentration in the flue gas climbed from about 5.5% recorded during the steady-state of 0.3MW to almost 8% during the first 15 minutes into the 0.6MW load stage, a maximum overshoot of 1% from the upper limit of the optimum band (5 to 7%) before settling down to about 7% as the combustion reached steady-state. As the setting of coal and air were at the operator's optimum, the CO emission remained low at about 25ppm at steady-state. The NO_x level rose from 100ppm to approximately 140ppm as a result of the load increase due to the higher bed temperature and air supply.

On load decrease - As can be seen in Figure 4.14, the transient CO emissions on load decrease was much higher (with peak of 700ppm). This can be attributed to the fact that combustion air was brought down first resulting in a situation where there was a sudden deficit in combustion air whilst the combustion intensity on the fire bed was still high (0.6MW). This resulted in the much higher emission of CO during the transient condition. A corresponding drop in the oxygen concentration to 3% from 7% (at steady-state of 0.6MW) can also be seen, before it gradually climbed up to 4% as the combustion rate moved towards 0.3MW. As for the NO_x emission, it went back down to about 100ppm from 140ppm following the drop in the load with hardly any undershoot.

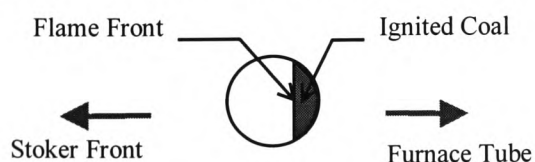
The first observation made of the flame front movement with this staging sequence on *load increase* is that it moved quite considerably only after the first 5 minutes into the 0.6MW load stage. As the combustion progressed the flame front moved further towards the furnace tube and as shown in Table 4.6, it wasn't visible through the inspection porthole at steady-state. This suggests that the ignition rate of the fresh coal was being delayed as compared to Test 1 when the flame front was seen at the right

edge of the circle at steady-state combustion. It wasn't until a drop in the load back down to 0.3MW before the flame front was brought back into sight. This was attributed to a slower grate speed and the higher combustion intensity on the fire bed initially. The first glimpse was 15 minutes after the load change from 0.6 to 0.3MW. At the lower load the location of the flame front was where it should be, as in the steady-state combustion of Test 1.

Table 4.6 Average Flame Front Movement from Test 6 with Staging Profile (SP) 1

Steady-State of 0.3MW at Optimum Air		0.3 to 0.6MW with SP 1 (0 min)	5 min	10 min
				
15 min	20 min	25 min	0.6 to 0.3MW with SP 1 (30 min)	35 min
				
40 min	45 min	50 min	55 min	60 min
				

Legend: Flame Front Location Through the Inspection Porthole



The transient CO emissions on load decrease were found to be higher than on load increase. This was due to an initially high combustion intensity on the fire bed which was starved of combustion air, as the air flow was reduced first before the coal feed. This also resulted in a dip in the oxygen level to almost 3% which was 2% below the

lower limit of the optimum band. A smaller overshoot in the oxygen level was seen on load increase with a peak of 8%, which was 1% higher than the upper optimum limit before settling to 7% at steady-state, although the flame front was more visible on load decrease than on load increase. NO_x emission was found to be highly acceptable during both transient and steady-state conditions.

4.2.2 Test 7 - Large Load Changes with Staging Profile 2

The boiler load was altered from 0.3 to 0.6MW and back down to 0.3MW with the staging sequence as illustrated in Figure 4.15 shown below.

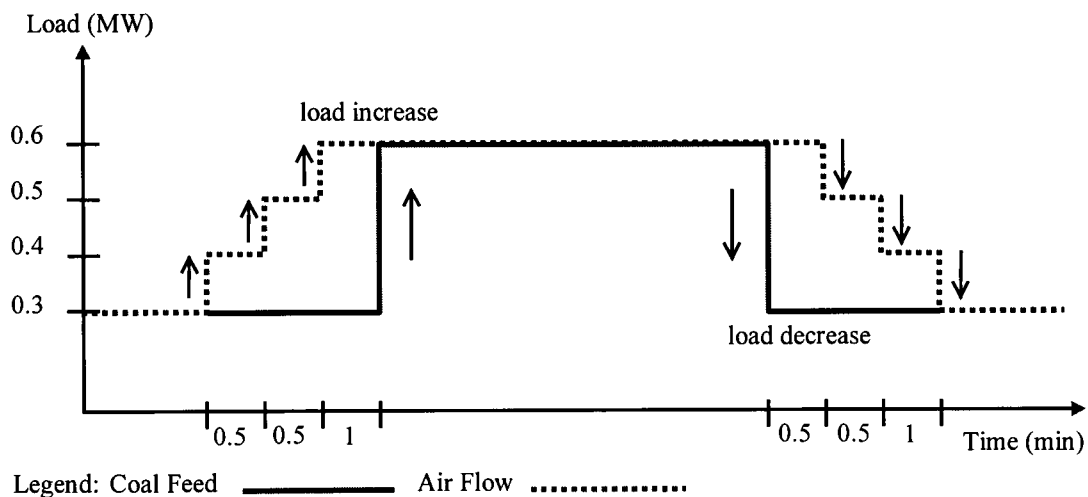


Figure 4.15 Coal Feed & Air Flow Staging Sequence Following Large Load Changes in Test 7 with Staging Profile 2

On load increase, the air flow was stepped up to the setting for 0.6MW in three 0.1MW steps over a time period of 1 minute, followed by increasing the coal feed one minute after that in a single step. Note that the time allowed for changes in the combustion air to complete was shortened by half compared to Test 6. The aim was to investigate the extent of overshoot or undershoot of the oxygen concentration following a more rapid change in the air flow. This staging sequence is referred to as air leading the coal feed on load increase.

Upon load decrease, the coal feed was brought down first in a single step to the setting of 0.3MW before reducing the air flow 1 minute after in three 0.1MW steps over a period of 1 minute. Similar to that for load increase, the time allowed for the staging of combustion air to complete was half than in Test 6. This staging sequence on load decrease is referred to as coal leading the air flow on load decrease. The boiler response particularly during the transients is discussed with reference to the CO and NO_x emissions, oxygen fluctuation in the flue gas and flame front movement.

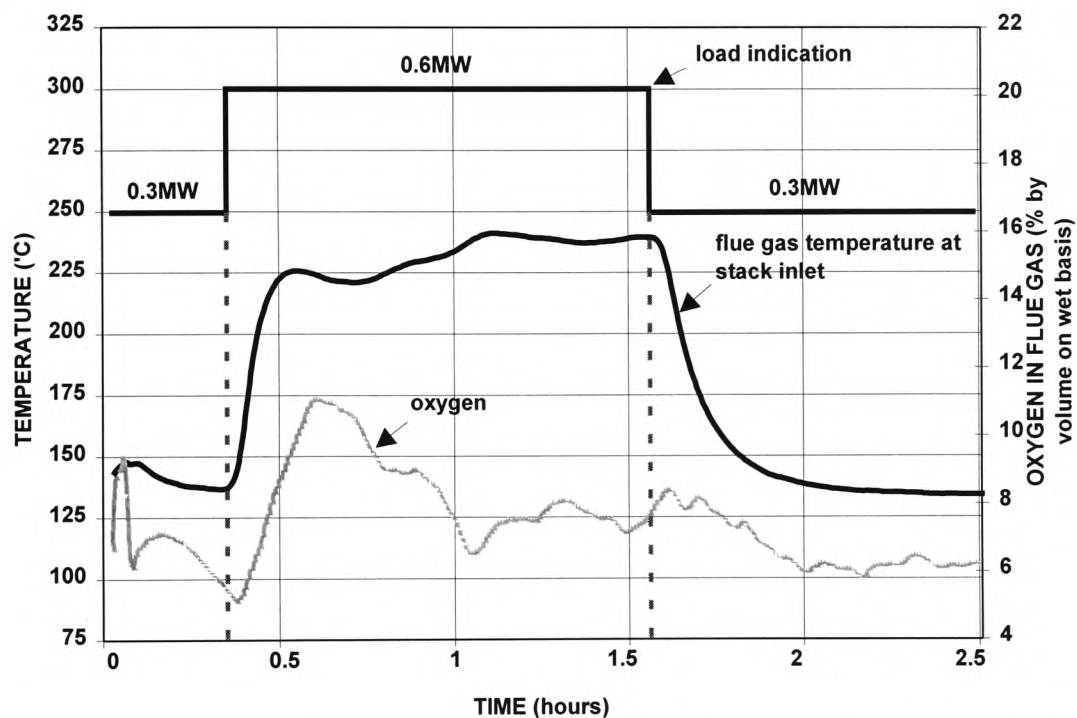


Figure 4.16 Flue Gas Temperature at the Stack Inlet & Oxygen Concentration in the Smoke Tube from Test 7 - Staging Profile 2

On load increase - Following Test 6, the aim was to provide a higher combustion intensity on the fire bed before introducing more coal onto the grate. As illustrated in Figure 4.17, the high CO emission before the load change (due to a previous experiment) dropped from an average of about 125ppm to less than 50ppm. This resulted from the combustion air increasing the combustion intensity with sufficient air turbulence to burn off the volatile matters prior to feeding more coal onto the grate. Increasing the air first and faster (than in Test 6) resulted in a surge in the oxygen concentration from 5% to 11%, 15 minutes after the load change to 0.6MW. As the

combustion on the fire bed steadied out the oxygen level fell gradually from 11% over the next 20 minutes hovering just above the 7% mark (Figure 4.16). In addition, the flue gas temperature took longer to steady out as compared to Test 6, which in a practical situation is highly undesirable as the main objective would be to achieve the target hot water or steam temperature as quickly as possible. Finally, NO_x emission rose from 85ppm to about 135ppm as a result of the load increase with hardly any overshoot despite the large oxygen fluctuation during the transient (Figure 4.17).

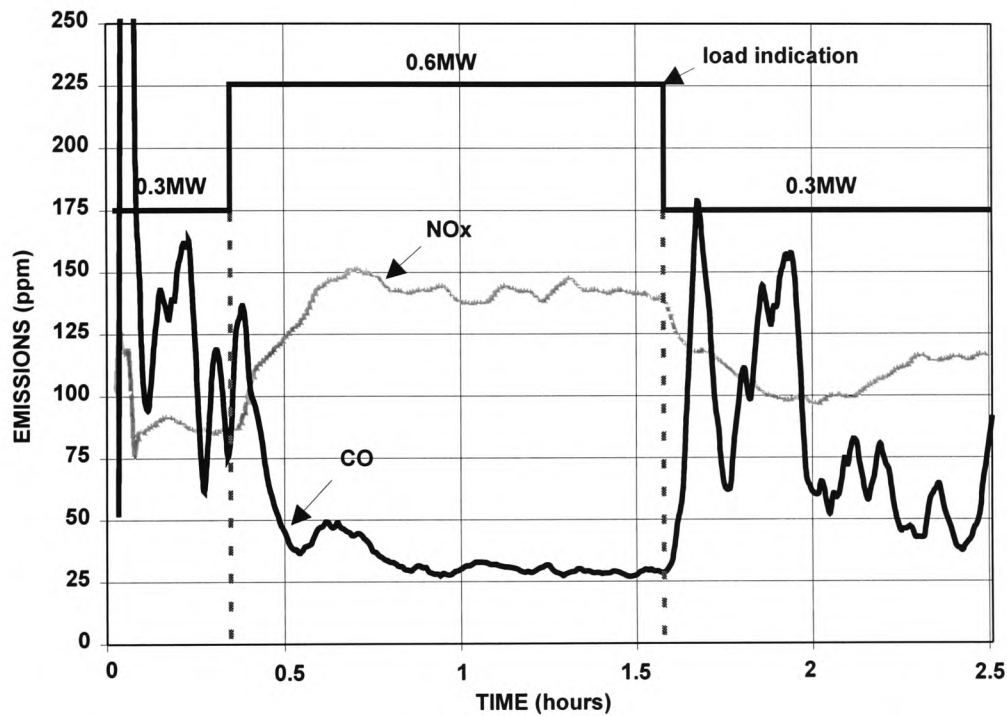


Figure 4.17 NO_x & CO Emissions in the Exhaust Duct from Test 7 - Staging Profile 2

On load decrease - A steadier oxygen trend can be observed during the transient period of load decrease as compared to Test 6, where it fell from about 7.5% at steady-state of 0.6MW to about 6% in 25 minutes with hardly any undershoot and remained at that level in the steady-state condition of 0.3MW (Figure 4.16). The flue gas temperature curve was also much smoother than on load increase. This improved response was a result of providing enough air during the first few minutes after the load change in order to meet the air demand of an initially intense fire bed before bringing the air down gradually to match the less intense fire bed of 0.3MW. Since the boiler response time to changes in the coal feed was considerably longer than changes







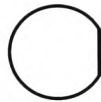
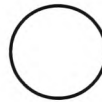
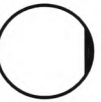
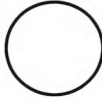
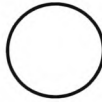
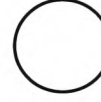
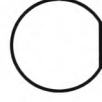
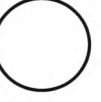
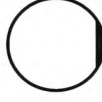
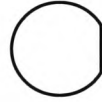
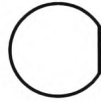


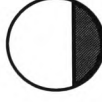









in the air feed, the fuel feed was brought down in just a single step. This improved condition is reflected in the low transient CO emissions with a peak of 175ppm, compared to the 700ppm of Test 6, before settling to around 60ppm at steady-state as illustrated in Figure 4.17. Finally, the NO_x level dropped from about 140ppm at a steady-state of 0.6MW to just under 100ppm before settling at about 110ppm and again posed little concern.

As in Test 6, the flame front was much more visible on load decrease than on load increase as shown in Table 4.7. Careful observation revealed that the rate at which the flame front moved forward was slower in the first 20 minutes, after the load increase from 0.3 to 0.6MW than during Test 6. This is in agreement with the statement made by Gunn (1982) on providing a higher combustion intensity on the fire bed prior to introducing more fresh coal will help to maintain an adequate ignition rate to match the higher grate speed. Furthermore the flame front was seen 75% of the time in the first 30 minutes after the load change to 0.6MW had occurred, compared to only 50% for Test 6. On load decrease, the flame front returned to the inspection porthole much faster than in Test 6 and this can be explained by the initial provision of a higher combustion intensity on the bed following the load change to 0.3MW. Here the air flow was kept to the 0.6MW setting for a few minutes after the coal feed had been dropped to 0.3MW. The flame front was seen throughout the entire remaining duration of this test compared to only half of the 30 minutes test duration in Test 6.

The transient emission of CO on load decrease was improved in this experiment, compared to Test 6, along with maintaining a steadier oxygen response by bringing down the coal feed first before the combustion air. Changing the air faster did not have any adverse effect on load decrease but on load increase, this attempt resulted in large oxygen overshoot and as a consequence caused pro-longed transient behaviour. This was clearly shown in the flue gas temperature profile, where the time taken to reach steady-state (235°C) was almost 50 minutes from the point of load change compared to 25 minutes in Test 6. The NO_x emissions at both transient and steady-state conditions proved to be acceptable. Ignition plane movement was minimised on both load

increase and decrease in this test than in Test 6, suggesting that the ignition rate was better maintained during the large load changes with Staging Profile 2.

Table 4.7 Average Flame Front Movement from Test 7 with Staging Profile (SP) 2

Steady-State of 0.3MW at Optimum Air		0.3 to 0.6MW with SP 1 (0 min)	5 min	10 min
				
15 min	20 min	25 min	30 min	35 min
				
40 min	45 min	50 min	55 min	60 min
				
65 mins	0.6 to 0.3MW with SP 2 (70 min)	75 min	80 min	85 min
				
90 min	95 min	100 min	105 min	110 min
				
115 min	120 min	125 min	130 min	
				

Legend: Flame Front Location Through the Inspection Porthole (Figure 4.1)

4.2.3 Conclusions of Section 4.2

The aim of the experiments conducted in this Section was to determine the best possible means of manipulating the input parameters in order to meet large demands in load. This ‘knowledge’ is essential in order to enable the NNBC to operate the stoker test facility efficiently during large load following conditions. The following conclusions can be drawn.

On load increase – changing the air flow first over a period of *at least 2 minutes* before increasing the coal feed rate shortly (1 minute) after. Both the CO and NO_x emissions during the transient period following such staging profile have been found to be of little concern. Leading the air gradually before the coal feed on load increase also helped to minimise the oxygen overshoot and maintained a better rate of ignition.

On load decrease - the coal feed must be brought down before gradually reducing the air flow over a period of *at least 1 minute*. Considerable improvements in the transient CO emission and oxygen response have been demonstrated in comparison to the reverse staging profile. In addition, it has also been shown to maintain the flame front within the view of the porthole for the entire duration of the test period. The NO_x emissions during both transient and steady-state periods were highly acceptable.

5. Development & Testing of the Neural Network Based Controller & Black Box Models

This Chapter is concerned with the artificial neural networks development aspect of the research project. It essentially involves two distinct areas, namely the development and testing of the neural network based controller, and the development of the black box models of the combustion process.

The controller development involved careful selection of the actual plant data (training data) which were presented to the neural networks during the learning phase and subsequently these neural network components were integrated within a carefully devised control strategy, based on expert human operator experience. Upon completion, the prototype controller was commissioned and its performance tested. The plant response under the influence of the neural network based controller was compared against operator's best practice. Test results have been discussed and conclusions drawn.

The neural modelling was concerned with the identification of the underlying dynamics of pollutant formation, namely carbon monoxide and nitrogen oxides, and also the combustion process itself using ANNs. The feed-forward Multi-Layered Perceptron (MLP) neural network was used in conjunction with the Auto Regressive with eXogenous inputs (ARX) regressor structure for the task of identifying the dynamics of the processes. The developed models were refined and validated with unseen data sets in order to examine the model's prediction capability. Finally conclusions are drawn in the last section of this Chapter.

5.1 The Concept of the Control Strategy - Minimising Boiler Losses

This section serves as a prelude to illustrate the fundamental concept of the control strategy before progressing into the next two sections which deal with the software development aspect and the real-time testing of the neural network based controller. Justifications are made with respect to the adopted control strategy, its logical decision making paths, the knowledge base components (constructed with feed forward neural networks) and the way in which these components were integrated. Since the dynamics of the plant cannot be established from a conventional control view point, the strategy adopted here was essentially based on the experience and decision making process of an expert human operator, and artificial neural networks were used to encapsulate the expert operator's knowledge. The following subsections are arranged as follows; a little background to summarise the aspects of lump coal combustion on grates, followed by the target areas where heat losses can be practically minimised without incurring any additional expenditure, hence areas where combustion efficiency can be salvaged, and lastly a detailed description of the proposed control strategy in order to optimise the operation of the stoker boiler plant in ways which the expert human operator would.

5.1.1 Background

As has already been discussed in Chapter 2, the combustion of lump coal on grates is a complex combination of chemical reactions, heat transfer and mass transfer processes which can result in inefficient burning with increased pollutant emissions if the governing factors are not properly controlled. Therefore, it is vital to maintain stable ignition and combustion on the grate, whilst allowing sufficient air and time for a high degree of carbon burn out and also to maximise the combustion of volatile matters and carbon monoxide. In addition, thorough mixing of the reacting substances with oxygen is required to ensure near complete combustion and since ideal stoichiometric conditions are difficult to attain, excess air is needed to provide turbulence for better mixing and completeness of combustion. This is particularly true for the burning of

solid fuels since the air required for combustion is less readily available to the mass of fuel when compared to oil or gas. However, the minimum level of excess air is required as the sensible heat loss in the flue gas increases with the excess air level. It is also equally important to distribute the primary air to suit the requirements of the different fuel bed profiles on the grate at different loads - i.e. the fire bed at turndown is shorter than at full load. In addition, an adequate air supply must be made available at the end section of the grate to provide sufficient cooling for the safe operation of the plant, particularly when burning coals with relatively low ash content (4% in this work - NCB Rank Code 802). However, the quantity must be kept to a minimum since the air that passes through this final section of the grate will have little effect on the combustion of both char and volatile matters therefore contributing towards the sensible heat loss from the boiler. Details of the empirically derived 'near optimum' primary air (oxygen in the flue gas of between 5 to 7%) and its distribution profile in the four wind-boxes for each boiler load (0.3, 0.4, 0.5 & 0.6MW) can be found in Section 3.3.2. The chain grate test facility when operated at operator's best practice at 0.3, 0.4, 0.5 and 0.6MW, had an average excess air level with reference to the oxygen content in the flue gas of 40%. This value is lower than its industrial counterparts which register a typical excess air level of 55% or more, owing to a better air distribution system on the test facility. Details of the air distribution facility can be found in Section 3.1.2.

5.1.2 Minimising Boiler Losses

In essence, to improve the combustion efficiency of the chain grate stoker test facility, one must first identify the areas where heat losses are most likely to occur. The three main target areas where heat losses can be minimised are; the sensible heat loss in the flue gas, heat loss due to smoke/carbon monoxide and losses due to the unburned combustibles in the grate ash [Good Practice Guide 30, 1992; Good Practice Guide 88, 1993]. Table 5.1 below summarises the likely cause(s) of these losses, the implications on the plant performance and also practical remedies to salvage valuable efficiency from these aspects of energy losses.

Table 5.1 Target Areas for Minimising Boiler Losses, Implications on the Plant & Practical Remedies [Good Practice Guide 30, 1992]

Target Areas	Main Causes, Implications on the Plant and Practical Remedies
Sensible heat loss	<ol style="list-style-type: none"> 1. Cause - High excess air level. 2. Implications - Lowering of thermal efficiency (6% increase in O_2 translates to a further 6.5% loss of ζ) and possibly higher grit carryover if a high percentage of fines in the fuel is present. 3. Remedies - Use the correct coal size, proper stoking practices and better control of both on-grate and over-grate combustion air.
Heat loss due to CO	<ol style="list-style-type: none"> 1. Cause - Air starvation, inadequate turbulence for proper air/fuel mixing, and/or ingress of cold air 'freezing' parts of the fire bed due to improper body insulation. 2. Implications - Small ζ loss in terms of non-conversion of carbon to CO_2, however the penalty in boiler fouling can be severe. De-rated plant performance if operated in such reduced conditions over an extended period of time. 3. Remedies - Correct level of excess air with proper air distribution on the fuel bed. The correct fuel size must be used to prevent clogging of fine spacing between grate links in order to allow under-grate air to pass and achieve good fuel/air mixing.
Grate ash loss	<ol style="list-style-type: none"> 1. Cause - Air starvation, fuel bed too thick (ignition plane shifting into the furnace tube), poor fuel distribution on the grate due to improper stoking practices giving rise to 'holes' in the bed (therefore allowing under-grate air to escape). 2. Implications - Increased ζ loss in unburned carbon, and possibly boiler fouling due to insufficient air supply. There is a danger of losing the fire if further ignition plane movement into the furnace tube is not rectified soon enough. 3. Remedies - Correct stoking practices, near optimum set-up of matching coal and air feed is essential throughout the entire load range. Regular inspection through the porthole to check for flames in order to ensure stability of combustion.

5.1.3 The Control Approach

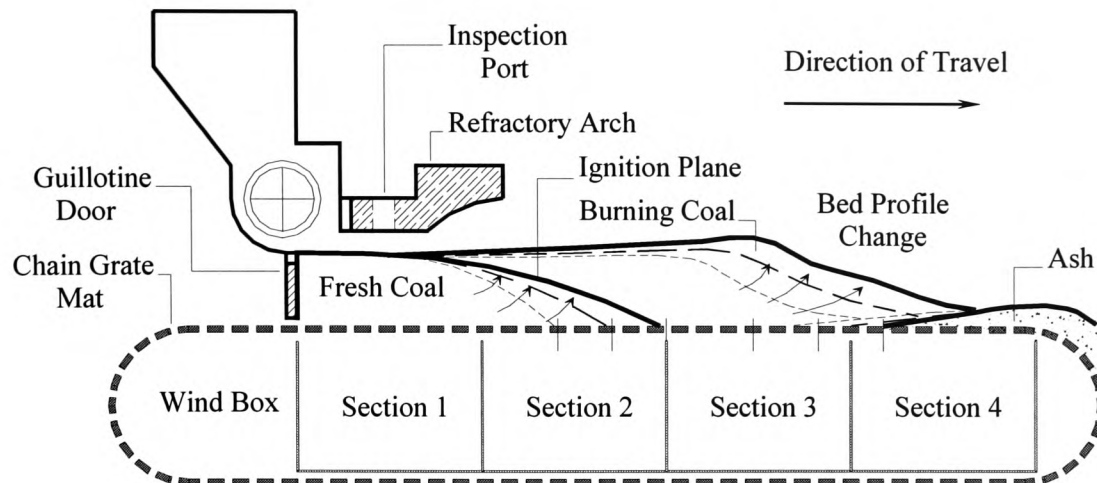
Before progressing further it is important to note that when the experiments were carried out, the test facility was in a good condition, and the fuel used in both manual and control experiments were to the expected quality and size distributions. Therefore in the discussions and analysis that follows, it can be safely assumed that coal was delivered correctly onto the grate by the mechanical stoker, both the forced and induced draughts were under close scrutiny from the plant PID control system, the appropriate fuel size and type was used and that the shell boiler itself was in a good working condition. It is clear that these are essential pre-requisites before any sort of control system can be applied to optimise the operation of the plant.

From Table 5.1, it can be seen that the first requirement would be to provide the plant with the near optimum settings of air flow (i.e. with a suitable excess air level) to match the coal feed rates, therefore minimising the sensible heat loss. These initial ‘near optimum’ settings (of coal and air) have been tested with an empirically derived under-grate air distribution profile based on operator’s experience. Test results, namely the emissions, grate ash loss, grate surface temperature, concentration of oxygen in the flue gas and the location of the ignition plane have proven to be satisfactory when operated under these conditions. Details of the test results can be found in Section 4.1.1. With adequate combustion air being supplied to meet the coal feed, good combustion conditions will prevail in the furnace tube and this in turn will maintain carbon monoxide and smoke emissions at a minimum during steady-state combustion.

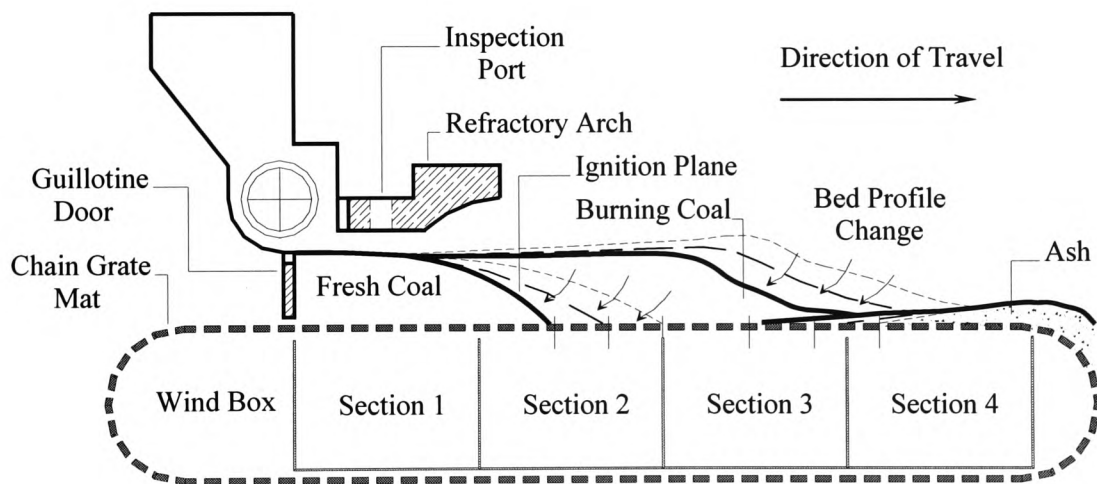
Having addressed the requirement of initial ‘near optimum’ settings of matching coal feed and air flow, the next issue will be the manner in which the boiler load can be altered in the shortest time possible to meet the demand. Undesired ignition plane movement and high transient carbon monoxide emissions can result if the input parameters are not properly regulated even though the initial settings are satisfactory, particularly during frequent large load changes [Chong *et al.*, 1997]. It has been found in this work that proper coal and air staging can help to promote good combustion during transients after a large load change. For instance, air must lead the coal feed on load decrease since there will be an initial oxygen starvation due to a higher rate of

combustion on the grate if the combustion air is decreased suddenly, and vice versa on load increase [Chong *et al.*, 1997; Gunn, 1982]. In modern shell and water tube boilers, 70% of the total heat transfer takes place in the fire tube or combustion chamber by radiation with the remaining 30% by convection from hot flue gases. Therefore, it is vital to operate the boiler plant as efficiently as possible during both transient and steady-state conditions, in order to minimise fouling. This staging effort will also in turn ensure good carbon burnout, since favourable conditions also exist during the shift from one load stage to another. In practice, the boilerman would visually inspect the grate ash and check the flame front through the inspection porthole from time to time to ensure that the combustion process itself was stable and that there are no 'holes' in the bed, i.e. the freshly supplied coal is ignited at the appropriate location. After 'optimum' staging of both coal feed and air flow have been carried out, the combustion process must then be allowed to re-establish itself to the new final settings if the load change is greater than a pre-determined limit, before any adjustment of the primary air can be made to optimise the air/fuel ratio.

Figure 5.1 illustrates the changes on the fire bed from one steady-state condition to another for two operating procedures; namely from full load to turndown and vice versa to highlight the transient characteristics. As can be seen from Figure 5.1, the fire bed will need to re-establish itself to the new settings and in doing so, changes the fire bed profile on the grate. A smooth transition from one state to the other is essential to avoid unwanted losses in unburned carbon and undesirable transient CO emission, thereby preserving the stability of combustion and this has been shown to be possible with the correct staging profile (Section 4.2). However once the coal feed rate and airflow has been brought to the new settings, sufficient time must be allowed for the combustion on the bed to steady-out, before any adjustment of the combustion air can be made. The only exception is that when the load change is of a small step (i.e. less than 0.1MW or in the case of an industrial stoker, less than 5% of the MCR), combustion air tuning can be carried out almost immediately without disturbing the combustion process.



(a) Fire Bed Transition when Operated from Turndown to Full Load



(b) Fire Bed Transition when Operated from Full Load to Turndown

Figure 5.1 Fire Bed Profile During Transients following Large Load Changes

After the transients have elapsed, which is typically 20 minutes after the last load change, the primary air to the main combustion zone must be adjusted according to the fire bed demand. Unless there is a system for regularly checking the flue gas constituents, such as the oxygen or carbon dioxide content, greater excess air will be required to allow for variations in the operating parameters which very often happens

in practice [Gunn and Horton, 1989]. Such parameters include changes in the fuel quality, variations in the fuel bed height and size distributions and the moisture content. For instance coal which has been stored in a bunker for a long period of time will have different characteristics than freshly supplied coal from the colliery. The reason for only adjusting the primary air to the main combustion zones (section 2 & 3) is that 80% of the total combustion air was supplied to these two sections with sections 1 and 4 essentially regulating the ignition plane and providing cooling of the grate and hence played a small role in the overall combustion [Butt and Pulley, 1996]. This was achieved by using oxygen in the flue gas reading with the adjustments of the initial air settings (in section 2 & 3) being dependent on the difference between the actual oxygen value and a pre-set target. In this case the target was 6% with the correction being delivered based on past experience.

5.2 The Development of the Neural Network Based Controller (NNBC)

This Section deals with the software development aspect of the Neural Network Based Controller (in the MATLAB™ computing environment). The basic idea was to provide the minimum airflow required for combustion, without having to sacrifice CO emission and carbon in ash losses, and in so doing improve the combustion efficiency of the stoker boiler plant. In addition, a desirable staging profile was taken into account when performing large step changes (load change greater than 0.1MW) and this knowledge was built into the control strategy. Feed forward Multi-Layered Perceptron (MLP) networks were utilised to construct the neural network components using gathered plant data (off-line) and were subsequently integrated into the overall control strategy, which was devised based on expert operator's experience. The bench mark of the NNBC was to achieve the lowest possible excess air level in light of other constraints of the stoker plant under study (see Section 4.1.1). The following subsections describe in detail the conceptual design of the overall control strategy and the manner in which the two neural networks were constructed.

5.2.1 Background - The Overall Controller Strategy

The NNBC essentially functioned by mimicking the human operator when operating the boiler plant after start-up. It detected changes in the load required (simulated by a request from the plant operator) and delivered the matching coal feed and air from the setting network. If the magnitude of the load change was higher than a pre-set limit (0.1MW), then an optimum staging profile of coal and air feed was delivered based on past experience, in order to preserve the location of the ignition plane, regardless of the magnitude and direction of the load change. The boiler was then left to respond to the new set of coal and air settings. It must be stressed again here that the combustion process *must* be allowed to re-establish itself to the new settings before any changes in the airflow can take place, as this will only upset the combustion process and can lead to pro-longed transient behaviour, particularly to large load changes – as detailed in Section 5.1.3.

After steady-state conditions were reached (typically 20 minutes after the final load change) the second phase of the neural network based controller was activated to fine tune the primary airflow rate, if necessary, in order to optimise the combustion process on the grate. This was achieved by monitoring the concentration of oxygen in the flue gas on-line and feeding the error (by comparing the actual reading with the target of 6%) into a corrective network which then delivered the amount of necessary adjustment in order to consistently maintain an optimum air/fuel ratio during steady-state combustion. The decision to perform fine tuning of the primary air was based on the boiler operator's experience. The NNBC was configured in the MATLAB™ computing language together with the necessary data acquisition and file writing accessories (RECIPE files) that enabled the controller to communicate with the host plant computer that managed the front end Tactician Control System (TCS) process controllers. Details of the NNBC program employed on the stoker test facility can be found in Appendix D. It is worth stating here that in order to allow the NNBC to retrieve information from the host plant computer through a network link (file sharing) the host computer had to run a Supervisory Control and Data Acquisition (SCADA) software (the TCS Paragon 2000) that was able to update the recipe files to and from the Tactician process controllers. The sampling rate of the plant host computer was set

to be 20 times faster than the NNBC controller sampling period in order to allow the NNBC to have a clear picture of the boiler's operating condition, and once a decision was made, the new instructions were promptly sent to the front end controllers. The structure of the NNBC devised for on-line control of the stoker boiler is as depicted in Figure 5.2 where the flow of information and instructions are regulated to and from the two neural network components including the staging program. Note that the target oxygen band imposed by the NNBC was narrower than that of boiler engineer's best practice (where acceptable limits were between 5 and 8%).

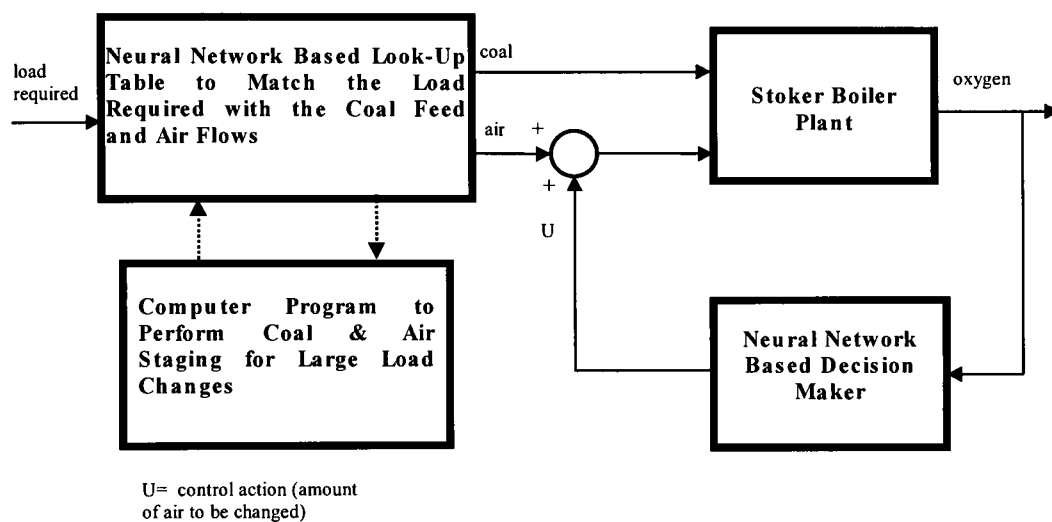


Figure 5.2 Overall Neural Network Based Controller Strategy

5.2.2 Setting Network

This network acted as a look-up table to provide the initial 'near optimum' settings of coal feed and primary airflow for the desired load. Table 5.2 and 5.3 list the settings of the coal feed (rotary valve and grate speed) and the primary airflow (in duct 1, 2, 3 & 4) for the four operating loads (0.3, 0.4, 0.5 & 0.6MW) for both Singles and Smalls grade coal used in the control experiments. This information was encoded in the form of two (one for Singles and the other for Smalls grade coal) Multi-Layered Perceptron (MLP) networks which were trained with the standard back-propagation algorithm to a

suitable error goal using the generic Neural Network Toolbox for use with MATLAB™ [Demuth and Beale, 1995; Chong *et al.*, 1996]. The input to the Setting Network was the desired load and the outputs were the six input parameters to the stoker boiler plant. In the interests of brevity details of the network construction have been omitted here, and can be found in Appendix E. It is sufficient for the purpose of this Section to state that the trained network could map the given boiler load to the desired coal feed and airflow settings with suitable accuracy.

Table 5.2 Near Optimum Settings of Coal Feed & Airflow for the Four Boiler Loads for Singles Grade Coal

Boiler Load (MW)	Rotary Valve Speed (rpm)	Grate Speed (cm/s)	Airflow in Duct 1 (l/min)	Airflow in Duct 2 (l/min)	Airflow in Duct 3 (l/min)	Airflow in Duct 4 (l/min)
0.3	2.15	6.2	1200	4200	3200	600
0.4	2.65	7.6	1200	5200	4200	800
0.5	3.3	9.52	1300	6000	5000	1000
0.6	3.9	11.25	3000	7000	7000	1500

Table 5.3 Near Optimum Settings of Coal Feed & Airflow for the Four Boiler Loads for Smalls Grade Coal

Boiler Load (MW)	Rotary Valve Speed (rpm)	Grate Speed (cm/s)	Airflow in Duct 1 (l/min)	Airflow in Duct 2 (l/min)	Airflow in Duct 3 (l/min)	Airflow in Duct 4 (l/min)
0.3	0.93	6.2	1400	4300	3300	900
0.4	1.18	7.6	1500	5400	4400	1000
0.5	1.54	9.52	1600	6000	5000	1200
0.6	1.81	11.25	2000	6500	6000	1700

5.2.3 The Corrective Network

The function of this network was to deliver a decision as to how much of the primary air to the main combustion zone (airflow in ducts 2 & 3) required pruning during steady-state operation in order to maintain the oxygen concentration at the optimum level. From the results gathered from Tests 1, 2 & 3, the correlation between the amount of air tuning required based on the oxygen deviation (from 5 to 6%) can be made, as tabulated in Tables 5.4 and 5.5 below. The boiler operating envelope was targeted at an oxygen reading of between 3 to 9% (excess air level between 15 to 80%), which can be considered large enough for the purpose of this work and hence this was the information used to train the corrective network [Chong *et al.*, 1997].

The gain factor derived from Table 5.5 was used to intuitively select two corrective network gains which were implemented in the first series of control experiments (Tests 8, 9, 10 & 11) to investigate the most suitable corrective gain factor. An empirical approach was inevitable as there are no other means by which the designer can determine a suitable value for the control parameters, as in linear control systems where the Ziegler-Nichols tuning method can be used to derive suitable controller parameters (proportional, integral and/or derivative gain) [Ogata, 1990].

Section 5.3 describes the fine tuning of the initial estimate until a satisfactory controller performance was obtained. As with the Setting Network, a MLP network architecture was adopted to construct the Corrective Network, which was developed using the method described for the Setting Network. The input to this network was the error in the oxygen reading (actual – target of 6%) and the output was the amount of tuning required based on the training data set (in terms of percentage of the initial setting). Again, in the interests of brevity the detailed description of its analysis has been omitted here and can be found in Appendix F.

Table 5.4 Total Primary Air Supplied with the Actual Oxygen in Flue Gas Band

Total Primary Air Supplied (litres/min)	Range of Oxygen Concentration (% by Vol. on wet basis)
Higher Excess Air (approximately +15% from the near optimum)	7 to 9
Near Optimum Excess Air (Best Operator's Practice)	5 to 7
Lower Excess Air (approximately -15% from the near optimum)	3 to 5

Note: The primary air distribution profile along the length of the bed was the same for all 3 tests.

Table 5.5 Relationship Between the Ranges of Oxygen Reading with the Band of
Primary Air

Range of Oxygen Readings (% by Vol. on wet basis)	Range of Airflow Tuning Required (percentage of the initial setting)
7.1 to 9.0 (Less Air Required)	-1 to -15% from the Optimum
5.0 to 7.0 (No Changes Required)	0%
3.0 to 4.9 (More Air Required)	+1 to +15 from the Optimum

Note: The resolution of the oxygen reading was to 0.1, hence the corrective network gain from the above was = $15\%/20 \text{ steps} = 0.75\%$ of the initial air setting for every 0.1 difference or 7.5% for every 1% difference in oxygen from the target band

5.3 Testing & Tuning of the Neural Network Based Controller (NNBC)

Upon completion, the prototype NNBC was initially tested on the chain grate stoker test facility to evaluate its performance before being tried on an industrial scale plant. A major part of the work involved experimenting with different controller parameters and these were the corrective network gain and also the controller sampling period. Four control experiments (Tests 8 to 11) were conducted whilst burning Singles grade coal (which was used in all the manual experiments, Tests 1 to 7) followed by one experiment whilst burning Smalls grade coal (Test 12) on the same test facility (in order to test the performance of the NNBC to burning a 'different' coal) and finally testing of the NNBC on an industrial scale 3.7MW_{th} chain grate stoker fired boiler (Tests 13, 14, 15, 16, 17a & 17b). Please refer to Section 3.4 for full details of the experimental procedures.

Before progressing further, it is worth stating again that the gain factor of the corrective network determined the amount of tuning made (in airflow to section 2 & 3 on the grate) based on the oxygen reading error (deviations from the target of 6%). Whilst the sampling period was the length of time between each successive decision made by the NNBC. It was equally important to investigate whether the same corrective gain factor was suitable for all the four operating loads (0.3, 0.4, 0.5 & 0.6MW), in addition to finding an appropriate sampling period.

From Table 5.5, it followed therefore that the corrective network gain factor should be approximately a 7.5% change of the initial airflow setting per every 1% difference from the green band (oxygen concentration above 6% or below 5%). Hence, two values of corrective network gains were intuitively chosen based on the derived value of 7.5 (an upper and lower limit) and these were 5 and 10. As for the controller sampling period, an initial value of 10 seconds was investigated and gradually increased until a suitable value was found. In the interests of brevity a summary of the first set of control experiments is provided in Table 5.6, and only one account of the 'bad' control scenario is illustrated along with the successful control experiment.

Table 5.6 Summary of Results of the Control Experiments with Singles

Controller Parameters			Summary of Results & Observations		
Corrective Network Gain Factor	Sampling Period (sec)	Changes in the Actuator's Output (Sections 2 & 3)	Changes in the Process Variable (Oxygen Level)	General Observations	
(a) Test 8	10	Large <i>diverging</i> oscillations of airflow with signs of instability	Sinusoidal fluctuations as a result of oscillating airflow. 50% of the total time (test duration of 3.25 hours) inside the desired green band (5 – 6%).	High CO peaks even when O ₂ remained within the green band, suggesting possible fuel bed build up at low loads, i.e. relatively thicker bed at low fire with insufficient combustion air. Controller changing the airflow too quickly, not allowing enough time for combustion to settle.	
(b) Test 9	30	Large diverging oscillations leading to pro-longed transient conditions (fuel bed build-up as the grate speed slowed down at low fire as a result of poor combustion at high fire.	Sinusoidal fluctuations as a result of oscillating airflow. 33% of the total test duration (of 2.25 hours) inside the green band	As in case (a), the controller output changed to quickly with respect to the process dynamics. Suggesting that the chosen gain was still too high and sampling period too short.	

(c) Test 10	5	60	Sustained sinusoidal pattern of oscillations although no clear sign of divergence was observed.	Clear pattern of sustained oscillations as a result of the fluctuating airflow delivered to the bed. 45% inside the green band in a test duration of 5.75 hours.	High CO peaks only when O ₂ fell below 4% for an average of 15 minutes, suggesting that the fuel bed build up was less significant, i.e. damping of controller response. In other words a better gain and sampling period had been chosen as compared to case (a) & (b).
(d) Test 12	5	120	Small gradual changes with signs of convergence – i.e. stability.	Minor sinusoidal pattern of fluctuations mostly within the narrow green band of 5 to 6% (decisive 71% within the green band during a 7.5 hours test duration, with only moderate peaks of 7.8% and 4.2%).	Stable plant operation with very positive results, whilst satisfying other operating constraints. Carbon in ash analysis later revealed a loss of 1.62% on a dry basis, which is highly comparable to those obtained from operator's best practice. Despite the absence of pollutant emissions data (faulty equipment), visual inspection revealed that combustion was good) and can be further justified with the pattern of arch temperature readings.

5.3.1 Control Experiments with Singles Grade Coal

Two control experiments whilst burning Singles grade coal are illustrated here, the first scenario is one which was implemented with unsuitable controller parameter settings and the other with suitable controller parameters (Tests 8 and 11). In the context of control experiments, the performance of the boiler is discussed with respect to the pollutant emissions, oxygen concentration in the flue gas and the flue gas temperature reading following changes in the load demand and also variations in the airflow following the tuning effort by the NNBC. In addition, emphasis is also placed upon the transient oxygen response and the pollutant emissions particularly when following large load changes.

5.3.1.1 Control Experiment (Test 8) with Unsuitable Controller Parameter Settings Burning Singles

Figure 5.3 shows the oxygen in the flue gas concentration following changes in the boiler load and subsequently variations in the airflow. A positive aspect that can be derived is that staging (of coal and air) has been successfully performed for the large load changes (on both load increase and decrease), and the evidence can be found in the satisfactory transient oxygen trend in the first 10 minutes from the point of load change. For instance a positive load change occurred at 0.33 hours and a negative load change at 1.08 hours into the experiment from the steady-state condition of 0.3MW to 0.6MW and vice versa. The peak transient oxygen reading following the load increase was 7.4%, as compared to 11% at boiler operator's best practice (see Section 4.2.2 for Test 7) and on load decrease an increasing oxygen trend was observed, indicating that the primary air was maintained before gradually being brought down to suit the lesser combustion intensity at low fire. The corresponding transient oxygen peak was 7.8% compared to a peak of 8.2% under good manual operation (Test 7). This was accompanied by satisfactory transient carbon monoxide emissions, falling from relatively high levels to about 50ppm on load increase from 0.3 to 0.6MW (at 0.33 hours and 2.15 hours). However, less flattering results were obtained when the boiler was operated from 0.6 to 0.3MW, due *not* to the staging process but to unwanted fuel bed build up as a result of fluctuating airflow at high fire. In other words, the fire bed

was made longer (more coal being left on the grate) due to the unsatisfactory supply of combustion air at high fire. Therefore when the grate slowed down at low fire, the amount of combustion air provided for a supposedly shorter bed was made insufficient. This is evident by the high carbon monoxide emission peaks of up to 980ppm. Hence one can conclude that with respect to the transient oxygen response and carbon monoxide emission, the incorporation of the staging profile can be justifiably considered an improvement to the control of the process.

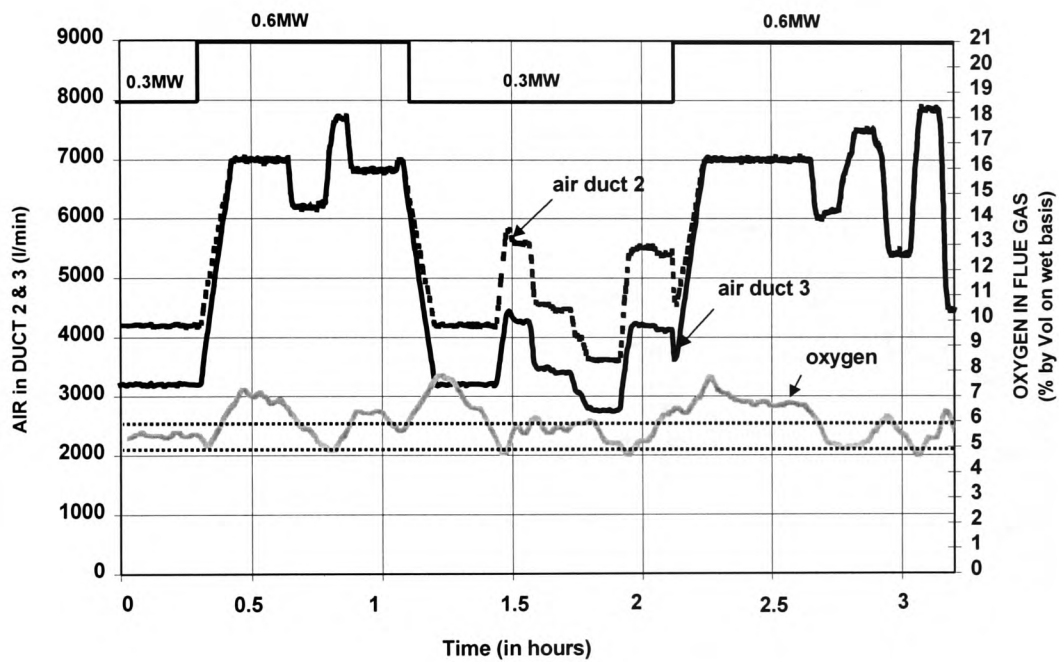


Figure 5.3 Oxygen Response to Undesirable Controller Gain & Sampling Period with Burning Singles - Test 8

However, the controller effort at steady-state was not quite as satisfactory. The NNBC made its decisions too quickly and did not allow enough time for the boiler to respond to the previous alteration of the airflow (sampling period of 10 seconds), and the magnitude of these changes were too large (corrective gain of 10). As a result, the oxygen reading fluctuated following the sinusoidal airflow patterns when oxygen trimming was carried out by the NNBC. As shown in Figure 5.3, in the last tuning exercise (NNBC started pruning the oxygen at 2.65 hours), the airflow pattern (to the main combustion zone) diverges from the initial settings. This is clearly undesirable as

it shows signs of controller instability, and this is also reflected in the flue gas temperature pattern (Figure 5.4). Although there was no apparent negative effect on the nitrogen oxides emission, it has been shown from Test 1 that increasing the excess air level will enhance its production. As described earlier in this Section, a high carbon monoxide reading was registered at low fire (0.3MW) and this is attributed to the unsatisfactory combustion conditions that prevailed at low load as a result of poor combustion at high fire (Figure 5.5). Such fluctuations in the primary airflow to the mid sections were undesirable, as it can lead to unstable boiler operation (with respect to the ignition plane) and a tendency for increased carbon in ash losses.

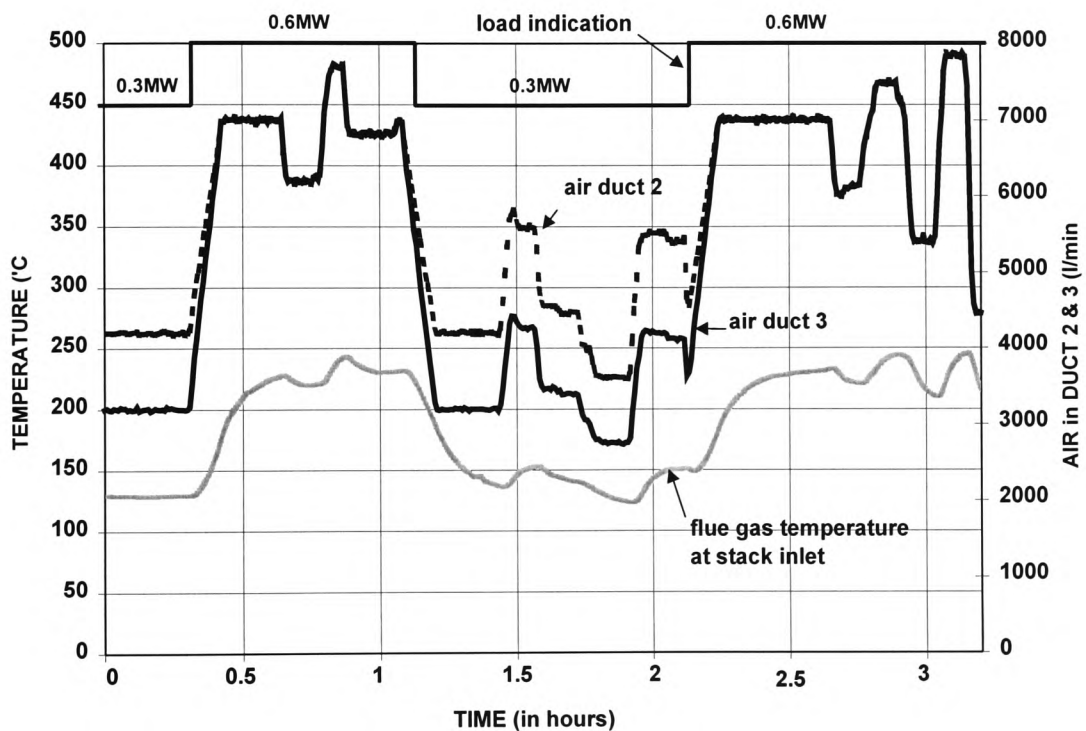


Figure 5.4 Flue Gas Temperature Response to Undesirable Controller Gain & Sampling Period with Burning Singles – Test 8

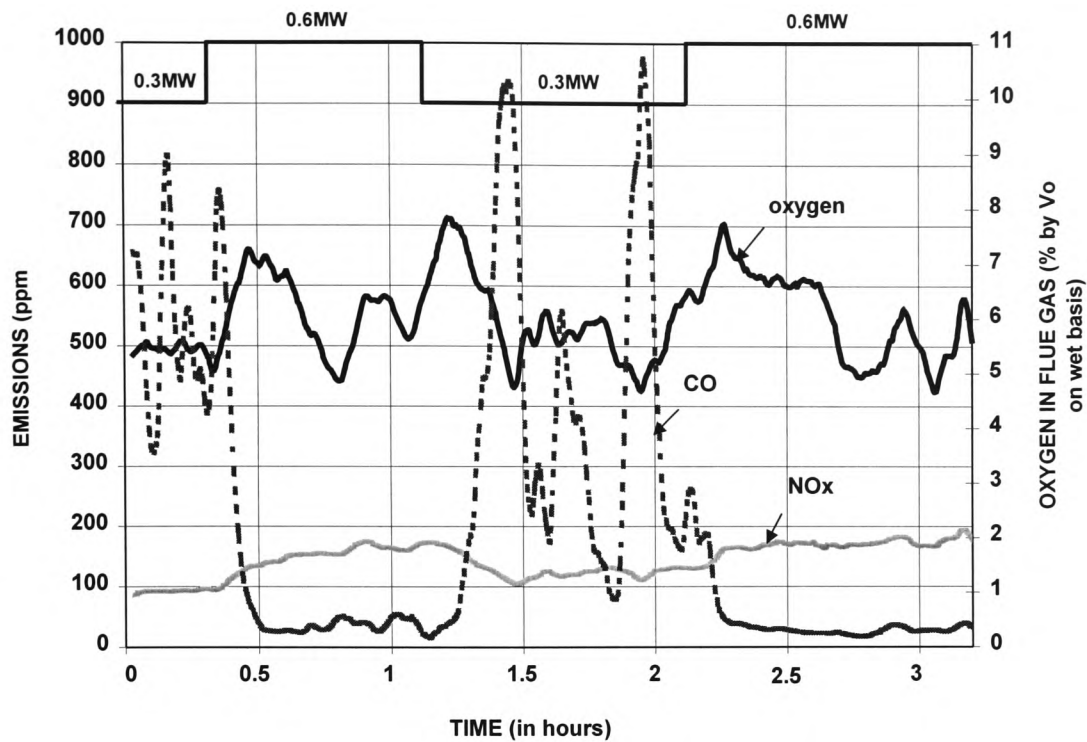


Figure 5.5 NO_x & CO Emissions to Undesirable Controller Gain & Sampling Period with Burning Singles – Test 8

5.3.1.2 Control Experiment (Test 11) with Suitable Controller Parameter Settings Burning Singles

Suitable values for the controller gain and sampling time were found during the course of the experiments and the boiler performance under the influence of these suitable settings is described here. The results are shown in Figures 5.6, 5.7 and 5.8, which consist of the oxygen concentration, flue gas temperature and instead of emission readings the arch temperature readings. The portable gas analyser was unfortunately *faulty* for this only successful occasion (due to financial and time constraints) of the control experiment, therefore a series of arch temperature readings are provided here in order to supplement the statements made with respect to the positive controller performance. However, the suitability of the NNBC approach in controlling such a boiler plant is further substantiated with its implementation onto a full scale 3.7MW_{th} chain grate stoker boiler plant (in Section 5.3.3) in a case study that was carried out in the later course of the research project.

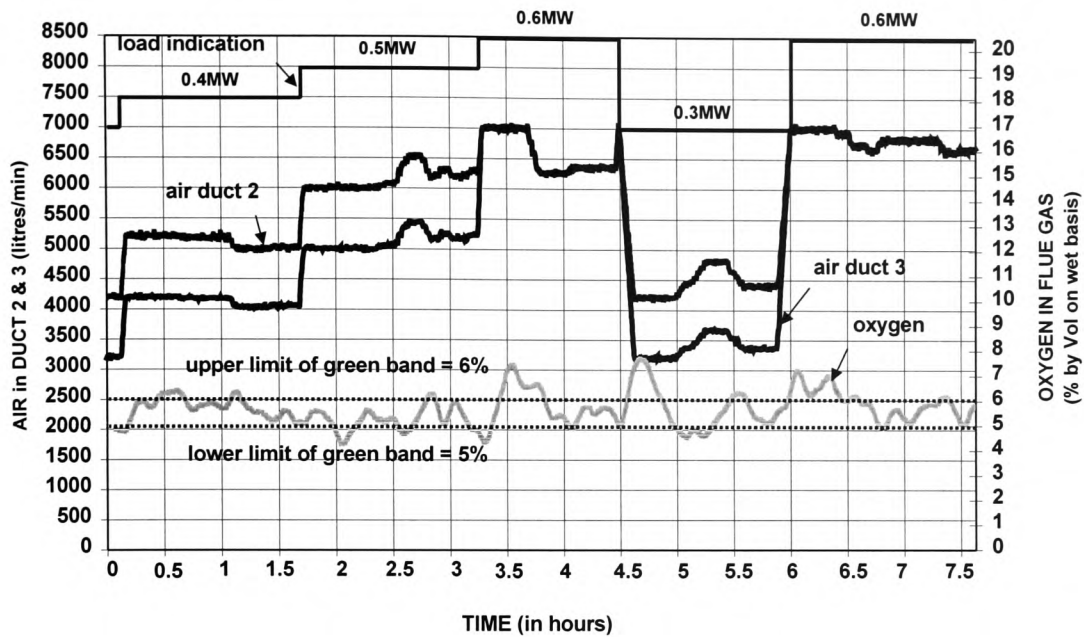


Figure 5.6 Oxygen Response to Desirable Controller Gain & Sampling Period with Burning Singles – Test 11

Please note that the oxygen trimming was only activated after 20 minutes from the point of load change to allow for transient boiler behaviour to elapse. Again the staging effect yielded good results with respect to the transient oxygen response following large load changes (at 4.5 hours going from 0.6 to 0.3MW and vice versa at 5.75 hours) where peaks of 7.5% and 4.5% were recorded, as shown in Figure 5.6. The oxygen concentration was found to be in the desired green band (5 and 6%, as indicated by dotted two lines in Figure 5.6) for 71% of the total test duration of 7.5 hours with only moderate fluctuations in what seems to be sustained steady operation (with respect to the oxygen reading) despite the load changes. The flue gas temperature pattern in Figure 5.7, shows little sign of fluctuations, and once a load change was performed the response was similar to that of a first order system which was to be expected, i.e. the flue gas temperature can be maintained to the corresponding level of the load. One ash sample was collected at the steady-state operation of 0.6MW (over a period of 1 hour) and sent to a commercial laboratory to analyse for unburned carbon (efficiency losses). The result was extremely encouraging, showing 1.62% on a dry basis, which was slightly better than good manual operation (1.69% at 0.6MW, Section

4.1.1). Although no pollutant emissions data were available, Figure 5.8 shows the pattern of a series of strategic arch temperature readings. For details of the location of the arch thermocouples and the significance of the trend, please consult Chapter 6. Essentially, these arch temperature patterns were designed to infer the movement of the ignition plane by allowing the user to study the distribution pattern of selected thermocouples over a period of operation. The three selected readings were from the front (T1 & T4) and back (T6) arch thermocouples. It follows therefore that any shift in the ignition plane towards the stoker front would result in an increase in the first two temperature readings and any shift backward into the furnace tube would result in an increase in the back temperature and a corresponding fall in the front two temperature readings.

As shown in Figure 5.8, a steady pattern can be seen in T1 and T4 as the load was gradually increased from 0.3 to 0.5MW followed by a steadily increasing trend of T6, suggesting that the arch was being warmed up as combustion in the furnace tube developed. The two front temperature readings fell following the load change from 0.5 to 0.6MW with an increase in T6, suggesting that the ignition plane shifted further into the furnace tube. However the trend in T6 over the duration of that load (0.6MW) remained almost constant, implying that the ignition plane settled in a location further away than at lower loads (as expected due to the higher grate speed) but confirming that the combustion was stable.

If the combustion wasn't stable, the ignition plane would have progressed further into the furnace tube, resulting in a fall in T6 as well. As the load dropped from 0.6 to 0.3MW, as one would expect with a lower grate speed, the ignition plane crept forward with an increase in T1 and T4 and a slight fall in T6. A similar but reverse trend can be observed on large load step up. Therefore, by concluding that the ignition of freshly supplied coal was satisfactory with good ash burnout (visual inspection and one laboratory analysed sample), one can confirm that the combustion on the bed was satisfactory. Therefore one can infer from this alternative evidence that the pollutant emissions would be satisfactory during the course of the experiments.

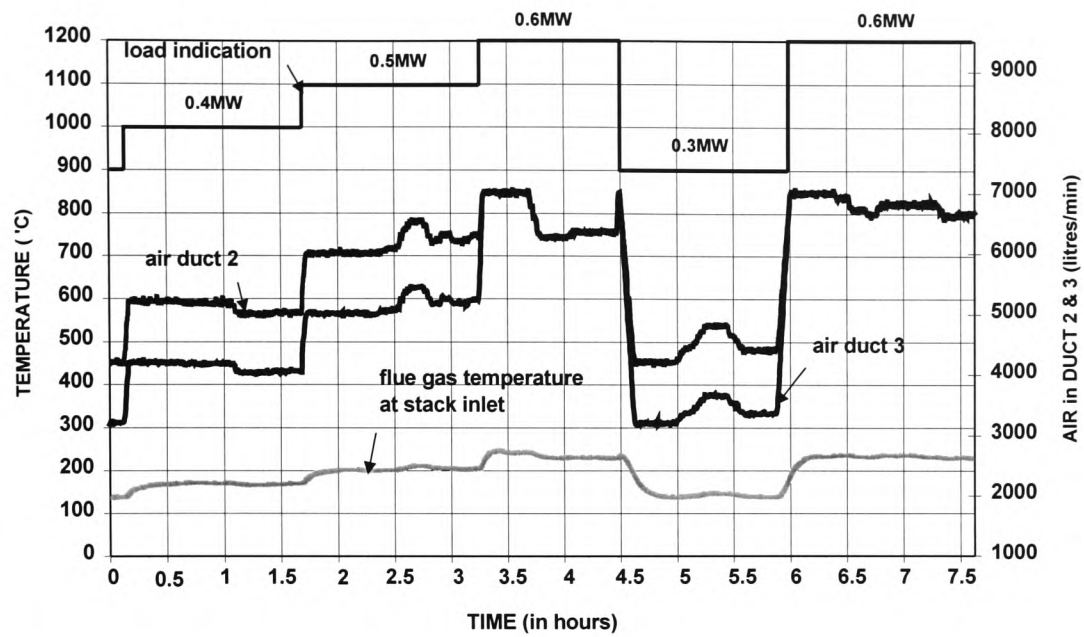


Figure 5.7 Flue Gas Temperature Response to Desirable Controller Gain & Sampling Period whilst Burning Singles – Test 11

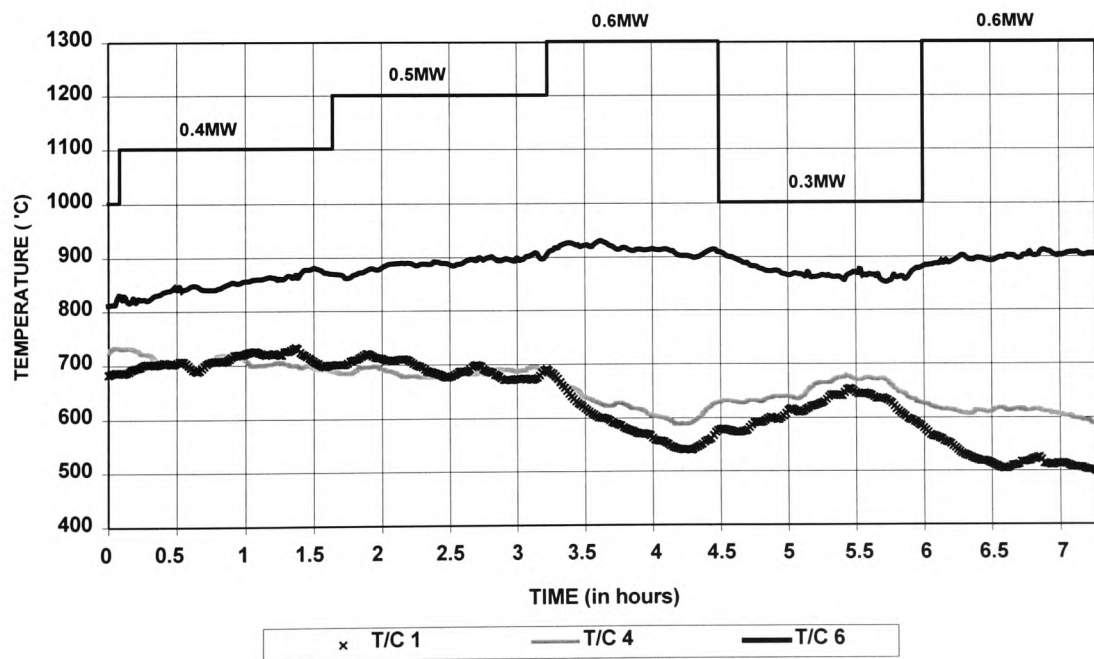


Figure 5.8 Arch Temperature Pattern to Desirable Gain & Sampling Period whilst Burning Singles – Test 11

5.3.2 Control Experiment (Test 12) with Burning Smalls Using NNBC Derived from Burning Singles

The performance of the NNBC was also evaluated whilst burning a different type of coal, and for this experiment the Daw Mill Smalls grade coal was used (smaller size distributions –12.5mm to 25mm). The primary objective of this experiment was to determine if the NNBC which was developed using data gathered from burning Singles, was able to deal with a different type of fuel. Before progressing further it must be stated that the fire bed was found to be shorter as compared to Singles, due to the smaller size distributions although no knowledge of this was available as this was the only experiment carried out with Smalls. The information required by the look-up table was provided by plant personnel (at Coal Research Establishment in Stoke Orchard, Cheltenham) based on previous experiments with Smalls. However, during the course of this experiment the fuel bed was found to be thicker than expected (expected fuel bed depth was approximately 100mm) and the problem was due to the settings of the rotary valve. In other words the initial ‘near optimum’ estimate of the input parameters for this experiment were not correct. Nevertheless the work conducted here was a valuable exercise to highlight the deficiencies of the NNBC and to identify areas where improvements could be made.

The results obtained by operating the boiler from 0.6 to 0.4MW in 0.1MW steps and a large single step change from 0.4 to 0.6MW and back down to 0.3MW, are shown in Figures 5.9, 5.10 and 5.11. The first observation was that during steady-state operation at 0.6MW the oxygen remained at an average of 4.5% suggesting that the amount of combustion air provided wasn’t sufficient. The load change from 0.6 to 0.5MW occurred at 0.13 hours into the experiment and oxygen trimming was initiated 20 minutes after the load change. The control effort by the NNBC to supply more air resulted in a huge oscillation in the oxygen response, suggesting that the gain was too high. In other words the suitable gain derived from burning Singles was not suitable for burning Smalls. On reflection this was not surprising as the bed profile for Smalls was shorter, hence a proportion of the air supplied to the mid sections passed unreacted, thereby giving rise to high oxygen peaks before being detected by the

NNBC and as a result the air was reduced significantly. At a steady-state of 0.4MW, the gain was halved (to 2.5% of initial setting for every 1% difference in oxygen) and the sampling period increased to 240 seconds, in order to damp the NNBC response. This resulted in less oscillation in the controller action as demonstrated in the load change from steady-state of 0.4MW to 0.6MW but on the whole an unsatisfactory response in the oxygen reading prevailed. Hence it can be concluded that the NNBC which was developed using data gathered from burning Singles was not capable of dealing with the different coal type although the unavailability of a good look-up table is thought to have some weight over the reduced performance.

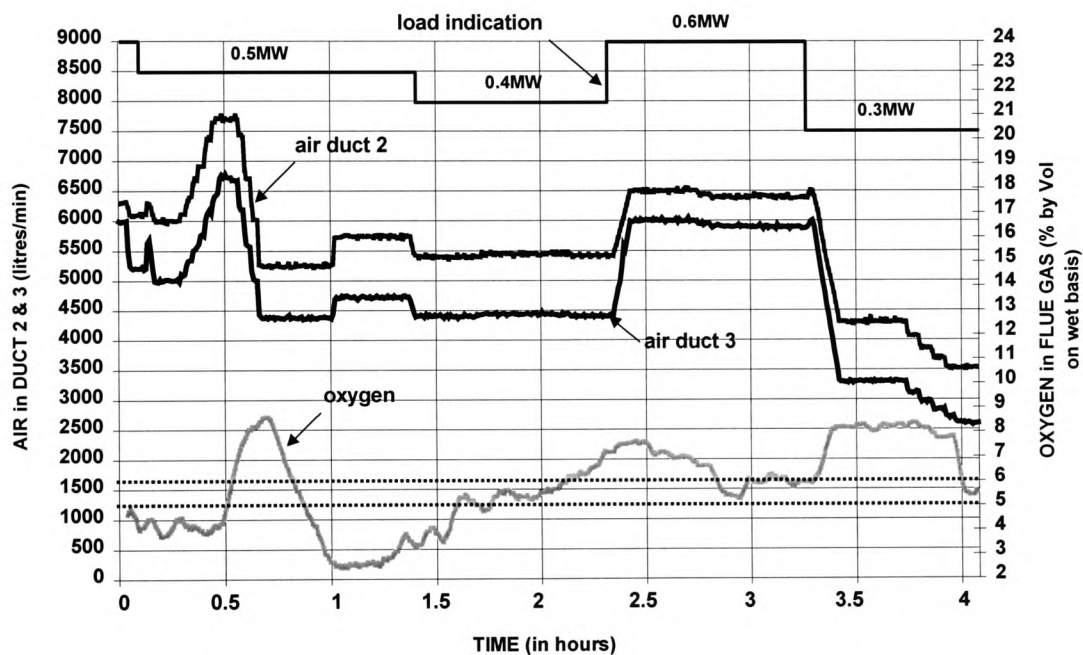


Figure 5.9 Oxygen Response with Burning Smalls – NNBC Derived from Burning Singles (Test 12)

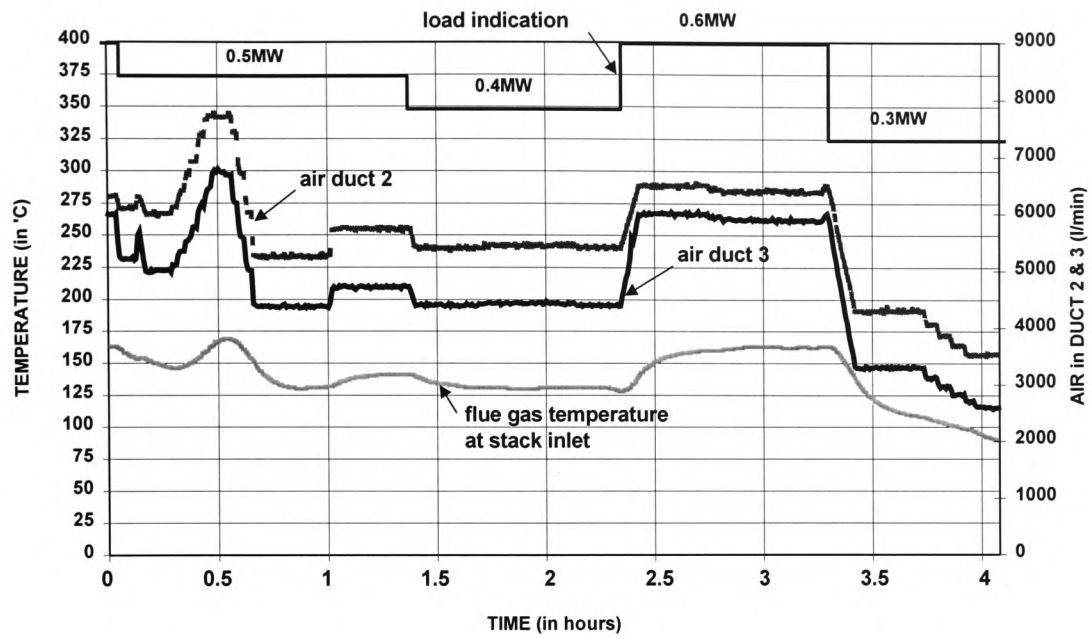


Figure 5.10 Flue Gas Temperature with Burning Smalls – NNBC Derived from Burning Singles (Test 12)

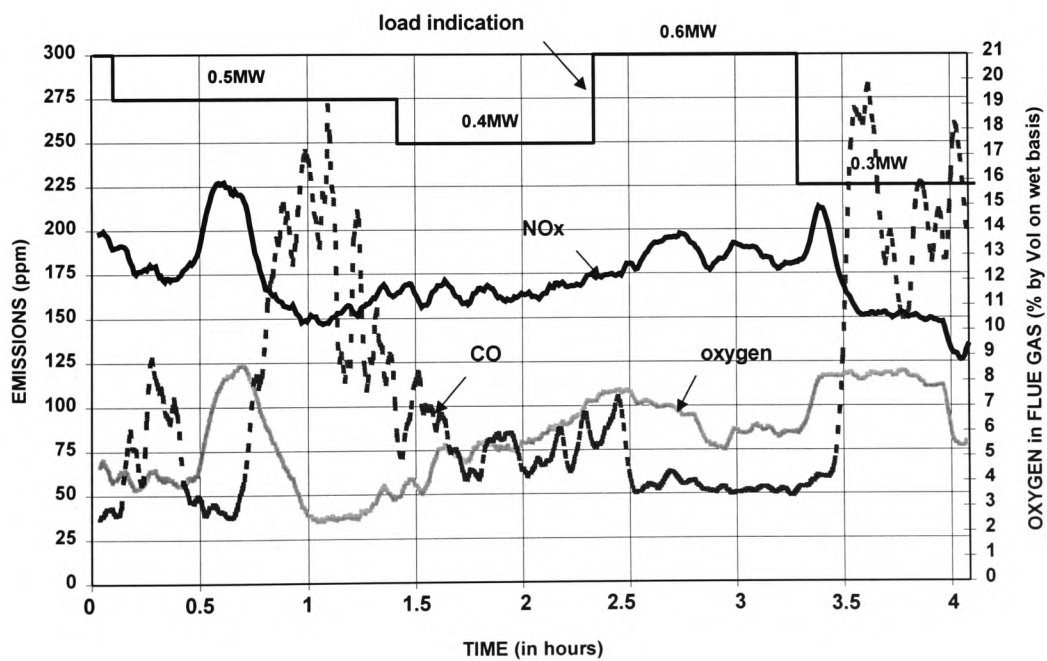


Figure 5.11 NO_x & CO Emissions from Burning Smalls – NNBC Derived from Burning Singles (Test 12)

5.4 Case Study – Implementation of the NNBC to an Industrial Chain Grate Stoker Fired Shell Boiler

This case study was concerned with the implementation of the prototype NNBC to control one of the three chain grates stoker fired shell boilers at Her Majesty's Prison (HMP) Garth in Leyland, Lancashire. These plants were sheltered in a state of the art boiler house featuring colossal tipping hoppers, pneumatic coal feeding and grate ash disposal system, equipped with an industrial digital control system. The boiler house was manned on a 24 hour basis and supplied hot water for space heating and domestic purposes for approximately 500 inmates from two separate prison compounds (Wymott and Garth).

Each of these coal fired stoker boilers could deliver up to 3.7MW of thermal capacity (coal consumption rate of approximately 600kg per hour at MCR) with a claimed combustion efficiency of near 80%. One natural gas boiler of similar capacity was also available to provide occasional backup load during the winter months and in the summer when the coal fired boilers were decommissioned for maintenance and inspection purposes. This exciting work was carried out in conjunction with a Lancashire based chain grate stoker manufacturer (James Proctor's Limited) and HMP Garth. The concept and methods adopted here were adapted and enhanced from the earlier work with the chain grate stoker test facility at CRE, so as to adaptively alter the gain of the adjustments made by the NNBC. The NNBC was then compared with the plant PID control system at providing the load demanded. The load demand in this case was reflected in the process variable being the pressurised hot water temperature, however no oxygen trimming system was available on the industrial boiler plant.

5.4.1 Description of the 3.7MW Industrial Scale Chain Grate Stoker Fired Shell Boiler & Plant Instrumentation

The key features of this state of the art chain grate stoker fired boiler were; the Proctor's fire break unit, pneumatic coal and ash handling system, an effective fire bed

area of 0.91m (width of grate) \times 3.05m (length of fire bed) made up of grey cast iron links, variable speed drives (VSD) installed onto the forced draught (FD) fan motor for better characterisation of the air distribution curve over the entire firing range, 3-pass shell boiler producing hot water at 4 bar and a 120°C set point temperature and a high efficiency cyclone before the flue gas was discharged through the stack. The thermal capacity of this boiler was 3.7MW with a turndown ratio of 6:1 (i.e. the lowest operable load was 0.62 MW which corresponded to 100kg per hour of bituminous coal consumption).

The stoker boiler was equipped with an industrial PID digital control system (the Honeywell UDC3000 process controller) which regulated the coal feed and airflow (the firing rate), in order to attain the desired set point hot water temperature. There was no secondary air involved, as free burning bituminous coal was used. Two process sensors were available from the plant and these were thermocouple signals from the outgoing hot water pipe and also the refractory arch. The stoker arch thermocouple was used together with an analogue dial to give the plant operator an indication of the approximate temperature of the refractory arch ($\pm 20^\circ\text{C}$). Individual signals to the various actuators (rotary valve, grate and damper motor) and VSD drives was ratio off the PID controller signal (4 - 20mA, 0 - 10v) as the on-board PID controller was a single loop process controller.

The type of coal burnt in this set of experiments was a Scottish bituminous Smalls grade coal (NCB Rank 802) with similar specification to the Daw Mill type burnt in earlier tests. The 'as received basis' were as follows; ash-8%, Volatile Matter-30%, Fixed Carbon-50%, Sulphur-1.3%, Gross CV-27,000 kJ/kg [Appendix B]. Note that the coal ash content for these commercial boilers is around 8%, since the commonly used link type is of the grey cast iron, which has a lower maximum operating temperature than the chrome cast iron links (the stoker test facility, which can be used with lower ash coal, $< 4\%$).

A stand-alone data logging system was developed for the purpose of automatically recording the input (firing rate) and the required process parameters (hot water and arch temperature). The input signal was passed through a low pass filter (RC circuit, $1\mu\text{F}$ & $1\text{M}\Omega$) for noise attenuation before being recorded. A conditioning circuit was also necessary for each of the two thermocouple readings for amplification of the weak signal (in the range of $45\mu\text{V}/^\circ\text{C}$) to the range of $10\text{mV}/^\circ\text{C}$ via the use of an AD595A integrated circuit chip. These 3 filtered analogue signals were then transferred to a MIO16-National Instruments card fitted into a P133MHz PC running LabVIEW™ for automatic logging every 30 seconds (the same sampling rate employed on the Tactician system of the chain grate stoker test facility at CRE). As with the earlier work on the stoker test facility, other measurements included the pollutant emissions (carbon monoxide, nitrogen oxides and sulphur dioxide normalised to 6% oxygen), concentration of oxygen in the flue gas, flue gas temperature (at the exhaust duct just before the cyclone) and flame front data (via the flame front monitor – see Chapter 6).

5.4.2 Preliminary Test on the 3.7MW Chain Grate Stoker Fired Shell Boiler (Test 13)

The objective of this experiment was to gather information about the behaviour of the stoker boiler and in particular the excess air level at various load stages and the associated pollutant emissions when manually operated under the boiler engineer's best practice. A turndown ratio of 5 to 1 was achieved due to a lack of heat demand at full load, however for the purpose of testing the NNBC this was found to be sufficient. The firing rate (boiler load) was defined as a percentage of the Maximum Continuous Rating (MCR) of the boiler and was regulated from turndown at 17% of MCR to 83% of MCR and back to turndown in 17% MCR steps. Figures 5.12 and 5.13 illustrate the excess air level, flue gas temperature and the pollutant emissions data gathered from this experiment following these gradual step load changes.

As can be seen in Figure 5.12, the industrial chain grate stoker boiler was set-up to operate at a higher excess air level except at high fire (at 67% of MCR or higher) and

the rationalisation was to ensure a short fire bed to avoid discharging live fire from the back of the grate. It is worth noting that the air distribution facility on this industrial stoker was manipulated by a damper motor (located half way along the length of the grate inside the windbox) that distributed the air into two sections on the grate. For instance at turndown, the damper will be closed (vertical) to provide air only to the first half of the grate owing to the short fire bed. The profile of the damper over the stoker turndown range was pre-set by the external commissioning engineer to suit the type of coal burnt. A relatively high excess air at medium fire (10 to 12% oxygen) to low fire (13 to 16% oxygen) was also necessary in order to create the required turbulence to ensure proper mixing of the volatile gases and promote char combustion in addition to providing cooling for the grate.

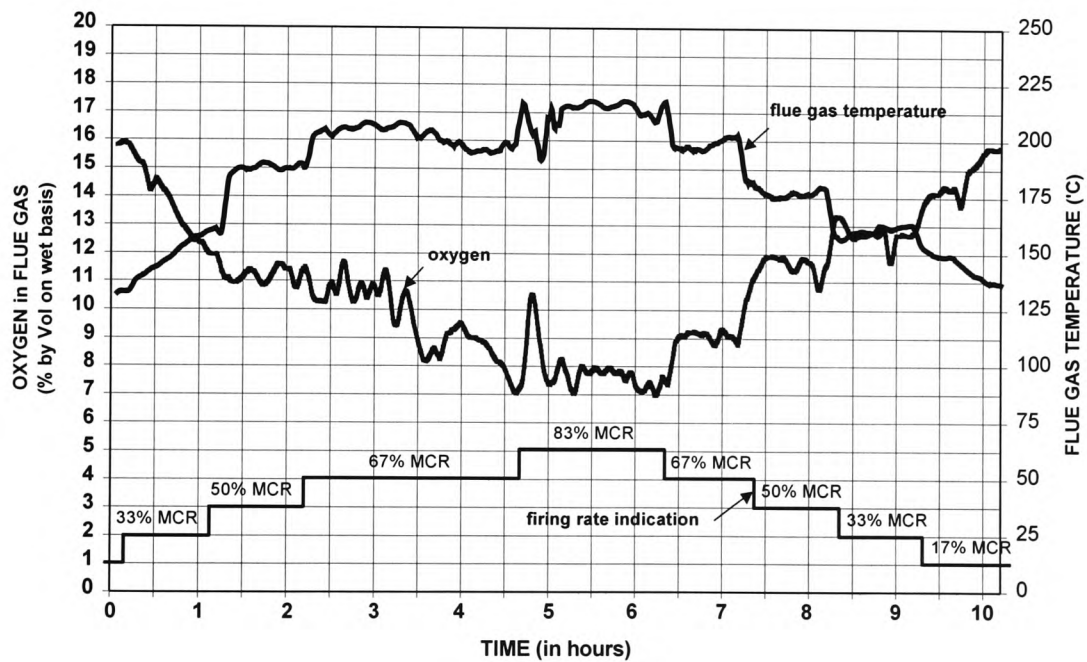


Figure 5.12 Oxygen Concentration & Flue Gas Temperature under Operator's Best Practice following Gradual Load Changes for the Industrial Stoker

In parallel to the previous findings on the chain grate stoker test facility at CRE and also from the literature, data here shows no concern over the concentration of nitrogen oxides (an average of approximately 250ppm normalised to 6% oxygen) owing to the natural form of air staging along the fire bed [Livingston *et al.*, 1995]. The carbon monoxide emission (average of 355ppm normalised to 6% oxygen) was satisfactory and it must be stated here that smoking only occurred when the CO level was in excess of 2000ppm. The sulphur dioxide emission in this particular experiment was higher than the limits applicable to the larger stoker plants (individual capacity of between 20 to 50MW_{th} or individual/aggregated total of higher than 50MW_{th} – Section 2.1.4.1) with an average emission of 986ppm (normalised to 6% oxygen). The grate surface temperature at the stoker front was found to be very cool, about 25°C throughout the entire firing range offering a much higher margin for secure plant operation which is to be expected in industrial practice.

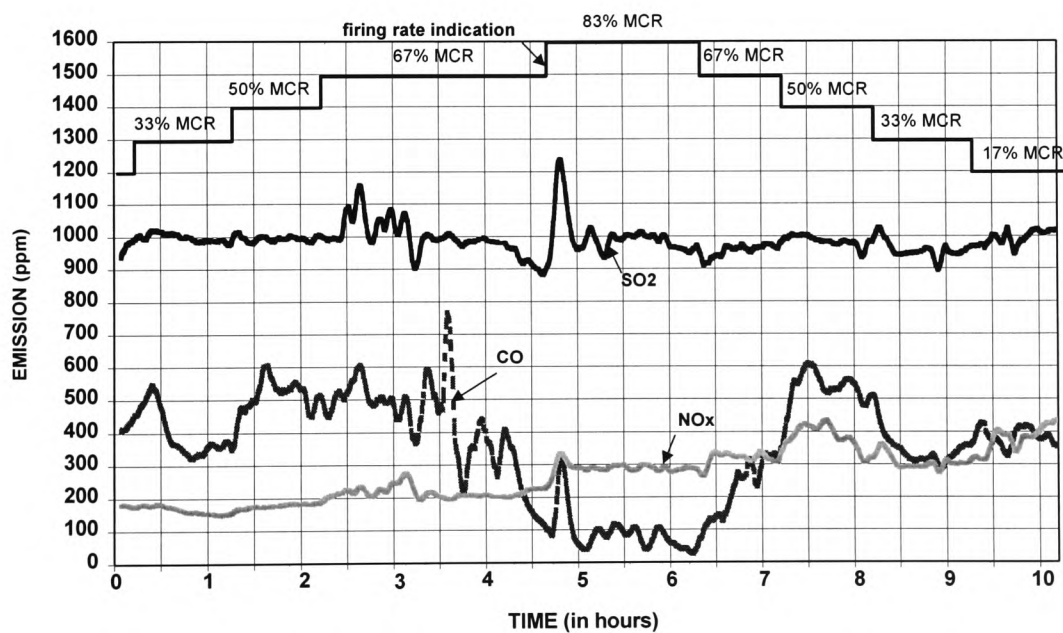


Figure 5.13 Pollutant Emissions under Operator's Best Practice following Gradual Load Changes for the Industrial Stoker

5.4.3 Plant Response Following Automatic Operation of the Boiler under Conventional PID Control (Test 14 & 15)

These two experiments, Test 14 & Test 15, were aimed at studying the performance of the on-site PID controller in tracking the desired hot water temperature set point (120°C) and also to a step change in the hot water temperature set point from 105°C to 120°C and vice versa.

5.4.3.1 Plant Response Under Automatic Conventional PID Controller Mode Tracking Hot Water Temperature Set Point (Test 14)

As shown in Figure 5.14, the PID controller hunted over almost the entire firing range (from full turndown to almost 90% of the MCR in less than 10 minutes) in attempting to bring the process variable (hot water temperature) to the desired set point. A small deviation in the hot water temperature ($\pm 5^\circ\text{C}$) from the set point of 120°C resulted in a huge oscillation of the controller output in order to cope with the error.

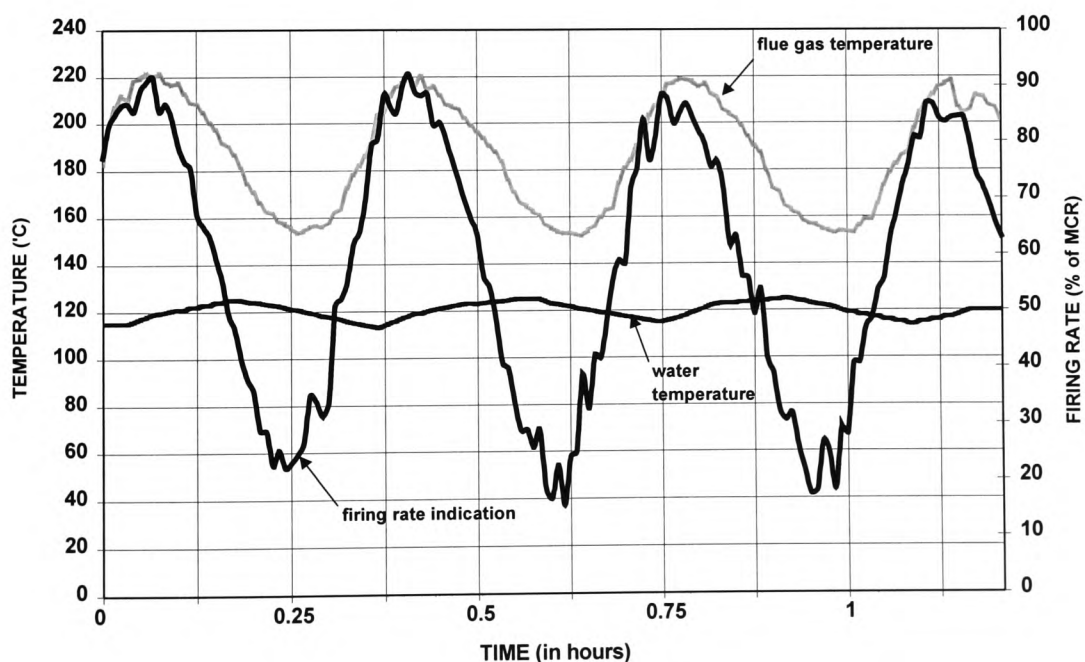


Figure 5.14 Oxygen Concentration & Water Temperature under PID Controller Effort to Tracking the Set Point Temperature

The pattern of oscillation in the controller output (firing rate) resembles those of critical stability covering a wide range of firing rate (changing the grate speed) within a relatively short period of time with no indication of the process attaining stability. The reasons for the large sustained fluctuation in the firing rate can be attributed to the high sampling rate (elapsed time between each successive control decision) and the non-optimal setting of the control parameters adopted by the plant PID controller. The flue gas temperature has a similar pattern to the sinusoidal wave of the firing rate, as expected.

Figure 5.15 shows the oxygen concentration and the carbon monoxide level in the flue gas following the sinusoidal change in the firing rate. As described in Section 5.4.2 with Test 13, a lower excess air level prevailed at high fire (less than 7% oxygen) and vice versa at full turndown (more than 12% oxygen) with a similar sinusoidal pattern to the firing rate but in the opposite direction. The CO emission at turndown was relatively lower than at high fire, although the average CO emission over the duration of the test was almost 3 times as much as those obtained from the operator's best practice. The high CO peaks (maximum of 1620ppm) can be explained by the fact that on load increase, more coal was fed onto a bed of initially lower combustion intensity with a lower excess air level (at high fire, the oxygen concentration was less than 8%), thereby starving the combustion process on the grate, at high loads, of air.

Although the coal and air feed was modulated (in 5% MCR steps) between turndown and full load and vice versa, both parameters were changed simultaneously without allowing sufficient time for the combustion process to steady out before the next load change. In other words, the heap of coal piled from the previous load change was not given sufficient time to burn off (about 10 minutes) before the next change of load, further adding to the cyclic oxygen and CO pattern. It is due to this reason that a high excess air is required especially at the low firing rate to burn off the additional coal on the grate in order to enable the plant PID controller to function without causing too much of a problem. As both NO_x and SO_2 emissions were primarily dependent on their content in the fuel burned and the availability of combustion air, the production of these two derivatives of combustion closely followed the firing rate. The emission of

both NO_x and SO_2 (Figure 5.16) pose no concern and although there are no emission limits for a boiler in this range, their emission limit matched those of the 20 to 50MW_{th} range (UK Emission Limits for Boiler between 20 to 50MW thermal capacity - $\text{NO}_x < 500\text{mg/Nm}^3$ or 244ppm and $\text{SO}_2 < 2000\text{mg/Nm}^3$ or 700ppm, at 6% oxygen for coal fired boilers) [IEA Statistics, 1997].

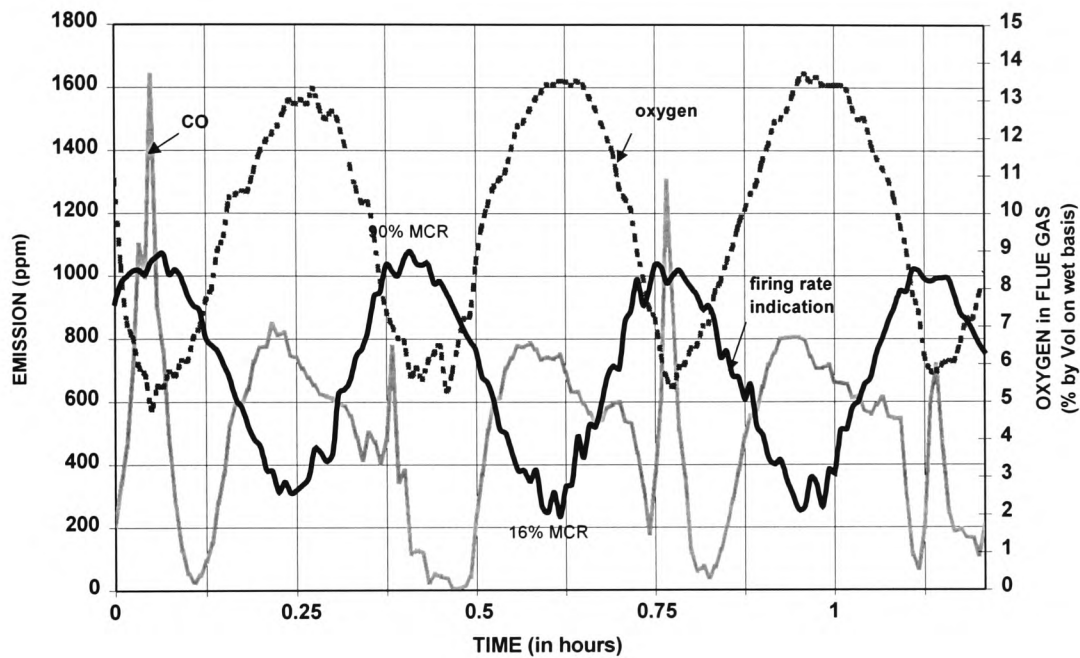


Figure 5.15 Oxygen Concentration & CO Emission under PID Controller Effort to Tracking the Set Point Temperature

The flame front (stability of combustion) was found to be extremely tolerant to load changes. This was reflected in the refractory arch temperature pattern following the cyclic load changes as shown in Figure 5.17. Despite the oscillatory nature of the change in grate speed, a marginal increase (8°C) in the refractory arch temperature was observed over the test duration of 1.2 hours. This increasing pattern is a clear indication of the robustness of the chain grate stoker and in fact it was largely due this that the chain grate stoker can be used with the conventional PID control system for hot water set-point temperature tracking.

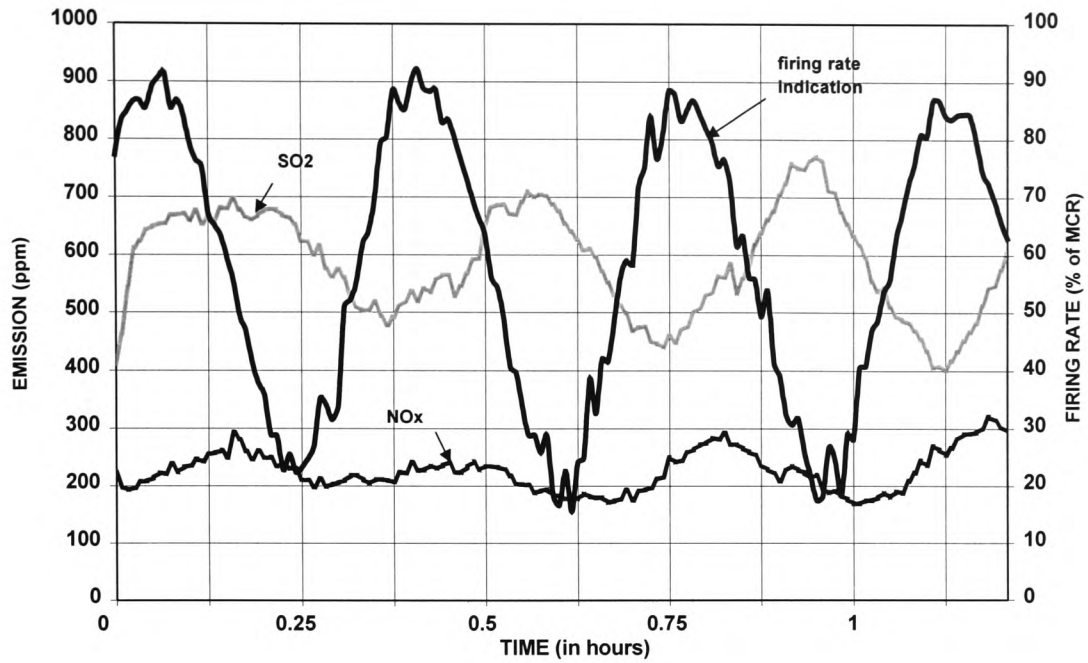


Figure 5.16 SO₂ & NO_x Emissions under PID Controller Effort to Tracking the Set Point Temperature

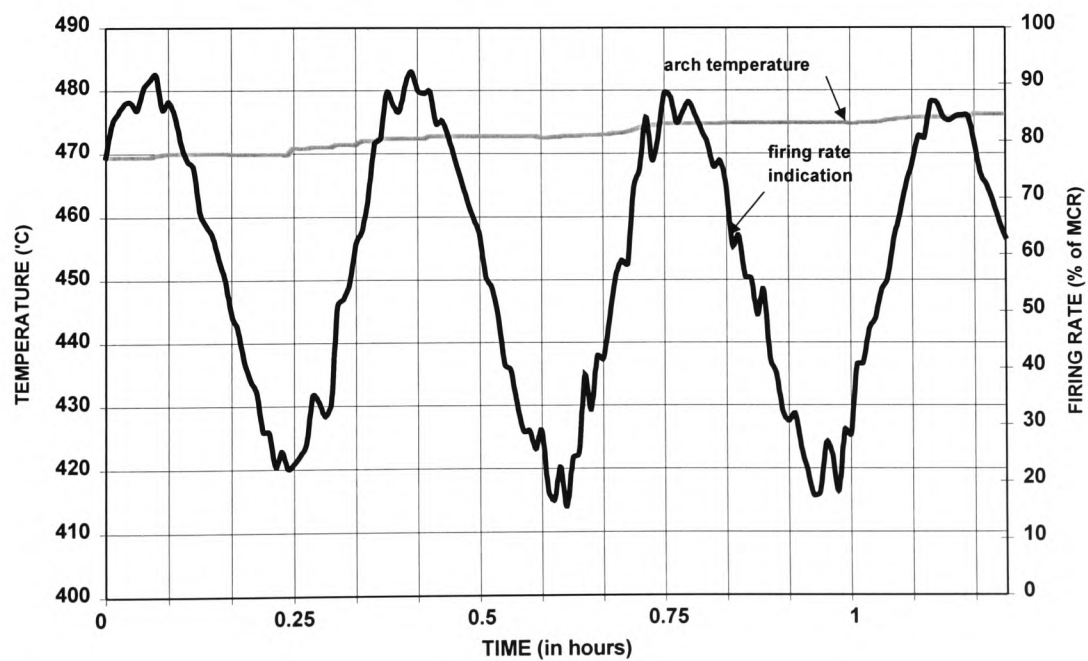


Figure 5.17 Refractory Arch Temperature Pattern under PID Controller Effort to Tracking the Set Point Temperature

5.4.3.2 Plant Response Under Automatic Conventional PID Controller Mode Following Temperature Set Point Change (Test 15)

This test was aimed at evaluating the transient characteristics of the stoker boiler plant under the influence of the conventional PID controller. The response of the plant to the set point changes was recorded and the results are presented in Figures 5.18 and 5.19. At 0.42 hours into the experiment, the process variable set point of the PID controller was altered from 105°C to 120°C, and upon detection of the error between the actual temperature and the desired set point the controller ramped up the firing rate to full load in order to meet the demand. An overshoot of 5°C in the water temperature can be seen in Figure 5.18 before the firing rate was gradually brought down. The corresponding oxygen concentration at high fire was on average about 10% which was comparable to the findings in Test 13. After 30 minutes into the experiment the set point was brought down to 105°C which resulted in the firing rate plunging to full turndown with the corresponding oxygen concentration gradually climbing to 16%.

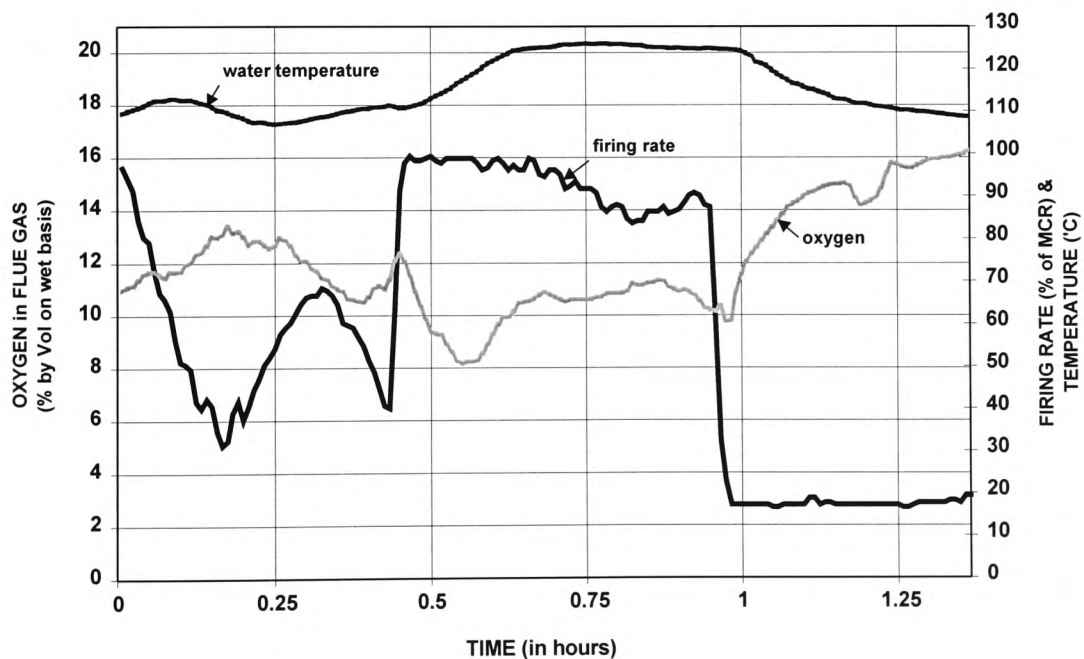


Figure 5.18 Oxygen Concentration & Water Temperature following A Step Change in the Hot Water Temperature Set Point under Conventional PID Control

The CO emission was fairly acceptable although the transient level from full load to turn was almost twice as much as from turndown to high fire, probably due to a fuel bed build up as depicted in Figure 5.19. Both sulphur dioxide and nitrogen oxides emissions were within acceptable limits.

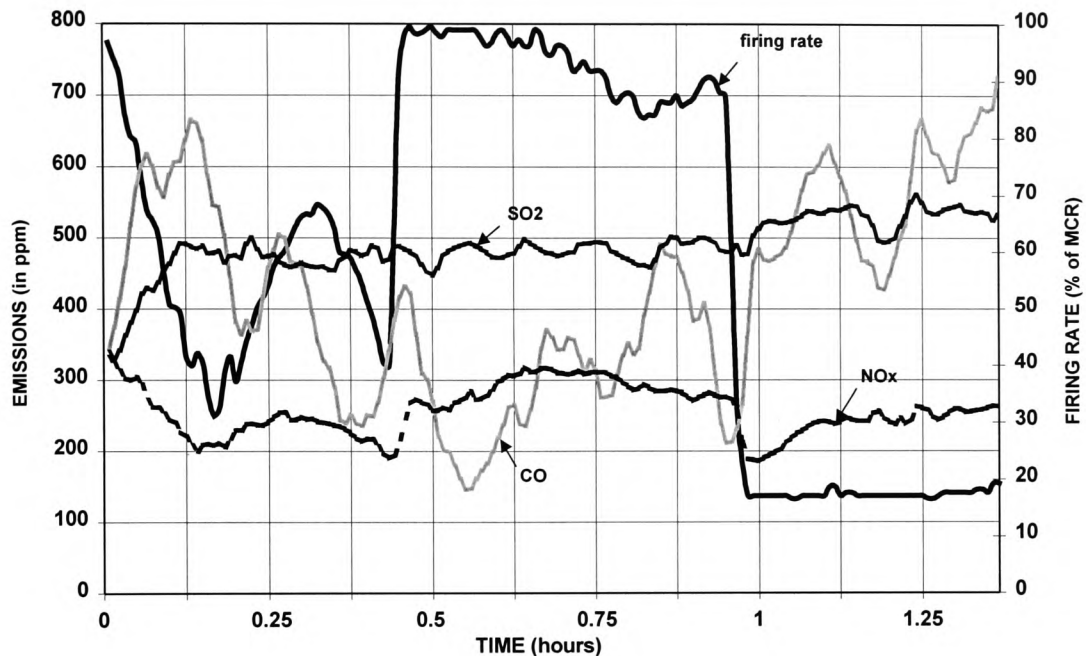


Figure 5.19 Pollutant Emissions following a Step Change in the Hot Water Temperature Set Point under Conventional PID Control

5.4.4 Plant Response Following Neural Network Based Controller (NNBC) Operation (Test 16, 17a & 17b)

The modifications to the NNBC structure (developed from earlier work) involved incorporating an adaptive gain tuning capability for the corrective network based on the rate of change of the process parameters, i.e. automating the task of iterating for a suitable corrective network gain (multiplying an initial estimate with an increasing or decreasing factor) by checking whether the rate of change of the parameter was within suitable limits or not. Since there were two parameters which the NNBC needed to control, a second control loop for the tracking of the process parameter set point was

built into the earlier NNBC architecture. The target oxygen green band in this case was dependent on the firing rate and from the information gathered from Test 13 an oxygen target table (Table 5.7) was adopted for the purpose of the oxygen trimming loop.

Table 5.7 Oxygen Target Band with the Corresponding Range of Firing Rate

Range of Firing Rate (% of MCR)	Target Optimum Oxygen Band
$17 \leq FR \leq 35$	11 to 13
$36 \leq FR \leq 70$	9 to 11
$71 \leq FR \leq 100$	7 to 9

The staging program took the difference between the current and newly evaluated firing rate (by the corrective network for the process variable loop) and if the change was greater than the predefined limit of 5% MCR, it performed the necessary staging of coal feed and air flow in 2.5% MCR steps depending on the direction of the load change. Figure 5.20 shows the flow chart of the modified NNBC controller developed for the purpose of controlling the industrial stoker plant. Details of the MATLAB™ code of the modified NNBC can be found in Appendix G.

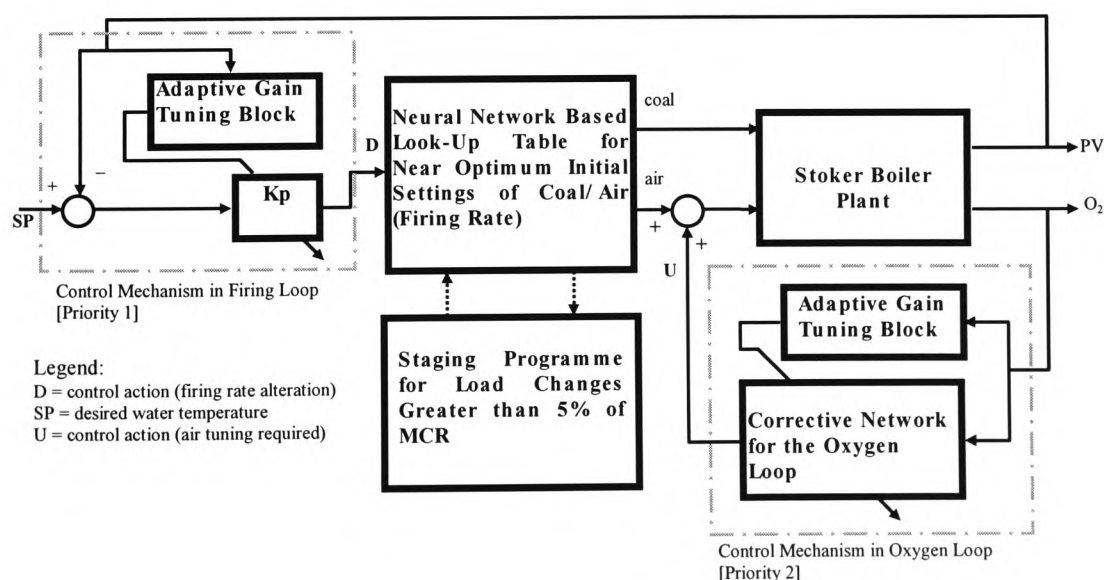


Figure 5.20 Modified NNBC Structure for the Control of the Industrial Chain Grate Stoker Plant

The modified NNBC was implemented on a supervisory level, retrieving necessary feedback parameters via the slave process controller (the Honeywell UDC3000 was replaced by a Bristol Babcock RTU3305 process controller in order to obtain the remote set point adjustment capability) and sending the control decisions back to the slave unit via a serial communication cable to alter the actuator set point. As with Section 5.4.3, the three experiments carried out with the NNBC (Tests 16, 17a and 17b) were aimed at evaluating the performance of the NNBC at maintaining the desired hot water temperature set point (120°C) and also to step changes in the process variable set point (from 88°C to 105°C and 105°C to 120°C).

5.4.4.1 Plant Response Under Automatic NNBC Mode Tracking Hot Water Temperature Set Point (Test 16)

The target set point in this experiment was 120°C, as in Test 14, and the response of the plant under the influence of the NNBC is shown in Figure 5.21 and 5.22 below. It is clearly evident that a smaller fluctuation in the firing rate occurred whilst keeping the hot water temperature at the desired 120°C with a maximum peak load of just over 60% compared to 90% in Test 14. With a more stable adjustment of the firing rate the corresponding oxygen concentration, sulphur dioxide and nitrogen oxides emissions also demonstrated a much more stable pattern. In addition to maintaining the water temperature set point, the NNBC also trimmed the oxygen at steady-state combustion (after 20 minutes of the last load change, or a load change smaller than 5% of MCR), indicated by the grey dashed line that deviates from its initial setting (coinciding with the coal feed). As a result, the excess air level in this experiment, depending on the firing rate, was lower than that attainable during operator's best practice. In other words, the NNBC was able to deliver the load required with less fluctuation than the plant PID controller with a lower excess air level, hence minimising the sensible heat loss from the boiler. In so doing it improved the overall carbon monoxide emission tremendously, with an average steady-state emission of 150ppm and occasional peaks at turndown (as a result of fuel bed build up from high fire) of up to 800ppm. Sulphur dioxide and nitrogen oxides showed no cause for concern.

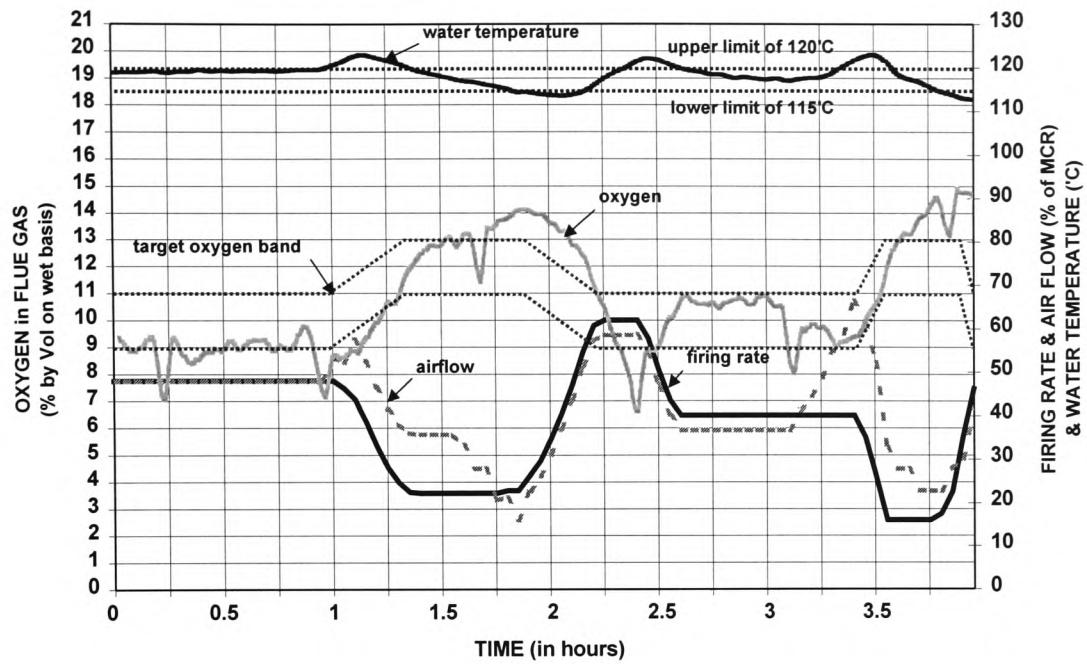


Figure 5.21 Oxygen Concentration & Water Temperature under NNBC Effort to Tracking the Set Point Temperature

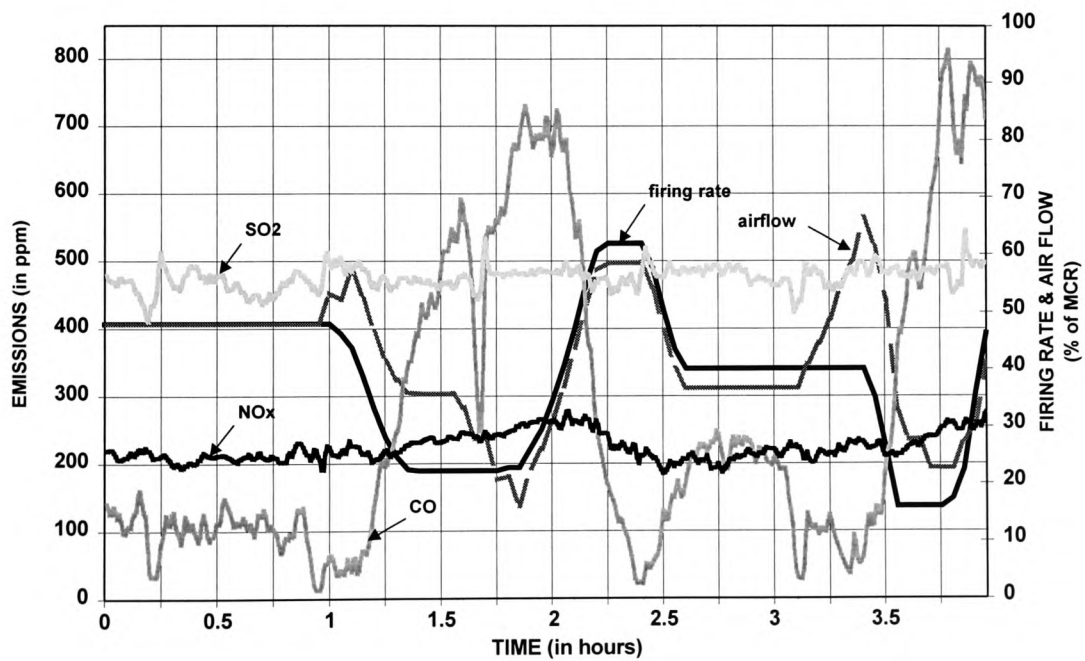


Figure 5.22 Pollutant Emissions under NNBC Effort to Tracking the Set Point Temperature

5.4.4.2 Plant Response Under Automatic NNBC Mode Following Temperature Set Point Change (Test 17a & 17b)

The performance of the NNBC at handling a set point change in the hot water temperature was carried out in this set of experiments which involved two experiments namely:

- (i) *Test 17a* – NNBC to Perform a Step Set Point Change from 88°C to 105°C;
- (ii) *Test 17b* – NNBC to Perform a Step Set Point Change from 105°C to 120°C.

The results from Test 17a are illustrated in Figure 5.23 and Figure 5.24, whilst the result from Test 17b are depicted in Figure 5.25 and 5.26. These are discussed with respect to the excess air level and pollutant emissions and the NNBC performance is compared to the conventional PID controller.

(i) Test 17a - NNBC to Perform a Step Set Point Change from 88 °C to 105 °C

As shown in Figure 5.23, there was little overshoot of the water temperature as the NNBC increased the firing rate gradually to meet the new demand. The inclusion of the staging profile is justified from this Figure where the initial near optimum settings of coal feed and airflow has resulted in little overshoot of the oxygen concentration and as the firing rate steadied out at about 50% of MCR the oxygen concentration fluctuated within the associated desired green band of 9 to 11%. It is worth stating that this experiment was carried out 1.5 hours after the boiler was fired up (boiler was in a banked state prior to start up), hence the longer period of time (40 minutes as compared to 10 minutes with the conventional PID controller) taken for the water temperature to reach the new set point. This can be observed with the flame front data showing a trend towards the combustion process establishing itself (please consult the Section 6.2.1). Test 17b was conducted later on that day (3.5 hours after start-up) and took a comparable 15 minutes to attain the new set point. The corresponding carbon monoxide level in this experiment was considerably lower than those obtained from Test 15, whilst similar trends of SO₂ and NO_x to those of Test 15 can be observed from Figure 5.24. It must be stressed here however, that by providing a lower level of excess air the level of NO_x was also reduced.

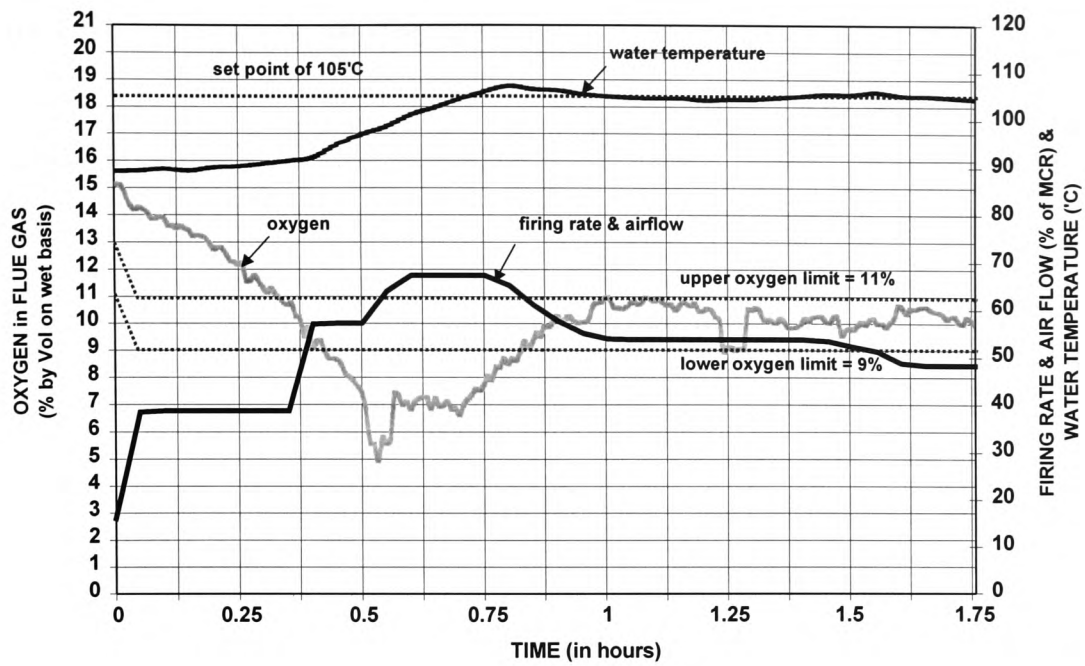


Figure 5.23 Oxygen Concentration & Water Temperature following A Step Change in the Hot Water Temperature Set Point with the NNBC (Test 17a)

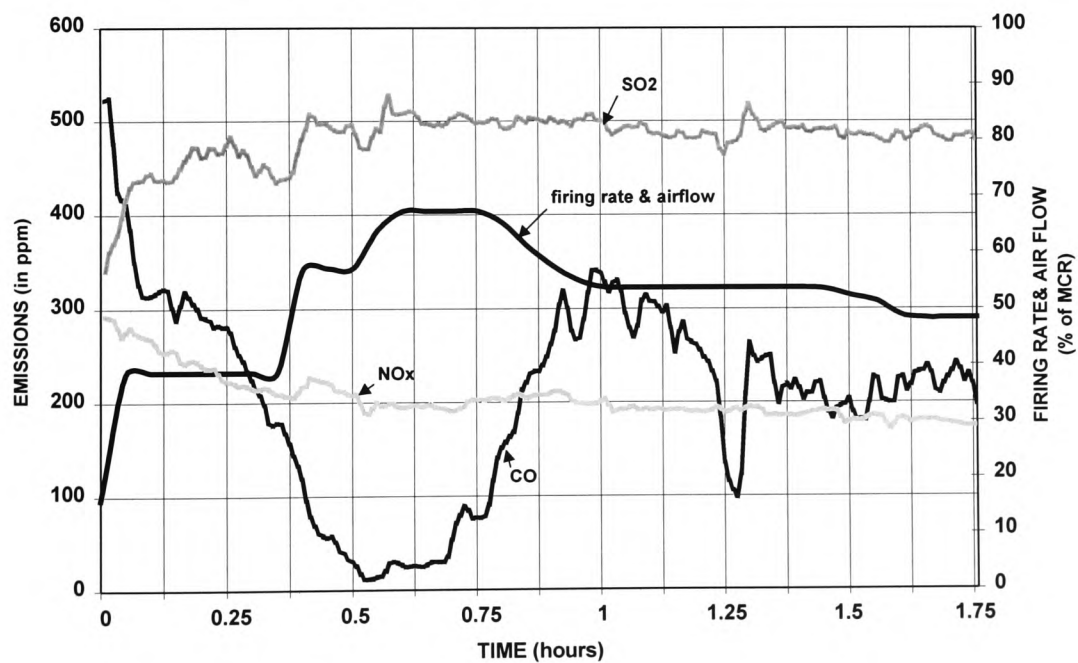


Figure 5.24 Pollutant Emissions following A Step Change in the Hot Water Temperature Set Point with the NNBC (Test 17a)

(ii) Test 17b - NNBC to Perform a Step Set Point Change from 105 °C to 120 °C

As shown in Figure 5.25 the time taken for the water temperature to increase from 105°C to 120°C was 15 minutes with gradual increases in the firing rate. The fuel bed in this particular experiment appeared to be thicker than usual and the evidence that points to this can be found in the relatively lower oxygen concentration in the first 15 minutes of the experiment which also resulted in a high CO peak of 1300ppm, before the condition deteriorated with the oxygen level dropping below the lower green oxygen limit of 7% and at 0.5 hours the CO emission reached 3600ppm (the stack was noticed to be smoking).

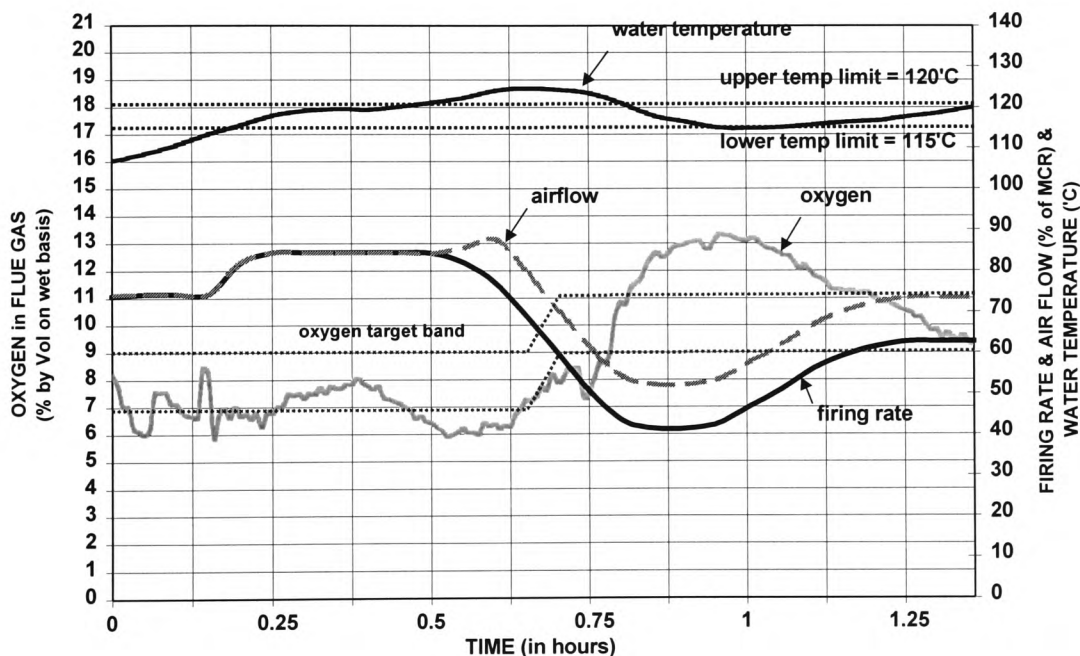


Figure 5.25 Oxygen Concentration & Water Temperature following A Step Change in the Hot Water Temperature Set Point with the NNBC (Test 17b)

This reduced operating condition shown in Figure 5.26, was probably as a result of *disturbances* in the fuel bed which was detected by the NNBC (error in the oxygen reading). The initial estimate of the airflow was increased, shown by the dashed grey line deviating from the initial setting (coincident with the coal feed), to cope with the

deficit in combustion air and the situation was brought back under control after 12 minutes. Following this *corrective action* by the NNBC, the CO emission fell to a much more acceptable level of below 600ppm with the oxygen level rising above the lower limit of 7%. This situation could not have been dealt with by the conventional PID controller, as there was simply no mechanism to detect such reduced operating performance and the deficit in the combustion air flow would have been left uncorrected until such a condition was discovered by the plant personnel.

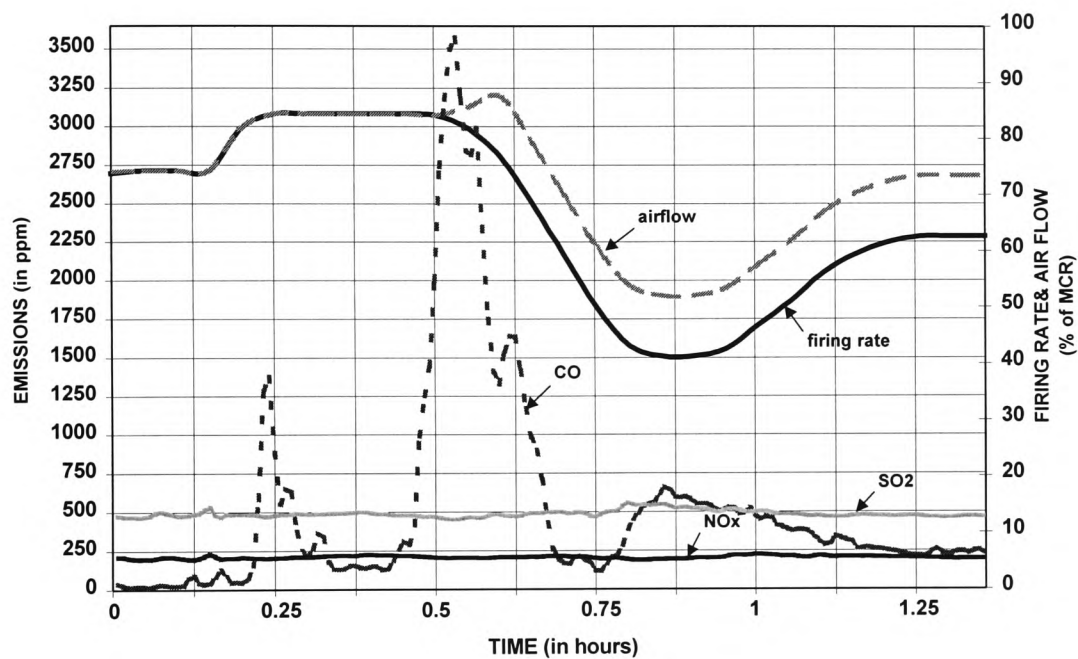


Figure 5.26 Pollutant Emissions following a Step Change in the Hot Water Temperature Set Point with the NNBC (Test 17b)

5.5 Neural Network Based System Identification – Black Box Modelling Using ANNs

This Section is dedicated to the use of the feed-forward Multi-Layered Perceptron (MLP) network to identify the combustion process (oxygen concentration in the exhaust flue gas) and pollutant formation (nitrogen oxides and carbon monoxide) of the chain grate stoker boiler test facility at CRE. The identification work presented here addresses the current deficiencies in modelling work as pointed by a survey of coal research and development conducted by Smoot (1984) and Hobbs *et al.* (1992, 1993). The ‘Neural Network Based System Identification Toolbox’ developed by Noorgard (1995) for use with MATLAB™, has been extensively used in this work for the system identification task although much of the basic understanding of the neural network ‘language’ was obtained from the ‘Neural Network Toolbox’, also for use with MATLAB™, developed by Demuth and Beale (1995).

5.5.1 System Identification Procedure

Identification is concerned with observing the signals produced by the system or plant under investigation, to known inputs and find a model that best regenerates the original output signals when subjected to the same input signals [Ljung, 1987; Soderstrom and Stoica, 1989]. It is an extremely useful tool that can be used to ‘model’ a process without having to consider many complex physical laws that govern a process, which very often happens in real life situations. Identification using neural networks in many ways is similar to the parametric identification approach, as multi-layered neural networks are versatile non-linear maps [Chen and Billings, 1991]. Indeed ‘parametric identification methods’ are techniques to estimate the parameters in a given model structure, which essentially involves a numerical search for suitable values of the associated parameters of the model to yield satisfactory results [Ljung, 1995]. However, in the case of system identification using feed-forward neural networks, the designer will have to provide the hidden layer with enough neurons to model the complexity of the input-output relationship being fitted, and this is generally determined through trial and error. This exercise can be seen as effectively increasing

the class of the ‘un-parameterised’ model to satisfy the underlying complexity of the input-output data set, before commencement of network training which ultimately determines the appropriate values of the network parameters through learning. Therefore, the system identification problem associated with artificial neural networks essentially involves finding a suitable model structure and subsequently good numerical values for its parameters (weights and biases of the network). The theoretical basis of non-linear modelling by using neural networks has been well established in the last decade by authors such as Hornik *et al.* (1989). These authors have shown that a two layer feed-forward Perceptron network containing enough neurons with the non-linear sigmoidal (continuous, bounded and non-constant) activation function in the hidden layer, can approximate any continuous function acting on a compact subset of \mathcal{R}^n , denoted by D , onto an output space \mathcal{R}^m . In mathematical form this can be written as $f:D \subset \mathcal{R}^n \rightarrow \mathcal{R}^m$, where n and m are the number of input and output vectorial elements respectively, and f is the theoretical function. Therefore, the overall input-output relationship of an n -input and m -output network with one (or more) hidden layers can be denoted as $f:D \subset \mathcal{R}^n \rightarrow \mathcal{R}^m$, where f is the approximation of the theoretical vectorial function f , realised by the network.

The work involved in identifying the dynamics of a process can be summarised into four basic steps. Figure 5.27 below depicts the four steps which involve gathering of data from experiments, selecting a model structure, estimating the model and finally validating the identified model with new data sets. With respect to the first step, it is essential that the training data covers the entire operating region of interest and is gathered with the correct choice of sampling frequency [Ljung, 1995; Noorgard, 1995]. Ideally the process to be modelled should be persistently excited so that all the dynamic modes of response (in this work these were plant responses to gradual, large load changes, variation in the airflow and the two staging profiles) are reflected in the data collected which will be used to teach the black box neural network model. In addition, this information must come from a continuous stream of data gathered from the same experiment in order to avoid any discontinuities or irregularities in ‘describing’ the dynamics of the process. The next stage was the selection of a model structure and in this work a MLP neural network architecture was adopted as the

framework of the model structure. Furthermore, since the process to be identified was non-linear in nature, it also involved choosing an appropriate set of regressor vectors [Noorgard, 1995]. The ARX (Auto Regressive with eXogenous inputs) regressor structure was chosen based on its popularity in linear system identification and hence was extrapolated to include the neural network models [Premier *et al.*, 1999]. More sophisticated regressor forms could well reduce the sum square error during neural network training but the added complexity of the model was not justified by the possible improvement in forecasting [Premier *et al.*, 1997]. The structure of the ARX regressor uses previous inputs and outputs in order to deliver a prediction of the current output at one or more sample periods in the future [Premier *et al.*, 1997; Ljung, 1995]. The function NNARX in the Neural Network System Identification Toolbox, allows the user to utilise such a regressor structure in the context of neural network modelling. The associated regressor vector term is defined as:

$$\varphi(t) = [y(t-1)...y(t-n_a), u(t-n_k)...u(t-n_b-n_k+1)]^T;$$

and the predictor can be expressed as $g(\varphi(t), \theta)$;

where $\varphi(t)$ is a vector containing the regressors, θ is a vector containing the weights and biases of the network and g is the function realised by the neural model through learning. The terms n_a and n_b denote the number of past outputs and inputs that are required and the term n_k denotes the delay of the system, in terms of the number of sampling periods. According to Noorgard, the function NNARX has a static predictor (feed-forward only with no feedbacks), which is more stable in its prediction than other model types which are recurrent (future network inputs depend on past network outputs) and further suggested its use as a general rule of thumb. In addition, the presence of noise in the signals from the Tactician front end controllers (coal, air and oxygen in flue gas) and the portable gas analyser (Testo 33) can be considered to be insignificant, which further warrant the use of the NNARX function [Noorgard, 1995].

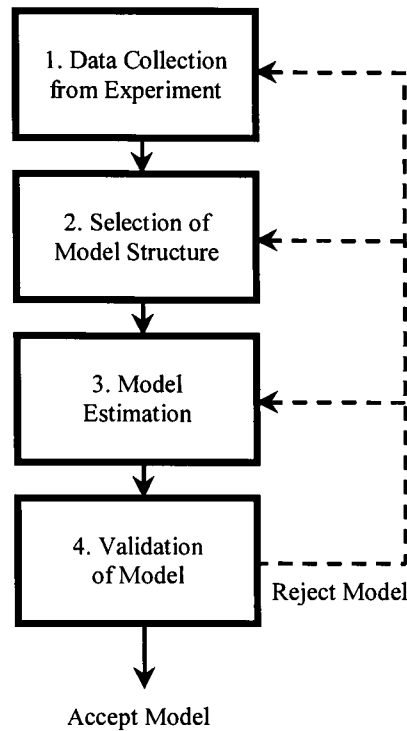


Figure 5.27 The Four Basic Steps Towards System Identification

The tasks of choosing the appropriate model order (number of past inputs and outputs) and also the delay of the system is relatively difficult for a non-linear process. Even in the absence of more precise knowledge, some physical insight through experience will to some extent enable the designer to intuitively suggest the orders and delays of the system [Noorgard, 1995; Ljung, 1995]. Once the model(s) has been generated with the desired error goal during neural network training, the final stage is to validate the black box model(s). This was carried out by passing unseen data to the model(s) and visually inspecting the plot comparing the actual measurements to the model predictions. The average sum square error (ASSE) between the actual response and the model prediction for the validation data set as defined below:

$$ASSE = \frac{\sum_{i=1}^N (Y_i - y_i)^2}{N} \text{ was used as an index for comparison, where;}$$

Y_i is the actual plant response;

y_i is the model prediction and N is the number of samples within the data set.

This validation exercise is of paramount importance, as it provides an indication of the model's ability to generalise. In linear system identification, the auto-correlation function of the residuals and cross correlation function between the input signals and residuals are used to measure the performance of a model, but in the case of non-linear models, the most important tool is the comparison of the predictions of the derived model with the actual plant response of the validation data sets. As such the selection of the test data must be done with care in order to fully investigate the predictive ability of the model. Should the model predictions prove to be unsatisfactory, then the designer will have to refer back to the two previous steps (shown in dashed line), as illustrated in Figure 5.27.

Very often this will involve either the selection of a different regressor structure (altering the delays, number of past inputs and outputs) or adopting a different network architecture, for example changing the number of neurons in the hidden layer. Unfortunately this empirical analysis will have to be carried out on a trial and error basis until satisfactory results are obtained. If the predictions still proved to be unsatisfactory, it would be worth considering additional feature(s) as inputs to the model in order to improve the neural network learning of the functional relationship [Premier *et al.*, 1999]. Again, the adoption of the additional feature(s) hinges solely on the degree of influence that the particular feature(s) have on the process being modelled and in general the experience of expert operator(s) is highly sought after.

5.5.2 Feed-Forward Multi-Layered Perceptron (MLP) Neural Network – Architecture of the Neural Network ARX Models

Many neural network applications to input-output modelling and data classification involves the so-called feed-forward Multi-Layered Perceptron (MLP) neural networks [Chong *et al.*, 1997; Narendra and Parthasarathy, 1990]. As the name implies the signals in these type of networks only flow in one direction, from the input to the output (final) layer. There are no feedback connections between the individual layers and no links between the neurons (simple processing elements) in each layer and hence

these types of network are only capable of statically mapping the input vectors to their corresponding targets, i.e. they have no dynamic memory. Although feed-forward networks do not have internal dynamic memory, they are still widely used in dynamic system identification by feeding the past discrete-time inputs and outputs of the system to the network as inputs. This can be achieved by employing the tap-delay-line technique to the system and using the next time step output of the system as the target output [Chen and Billings, 1990; Narendra and Parthasarathy, 1990]. Thus the tap-delay-line method basically converts the temporal modelling problem (learning the dynamic behaviour of the system in real time domain) into a spatial modelling problem (statically mapping the tapped-delayed inputs and outputs to the next output).

A black-box model approach is useful in situations where the relationships between the input and output data are more important than an in-depth understanding of the process being modelled [Ljung, 1987; Premier *et al.*, 1999]. The difficulties in formulating mathematical models based on the underlying dynamics of the combustion process is well known, and much literature has been reported with respect to this issue [Smoot, 1984; Hobbs *et al.*, 1992]. The feed-forward MLP network is currently the most widely used artificial neural network and the extent of its utilisation has been proven in numerous practical applications [Demuth and Beale, 1995].

The main reason for this popularity is due to its ability to model complex functional relationships between the given input and output data sets by learning from examples. Over the last decade it has been demonstrated to be a valuable tool for the synthesis of black box models for various non-linear processes (please consult Section 2.4.3). The type of MLP network structure adopted for the identification tasks here was confined to one hidden layer of hyperbolic activation function neurons and a single neuron in the output layer of linear activation function [Noorgard, 1995]. Figure 5.28 depicts the architecture of the MLP network employed for the modelling work.

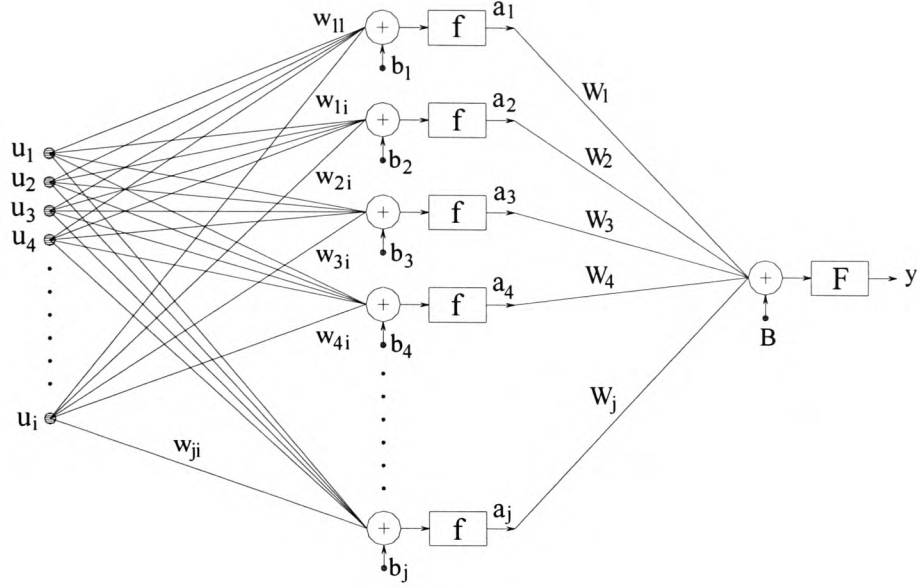


Figure 5.28 The Feed-Forward MLP Network Architecture for the ARX Neural Model Structure

From Figure 5.28 the following analysis can be established:

$$y(w, b, W, B) = F\left(\sum_{j=1}^{10} a_j W_j + B\right) = F\left(\sum_{j=1}^{10} W_j f\left(\sum_{i=1}^n u_i w_{ji} + b_j\right) + B\right), \text{ where } n \text{ is the}$$

number of features in the input vector;

$y(w, b, W, B)$ is the model prediction, as a function of the network weights and biases;

F is the linear activation function of the output layer;

W_j are the weights of the connections between the hidden and the output layer;

B is the bias of the output layer;

f is the activation function of the hidden layer, which is of the hyperbolic tangent;

w_{ji} are the weights through which u_i is connected to the hidden neuron j and b_j is the bias of the hidden layer and;

u_i represents the feature input vector of length n , presented as the input to the feed-forward MLP network.

As shown in Figure 5.28, the fully connected network structure consisted of a hidden layer with 10 neurons of hyperbolic tangent transfer function and an output layer with a single neuron of linear transfer function. Please note that the type of model

considered here consisted of multiple inputs (more than one attributes) but having only one output, i.e. multiple input and single output (MISO) models. The weights and biases (specified by the vector θ , which is a function of matrices w , b , W and B) are the adjustable parameters of the network, where suitable values are determined through learning from a training data set provided by the designer/teacher. The training set is normally expressed by:

$Z^N = \{[u(t), y(t)] \mid t = 1, 2, \dots, N\}$, where N is the number of data samples or vectors. The ultimate aim of the training process was to realise the functional mapping from the examples to a set of possible weights and biases of the network:

$$Z^N \rightarrow \theta,$$

So that the network predictions $Y(t)$ will come close to the actual plant output $y(t)$ based on the introduction of a measure of closeness in terms of a mean square error criterion. A Gauss-Newton based Levenberg-Marquardt method was used here to minimise the mean square error criterion, owing to its rapid convergence and robustness. The method adopted by Noorgard in his function MARQ can be found in Fletcher (1987).

The training data set was obtained from Test 10, which reflected the dynamics of the stoker boiler plant to both gradual and large load changes, variations in the airflow whilst under constant coal feeds and finally the response of the plant to the two coal/air staging profiles. In other words, all of the possible modes of excitation that can be exerted on the plant. Four validation data sets were selected for the purpose of testing the network, and these were carefully chosen to examine the ability of the neural model to re-enact the different operating scenarios, namely gradual load changes (Test 1), large load changes (Test 6) and finally the data gathered from two other control experiments (Test 8, 9) over a wide range of load variations (including airflow variations whilst under constant coal feed rates). The latter two validation data sets were gathered when the boiler was operated under similar control parameters (the same gain but slightly different controller sampling period), and therefore can be used to test the *repeatability* of the model's prediction.

Training Data Set

1. Test 10 (control experiment with gain of 5 and controller sampling period of 60 seconds).

Validation Data Set

1. Validation Set 1 – Test 1 (load change from 0.3MW to 0.6MW in 0.1MW steps and back to 0.3MW at near optimum excess air level).
2. Validation Set 2 - Test 6 (single load change from 0.3MW to 0.6MW and vice versa with undesirable staging profile).
3. Validation Set 3 – Test 8 (control experiment with gain of 10 and sampling period of 10 seconds)
4. Validation Set 4 – Test 9 (control experiment with gain of 10 and sampling period of 30 seconds)

The first two validation data sets were 8 months apart from the training data set, which represents a significant temporal separation between the examples and unseen data sets and will therefore impose a stiffer test on the performance of the neural model. It should be noted however that any time varying characteristics due to influences such as boiler fouling, corrosion, etc., are assumed to be unpredictable and factors such as variations in the moisture, coal quality and bed distribution are tolerable and can be taken as disturbances to the process being modelled [Ljung, 1995; Premier *et al.*, 1999]. For details of the description of the test results for training and validation data sets, please refer to Sections 4.1 and 5.3.

5.5.2.1 Non-linear (Neural Network) ARX Model for Oxygen in the Flue Gas

The selected input parameters for this model were the coal feed (rotary valve and grate speed) and the air flows (in duct 1, 2, 3 & 4), which were easily available from the Tactician front end units. An initial attempt included the flue gas temperature reading at the reversal chamber (closest thermocouple to the fire bed, hence the most responsive one to any changes in the bed) as one of the input parameters. This however

resulted in a reduced performance by the neural model and hence was omitted from further identification work. Two graphs are provided at the end of this sub-section to justify the reason for leaving out the temperature reading. The scope for on-line neural models, if the margin of error is within tolerable limits, is to reduce the user's reliance on physical sensors which in turns reduces the operating costs. A feed-forward MLP network of 10 hidden neurons were selected from trials and has been found to produce satisfactory results. A delay of 4 sampling periods was chosen for the coal feed and a delay of 1 sampling period was chosen for the air flow. In other words, it will take at least 2 minutes before the oxygen reading changes following a change in the coal feed and similarly for the air flow [Butt and Pulley, 1996]. From experience, two previous inputs (coal feed and air flows) and output (oxygen in flue gas) were selected to form the regressor vectors (inputs to the MLP network). Increasing the order of the model (having more past inputs and output) would probably reduce the sum squared error during training but this will to a larger extent lead to over-fitting of the data and could reduce the model performance [Premier *et al.*, 1999]. Furthermore, the general oxygen response pattern to a step change in coal feed and air flow appeared on a heuristic level to be similar to that of a damped 2nd order response curve. An illustration of the neural network ARX model for oxygen in the flue gas is as shown in Figure 5.29.

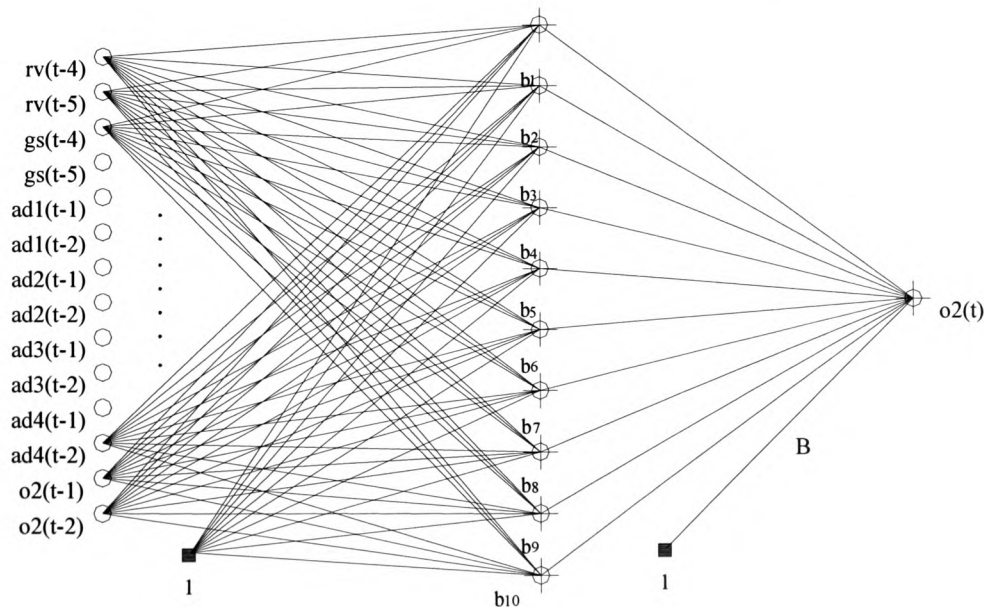


Figure 5.29 The Neural Network ARX Model for Oxygen in the Flue Gas

Training - The example data set was normalised to a mean of 0 and variance of 1, with the function DSCALE in order to improve network training [Noorgard, 1995]. It took less than 15 iterations with the Gauss-Newton based Levenberg Marquardt optimisation technique to reach the predefined normalised sum squared error (NSSE) goal of 0.015 with the training data set (more than 700 data samples of input and target pairs) as shown in Figure 5.30. Although the predefined error goal was probably not the global minimum it has been found by trail and error to be sufficiently low to provide good results, and was used in all three models. As can be seen in Figure 5.31, the model prediction has been found to be in good agreement (both in representing the dynamics of the process and in prediction accuracy) with the training targets (actual response). However this is to be expected since a good-fit model has been derived in response to the performance of an objective function through the learning process from the example data set. The average sum square error of the difference between the actual response and the model prediction for the training set was 0.047 and was taken as a bench mark for the purpose of comparing the model performance with the four validation plots.

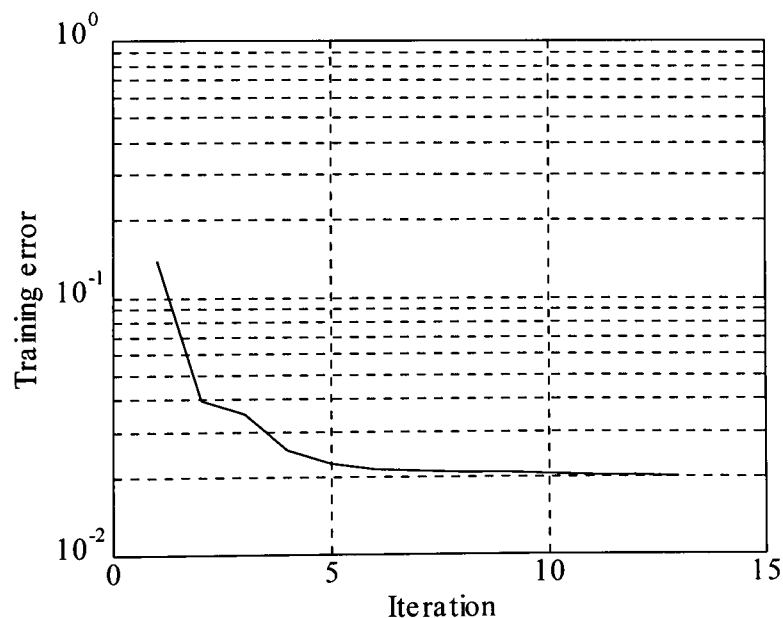


Figure 5.30 Training Error vs Number of Iterations for the Oxygen Model

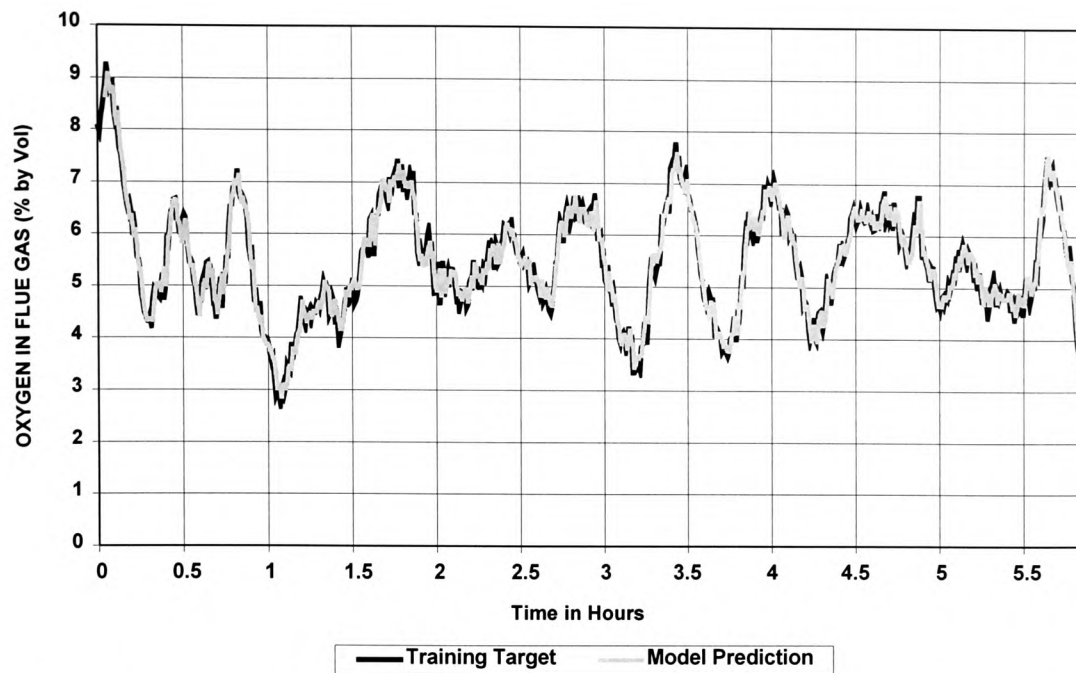


Figure 5.31 Targets vs. One Step Ahead Model Predictions for the Oxygen Model

Validation – The following Figures (5.32, 5.33, 5.34 & 5.35) illustrate the oxygen neural model’s one step ahead prediction as compared to the actual plant response with the four validation data sets.

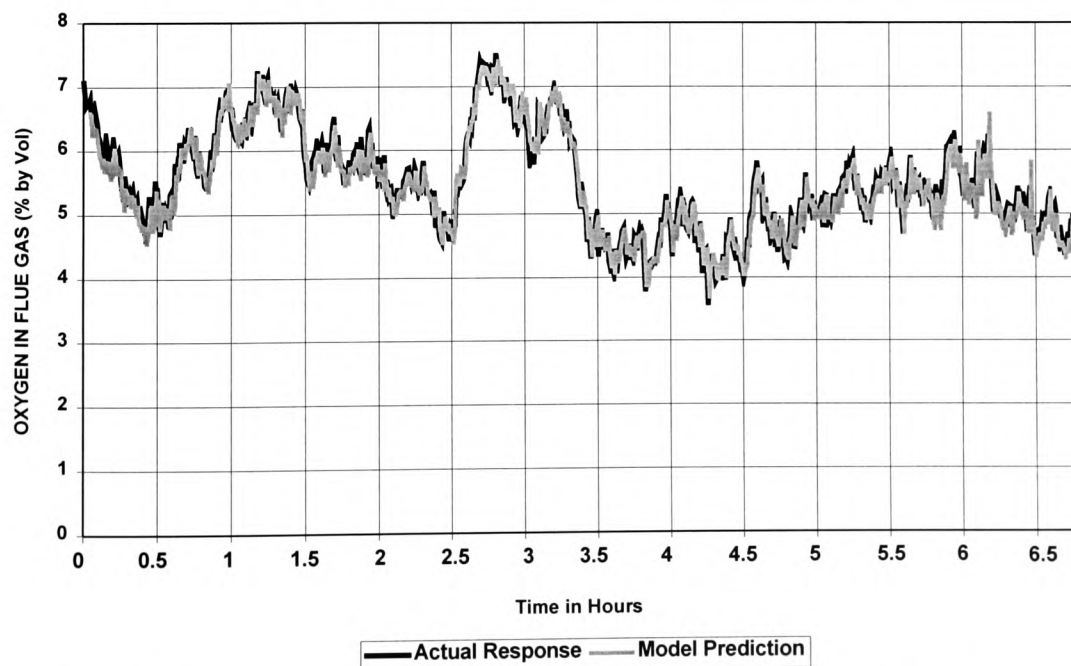


Figure 5.32 One-Step Ahead Prediction by the Neural Network ARX Model for Oxygen in the Flue Gas with Validation Data Set 1 (Test 1)

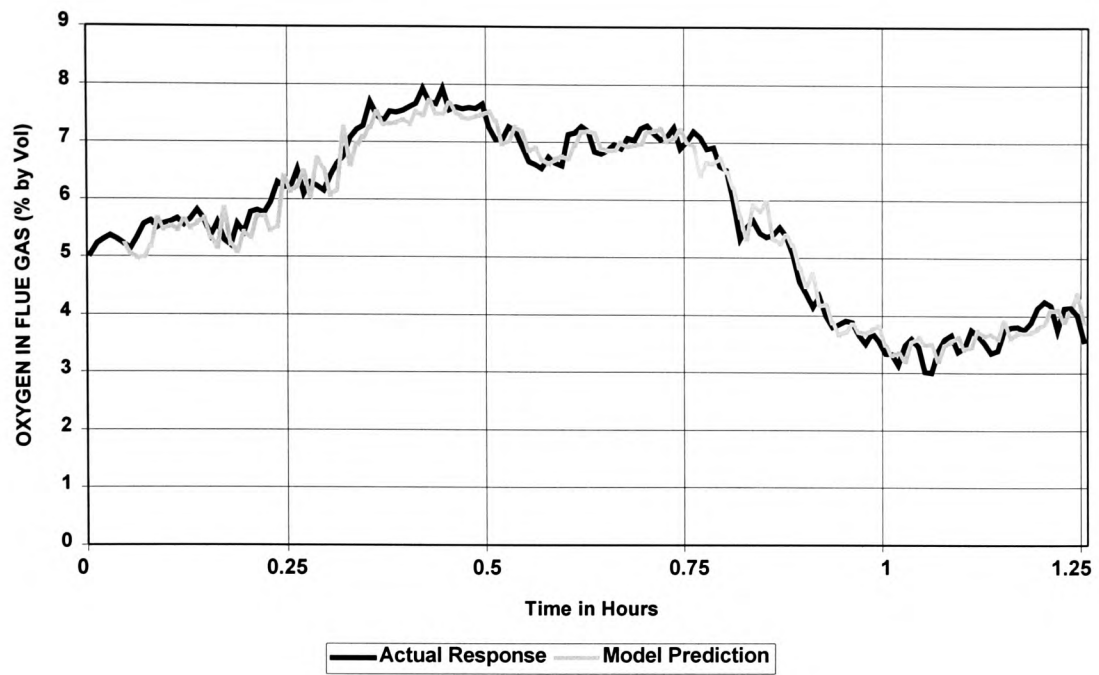


Figure 5.33 One Step Ahead Prediction by the Neural Network ARX Model for Oxygen in the Flue Gas with Validation Data Set 2 (Test 6)

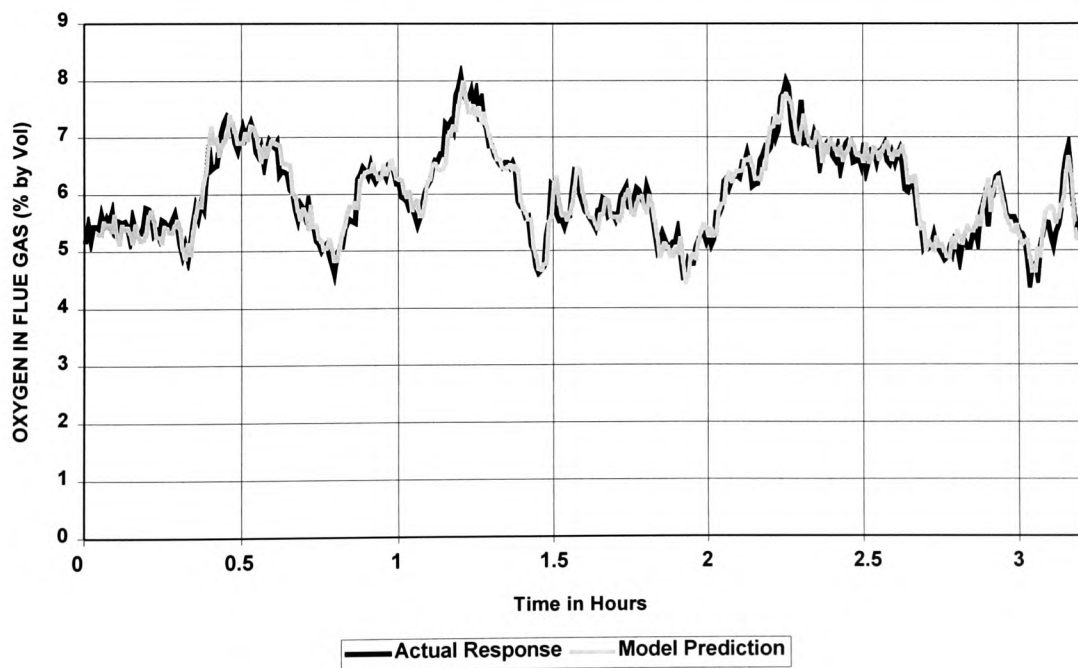


Figure 5.34 One Step Ahead Prediction by the Neural Network ARX Model for Oxygen in the Flue Gas with Validation Data Set 3 (Test 8)

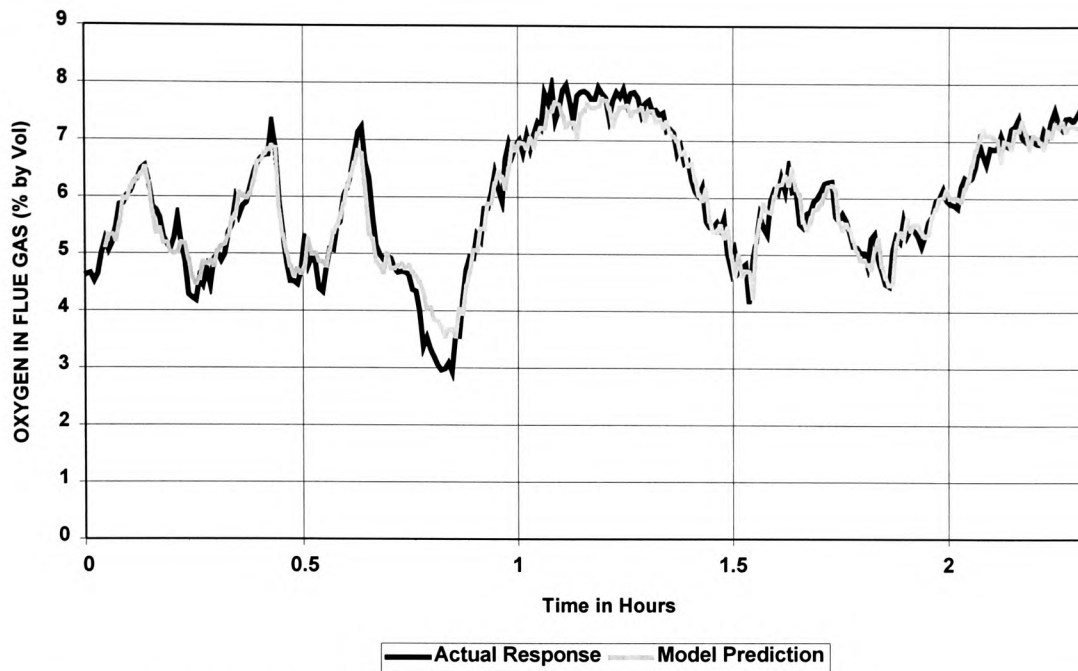


Figure 5.35 One Step Ahead Prediction by the Neural Network ARX Model for Oxygen in the Flue Gas with Validation Data Set 4 (Test 9)

Description of Results - Visual inspection of the four comparison plots clearly shows that the developed oxygen model was capable of delivering accurate one step ahead predictions for the oxygen concentration based on the past inputs and outputs (as defined by the regressor vector) of the four operating conditions. These highly accurate results, with the corresponding ASSE of 0.05, 0.07, 0.06 and 0.09 which were comparable to the ASSE of the training data set of 0.05, extended not only to the latter 2 validation sets but also the first two data sets despite the significant temporal separation (8 months). It can therefore be concluded from these results that the developed non-linear neural network ARX model of the oxygen concentration in the flue gas with the regression vector described earlier in this Section, has been able to represent the underlying dynamics of the actual process to sufficient accuracy.

Inclusion of Flue Gas Temperature in the Oxygen Model - The next two Figures (5.36 & 5.37) show the neural model's one step ahead prediction against the actual response when the flue gas temperature was included as one of the inputs to the model. The number of neurons in the hidden layer were the same as in the first neural model in order to allow a basis for comparison. It can be clearly seen from the two

plots that the prediction capability has been reduced considerably with respect to both representing the dynamics of the process and its accuracy. The corresponding ASSE for the two cases were 0.99 and 1.76 which were 19 and 35 times the magnitude of ASSE of the training set. The exclusion of flue gas temperature as one of the input parameters in the author's opinion, requires a valid justification as K-type thermocouple are readily available with relatively low cost (one unit of the industrial K-type low range thermocouple costs around £70) and can provide reliable measurements of the flue gas temperature. By virtue of the parallel structure of the ANNs (hence the term parallel distributed computing) one can argue that including the flue gas temperature reading as one of the input parameters would enhance the neural model's predictive capability. This has been demonstrated *not* to be the case and the cause was probably due to the reliability of the temperature reading itself over the 3 year period of boiler operation.

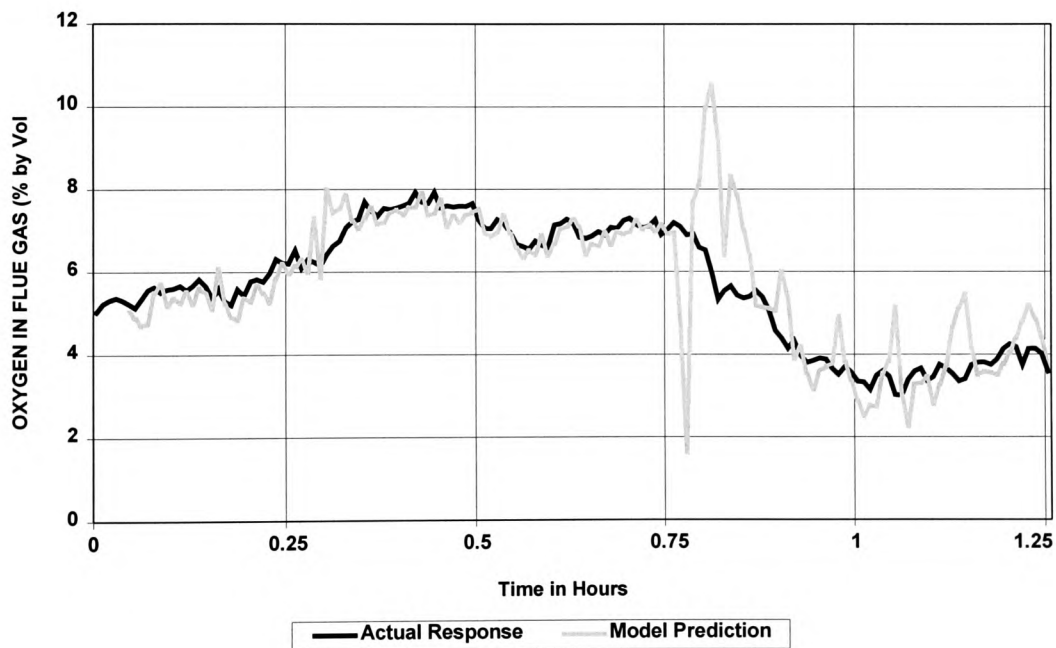


Figure 5.36 One Step Ahead Prediction by the Neural Network ARX Model for Oxygen in Flue Gas with Flue Gas Temperature as One of the Input to the Model with Validation Set 2 (Test 6)

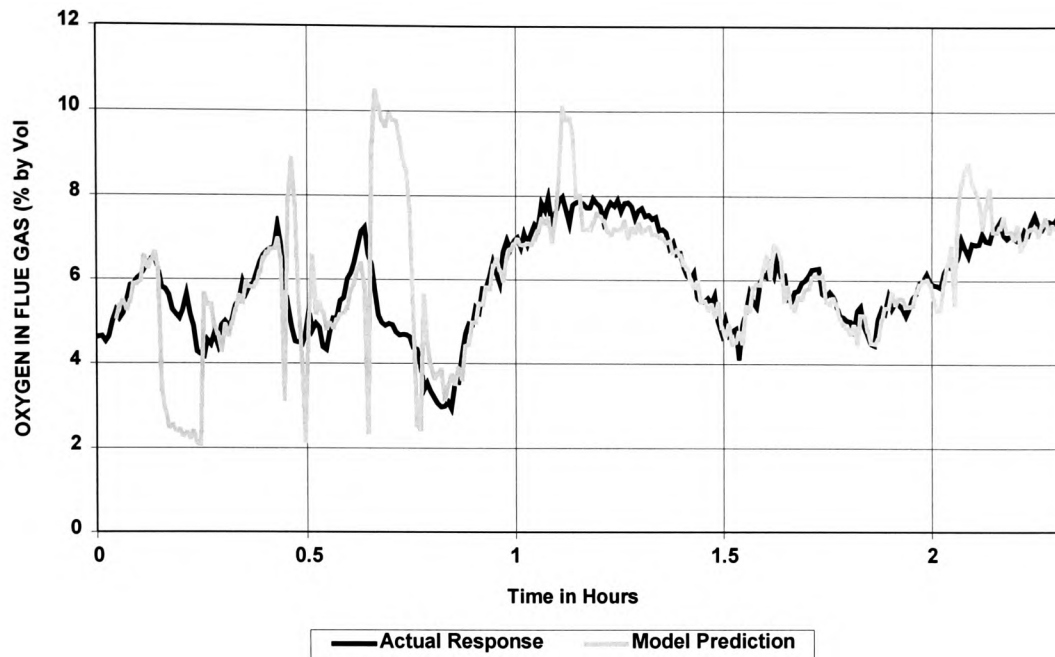


Figure 5.37 One Step Ahead Prediction by the Neural Network ARX Model for Oxygen in Flue Gas with Flue Gas Temperature as One of the Input to the Model with Validation Set 4 (Test 9)

5.5.2.2 Non-linear (Neural Network) ARX Model for Nitrogen Oxides (NO_x) Emission

The input parameters chosen for this model were the coal feed (rotary valve and grate speed), air flows (in duct 1, 2, 3 & 4) and the oxygen concentration in the flue gas (from the Zirconia analyser). The inclusion of the oxygen concentration into the model was necessary due to the fact that the oxygen level in the exhaust flue gas provided an indication of the amount of excess air being supplied for combustion. It is also a well known fact that the production of both thermal and fuel NO_x are highly dependent on the amount of combustion air and the temperature in the combustion zone.

Since the flue gas temperature reading has been omitted from further identification work, based on the findings from the oxygen model, it is evident that the oxygen reading was essential in order to enable the neural network model to identify the dynamics of the production of nitrogen oxides. It is in situations like this that an insight to the process being modelled can prove extremely useful when it comes to

selecting the appropriate parameters to use and the corresponding delays and orders of each of the parameters to form the regressor vectors as inputs to the neural model. As with the oxygen model, a MLP network architecture of 10 neurons in the hidden layer (of hyperbolic tangent transfer function), which was found by trial to be sufficient, was adopted as the framework of the non-linear ARX model.

The regressor vectors consisted of delayed input parameters (coal feed, air flow and flue gas oxygen concentration) and output (nitrogen oxides emission), and were batch fed to the MLP network during learning. The number of delays and order of the coal feed, airflow and oxygen reading were identical to the oxygen model, i.e. delay of 4 sampling periods before a change in coal feed affects the nitrogen oxides emission and a delay of 1 sampling period for a change in the airflow and the oxygen concentration, looking over a historical period of 1 minute (2 previous values) [Butt and Pulley, 1996]. The order of the nitrogen oxides emission however was increased by an additional sampling period to 3, as compared to the oxygen model.

This decision was made based on experience, as with the many intuitive assumptions associated with non-linear black-box modelling, following real time investigation of the response of nitrogen oxide emission following a step change in the firing rate (coal feed and air flow) which did not resemble a damped 2nd order response curve as observed for the oxygen reading. The only means by which the designer is able to decide whether it is a justifiable decision is to investigate the validation plots, which have been found to be exceptionally satisfactory after some modification to the network weights by an optimising algorithm in the Neural Network System Identification Toolbox [Noorgard, 1995]. A diagrammatic representation of the MLP network architecture adopted for the modelling task with the associated input nodes to accommodate the regressor vectors is shown in Figure 5.38.

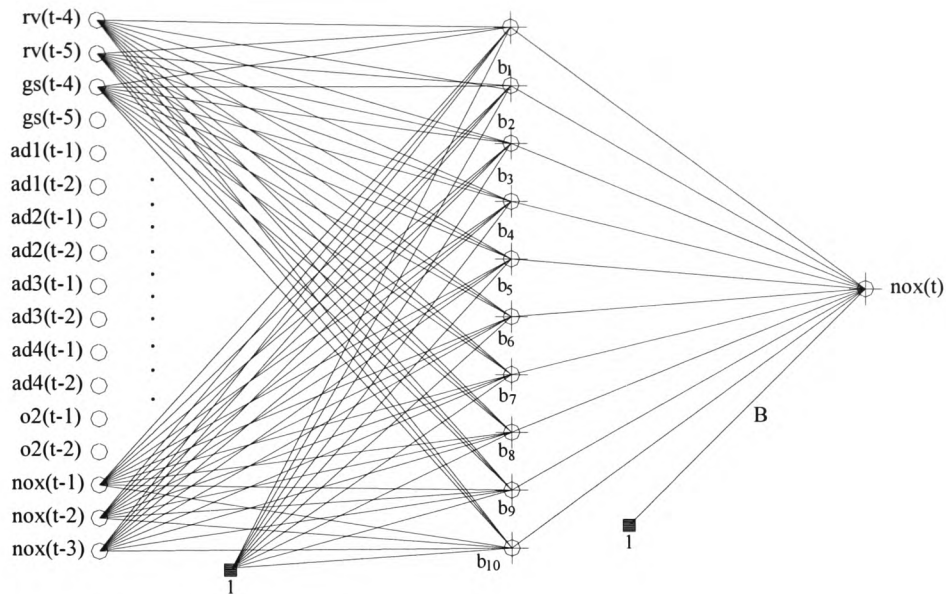


Figure 5.38 The Neural Network ARX Model for Nitrogen Oxides Emission

Training – As with the oxygen model, the training data set was normalised to a mean of 0 and variance of 1 by using the function DSCALE to improve network training [Noorgard, 1995]. The number of iterations required to reach an error goal of 0.015 was less than 5, as shown in Figure 5.39, which demonstrates the speed of convergence of the Gauss Newton based Levenberg Marquardt algorithm adopted by Noorgard in his function MARQ when considering batch training with an example data set of more than 700 vectors. The time required to reach such an error goal with the generic ‘Neural Network Toolbox’ by Demuth and Beale (1995) can easily take up to 48 hours or more.

Figure 5.40 shows the plot comparing the model predictions after learning with the actual targets and as one would expect, they are in good agreement. The average sum square error obtained by comparing the predictions to the targets when considering the actual physical units of the process parameter was 10.4 and will be used as the index by which to compare the validation plots with.

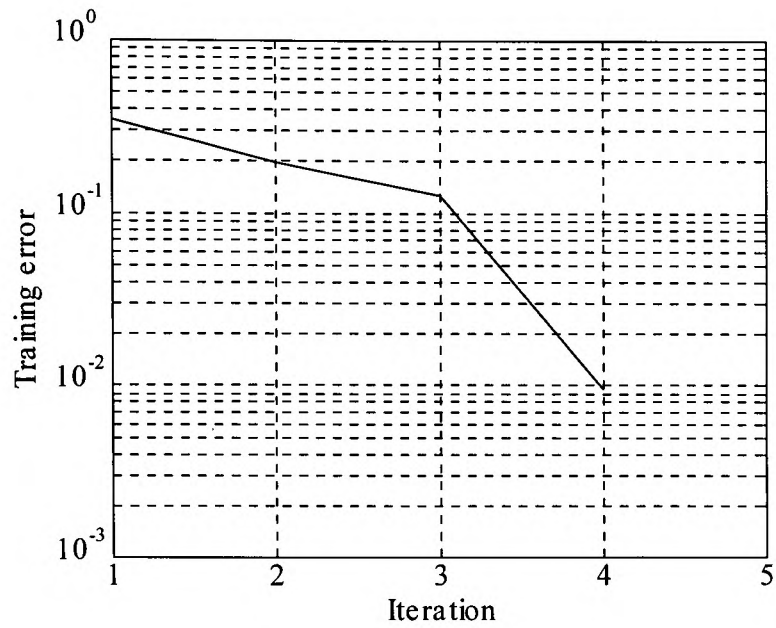


Figure 5.39 Training Error vs. Number of Iterations for the Nitrogen Oxides Emission Model

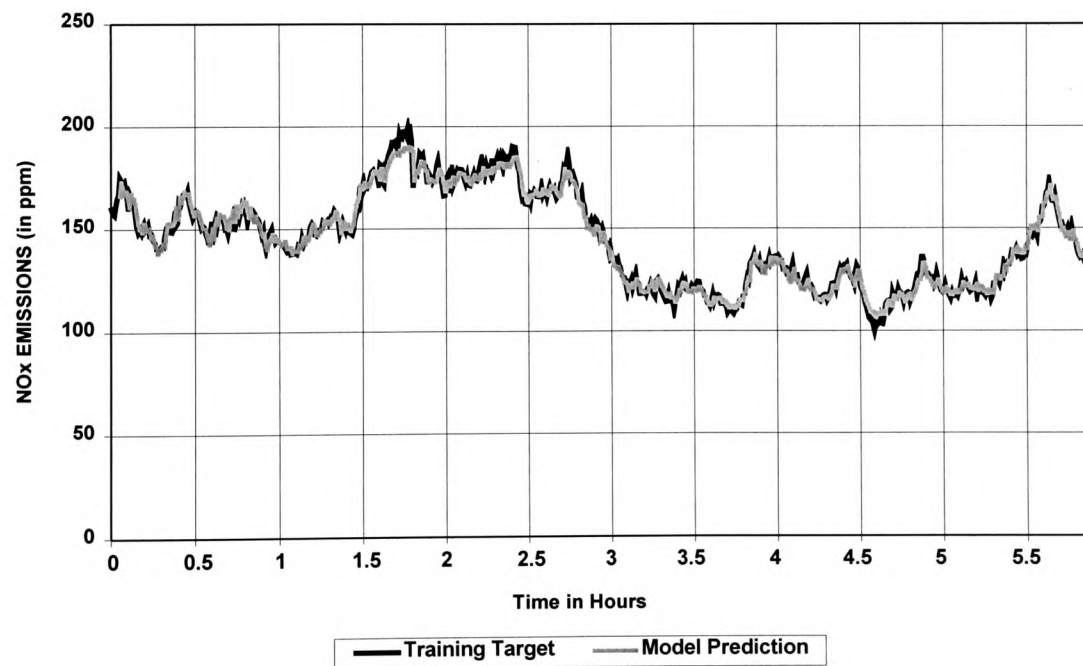


Figure 5.40 Targets vs. One Step Ahead Model Predictions for the Nitrogen Oxides Emission Model

Validation Sets – The neural model derived after the learning process was validated with the four test sets and was found to have slightly larger errors. The following two plots, Figures 5.41 and 5.42, demonstrate the inadequacy of the neural model’s one step ahead predictive capability as compared to the actual response of validation data set 1 and 2. The average sum square error for the two tests were 101.7 and 81.6 which represents a magnitude of 10 and 8 times the error encountered with the training examples. The following paragraph describes the steps taken to improve the neural model’s performance and to show the model’s predictive performance after optimisation.

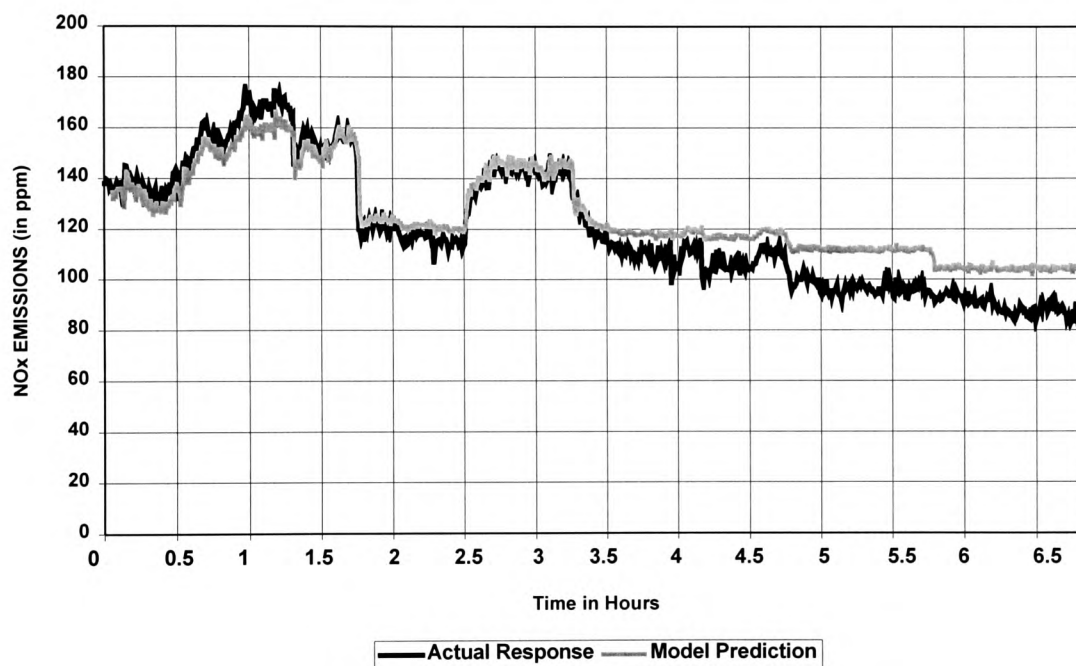


Figure 5.41 One Step Ahead Prediction by the Neural Network ARX Model for Nitrogen Oxides Emission with Validation Data Set 1 (Test 1)

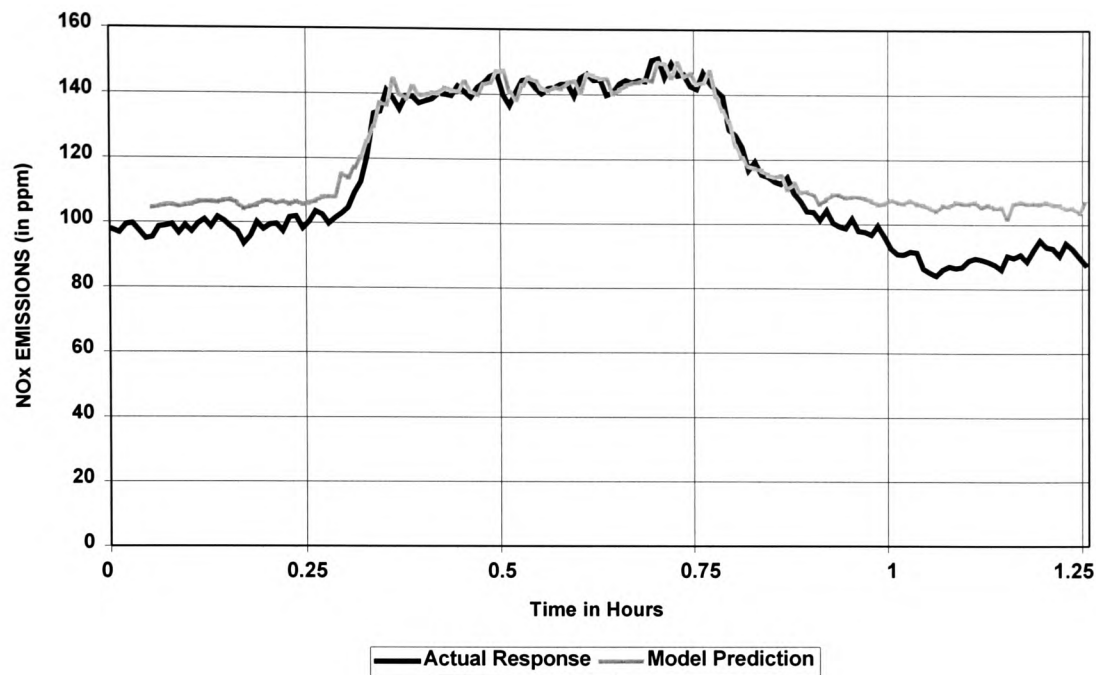


Figure 5.42 One Step Ahead Prediction by the Neural Network ARX Model for Nitrogen Oxides Emission with Validation Data Set 2 (Test 6)

At this point the designer can take a closer look at the delays and orders of the input parameters and intuitively fine tune these parameters and retrain the network to investigate for possible improvements. But visual investigation of the plots clearly shows that the neural model is able to represent the dynamics (response curve trends) despite a lower prediction accuracy, particularly in the lower load regions. It can therefore be concluded that the delays and orders of the inputs and output have been adequately chosen and a large enough network architecture has been adopted as the structure for the non-linear ARX model. A solution proposed by Noorgard (1995) is to reduce the dimensionality of the network by employing the so-called Optimal Brain Surgeon (OBS) algorithm to ‘prune’ the network in order to optimise its performance. This involves re-training the network for a number of iterations (50) in order to optimise the performance of the network with respect to both the training data set and a validation set, after some weights of the network are removed (5%). This algorithm ran until the global minima was reached and the network weights that delivered the best performance were adopted [Noorgard, 1995; Premier, 1999]. The time taken to prune the nitrogen oxides neural model was 6 hours with a P120MHz PC with 48MB of

memory and the end results were most encouraging. Figures 5.43, 5.44, 5.45 and 5.46, illustrate the improved neural model's performance with the four validation sets.

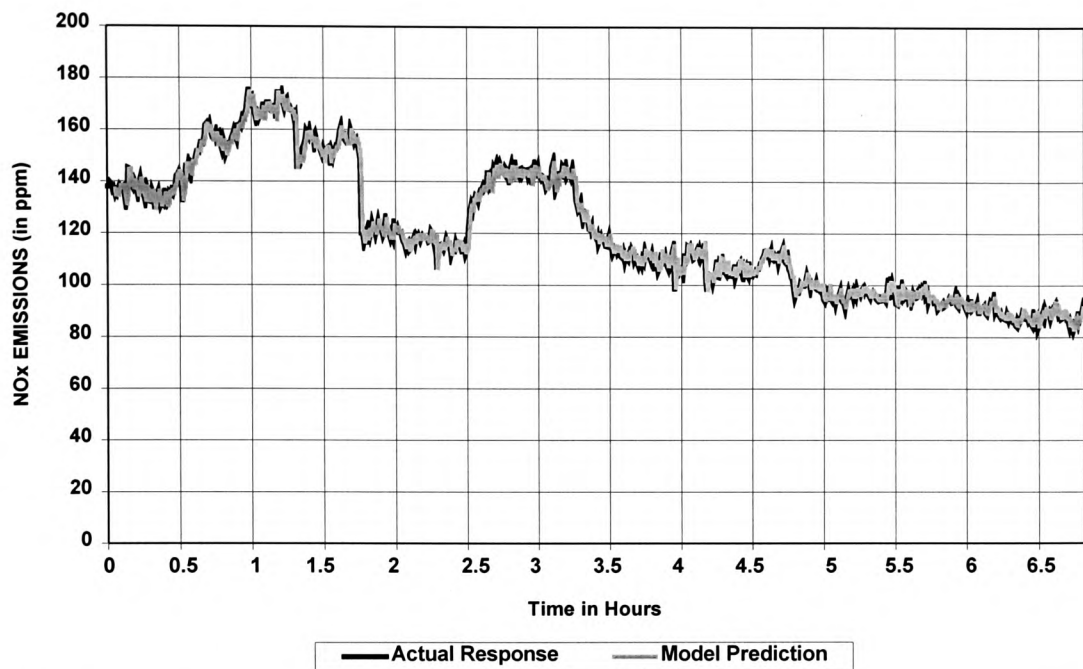


Figure 5.43 One Step Ahead Prediction by the Pruned Neural Network ARX Model for Nitrogen Oxides Emission with Validation Data Set 1 (Test 1)

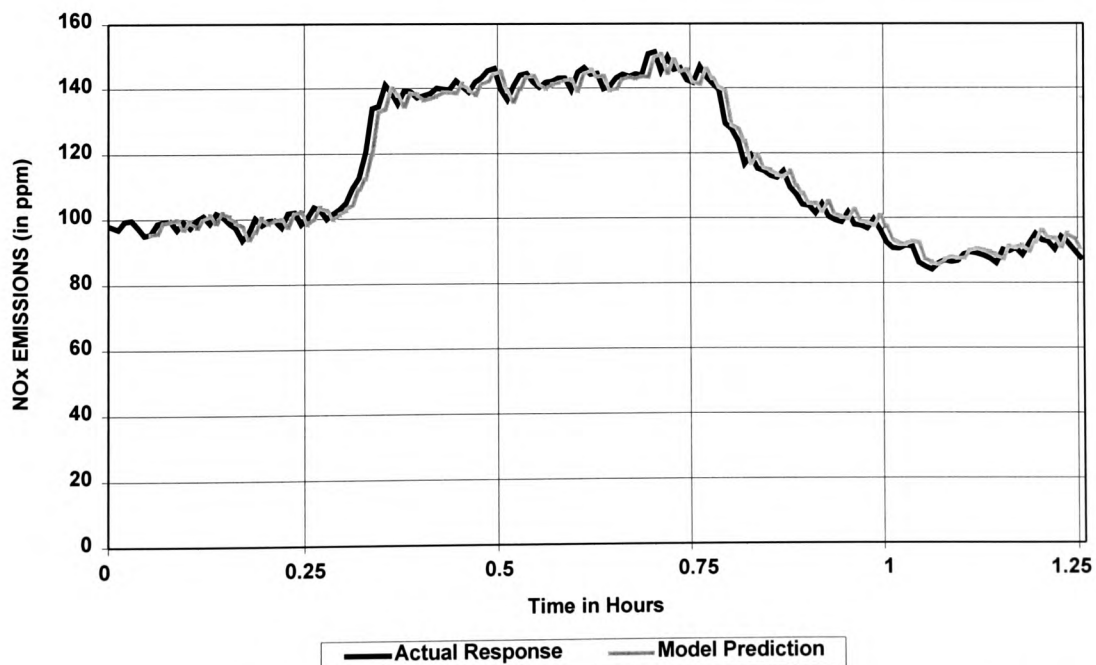


Figure 5.44 One Step Ahead Prediction by the Pruned Neural Network ARX Model for Nitrogen Oxides Emission with Validation Data Set 2 (Test 6)

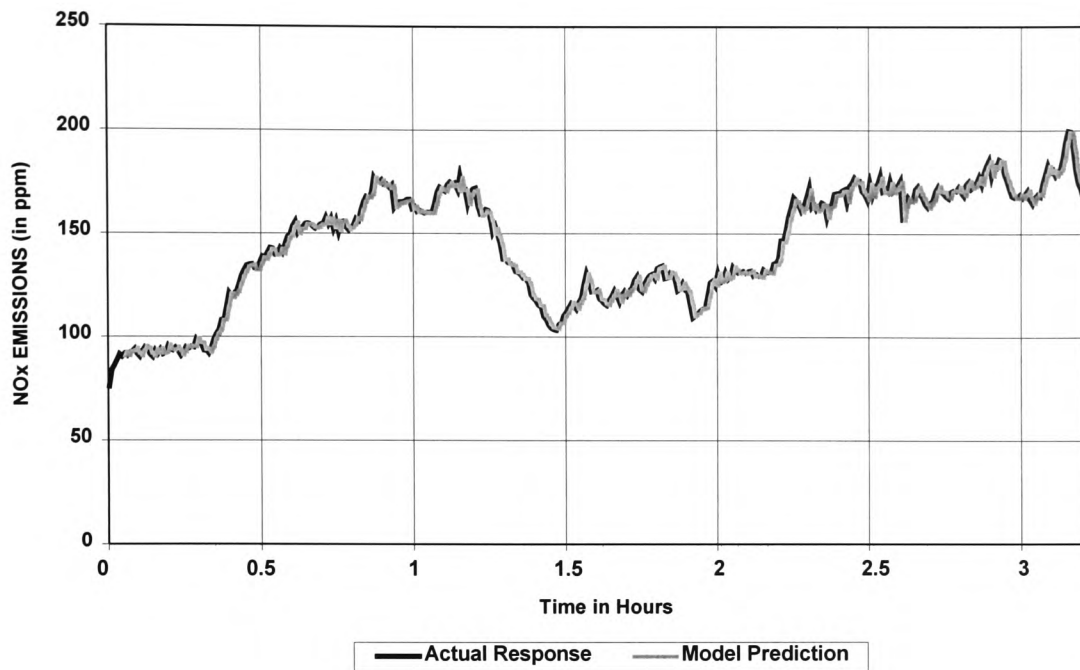


Figure 5.45 One Step Ahead Prediction by the Pruned Neural Network ARX Model for Nitrogen Oxides Emission with Validation Data Set 3 (Test 8)

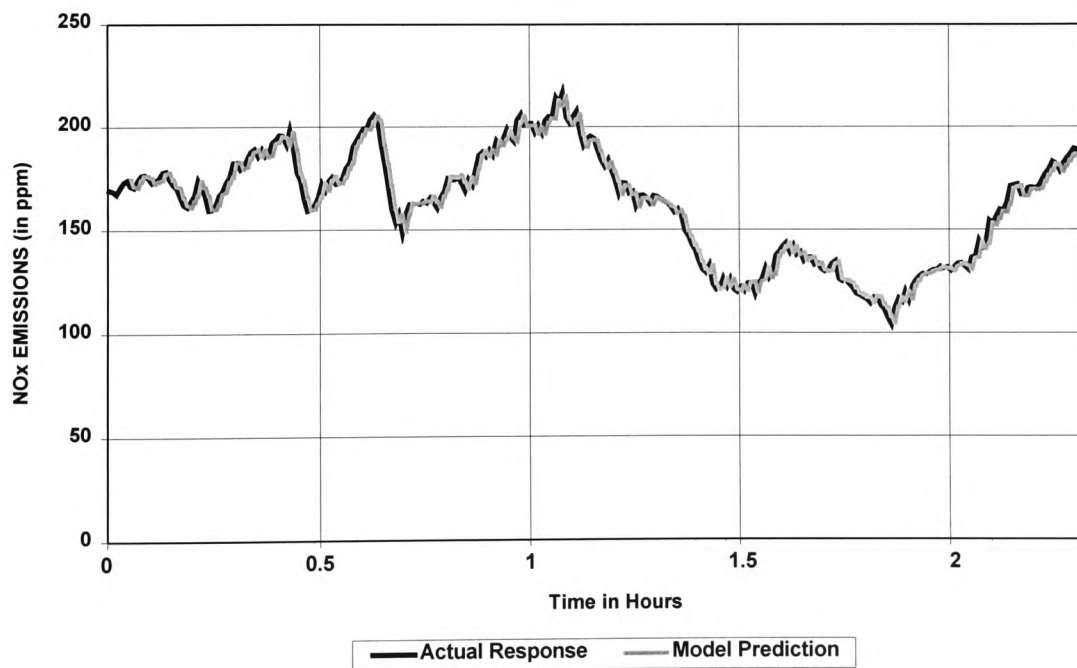


Figure 5.46 One Step Ahead Prediction by the Pruned Neural Network ARX Model for Nitrogen Oxides Emission with Validation Data Set 4 (Test 9)

Description of Results – As illustrated in the four Figures (5.43, 5.44, 5.45 and 5.46), the predictive capability of the optimised neural model has been significantly improved with respect to both representing the underlying dynamics of the process and also the prediction accuracy. The average sum square errors were 8.3, 10.2, 11.5 and 16.4 respectively, which were highly comparable to the ASSE of the training data set of 10.4. Again this demonstrated the validity of the model over the data span with significant temporal separation. Although it is not clear as to the extent in which a non-linear neural network model can be optimised (through the pruning algorithm), which is usually the case in system identification, the results shown here can be used to conclude the model's reliability in foreseeing the nitrogen oxides emission over a short time horizon (30 seconds) based on past inputs and output.

5.5.2.3 Non-linear (Neural Network) ARX Model for Carbon Monoxide Emission

There is a close resemblance between this model and the one for nitrogen oxides emission in the sense that the oxygen concentration in the flue gas was used as one of the input parameters to the model, based on the same argument that it provides a clear indication of the excess air level, and thus the combustion condition. In addition, the number of delays and orders of the coal feed (delay of 4 sampling periods, overlooking 2 previous values), air flow and oxygen level (delay of 1 sampling period overlooking 2 previous values) of the regressor vectors were also identical.

The number of past outputs (carbon monoxide emission) was increased to 4 and again the decision was based on an investigation of the real time response and on a heuristic level appeared to be of higher order than those of the oxygen level or nitrogen oxides emissions. Increasing this order could result in a lower error goal during training, but to a larger extent causes over-fitting of the data [Premier *et al.*, 1999]. It is worth stating here that the function LIPSCHIT in the Neural Network Based System Identification Toolbox can be used to calculate the order (lag space) for Single Input Single Output (SISO) models, however Noorgard (1995) emphasised that insight into the process being modelled is still the best means of synthesising a good model [Noorgard, 1995; He and Asada, 1993]. The derived network after training was pruned

using the optimising algorithm (OBS) to improve the model's prediction. A MLP network architecture of 10 neurons in the hidden layer (of hyperbolic tangent transfer function) and one output neuron of linear activation function was adopted as the structure for the ARX model. A diagrammatic representation of the non-linear neural network ARX model structure for the carbon monoxide production is as shown in Figure 5.47 below.

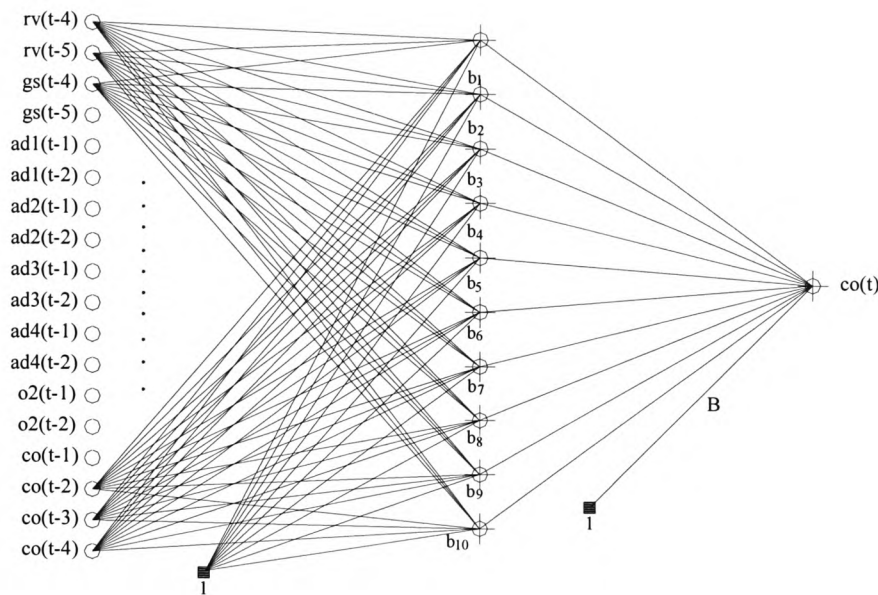


Figure 5.47 The Neural Network ARX Model for Carbon Monoxide Emission

Training – As with the first two models, the function DSCALE was used to scale the example data set to a mean of 0 and variance of 1, in order to improve network training [Noorgard, 1995]. It took 20 iterations to reach the predefined error goal of 0.015 as shown in Figure 5.48. Again this demonstrates the rapid convergence property of the training algorithm adopted by Noorgard in his function MARQ. Model predictions have been found to be in good agreement with the training targets, as shown in Figure 5.49. The average sum square error was found to be 1334 (by considering the actual scale) for the training set and will be used to compare the four validation data sets.

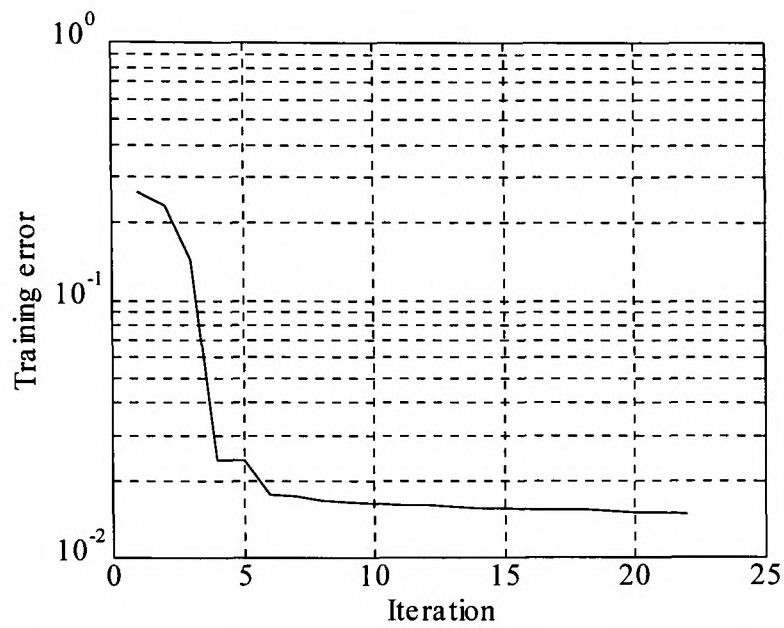


Figure 5.48 Training Error vs. Number of Iterations for the Carbon Monoxide Emission Model

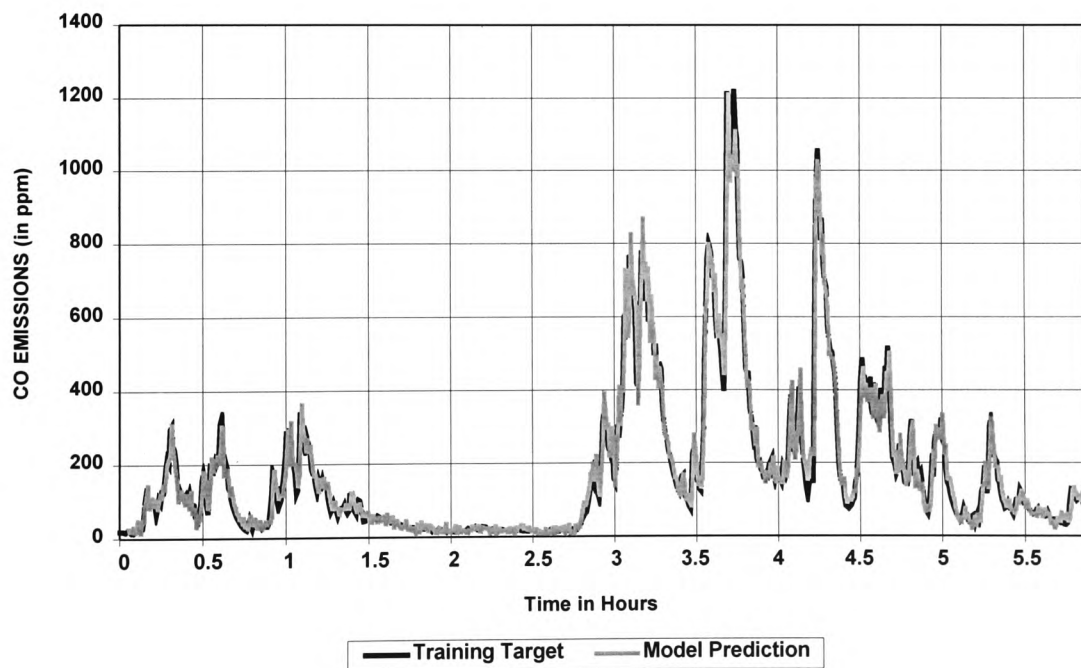


Figure 5.49 Training Targets vs. One Step Ahead Model Predictions for the Carbon Monoxide Model

Validation Sets – The derived neural model was tested with the four validation data sets and although the underlying dynamics of the process have been fairly well represented by the neural network model, the Optimal Brain Surgeon algorithm NNPRUNE, was employed to optimise the neural model's performance. The following two figures, Figure 5.50 and 5.51, compare the model predictions before network pruning with the actual response, with the corresponding ASSE of 7030 and 6177, which were 5.3 and 4.6 times the magnitude of the training ASSE respectively. Although the figures were not very far off the training ASSE, it was decided to compare the performance of the neural network model after pruning and the four figures which follow after, Figures 5.52 to 5.55, are provided to highlight the prediction improvement that was obtained. The pruning parameters for the function NNPRUNE was the same as in the nitrogen oxides model, requesting re-training of the network for 50 iterations after every 5% weight elimination from the network. The length of time taken by the same computer was almost 7 hours.

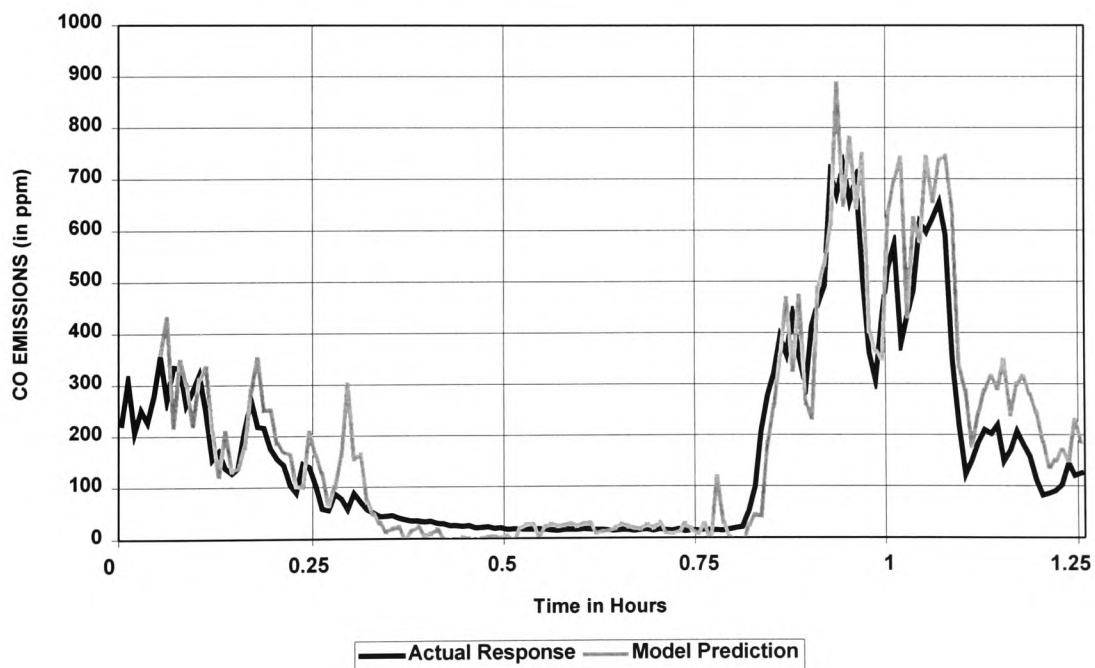


Figure 5.50 One Step Ahead Prediction by the Neural Network ARX Model for Carbon Monoxide Emission with Validation Data Set 1 (Test 1)

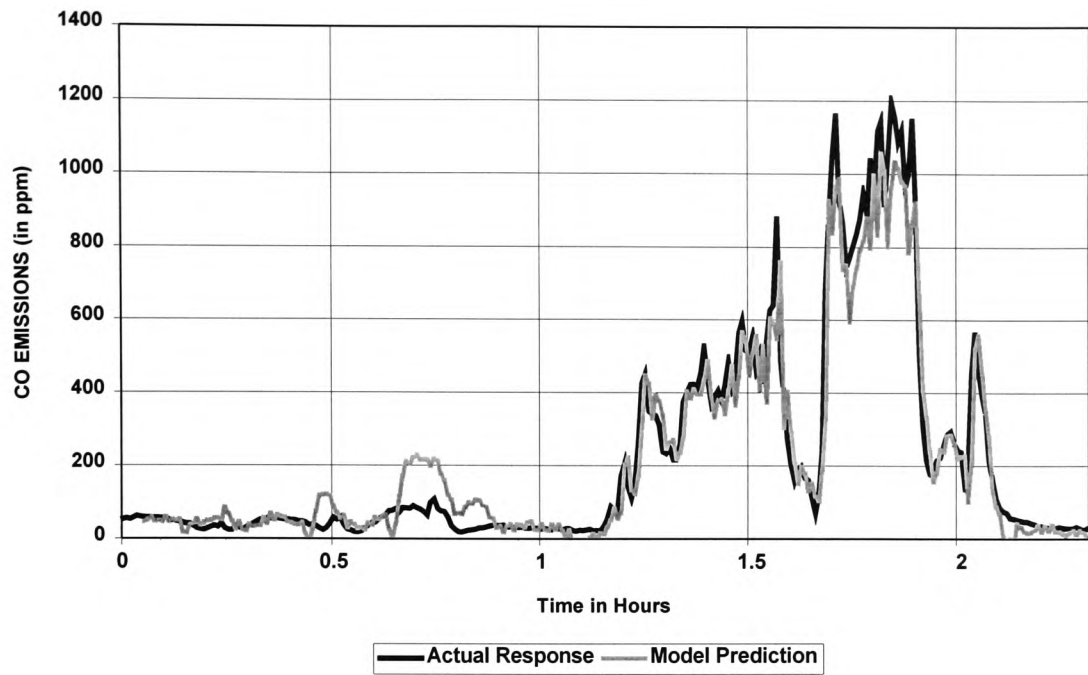


Figure 5.51 One Step Ahead Prediction by the Neural Network ARX Model for Carbon Monoxide Emission with Validation Data Set 4 (Test 9)

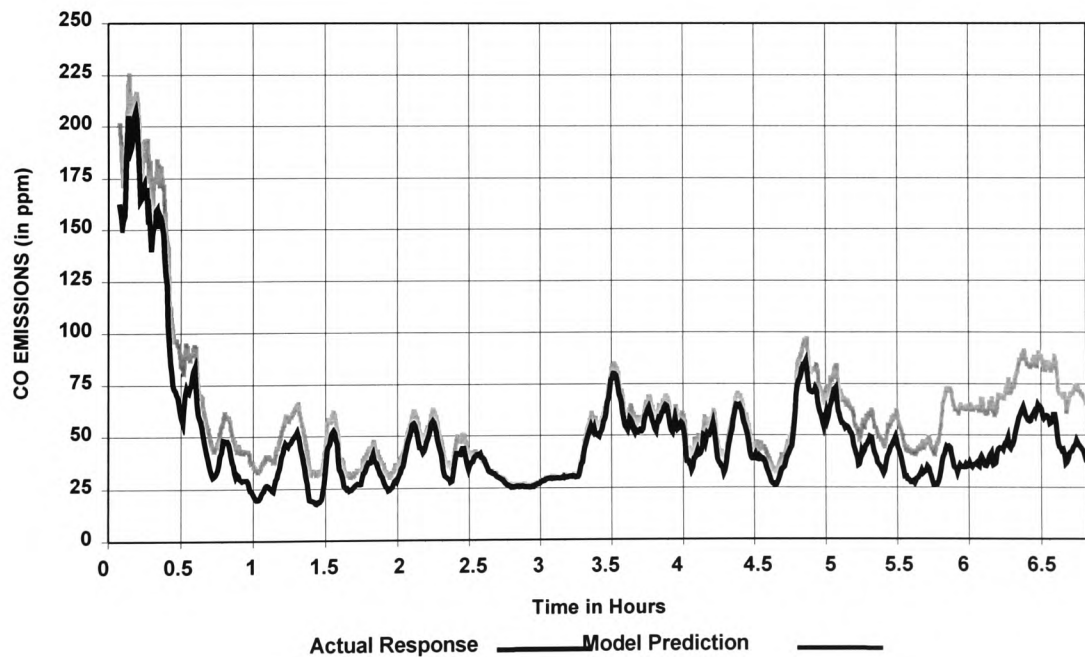


Figure 5.52 One Step Ahead Prediction by the Pruned Neural Network ARX Model for Carbon Monoxide Emission with Validation Data Set 1 (Test 1)

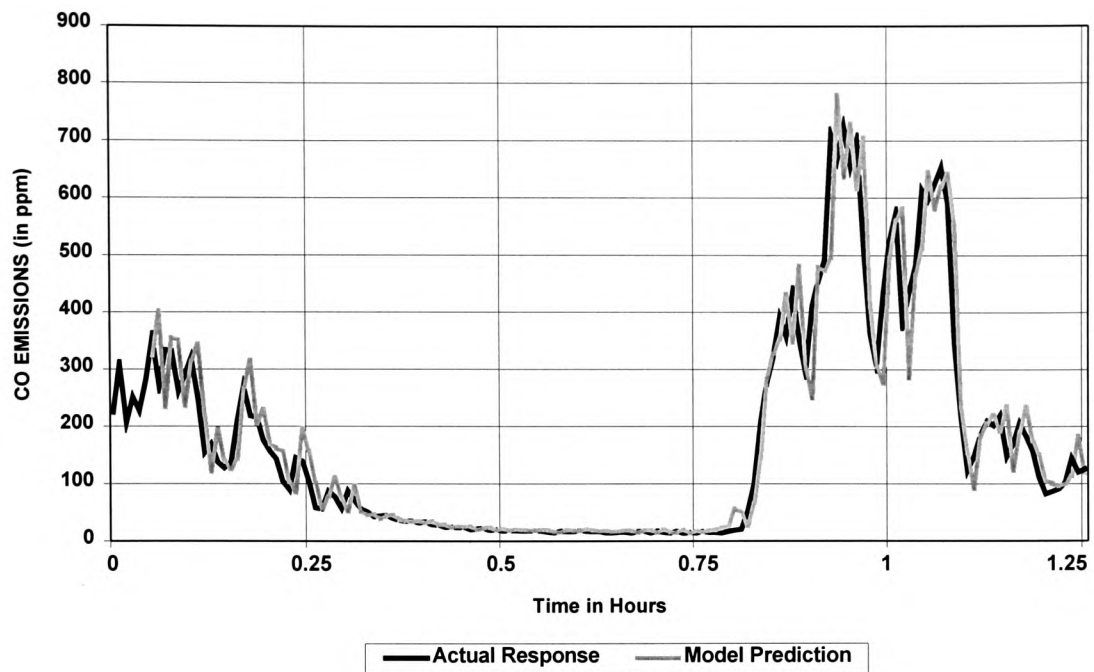


Figure 5.53 One Step Ahead Prediction by the Pruned Neural Network ARX Model for Carbon Monoxide Emission with Validation Data Set 2 (Test 6)

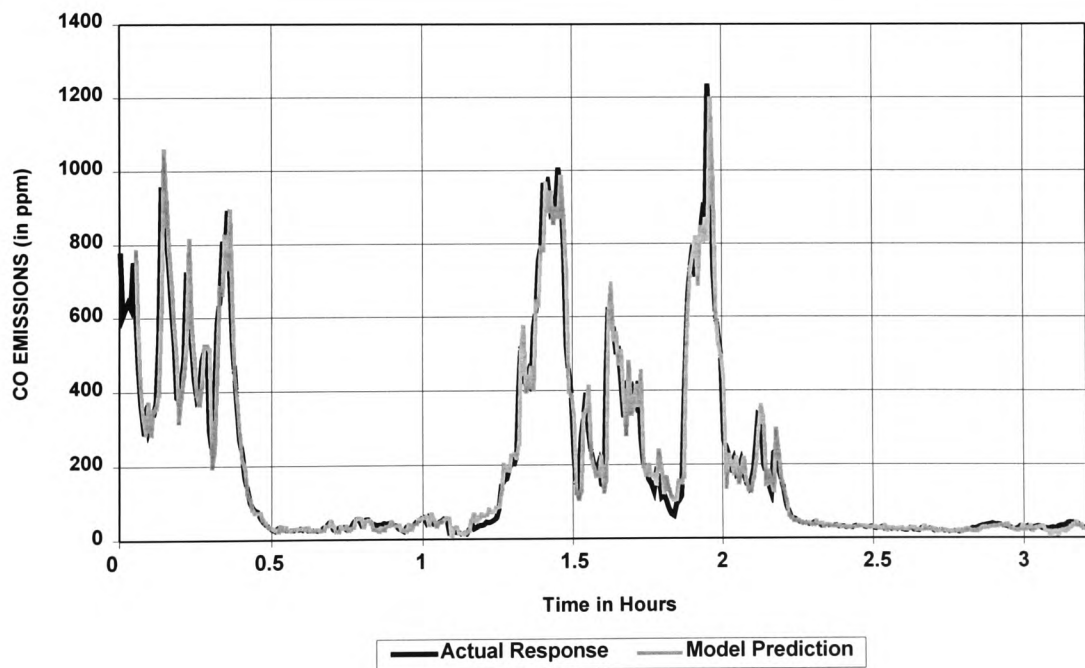


Figure 5.54 One Step Ahead Prediction by the Pruned Neural Network ARX Model for Carbon Monoxide Emission with Validation Data Set 3 (Test 8)

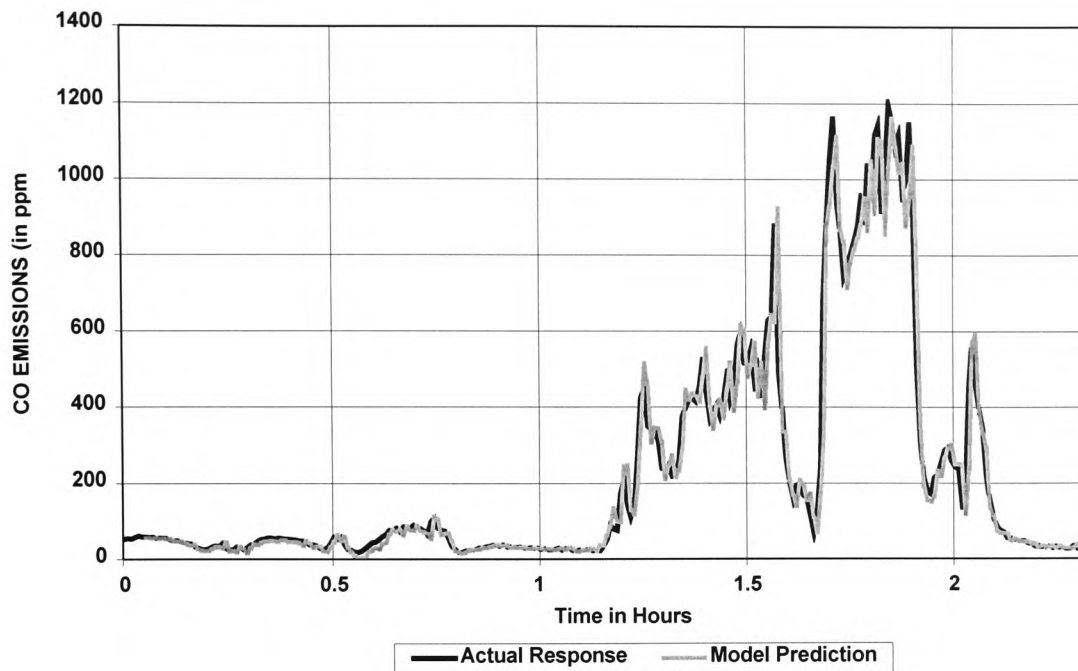


Figure 5.55 One Step Ahead Prediction by the Pruned Neural Network ARX Model for Carbon Monoxide Emission with Validation Data Set 4 (Test 9)

Description of Results – The model’s prediction capability has clearly been improved with the corresponding ASSE of 781, 3176, 3725 and 4248, which represents a magnitude of 0.6, 2.4, 2.8 and 3.2 of the training ASSE. Although the comparative error (with respect to the training ASSE) here was higher than those of the oxygen and nitrogen oxides emission models, it must be stressed that the dynamics of the carbon monoxide production was of a significantly higher order (as illustrated from the data gathered through the carefully designed experiments – Chapter 4). In addition, the system identification work here can be seen in many ways as a simplistic approach to that of the more daunting route of mathematically modelling the physical process. The alternative although lacking in model transparency and elegance, is able to produce one step ahead predictions of the derivatives of combustion with striking accuracy considering its relative simplicity in model design. This has been demonstrated not only with data sets that were obtained from the same series of experiments (which also demonstrated the repeatability of the model performance) but also from a large temporal separation of almost 8 months from the training data set. However the neural network model does require a large enough training data set

(covering if not all but the majority of the dynamical aspects of the process) in order to ensure adequate training.

6. Development & Testing of a Prototype Flame Front Monitoring Device

One of the commonly encountered problems in chain grate stoker firing is the non-uniformity of the fuel size and its distribution on the bed. In the event that the fuel size is not to the required specification with a reduced calorific value, coupled with possible disruption to the ignition process due to frequent load changes, could pose serious threat to the stability of combustion. In many modern chain grates, this would involve slowing the grate to allow more time for combustion in order to bring the ignition plane back to a suitable location. One of the objectives of this work was to develop a combustion monitoring system that would be capable of monitoring the combustion process on the bed, particularly during large load changes, where a sudden increase or decrease in the grate speed would disrupt the ignition plane.

This Chapter describes the development and testing of an optical device that was used to monitor the flame front location on the fire bed through the arch inspection porthole. The motivation behind this work also stemmed from the need to develop a better means to monitor the combustion process on the bed since conventional low-range K-type thermocouples are slow to respond owing to the high thermal inertia of the arch. Experience had shown that more than one thermocouple was required in order to have a clear representation (based on historical data) of the movement of the ignition plane which in the long run could be costly since thermocouple tips deteriorate due to the elevated working temperature of the arch. Furthermore, the standard industrial practice when operating a chain grate stoker is to visually inspect for flickers of flame through the arch porthole to ensure that fresh coal is being ignited at the appropriate location. Very often, one arch thermocouple is used to provide an indication of the readiness of the arch prior to the commencement of normal operation.

Consequently a pilot study was conducted by recording the image of the bed through the inspection porthole and the flame front location was manually logged every 30 seconds, off line (the same sampling period as the Tactician front end controllers), by an expert operator. The information obtained from the discrete time video images was

found to correlate well with the arch temperature patterns with respect to the ignition plane movement. This led to the development of a sensor using a Single Lens Reflex (SLR) camera with an array of 8 photodiodes as an alternative means to monitor the combustion process and this was subsequently tested on a full scale industrial chain grate boiler with encouraging results. Finally, a hybrid neural network classification system combining the Learning Vector Quantisation (LVQ) network and a standard feed-forward Multi-Layered Perceptron (MLP) network, was used to process the raw data gathered from the sensor in order to deliver an accurate assessment of the flame front location.

6.1 Flame Front Detector - Pilot Study to Investigate the Feasibility of Using Optical Means as An Alternative to Thermocouples

One of the key operating criteria for a chain grate stoker is a hot refractory arch. This in turn ensures quick ignition of the fresh charge and as the coal burns in the furnace chamber, the back radiation from the fire bed provides the heat required to maintain the temperature of the refractory arch making the whole combustion process to be self supporting. Therefore it is of vital importance to keep the arch hot, with the ignition plane at the appropriate location, before carrying out any load change (Section 2.2.3). This also ensures that the fresh charge can be combusted satisfactorily, and in practical cases any grate ash losses of less than 2.5% in terms of the overall combustion efficiency can be considered good [Good Practice Guide 88, 1993].

During normal boiler operation the only indication as to whether the ignition plane occurred at a suitable location is to visually inspect the fuel bed for flickers of flame through the inspection porthole. When commissioning the stoker test facility, the rate at which coal was transported into the combustion chamber (grate speed), was calibrated so that the fresh charge can be ignited within the visible range of the inspection porthole, so as to yield a good carbon burnout. In fact during normal operation, the operator would look for the flame front from time to time. The left most

edge (towards the stoker front) of the newly ignited coal is termed the flame front, and the ignition plane travels downward from that point, reaching the bottom of the bed at about half the grate length, if satisfactory conditions prevail.

In attempting to investigate the movement of the ignition plane following load changes, the test facility was fitted with an array of seven low range K-type thermocouples (up to 1100°C) embedded within the refractory arch, shown in Figure 6.1. In most industrial stokers, only one thermocouple is available, usually located in the centre of the stoker arch so as to indicate to the plant operator whether the arch is hot enough before the commencement of normal operation. During plant start-up, the operator would bank the fire under the arch and wait until the temperature of the arch (t₃) reached 700°C before gradually increasing the coal feed to meet the required load. When the boiler was in operation, the arch thermocouple was used only as an ‘alarm’ should the combustion conditions deteriorate.

For instance if the temperature of the arch fell below 400°C (losing the ignition), then the grate speed would be reduced in order to bank the fire under the arch, and raise the temperature to the required level before resuming normal operation. With the stoker test facility at CRE such a condition could occur if the coal feed and air flow were not properly regulated to meet a large fluctuating load demand. Therefore there was a need for a sensor that could provide a faster indication of the stability of the combustion process to enable early corrective actions to be taken (small adjustments of the grate speed) without having to sacrifice production. Hence, an inexpensive monitoring device that could provide a real time indication of the flame front location to the plant operator or the on-board control system could assist in maintaining good boiler operation.

A Charged Coupled Device (CCD) video camera was mounted on the stoker arch inspection porthole to continuously record the movement of the flame front following the series of manual experiments (Test 1 to Test 7). The images obtained from the video camera were then analysed off line by taking one snap-shot every 30 seconds for flame front movement during the entire duration of each test. This movement of the

flame front was then plotted together with the arch temperature readings (also logged every 30 seconds) and a close correlation was observed. The following Sub-Sections describe some of the more important results obtained that demonstrate the feasibility of using an optical approach, as an alternative to thermocouples, for monitoring the movement of the ignition plane.

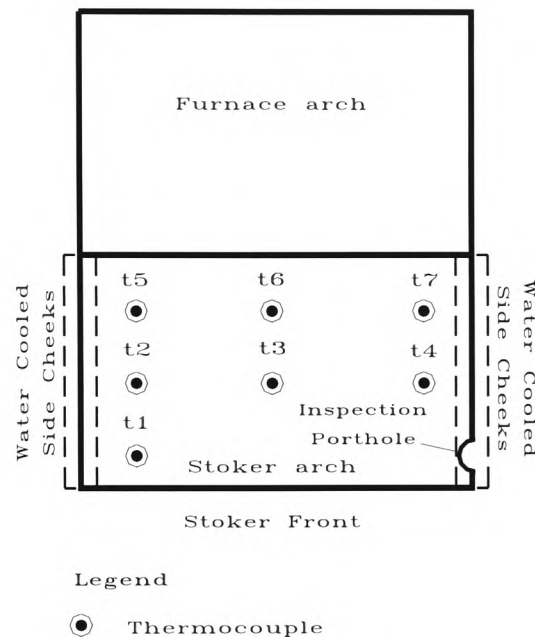


Figure 6.1 Plan View of the Refractory Arch with the Thermocouples

6.1.1 The Use of Thermocouples to Infer the Movement of the Ignition Plane

Before progressing into describing the results obtained from the discrete time video images, this section serves to demonstrate the movement of the ignition plane to gradual load changes at optimum operating conditions with respect to the arch temperature patterns. The location of the seven K-type thermocouples embedded in the refractory arch (6mm away from the inner surface of the arch) is shown in Figure 6.1. Thermocouples t3 and t6 best represented the actual arch temperature as these two thermocouples were located along the centre line where most radiant heat from the hot bed was directed. However for the purpose of illustration, thermocouple t1 is also included in Figure 6.2 to provide a better picture of the ignition plane movement. This

thermocouple was closer to the fire bed and towards the stoker front, thus making it more sensitive to the movement of the ignition plane at that region. These three thermocouple readings are used in Figure 6.2 to infer the movement of the ignition plane to gradual load changes at operator's best practice (Test 1).

In the case of load increase from 0.3MW to 0.6MW in 0.1MW steps, an upward trend in the temperature recorded by t_3 and t_6 (back thermocouples) can be seen with a corresponding downward trend in t_1 (front thermocouple). Please note that during plant commissioning the grate speed for the entire load range would have been calibrated so that the ignition of the fresh charge could take place within the visible range of the inspection porthole. It is also important to note that the ignition plane at the higher load was further away from the centre line of the inspection porthole (Chapter 4), as the ignition rate of the fresh charge was relatively slower than the coal feed rate. Therefore as the load increased, the ignition plane shifted from t_1 to settle at a position which was closer to t_3 and t_6 . Hence t_1 registered a decline whilst both t_3 and t_6 clearly demonstrated an increase.

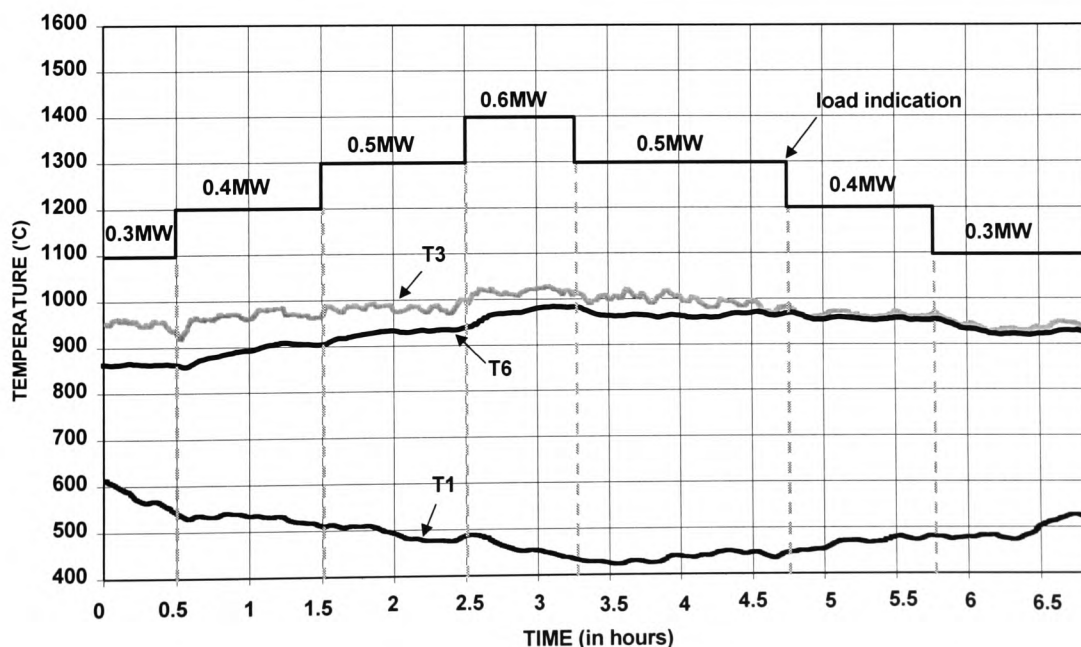


Figure 6.2 Arch Temperature Distributions Following Gradual Load Changes at Optimum Operating Conditions – Test 1

Conversely on load decrease, the gradual slowing of the grate meant that there was more time for the fresh coal to ignite (ignition rate was faster than the rate at which the fresh charge was brought forward), thus allowing the ignition plane to creep towards the stoker front. The initial higher combustion intensity after the load drop from 0.6MW together with a slower grate speed also contributed to the shift of the ignition plane back to the centre line of the porthole. Therefore, the temperature of t_1 gradually increased and this was accompanied by a downward trend in t_3 and t_6 .

Ideally, the input parameters to the boiler (coal feed and air flow) would be controlled in order to avoid excessive ignition plane movement either into the furnace chamber or back towards the hopper, especially in situations where large load changes are required on a frequent basis.

6.1.2 Classification of the Flame Front through the Inspection Porthole

This Section describes the use of a simple technique to evaluate the images obtained through the porthole which would allow the development of a monitoring system for ignition plane movement. An experienced operator would classify the edge of the flame into five distinct regions. These are shown in Figure 6.3 with the boundaries of these small regions being marked by broken lines. For the stoker test facility under study, each zone was 15mm wide. The location of the flame front was recorded every 30 seconds with respect to a classification table formulated from the five regions of the porthole shown in Table 6.1.

A moving average trend was then plotted using these discrete data points (-30, -15, 15, 30 and 45mm) for the purpose of comparing the information obtained from the images with the arch thermocouples (t_1 , t_3 & t_6). Figures 6.4 to 6.8 illustrate the average flame front movement following gradual (Test 1, 2 & 3) and large load changes (Test 6 & 7) at optimum and sub-optimum operating conditions (Chapter 3).

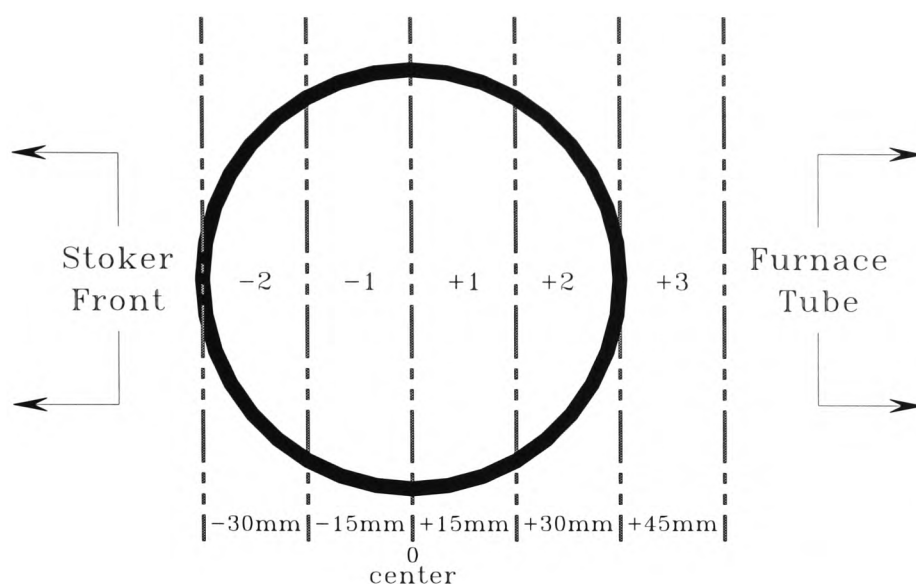


Figure 6.3 Reference Flame Front Zones through the Arch Inspection Porthole

Table 6.1 Flame Front Zones and their Discrete Location Relative to the Centre of the Inspection Porthole

Flame Front Zones	Discrete Zone Location Relative to the Centre Line (mm)
-2	-30
-1	-15
+1	15
+2	30
+3	45

6.1.3 Flame Front Movement Following Gradual Load Changes at Optimum Air – Test 1

In Test 1, the stoker test facility was operated at the engineer's best practice from turn down (0.3MW) to full load (0.6MW) and back to turn down (0.3MW) in 0.1MW steps, with an optimum air distribution profile along the grate (Section 3.4.1). As can be seen from Figure 6.4, increasing the boiler load from 0.3MW to 0.6MW resulted in the flame front moving towards the furnace tube (Section 4.1.1). This was expected since

the ignition rate of the fresh charge was slower than the rate at which the coal was being transported into the furnace tube, as the load increased.

The flame front location moved from an initial position of +5mm to an average of +25mm at 0.6MW (Figure 6.4). This shift in the ignition plane towards the furnace tube was also reflected in the three arch temperatures (t_1 , t_3 & t_6) as discussed for Figure 6.2. Conversely on load decrease, the gradually declining grate speed resulted in the ignition plane being brought back towards the stoker front as the rate of ignition was faster than the rate at which fresh coal was being fed. This is clearly shown by the downward trend of the flame front movement from an average of +25mm at 0.6MW to approximately +13mm at 0.3MW. This trend is also mirrored in the three arch temperatures (t_1 , t_3 & t_6). It can therefore be concluded that it is quite feasible to classify the flame front and utilise it as a means to dictate the movement of the ignition plane. In this test, the combustion process on the grate following gradual load changes can be deduced as stable through the availability of the flame front through the porthole throughout the entire test duration, with no signs of any unstable pattern.

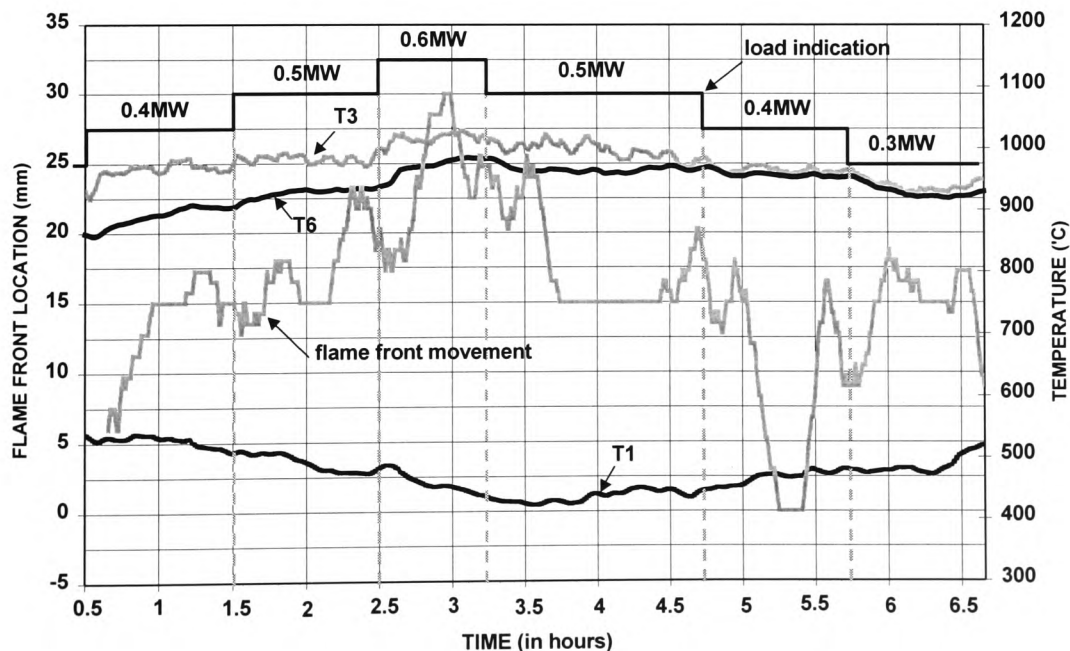


Figure 6.4 Flame Front Movement Following Gradual Load Changes at Optimum Air
(Test 1)

6.1.4 Flame Front Movement Following Gradual Load Changes at Lower Excess Air – Test 2

In this experiment the stoker test facility was operated from turn down (0.3MW) to full load (0.6MW) and back to turn down (0.3MW) in 0.1MW steps, with a lower excess air level (Section 3.4.1). In the interests of brevity, only the flame front movement relating to load increase is provided here since the trend on load decrease was a mirror image to that on load increase, as illustrated in Section 6.1.3.

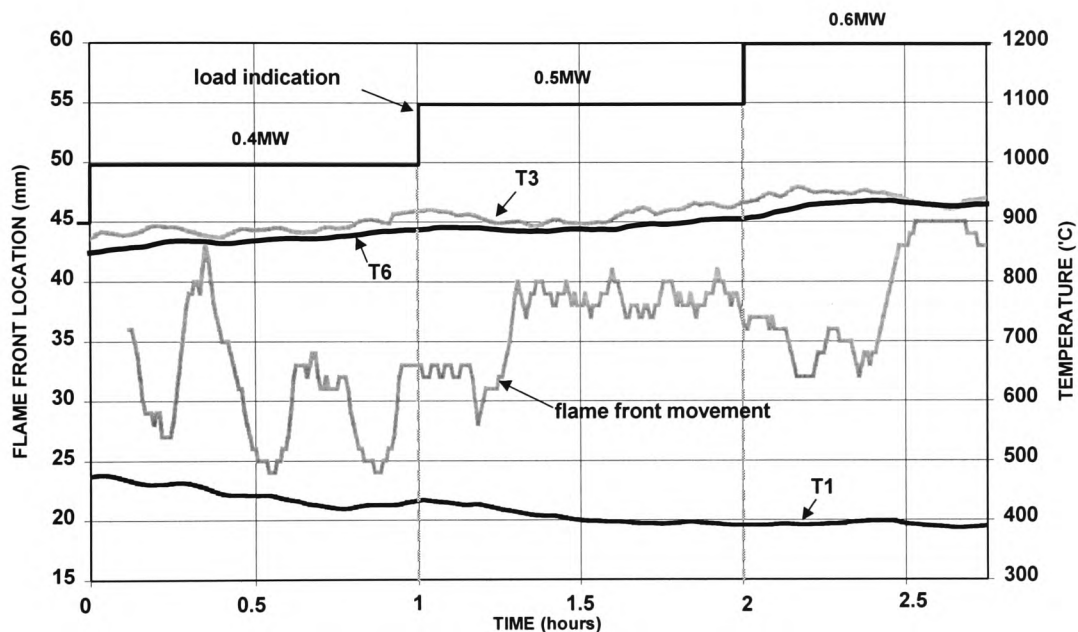


Figure 6.5 Flame Front Movement Following Gradual Load Changes at Lower Excess Air (Test 2)

As with Test 1, the load increase resulted in the ignition plane moving towards the furnace tube. This is shown in Figure 6.5, as the flame front moved from an average of +30mm at 0.3MW to approximately +40mm at 0.6MW. Throughout the entire duration of the test, the flame front occurred further towards the furnace tube than in Test 1. This can be explained by the reduced quantity of combustion air that was available in this test which inevitably retarded the ignition process of the fresh charge thus contributing towards a higher carbon in ash losses (Section 4.1.2). This was also

reflected in the thermocouple readings as illustrated in Section 6.1.1, demonstrating an increase in both t_3 and t_6 with a corresponding downward trend in t_1 .

6.1.5 Flame Front Movement Following Gradual Load Changes at Higher Excess Air – Test 3

The manner in which the boiler load was altered in this experiment was identical to Test 1 and Test 2 but was operated at a higher excess air level (Section 3.4.1). As in Section 6.1.4, only the flame front information relating to load increase is provided here to illustrate the ignition plane movement, since the trend on load decrease was a mirror image of the load increase.

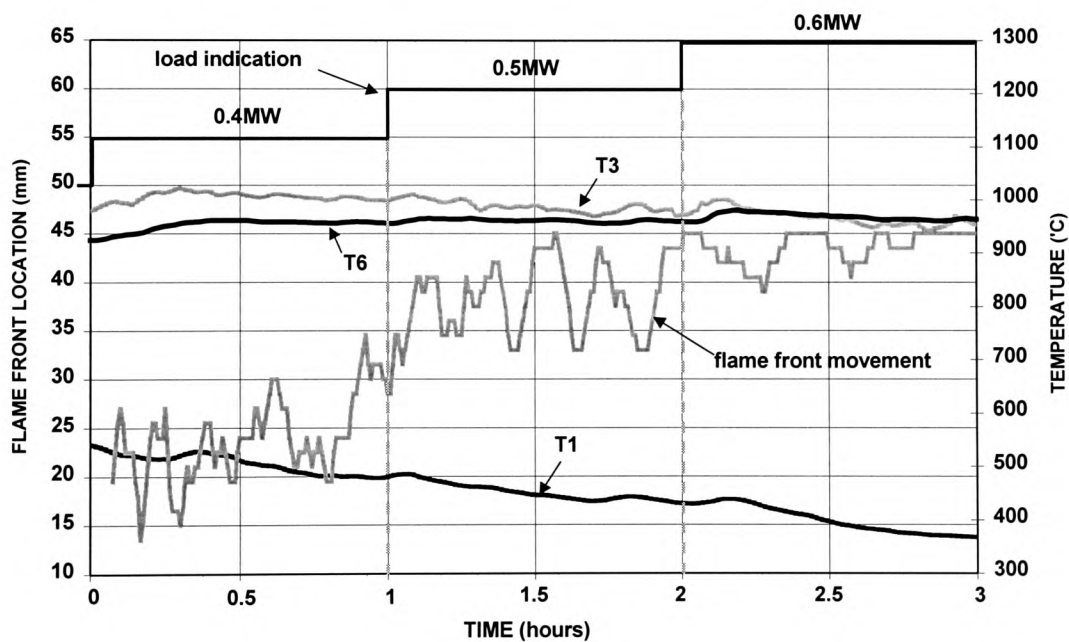


Figure 6.6 Flame Front Movement Following Gradual Load Changes at Higher Excess Air (Test 3)

Figure 6.6 is the sort of scenario that needs to be avoided at all costs, as it is a clear indication that ignition will be lost. This resulted in a longer fire bed, but because of the higher combustion intensity prevailing in the furnace chamber due to the increased availability of combustion air, the carbon in ash losses were marginally better than

those attainable at operator's best practice (Section 4.1.3). However, the marginal efficiency improvement offered in the carbon burnout did not justify the increased loss in the flue gas. As described in the previous Sections, an increase in the grate speed resulted in a shift of the flame front location towards the furnace tube, which is clearly shown in the escalating upward trend of the flame front (Figure 6.6). However, this movement of the flame front from an average of +23mm at 0.4MW to +38mm at 0.5MW and subsequently towards +45mm at 0.6MW was not accompanied by any increase of the two back arch thermocouples reading (t_3 and t_6), whilst t_1 clearly shows a steep downward trend from 550°C to 370°C. In other words, the ignition plane crept towards the furnace tube but the back arch thermocouples did not register any significant increase in temperature. This could possibly be attributed to the presence of more combustion air which could have imposed a cooling effect on the arch (Section 4.1.3) [Good Practice Guide 88, 1993]. The problem of arch cooling was exacerbated as increased suction by the induced draught fan was required in this experiment to achieve clean boiler operation.

6.1.6 Flame Front Movement Following Large Load Changes with an Undesirable Staging Profile – Test 6

In this experiment the boiler was operated from turn down (0.3MW) to full load (0.6MW) in a single step and vice versa with an undesirable coal and air staging profile (Section 3.4.2 – Test 6). The objective was to investigate the transient boiler response to changes in the coal feed onto an initially less intense fire bed. As such, the coal feed rate was stepped up before the air flow on load increase, and vice versa on load decrease (Section 4.2.1).

The average flame front location within the first 15 minutes after the load change from 0.3MW to 0.6MW was approximately +25mm and remained at that location until the load was brought back down to 0.3MW. This was accompanied by the expected trend in the three arch temperatures, where t_3 and t_6 registered an increase and t_1 exhibited a downward slope following the shift in the ignition plane towards the furnace tube

(Figure 6.7). On load decrease from 0.6MW to 0.3MW, the flame front remained towards the furnace tube (+25mm) despite the *reduced* coal feed rate for almost 20 minutes after the load change before settling at the expected location closer to the stoker front (+10mm). This delayed transition in the ignition process from full load to turndown was also reflected by only a small inclination in t_1 after 15 minutes following the load change along with t_3 and t_6 registering a slight downward trend.

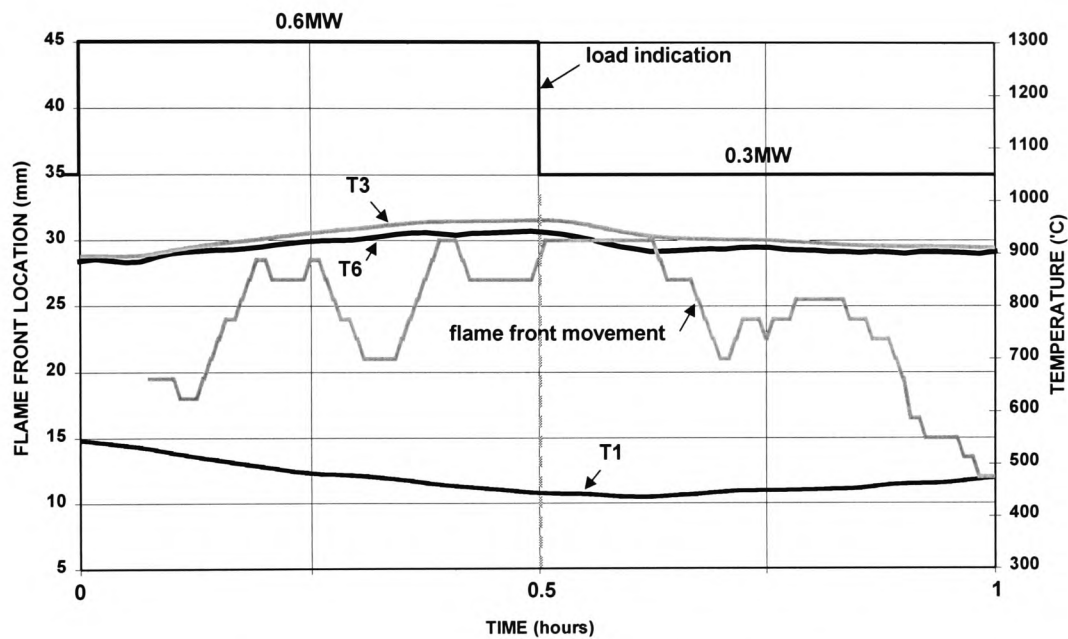


Figure 6.7 Flame Front Movement Following Large Step Changes with an Undesirable Staging Profile (Test 6)

6.1.7 Flame Front Movement Following Large Step Changes with a Desirable Staging Profile – Test 7

In this experiment the air flow was gradually stepped up before the coal feed on load increase from 0.3MW to 0.6MW, and vice versa on load decrease from 0.6MW to 0.3MW (Section 3.4.2). The objective was to obtain an intense fire bed before any change in the coal feed was carried out (Section 4.2.2). The flame front results from this experiment are used to demonstrate the improvements with respect to the transient

ignition plane movement, that were obtained by adopting the correct coal and air staging profile as compared to Test 6.

The load change from 0.3MW to 0.6MW occurred at 0 hour, which resulted in a higher temperature in the furnace tube as the combustion intensity was elevated by an increase in the air flow followed by the coal feed rate. As discussed in the previous sections, the flame front location at higher load occurred further towards the furnace tube due to the higher grate speed, therefore a clear displacement in the flame front position from +8mm (at 0.3MW) to an average of +25mm (at 0.6MW) can be seen in Figure 6.8, in the first 30 minutes after the load change. This was accompanied by a fall in thermocouple t_1 , although an increasing trend is shown in the first 10 minutes after the load change due to the increased airflow prior to the grate speed change (Section 4.2.2).

A similar trend can be observed in t_3 and t_6 in the first few minutes following the load change, before attaining a higher reading at the steady-state of 0.6MW. This clearly suggests that a stable transition had taken place from turn down to full load as the ignition plane settled into a new position towards the furnace tube. When the boiler load was brought back to full turndown, the flame front can be seen to move to an average of +12mm, 10 minutes after the load change (compared to 20 minutes in Test 6), before it settled at an average position of +17mm at the steady-state of 0.3MW. This displacement of the ignition plane towards the stoker front was also reflected by an increase in the front thermocouple (t_1), with a slight decrease in t_6 .

An important finding that can be drawn from these results, is that the thermocouple readings remained unchanged for several minutes after the load change whilst the discrete time flame front images showed clear signs of the ignition plane movement within this short time period. Therefore it can be concluded that the optical means could provide a better picture of the ignition plane movement than the array of arch temperatures. Also from comparison with Test 6, an improved transition in the ignition process from one load to another has been demonstrated with a desirable staging profile, i.e. on load increase the flame front moved *gradually* to settle at the new

location and was better maintained through the visible range of the porthole, whilst on load decrease, the flame front was brought back to settle in the new position in *half* the time required with an undesirable staging of coal and air.

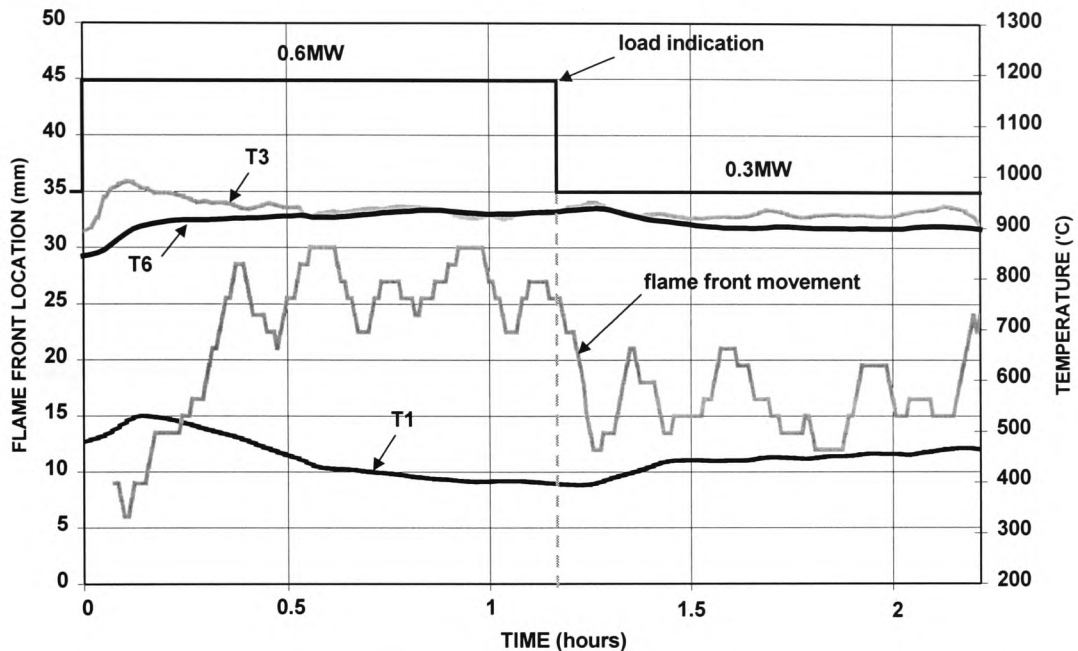


Figure 6.8 Flame Front Movement Following Large Step Changes with a Desirable Staging Profile (Test 7)

6.2 The Development & Testing of the Flame Front Monitor

A prototype flame front monitor was successfully developed following the pilot study conducted with the CCD video camera. This prototype monitor consisted of a Single Lens Reflex (SLR) camera, a linear array of eight photodiodes, signal amplifiers and a data acquisition card with built-in analogue to digital converter. A personal computer was employed to host the data acquisition card, which ran a Quick Basic data logging program in DOS for the automatic logging of the signal from the flame front monitor. Figure 6.9 illustrates the set-up of the monitoring system, where the image of the fire bed through the inspection porthole was focused onto an opaque screen via the use of the SLR camera. At this point, it must be mentioned that for the purpose of the flame

front monitor, only the reference zones viewable by the camera (zones -2, -1, +1 and +2) were considered. Reference zone +3 was used later in the description of results (Section 6.2.1) to denote a flame front location beyond the right corner of the porthole, for the purpose of illustrating the results (as employed in Section 6.1.2).

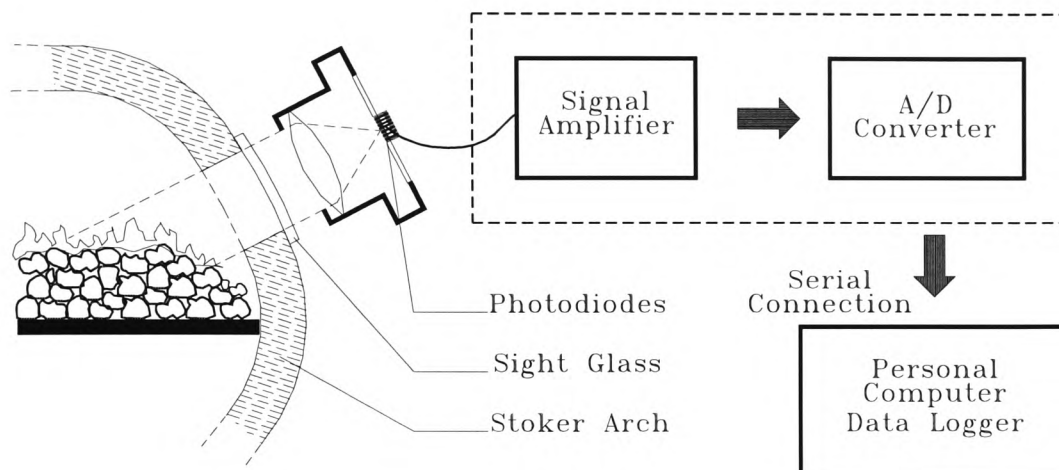


Figure 6.9 Block Diagram of Flame Front Monitor and Data Logger

An array of eight linear photodiodes, was mounted behind the opaque screen to detect the bright and dark regions of the image as shown in Figure 6.10. Two photodiodes were allocated for each of the four visible reference zones of the inspection porthole in order to obtain better clarity and therefore offered a higher degree of confidence when determining the flame front location. It was also important to ensure that the horizontal diameter of the image focused on the opaque screen coincided with the length of the photodiode array, in order to fully utilise the photodiodes for the purpose of monitoring the flame front movement within the entire visible range of the inspection porthole. Each photodiode then delivered an electric current (mA) based on the light intensity of the image at that particular location.

The typical response of the photodiodes employed in this work was 400 mA/W since the colour of the flame/light encountered on the bed was of orange/red spectrum (visible radiation wavelength of approximately 620nm). The signal from the photodiodes was then amplified to a suitable magnitude using operational amplifiers, which gave an analogue voltage output in the range of 0 to -10volt. These 8 analogue

voltage signals were fed to a 12 bit MPIBM3 BYTRONIC data acquisition card, fitted into a personal computer for conversion into digital signals and subsequently for automatic data recording. The data logging program delivered an output of 1 for a *bright* region of the image (digital signal over a threshold limit) while a *dark* region resulted in an output of 0 (signal below the threshold limit).

The flame front detector was tested on-line in the case study concerned with the implementation of the NNBC onto an industrial stoker-fired boiler plant (Section 5.4). The findings were most encouraging and the novel flame front monitor was able to detect the dark and bright regions of the image on the fire bed through the arch inspection porthole. A typical scenario is shown in Figure 6.10, where the first element of the photodiode to register a reading of 1, indicates the flame front position.

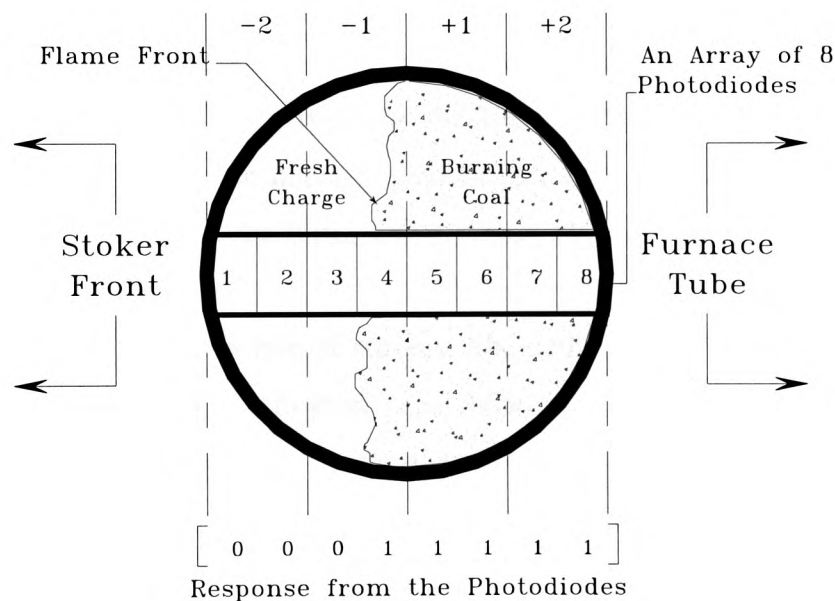


Figure 6.10 Typical Flame Front Monitor Response to the Image of the Fire Bed

The following Section presents the results (Test 16, 17a & 17b) obtained from the flame front monitor, through its implementation onto the 3.7MW_{th} industrial chain grate stoker-fired boiler plant to monitor the combustion process when the plant was operated under the influence of the NNBC.

6.2.1 Flame Front Monitor Results & the Hybrid Neural Network Classifier

The results from the on-line implementation of the flame front monitor (Tests 16, 17a & 17b) are presented here to evaluate its performance in providing information relating to the stability of combustion and also to demonstrate its reliability over hours of test duration. The gathered data was fed off-line to a hybrid classification neural network (combining the LVQ network and the MLP network), to determine the flame front distance with respect to the four reference zones as described in Section 6.1.2. Also, as described earlier in Section 6.2, zone +3 was used to denote an absence of the flame front from the porthole, i.e. all eight photodiodes registering a zero value.

Neural networks offer a convenient means for classifying the information recorded by the flame front monitor to infer the stability of the ignition plane through learning from the given set of examples rather than being laboriously programmed. A frequently adopted classification neural network is the Learning Vector Quantisation (LVQ) network (Section 2.4.2.2). An interesting application of the LVQ network for pattern classification was reported by Pham and Oztemel (1994), where it was used as a preventive measure against possible out-of-control situations in a production line and was claimed to have a 97% rate of success. The authors also demonstrated that the pattern recognition and classification capabilities of the LVQ network was more superior than the conventional statistical approach. In addition, once successfully trained, the LVQ network was able to generalise from the learning examples on unseen data set thus making it more robust. To demonstrate the LVQ's generalisation ability, the following Tables 6.2, for the training examples and 6.3, for the network's classification results on *unseen* data, are presented.

Table 6.2 Example Data Set for the Hybrid Neural Network Training

Flame Front Monitor Data		Desired Output from the Hybrid Neural
Stoker Front	Furnace Tube	Network Classifier
	[0 0 0 0 0 0 0 0]	+45 (no visible flame front)
	[0 0 0 0 0 0 0 1]	+30
	[0 0 0 0 0 0 1 1]	+30
	[0 0 0 0 0 1 1 1]	+15
	[0 0 0 0 1 1 1 1]	+15
	[0 0 0 1 1 1 1 1]	-15
	[0 0 1 1 1 1 1 1]	-15
	[0 1 1 1 1 1 1 1]	-30
	[1 1 1 1 1 1 1 1]	-30

Note: The LVQ network in MATLAB™ only gave binary output, hence a standard 3-layer MLP network was used to map the LVQ network's output into the actual discrete distance (in mm) for the purpose of plotting the flame front movement with the boiler firing rate.

Table 6.3 Hybrid Neural Network Classifier Output on Unseen Data

Unseen Flame Front Monitor Response		Output from the Hybrid Neural Network
Stoker Front	Furnace Tube	Classifier
(a)	[0 1 0 0 1 1 1 1]	+15 (despite the 1 in the 2 nd element. A conventional means seeking for the first element of 1 would have resulted in -30)
(b)	[1 0 0 0 0 0 0 0]	+45 (was able to indicate no flame front <i>despite</i> the 1 in the 1 st element)
(c)	[1 1 0 0 0 0 0 0]	+45 (similar sort of scenario to (b))
(d)	[0 0 0 1 0 0 0 0]	+45 (similar sort of scenario to (b))
(e)	[0 0 1 1 1 1 1 0]	-15 (flame front location at -15mm, <i>despite</i> the 0 in the last element)
(f)	[1 0 0 0 0 0 1 1]	+30 (flame front at the right corner of the porthole <i>despite</i> the 1 in the 1 st element)
(g)	[1 0 0 0 1 1 1 1]	+15 (similar sort of scenario to (f))

Although the ‘spurious’ data in Table 6.3, which was simulated to test the hybrid neural network classifier, weren’t encountered during the flame front monitor implementation, the ability of such a classification system to tolerate sensor loss or possible disturbances, could make the flame front monitor more attractive for on-line industrial implementation. The classified results from Tests 16, 17a and 17b were plotted with the boiler firing rate of each respective test for the entire test duration (Figures 6.11 and 6.12), and its implication of the ignition plane movement is discussed in the following three Sub-Sections.

6.2.1.1 Industrial Plant Response Under Automatic NNBC Mode in Tracking the Hot Water Temperature Set Point (Test 16)

In this experiment the NNBC was implemented to maintain the hot water temperature from the industrial stoker and upon attainment of steady-state combustion (no changes in load for more than 15 minutes), then fine tune the air flow in order to optimise the combustion process (Section 5.4.4.1). The flame front monitor was mounted onto the arch inspection porthole (having the same diameter as the test facility at CRE, of 60mm) and a constant jet of air was purged down the metal tube supporting the camera to avoid the lens from being contaminated by particles ejected from the fire bed. This *maintenance free* set up was used in Tests 16, 17a and 17b which covered over 7 hours of total tests.

As illustrated in Figure 6.11, the overall flame front location throughout the test duration of just under 4 hours, remained towards the stoker front, with no indication of any sort of unstable movement that could lead to the loss of the ignition plane. This *sustained* stable flame front position was observed despite the changes in the firing rate where the largest change was from 22% of MCR to 62% of MCR, covering a turndown ratio of 3 to 1. This was largely due to the stable ignition process on the bed, where the high thermal inertia of the arch was thought to have played a significant role in enabling the plant PID control system to be implemented without too many problems (Section 5.4.3).

The only clear movement of the flame front in Figure 6.11, was when the air flow was increased from its lower setting, which raised the combustion intensity on the fire bed, thereby enhancing the ignition rate. The flame front location (marked by the dotted oval) shifted from approximately the middle of the porthole to almost the left corner of the porthole before it gradually moved back to the initial location.

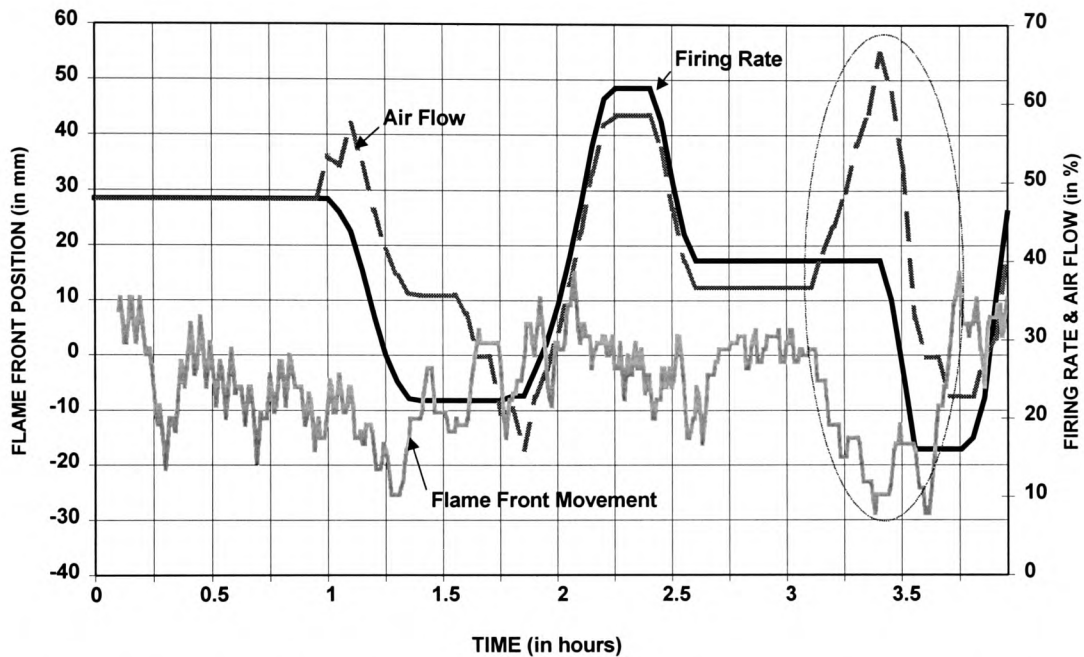


Figure 6.11 Flame Front Movement following Load Changes to Maintain the Hot Water Temperature Set Point of the Industrial Stoker Plant (Test 16)

6.2.1.2 Industrial Plant Response Under Automatic NNBC Mode to a Step Change in the Hot Water Temperature Set Point (Test 17a)

The required hot water temperature set point from the industrial boiler was stepped up from 88°C to 105°C, and the NNBC responded by increasing the firing rate to meet the increase in demand (Section 5.4.4.2). It must be noted that this experiment was carried out shortly after (1.5 hours) plant start up, which means that the ignition process of the fresh charge was establishing itself, although the arch was already hot enough (temperature higher than 500°C) to permit normal operation.

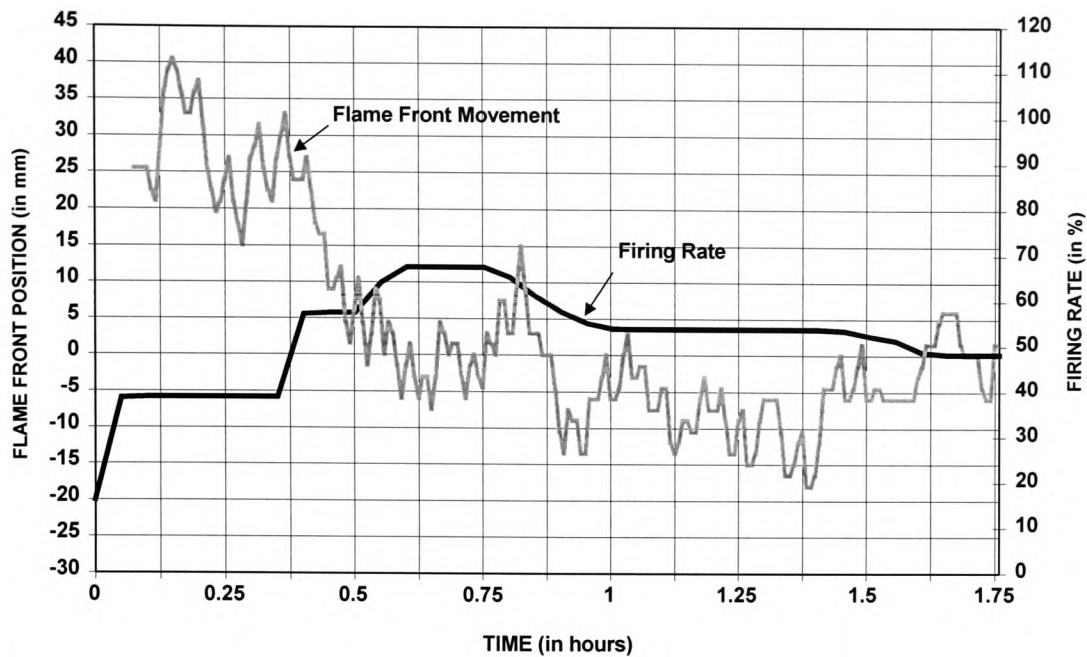


Figure 6.12 Flame Front Movement following a Step Change in the Hot Water Temperature Set Point of the Industrial Stoker Plant (Test 17a)

As the combustion process on the bed steadied out with time, one would expect the flame front to creep back to a location closer towards the stoker front (calibrated during commissioning), as illustrated in Test 16 during a normal plant operation. This expected trend was observed, as shown in Figure 6.12, where the flame front moved from a position somewhere beyond the visible range of the porthole ($>+30\text{mm}$) towards the stoker front and was found to be visible at an average location of -5mm at steady-state operation. Therefore, this monitoring device was capable of providing the plant operator with reliable on-line data regarding the flame front movement following changes in the boiler load.

6.2.1.3 Industrial Plant Response Under Automatic NNBC Mode to a Step Change in the Hot Water Temperature Set Point (Test 17b)

This was a similar experiment to Test 17a, where the hot water temperature set point was stepped up from 105°C to 120° . It is worth stating that this test was carried out after Test 17a, whereby the combustion process on the bed had already steadied out. As one would expect the flame front location occurred within the range very similar to Test 16, indicating that the ignition of the fresh charge was satisfactory.

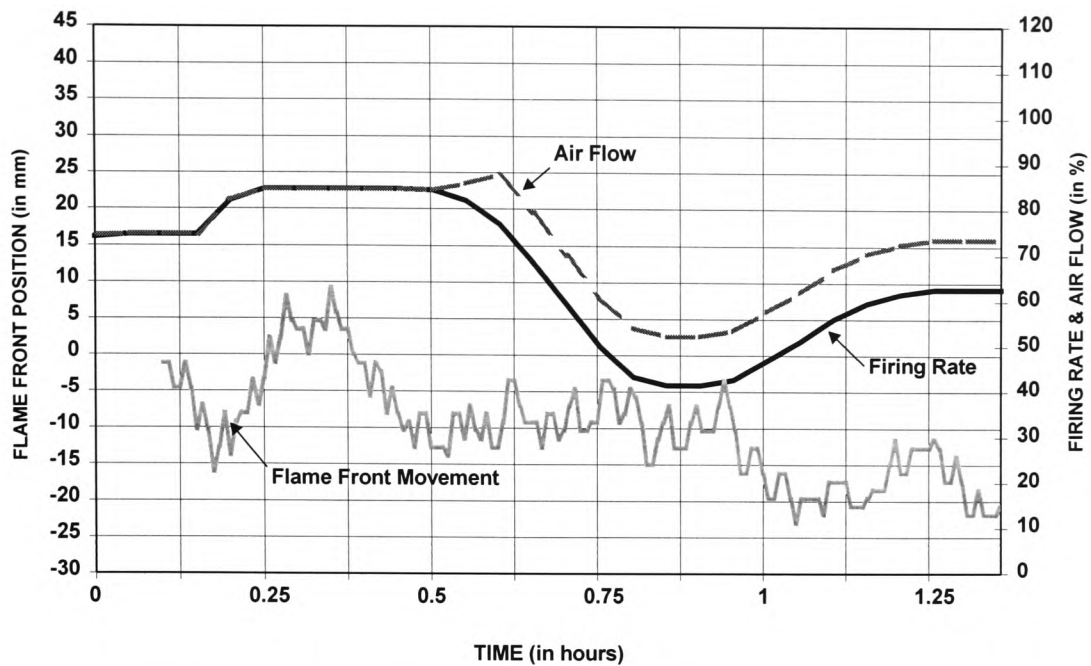


Figure 6.13 Flame Front Movement following a Step Change in the Hot Water Temperature Set Point of the Industrial Stoker Plant (Test 17b)

6.3 Conclusions

A novel combustion monitoring system was developed following a pilot study on the stoker test facility at CRE to investigate flame front movement through the arch inspection porthole following load changes. It has been demonstrated on an industrial chain grate that the flame front monitor can provide reliable on-line data regarding the ignition plane movement over long hours of plant operation. Such a monitoring system coupled with the robust neural network classifier can be used to enhance the integrity of the on-board conventional controller and/or simply act as an on-line advisor to the plant personnel to cope with possible bed disturbances. This monitoring system can be installed onto any chain or travelling grate stokers with ease, being maintenance free and offer ease of digital interfacing.

7. Conclusions & Recommendation for Further Work

There is a strong indication that coal could be the primary source of energy for the commercial and industrial sector in the not too distant future, let alone the power generation and iron production industry which currently consumes over 2/3 of the world's coal production. Along with concerns over the influence of human activity towards grave environmental issues, implications from fossil fuel combustion has been globally voiced, particularly among the industrialised nations. In Europe this has already been reflected in the ever tightening legislation on emission limits, with distinctive attention on the emission of green house gases (GHGs). This has clearly called for improved means and methods of more efficient and cleaner ways in which coal can be utilised for heat generation. As a matter of fact, it is the main motivation behind this research project which received financial support from the British Coal Utilisation Research Association (BCURA) and the UK Department of Trade & Industry (DTI) which aimed to optimise the combustion process on small to medium size coal fired boiler plants. The mechanical chain grate was nominated as the main stoking candidate for lump coal combustion in mostly shell boilers owing to its sustained popularity over many decades as the preferred means of combusting solid fuel(s). In the UK this have been reflected in the large proportion of the 3.2 million tonnes of coal currently consumed annually (approximately £160 million pounds worth) in this small to medium boiler range capacity, in which chain grates dominate as the primary stoker.

From the literature search, it appears that Artificial Intelligence (AI) techniques have escalated in use over the last decade or so in addressing problems associated with real life situations when conventional means failed to offer adequate solutions. In the aspect of monitoring and subsequently the control of non-linear processes (such as the task at hand) so as to yield a desirable performance, AI techniques have proven to be an immense success over a wide spectrum of fields. Artificial Neural Networks (ANNs) can process incomplete information or corrupted signals to deliver an output based on past experience, which in a real-world environment offers the much sought

after *robustness* to a control system. In addition to being able to see through ‘noisy’ signals, it can approximate *any continuous* functional mapping between the given boundary of input and output data, therefore providing many engineers and scientists with a versatile tool in identifying complex processes without having to consider the complex underlying physical dynamics associated with mathematically modelling these processes.

7.1 Performance of the Neural Network Based Controller (NNBC)

In this study, ANNs have proved to be suitable for the tasks of encoding the operator’s knowledge in the form of modules/data bases which were integrated in a framework of rules written in a computer programme (MATLAB™) to function as an expert boiler operator. The novel NNBC strategy utilised the learned experience of these neural network modules to cope with unwanted situations and delivered the appropriate corrective actions so as to improve the plant performance. By comparing the results obtained from operating the boiler plant manually (0.75MW_{th} test facility at CRE) and under the influence of the conventional plant PID controller (3.7MW_{th} plant at HMP Garth) against the performance of the NNBC have clearly demonstrated the superiority of the NNBC in outperforming the former approaches. With respect to manual operation, although operated under the boiler engineer’s best practice, the NNBC was much more *consistent* in its effort at maintaining a minimum excess air level, in addition to executing the staging sequence for large load changes with better *precision* (magnitude of change and time between successive stages). The optimised parameter was the excess air level (reflected by the oxygen in the exhaust flue gas concentration) and the NNBC endeavoured to provide a minimum amount of combustion air (as specified by the desired optimum band) without having to sacrifice smoke/carbon monoxide emission or unburnt carbon in the ash, thereby improving the combustion efficiency, and in so doing managed to reduce the overall nitrogen oxides emission. On the 3.7MW_{th} industrial chain grate boiler plant, the NNBC demonstrated an overall improvement of 2 to 3% in combustion efficiency by reducing the excess air level

consistently to the minimum requirement by 2%, which also resulted in an overall nitrogen oxides emission reduction of 15% and decreased the carbon monoxide emission by 60%. However it must be stressed that the carbon monoxide emission from the 3.7MW_{th} industrial chain grate under conventional PID control (average peak of 1200ppm at turndown) has yet to cause any concern over smoke emission although the NNBC could well offer these combustion plants better compliance with future legislation that could be imposed as indicated by the European Commission. The success of the NNBC stemmed from its intimate understanding of the behaviour of the combustion process through the formulation of good estimates of the input parameters before staging these parameters in order to achieve better transient operation. Upon the attainment of steady-state combustion, the NNBC then consistently attempted to keep the excess air level to a minimum hence improving the combustion efficiency whilst keeping pollutant emissions at an acceptable level in addition to maintaining safe boiler operation (such as no live fire over the grate, no smoking at stoker front and a cool grate surface temperature).

7.2 Identified Models of Combustion Derivatives by Using the ‘Black-Box’ Modelling Technique of ANNs

In addition to the on-line condition monitoring and control of the coal fired plant, the research project also addressed the current deficiencies in combustion modelling as reported in the literature by employing the ‘black box’ identification technique of ANNs. Encouraging results were obtained with respect to both representing the dynamics of the combustion process (reflected in the exhaust flue gas oxygen concentration) and also the pollutant emissions (nitrogen oxides and carbon monoxide) as well as providing accurate one-step-ahead predictions of the three combustion derivatives, based on the past input and output signals. It must be stressed that these models were developed and tested using data gathered from the 0.75MW_{th} chain grate stoker test facility burning Singles grade bituminous coal. Upon completion of model training (learning with an example data set), these models were also validated with data gathered from a significant temporal separation (training and validation data sets

were 8 months apart) which should have allowed for any time-varying characteristics of the combustion process to develop such as boiler fouling to a small extent and were found to be highly acceptable. Although the developed models could only provide an accurate prediction over a short time horizon in the future (30 seconds) it demonstrated the ability of ANNs to represent complex functional relationships which existed in the example data set, and employed previously learned experience to deliver an accurate one step ahead prediction. This could be used as an on-line 'software' sensor in conjunction with a more sophisticated control strategy to control such a boiler plant, although the added complexity (as compared to the NNBC) would have to be justified if it is reflected in the end cost of commercially developing such a control system. It is to the author's opinion not to be currently feasible due to the reluctance of users to make such a capital investment for boilers within this operating range.

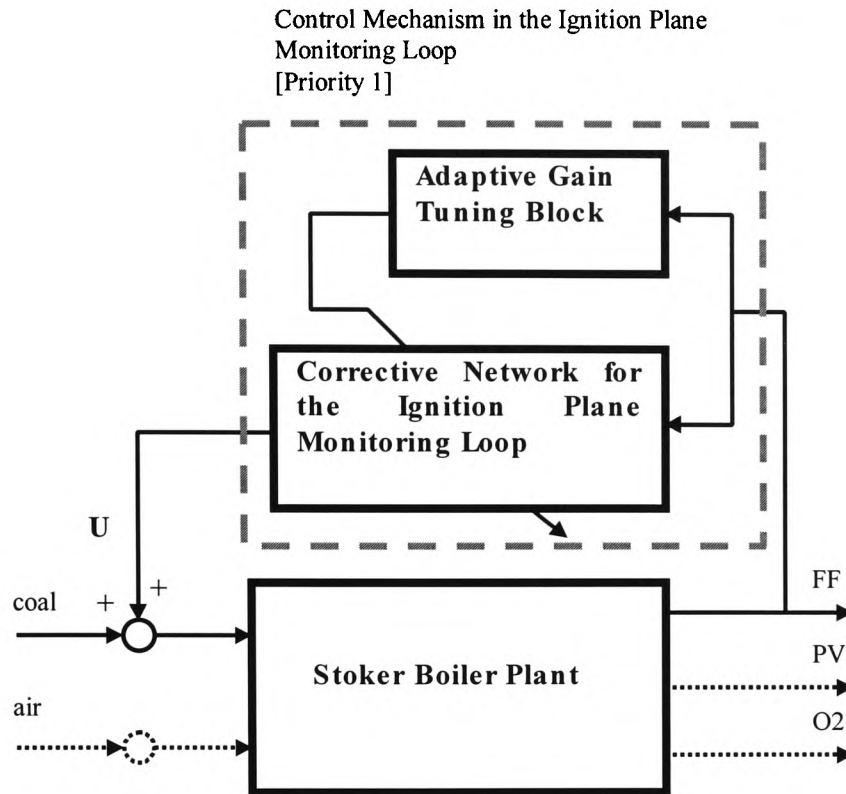
7.3 Novel Flame Front Monitoring System

A novel combustion monitoring system was also developed during the course of the research project by using an optical means to record the flame front location (providing an indication of the ignition plane) through the stoker arch inspection porthole. The optical monitoring system was a result of a pilot study conducted by analysing the images taken by a video camera at discrete time (30 seconds) and plotting the historical data over a period of boiler operation. Information provided by these discrete time images mirrored the action of the boiler operator who ensured that the freshly supplied coal was ignited at the correct location (where visible from the inspection porthole) in order to achieve satisfactory combustion on the bed. Following the results of the pilot study, a novel flame front monitoring system was developed using an array of photodiodes to detect the varying light intensity of the bed image through the porthole which was focused on a screen mounted in a Single Lens Reflex (SLR) camera. The information gathered was subsequently fed to a hybrid ANN for classification to provide an output as to the exact location of the flame front. This novel monitoring system was tried on the 3.7MWth industrial chain grate stoker boiler and was found to perform well over hours of continuous operation without requiring any maintenance. The flame front monitoring system could be interfaced with the plant Digital Control

System (DCS) or integrated into the Building Management System (BMS) as a safety interlock i.e. should the flame front be found to move towards the furnace tube at a fast rate (losing the ignition plane), it could trigger an alarm or shut down the grate motor until ignition was brought back, before resuming normal operation. Clearly this can better equip the on-plant control system to deal with bed disturbances (coal quality and/or bed distribution) of a larger extent – which is a primary concern to both stoker manufacturers and users alike. Finally the novel flame front monitoring system can offer these facilities without incurring any heavier costs than those of installing K-type thermocouples into the boiler refractory arch. In order to have a clear picture of the ignition plane movement, experience has shown that at least 3 thermocouples are required namely front, middle and back and would need replacement at least once a year. The current cost of one industrial thermocouple is around £50, and over two years of operation, the costs on the thermocouples themselves would be £300. Apart from a low range Personal Computer (DX386) with a data acquisition card, the sensor part of the flame front monitoring system (consisting of an array of photodiodes, camera and amplification circuit) can literally be constructed with under £100 and unlike the thermocouples it requires no maintenance, as it is not subjected to deterioration due to extreme working temperature. Furthermore the information from the flame front monitoring system is more reliable and can provide a better representation of the actual ignition plane movement.

7.4 Recommendation for Further Work

It is the author's conviction that the novel flame front monitoring system with the classification neural network when incorporated into the NNBC strategy could offer better reliability and confidence to prospective users when the stoker boiler plant is left on automatic operation under the influence of the NNBC. The following block diagram in Figure 6.1 proposes the inclusion of the flame front monitoring system in the overall NNBC control strategy for the industrial chain grate stoker. The dotted lines represent the original NNBC structure as depicted in Figure 5.20 in Section 5.4.4 whilst the solid lines denote the control loop associated with the ignition plane monitoring system.



Legend:

U = magnitude of grate speed to be changed

FF = location of the flame front from the monitoring system

Figure 7.1 The Inclusion of Flame Front Monitoring Network into the NNBC Strategy

The control philosophy of the flame front monitoring loop would be similar to the oxygen trimming loop, shown in the dashed grey box, where a corrective network was employed to deliver the necessary corrective action based on past experience, i.e. if the flame front has moved towards the furnace tube reduce the initial grate speed by say 10%, or increase the grate speed by 10% if the flame front has moved towards the stoker front (possible burnback with an older stoker). As with all empirical work, data would have to be gathered from carefully designed experiments in order to generate a reliable information data base for neural network training. An adaptive gain tuning block could be employed to automatically fine tune the gain factor (magnitude of grate speed change) of the corrective network to yield a desirable performance, by constantly inspecting the rate of ignition plane movement (based on past data) following a control decision by the corrective network. However the first priority of the NNBC with the inclusion of the monitoring loop, would be establishing good ignition of the freshly

supplied coal before tracking the process variable (e.g. hot water temperature) set point or trimming the excess air level for optimum combustion.

Perhaps the other more speculative area that could be investigated would include encoding a self-learning neural network module within the overall NNBC to deal with other long term factors or time varying characteristics such as boiler fouling. Such work will perhaps involve the so-called unsupervised learning neural networks for such independent classification tasks within a hybrid expert system architecture to deliver an accurate diagnosis.

References

- Allen, M.G., Butler, C.T., Johnson, S.A., Lo, E.Y. and Russo, F (1993) An Imaging Neural Network Combustion Control System for Utility Boiler Applications. *Combustion and Flame*, **94**, 205-214.
- Anson, D., Clarke, W.H.N., Cunningham, A.T.S. and Todd, P. (1971) Carbon Monoxide as a Combustion Control Parameter. *Journal of the Institute of Fuel*, **44**, 191-195.
- Babcock International (1995) Minimise NO_x Emissions while Optimising Combustion. *Private Communication*.
- Bailey, D. and Thompson, D. (1990) How to Develop Neural Network Applications. *AI Expert*, 38-47.
- Baker, P.C. and Loveridge, D.J. (1965) Dynamic Response of a Coal Fired Shell Boiler. *Journal of the Institute of Fuel*, **38**(483), 483- 492.
- Berger, D., Landau, M.V., Herskowitz, M. and Boger, Z. (1996) Deep Hydrodesulphurisation of Atmospheric Gas Oil: Effects of Operating Conditions and Modelling by Artificial Neural Network Techniques. *Fuel*, **75**(7), 907-911.
- Birkby, C., Brown, J. and Street, P.J. (1973) The Early Detection of Mill Fires by Monitoring for Carbon Monoxide. *CEGB Digest*, **25**(3), 7-10.
- Boger, Z. (1997) Experience in Industrial Plant Model Development Using Large-Scale Artificial Neural Networks. *Information Sciences*, **101**, 203-216.
- BS1016: Part 104.2 (1991) *Methods for Analysis and Testing of Coal and Coke: Determination of Moisture Content of the General Analysis Sample of Coke*. British Standard Institution.
- BS1016: Part 104.4 (1991) *Methods for Analysis and Testing of Coal and Coke: Determination of Ash*. British Standard Institution.
- BS845: Part 1 (1987) *Assessing Thermal Performance of Boilers for steam, Hot Water and High Temperature Heat Transfer Fluids*. British Standard Institution.
- Butt, A.R. and Pulley, M.V. (1996) *On-Line Condition Monitoring in Coal Utilisation*. Coal Technology Development Division, Materials Report 031.
- Chen, S. and Billings, S.A. (1990) Non-Linear System Identification using Neural Networks. *International Journal of Control*, **51**(6), 1191-1214.

- Chen, S. and Billings, S.A. (1991) *Neural Networks for Non-Linear Dynamic System Modelling and Identification*. Dept. of Automatic Control and Systems Engineering, Univ. of Sheffield, Research Report: 436.
- Chong, Z.S., Wilcox, S.J. and J. Ward (1999) BCURA Project B35: *7th Progress Report on the Monitoring and Control of Stoker Fired Boiler Plants by Neural Networks*. BCURA Library, CRE Ltd., Cheltenham.
- Chong, Z.S., Wilcox, S.J., Ward, J. and Butt, A. (1996) The Monitoring and Control of Stoker Fired Boiler Plant by Neural Networks. *Proceedings of the 9th International Conference on Condition Monitoring and Diagnostic Engineering Management*, 289-298, 1996.
- Chong, Z.S., Wilcox, S.J., Ward, J. and Butt, A. (1997) The Development of a Neural Network Controller for Chain Grate Stoker Boiler. *Proceedings of the 4th European Conference on Industrial Furnaces and Boilers: Furnace/Boiler Operation and Design*, 1.
- Clarke, A.G. and Williams, A. (1992) The Formation and Control of NO_x Emission. *Chemistry and Industry*, **24**, 917-920.
- Coal R&D Project Summary 051 (1997) *On-Line Condition Monitoring in Coal Utilisation*. Energy Technology Support Unit (ETSU) for the DTI.
- Coal R&D Project Summary 057 (1996) *The Control of Nitrogen Oxides Emissions from Stoker Fired Boilers*. Energy Technology Support Unit (ETSU) for the DTI.
- Coal Research Establishment (CRE) (1994) Petroleum Coke as a Domestic Fuel: An Evaluation of Sulphur Retention Using a Sorbent Additive in Solid Fuel Briquettes. *Private Communication*.
- Coal Technology Development Division (CTDD) (1995) Material Division Report on PB29: Chain Grate Stoker Test Facility. *Private Communication*.
- Combustion Developments Ltd. (CODEL) (1998) 1000 Series CO, SO₂ or NO Analysis. Emission or Process Stack Gas Analysis: Purpose Designed for Large/Dirty Processes. *Private Communication*.
- Cooke, M.J. (1991) The Environmental Implications of Clean Coal Technologies. *Proceedings of the Conference on New Technologies for Power Generation and Industrial Plant*, 209-226.

- Cooke, M.J. and Pragnell, R.J. (1989) Technology to Meet Proposed Environmental Standards. *Proceedings of the First European Fine Coal Conference*, 23-25.
- DeClaris, N. and Su, Mu-Chun (1993) A Neural Network Based Approach to Knowledge Acquisition and Expert System. *Proceedings of the IEEE International Conference on System, Manufacturing and Cybernetics*, **2**, 645-650.
- Demuth, H. and Beale, M. (1995) *Neural Network Toolbox Manual for Use with MATLAB™*. The MathWorks Inc., USA.
- DTI Case Study 004 (1998) *Industrial Boiler Control*. DTI Cleaner Coal Technology Programme.
- DTI NeuroComputingWeb (1998) <http://www.clients.globalweb.co.uk/nctt/guide>. The Department of Trade and Industry.
- European Coal and Steel Community (ECSC), (1996) *Modelling the Burning of Multicomponent Solid Fuel Briquettes in Domestic and Industrial Combustors*. Agreement No. 7220-ED-084.
- EEC Directive 88/609 (1988) On the Limitation of Emissions of Certain Pollutants into the Air from Large Combustion Plants. *Official Journal of the European Communities*, IBICL, L336, 1-13.
- Eki, Y., Hirasawa, K., Nakamura, M. and Oouchi, K. (1997) New Method of Off-Line Adjustment of Feed-Forward Control for Fossil-Fired Plant Main Control System. *Electrical Engineering in Japan*, **119**(1), 55-61.
- Ekman, B. and Wang Jensen, J. (1990) Infurnace SO_x Reduction. *Proceedings of the Costs of Flue Gas Desulphurisation*, 1-12.
- Esteves, S.R.R., Hawkes, D.L., Hawkes, F.R., Guwy, A.J., O'Neill, C., Dinsdale, R.M. and Wilcox, S.J. (1998) Prediction of Remedial Actions during the Biological Degradation of Industrial Effluents by Neural Networks. *Proceedings of the 11th International Congress on Condition Monitoring and Diagnostic Engineering Management*.
- Fletcher, R. (1987) *Practical Methods of Optimisation*, Wiley.
- Ford, N.W.J., Cooke, M.J. and Gibbs, B.M. (1991) Control of SO₂ Emissions from Stoker Fired Coal Combustion by On-Grate Addition of Limestone. *Transactions of the IChemE*, **69**(B), 167-172.

- Ford, N.W.J., Cooke, M.J. and Pettit, M.D. (1992) The Use of a Laboratory Fixed-Grate Furnace to Simulate Industrial Stoker-Fired Plant. *Journal of the Institute of Energy*, **65**, 137-143.
- Francis, W. and Peters, M.C. (1980) *Fuels and Fuel Technology*. Pergamon Press: Oxford.
- Fuel Efficiency Booklet 17 (1994) *Economic Use of Coal Fired Boiler Plant*. The Department of the Environment: Best Practice Programme.
- Giammar, R.D., Hopper, D.R., Webb, P.R. and Radhakrishnan, E. (1979) Evaluation of Emissions and Control Technology for Industrial Stoker Boilers. *Proceedings of the 3rd Stationary Source Combustion Symposium*, **1**, 3-35.
- Good Practice Case Study 35 (1991) *Variable Speed Drive on a Boiler Fan*. The Department of the Environment: Best Practice Programme.
- Good Practice Case Study 352 (1997) *Improved Turndown and Fuel Savings on a Coal-Fired Boiler Using Chain Grate Stokers*. The Department of the Environment: Best Practice Programme.
- Good Practice Guide 2 (1998) *Energy Savings with Electric Motors and Drives*. Energy Efficiency Office: Best Practice Programme.
- Good Practice Guide 30 (1992) *Energy Efficient Operation of Industrial Boiler Plant*. Energy Efficiency Office: Best Practice Programme.
- Good Practice Guide 88 (1993) *Energy Efficient Use of Boilers Using Chain Grate Stokers*. Energy Efficiency Office: Best Practice Programme.
- Grainger, L. and Gibson, J. (1981) *Coal Utilisation: Technology, Economics & Policy*. Graham and Trotman Limited.
- Gunn, D.C. (1952) The Effect of Coal Characteristics on Boiler Performance. *Journal of the Institute of Fuel*, **July**(25), 148-154.
- Gunn, D.C. (1982) Conventional Coal Firing Equipment. *Private Communication*.
- Gunn, D.C. and Horton, R. (1989) *Industrial Boilers*. Longman Scientific & Technical.
- Guo, B., Shen, Y.T., Li, D.K. and Zhao, F. (1997) Modelling Coal Gasification with a Hybrid Neural Network. *Fuel*, **76**(12), 1159-1164.
- Gupta, A.K. and Lilley, D.G. (1987) The Grey Areas in Combustion Research. *Journal of the Institute of Energy*, 108-120.

- Gutmark, E., Parr, T.P., Hanson-Parr, D.M. and Schadow, K.C. (1990) Use of Chemiluminescence and Neural Networks in Active Combustion Control. *Proceedings of the 23rd International Symposium on Combustion: The Combustion Institute*, **23**, 1101-1106.
- Hadvig, S. (1989) Advanced Air Control for Combustion on Travelling Grates. *Proceedings of the Applied Energy Research Conference*, 207-220.
- Harris, C.J., Moore, C.G. and Brown, M. (1993) *Intelligent Control*. World Scientific.
- Harris, M., Rivett, W.L. and Thurlow, G.G. (1962) Some Experiments and Developments Towards Improved Coal and Ash Handling for Small Boiler Plant. *Journal of the Institute of Fuel*, **35**, 523-531.
- Harris, M., Rivett, W.L. and Thurlow, G.G. (1962) Some Experiments and Developments Towards Improved Coal and Ash Handling for Small Boiler Plant. *Journal of the Institute of Fuel*, **35**, 523-531.
- Hayward, C.H.G. (1951) Developments in the Firing of Shell Boilers by Means of Chain-Grate Stokers. *Journal of the Institute of Fuel*, **May**(24), 109-115.
- He, X. and Asada, H. (1993) A New Method for Identifying Orders of Input-Output Models for Non-Linear Dynamic Systems. *Proceedings of the American Control Conference*, 2520-2523.
- Hebb, D.O. (1949) *The Organisation of Behaviour: A Neural Psychological Theory*. John Wiley, New York.
- Hobbs, M.L., Radulovic, P.T. and Smoot, L.D. (1992) Modelling of Fixed-Bed Gasifiers. *Journal of the American Institute of Chemical Engineers*, **38**(5), 681-702.
- Hobbs, M.L., Radulovic, P.T. and Smoot, L.D. (1993) Combustion and Gasification of Coals in Fixed-Beds. *Progress in Energy and Combustion Science*, **19**, 505-586.
- Hopfield, J.J. (1982) Neural Networks and Physical Systems with Emergent Collective Computational Abilities. *Proceedings of National Academy of Sciences*, **79**, 2554-2558.
- Hornik, K., Stinchcombe, M. and White, H. (1989) Multi-Layered Feed-Forward Networks are Universal Approximators. *Neural Networks*, **2**, 359-366.

- Houghton, J.T., Jenkins, G.J. and Ephraums, J.J. (1990) *Climate Change: The Intergovernmental Panel on Climate Change (IPCC) Scientific Assessment*. Cambridge University Press.
- Huang, S.H. and Zhang, H.C. (1994) Artificial Neural Networks in Manufacturing: Concepts, Applications and Perspectives. *IEEE Transactions on Components, Packaging and Manufacturing Technology: Part A*, **17**(2), 212-228.
- IEA Coal Research (1993) *An International Project for Coal Information*. International Energy Agency.
- IEA Statistics (1997) *Coal Information*. International Energy Agency.
- Jain, A.K., Mao, J.C. and Mohiuddin, K.M. (1996) Artificial Neural Networks: A Tutorial. *Computer*, **29**(3), 31-44.
- Johnson, A.J. and Auth, G.H. (1951) *Fuels and the Combustion Handbook*. 1st Edition, McGraw-Hill Book Company.
- Kautz, K., Reichel, H.H. and Schwarz, G. (1983) Relationship Between Coal Properties and the Incidence of Slagging, Fouling and Corrosion in Travelling-Grate Boilers. *VGB Kraftwerkstechnik*, **63**(8), 605-609.
- Kohonen, T. (1989) *Self-Organisation and Associative Memory*. Springer-Verlag, Berlin.
- Land Combustion (1998) Stack Gas Analysis and Total Efficiency: Combustion and Environmental Monitoring. *Private Communication*.
- Langsjoen, P.L. (1981) *A Guide to Clean and Efficient Operation of Coal Stoker Fired Boilers*. Report for the American Boiler Manufacturers Association, U.S. Department of Energy & U.S. Environmental Protection Agency, Contract No. IAG – D7E681 (EPA).
- Langsjoen, P.L., Burlingame, J.O. and Gabrielson, J.E. (1981) *Emissions and Efficiency Performance of Industrial Coal Stoker Fired Boilers*. Report for the American Boiler Manufacturers Association, U.S. Department of Energy & U.S. Environmental Protection Agency, Contract No. IAG – D7E681 (EPA).
- Livingston, W.R., Chakraborty, R.K. and Birch, M.C. (1995) The Control of NO_x Emissions from Stoker Fired Boilers. *Proceedings of the 2nd Combustion and Emissions Control Conference*, 273-283.

- Ljung, L. (1987) *System Identification: Theory for the User*. Prentice-Hall, Inc., Englewood Cliffs, New Jersey.
- Ljung, L. (1995) *System Identification Toolbox Manual for Use with MATLAB™*. The MathWorks Inc., USA.
- Lu, S. (1997) Towards Intelligent Systems for Boiler Design. *Journal of Power and Energy: Proceedings of the IMechE: Part A*, **211**(5), 399-409.
- Luxl, F.C. (1961) Sampling, Analysing and Control of Oxygen in Boiler Flue Gas. *Proceedings of the ASME Winter Annual Meeting*, 3-8.
- MacDonald, E.J. and Murray, M.V. (1953) Effect of Ash on the Performance of Shell Boilers: Part 1. *Journal of the Institute of Fuel*, 308-317.
- MacDonald, E.J. and Murray, M.V. (1953) The Effect of Ash on the Performance of Shell Boilers. *Journal of the Institute of Fuel*, **Jan**(1), 308-317.
- MacDonald, E.J. and Murray, M.V. (1955) The Effect of Coal Quality on the Efficiency of a Shell Boiler Equipped with a Travelling-Grate Stoker. *Journal of the Institute of Fuel*, **Oct**(28), 479-498.
- Marks, W.L. (1987) Coal Fired Industrial Steam Boilers: Principle of Automatic Regulation of Pressure for Stability during Load Following. *Journal of the Institute of Energy*, **60**(442), 8-14.
- McCulloch, W.S. and Pitts, W.H. (1943) A Logical Calculus of the Ideas Imminent in Nervous Activity. *Bull. Mathematical Biophysics*, **5**, 115-133.
- McGhee, J., Grimble, M.J. and Mowforth, P. (1990) *Knowledge-Based Systems for Industrial Control*. Peter Peregrinus Ltd.
- McHale, A.P. (1988) Business Opportunities in Boiler Control Systems. *Energy World: Electronic Energy Management*, **156**, 7-9.
- Minsky, M. and Papert, S. (1969) *Perceptrons: An Introduction to Computational Geometry*. MIT Press: Cambridge, Massachusetts.
- Naidu, S.R., Zafiriou, E. and McAvoy, T.J. (1990) Use of Neural networks for Sensor Failure Detection in a Control System. *IEEE Control Systems Magazine*, **10**, 49-55.
- Narendra, K.S. and Parthasarathy, K. (1990) Identification and Control of Dynamical Systems Using Neural Networks. *IEEE Transactions on Neural Networks*, **1**(1), 4-27.

- Neuffer, D., MacConnell, P.F., Owens, D.H., Patrick, M.A., Biss, D. and Butt, A.R. (1995) An Automatic Control System for Clean Coal Combustion on a Chain Grate Stoker. *The Proceedings of the 8th International Conference on Coal Science*, 559-562.
- Neuffer, D., MacConnell, P.F., Patrick, M.A. and Owens, D.H. (1996) A Two-Dimensional Heterogeneous Model for the Control of a Chain Grate Stoker. *Physical Modelling as a Basis for Control*. Digest No. 96/042, IEE, London.
- Neuffer, D., Owens, D.H., MacConnell, P.F.A. and Dando, R. (1997) Optimised Control of Coal Fired Boilers. *Private Communication*.
- Noguchi, K., Takamichi, A., Iwatsuka, C. and Nakamura, K. (1993) How can ANNs Contribute to Industrial Development ?. *Proceedings of the International Joint Conference on Neural Networks*, 1(1), 1061-1064.
- Noorgard, M. (1995) *Neural Network Based System Identification Toolbox Manual: For Use with MATLAB™*. Technical Report 95-E-773, Institute of Automation, Technical University of Denmark.
- Ogata, K. (1990) *Modern Control Engineering*. Prentice-Hall International Editions.
- Ormerod, W.G. (1981) Automatic Trimming of Combustion Air to a Pulverised Coal-Fired Boiler Using the Flue Gas Carbon Monoxide Signal. *Journal of the Institute of Energy*, 174-175.
- Ormerod, W.G. and Read, A.W. (1979) An Improved Method of Combustion Control of Coal-Fired Boilers Using Flue Gas Carbon Monoxide Analysis. *Journal of the Institute of Energy*, 23-26.
- Ounstead, B.A. (1969) A Rapid, Multipoint, Oxygen Analyser for Power Station Flue Gases. *Journal of the Institute of Fuel*, **42**, 408-411.
- Pal, S.K. and Srimani, P.K. (1996) Neurocomputing: Motivation, Models and Hybridisation. *Computer*, **29**(3), 24-27.
- Pham, D.T. (1994) Neural Networks in Engineering. *Proceedings of the 9th Conference of Artificial Intelligence in Engineering*, 3-36.
- Pham, D.T. and Liu, X. (1995) *Neural Networks for Identification, Prediction and Control*. Springer-Verlag, London Limited.

- Pham, D.T. and Oztemel, E. (1994) Control Chart Pattern Recognition Using Learning Vector Quantisation Networks. *International Journal of Production Research*, **32**(3), 721-729.
- Premier, G.C., Dinsdale, R., Guwy, A.J., Hawkes, F.R., Hawkes, D.L. and Wilcox, S.J. (1999) A Comparison of the Ability of Black Box and Neural Network Models of ARX Structure to Represent a Fluidised Bed Anaerobic Digestion Process. *Water Research*, **33**(4), 1027-1037.
- Premier, G.C., Dinsdale, R., Guwy, A.J., Hawkes, F.R., Hawkes, D.L. and Wilcox, S.J. (1997) Simple Black Box Models Predicting Potential Control Parameters during Disturbances to a Fluidised Bed Anaerobic Reactor. *Water Science and Technology*, **36**(6-7), 229-237.
- Prizzi, J.J. (1985) A Low Cost Option for Controlling Particulate Emissions from Chain Grate Stoker Fired Boilers. Proceedings of the 76th Annual Conference of the International District Heating Association, **76**, 207-218.
- Proctor, A. (1999) Energy Efficient Boiler Operation Utilising Chain Grate Stokers. *Private Communication*.
- Radl, B.J. (1999) Neural Networks Improve Performance of Coal-Fired Boilers. *CADDET Energy Efficiency: Boilers and Burners*, Newsletter No. 1, 4-6.
- Rawlings, C.M., Roderick, D.J.I. and Thurlow, G.G. (1962) Note on Heat-Transfer Rates Occurring in the Furnace Tubes of Coal-Fired Shell Boilers. *Journal of the Institute of Fuel*, **Feb**, 56-59.
- Reifman, J. and Feldman, E.E. (1998) Identification and Control of NO_x Emissions Using Neural Networks. *Journal of the Air and Waste Management Association*, **48**, 408-417.
- Reinschmidt, K.F. and Ling, B. (1994) Neural Networks with Multiple State Neurons for Nitrogen Oxide Emissions Modelling and Advisory Control. *Proceedings of the IEEE International Conference on Neural Networks*, **6**, 3834-3839.
- Ribeiro, B., Dourado, A. and Costa, E. (1993) A Neural Network Based Control of a Simulated Industrial Lime Kiln. *Proceedings of the International Joint Conference on Neural Networks*, **2**(2), 2037-2040.

- Robson, B.T., Johnstone, C.D. and Crowther, M. (1988) Fully Automatic Unmanned Solid and Multi-Fuel Shell Boilers. *IMechE Seminar on the Continuing Role of Steam*, 7-17.
- Rolfe, T.J.K. (1961) Distribution of Primary Air in Chain Grate Stokers. *Journal of the Institute of Fuel*, **34**, 481-443.
- Rolfe, T.J.K. (1961) Distribution of Primary Air. *Journal of the Institute of Fuel*, **34**, 481-493.
- Rolfe, T.J.K. (1962) Tests on an Automatically Controlled Chain Grate Fired Shell Boiler. *Journal of the Institute of Fuel*, 532-550.
- Rolfe, T.J.K. (1962) Tests on an Automatically Controlled Chain-Grate-Fired Shell Boiler. *Journal of the Institute of Fuel*, **Dec**, 532-550.
- Rosenblatt, R. (1962) *Principles of Neurodynamics*. Spartan Books, New York.
- Rumelhart, D.E. and McClelland, J.L. (1986) *Parallel Distributed Processing: Exploration in the Microstructure of Cognition*. MIT Press, Cambridge, Massachusetts.
- Saha, P.K., Shoib, M. and Kamruzzaman, J. (1998) Development of a Neural Network Based Integrated Control System of 120ton/h Capacity Boiler. *Computers and Electrical Engineering*, **24**, 423-440.
- Salehfar, H. and Benson, S.A. (1998) Electric Utility Coal Quality Analysis Using Artificial Neural Network Techniques. *NeuroComputing*, **23**(1-3), 195-206.
- Sanyal, A. and Williamson, J. (1981) Slagging in Boiler Furnaces: An Assessment Technique Based on Thermal Behaviour of Coal Minerals. *Journal of the Institute of Energy*, 158-162.
- Sarofim, A.F. and Flagan, R.C. (1976) NO_x Control for Stationary Combustion Sources. *Journal of Progress in Energy and Combustion Science*, **2**(1), 1-25.
- Sarofim, A.F. and Hottel, H.C. (1978) Radiative Transfer in Combustion Chambers: Influence of Alternative Fuels. *Proceedings of the 6th International Heat Transfer Conference*, 199-217.
- Schobert, H.H. (1987) *Coal: The Energy Source of the Past and Future*. American Chemical Society.
- Shaw, W.T. (1990) Multivariable Alarming Using Neural Networks. *ISA Transactions*, **29**(1), 57-62.

- Silva, R.G. (1997) *Cutting Tool Condition Monitoring of the Turning Process Using Artificial Intelligence*. Doctoral Dissertation, The University of Glamorgan, South Wales, UK.
- Sinnasamy, R.N., Zafiriou, E. and McAvoy, T.J. (1990) Use of Neural Networks for Sensor Failure Detection in a Control System. *IEEE Control System Magazine*, **10**, 49-55.
- Smoot, L.D. (1984) Modelling of Coal Combustion Processes. *Journal of the Progress in Energy and Combustion Science*, **10**, 229-272.
- Smoot, L.D. and Hill, S.C. (1983) Critical Requirements in Combustion Research. *Progress in Energy and Combustion Science*, **9**, 77-103.
- Soderstrom, T. and Stoica, P. (1989) *System Identification*. Prentice-Hall, USA.
- Staib, W.E. and Bliss, N.G. (1992) Developments in Neural Network Applications: The Intelligent Electric Arc Operation. *Iron and Steel Engineer*, **69**(6), 29-32.
- Starley, G.P., Bradshaw, F.W., Carrel, C.S. and Pershing, D.W. (1985) The Influence of Bed-Region Stoichiometry on Nitric Oxide Formation in Fixed-Bed Coal Combustion. *Combustion and Flame*, **59**, 197-211.
- The Open University (1973) *Coal, the Basis of 19th Century Technology*. AST281: Block 2, Unit 4. Bletchley: Open University Press.
- Thurlow, G.G. (1962) The Mechanisation and Automatic Control of Coal Fired Shell Boilers: A Summary of Work Carried Out by the BCURA. *Journal of the Institute of Fuel*, **35**, 516-522.
- Thurlow, G.G. (1962) The Mechanisation and Automatic Control of Coal-Fired Shell Boilers: A Summary of Work Carried Out by the BCURA. *Journal of the Institute of Fuel*, **35**, 516-522.
- Toole-O'Neil, B. (1990) Furnace Sorbent Injection. *Journal of Air and Waste Management*, **40**(12), 1716-1718.
- Venkatasubramanian, V. and Chan, K. (1989) A Neural Network Methodology for Process Fault Diagnosis. *Journal of the American Institute of Chemical Engineers*, **35**(12), 1993-2002.
- Wilcox, S.J., Hawkes, D.L., Hawkes, F.R. and Guwy, A.J. (1995) The Use of a Neural Network to Monitor Anaerobic Digestion with an On-Line Bicarbonate Alkalinity Sensor. *Water Research*, **29**(6), 1465-1470.

- Yoon, Y., Guimaraes, T. and Swales, G. (1994) Integrating Artificial Neural Networks with Rule Based Expert Systems. *Decision Support Systems*, **11**, 497-507.
- Zimmermeyer, G. (1992) Coal as a Primary Energy Source: The Problem of CO₂. *Journal of the Control of Emissions from the Combustion of Coal: New Technologies for Power Generation and Industrial Plant*, 395-416.
- Zurada, J.M. (1992) *Introduction to Artificial Neural Systems*. West Publishing Company.

Appendix A – Fuel Specification for Experiments on the Stoker Test Facility

CRE Group Limited,
Stoke Orchard,
Cheltenham, Gloucestershire,
GL52 4RZ.

Subject: Coal Analysis in Accordance with British Standard
BS1016

Colliery: DAW MILL
Grade: Singles
Size: 31.5 x 12.5 mm
Quarter/E: 26-DEC-1992
Seams: 100% - WARWICKSHIRE THICK
Code: 26080327

As Received Basis	Mean	Min			
Moisture %	9.9	7.2	12.1	0.77	-
Ash %	4.5	3.4	6.0	0.51	0.56
Volatile Matter %	35.1	33.8	35.4	0.44	-
Fixed Carbon %	50.5	-	-	-	-
Sulphur %	1.50	1.35	1.69	0.078	0.086
Chlorine %	0.23	0.22	0.25	0.009	0.010
Calorific Value (KJ/Kg)	28,573	27,662	28,899	314	-
Phosphorus %	0.009	-	-	-	-
Carbon Dioxide %	0.43	-	-	-	-
Mineral Matter %	5.7	-	-	-	-

Coking Properties	
Gray King Coke Type	C
Swelling Index	1.5

Rank	
Reflectance	0.61
Coal Rank Code	802

Ash Fusion Temperature °C (Reducing Atmosphere)	
Initial Def.	1150
Hemisphere	1260
Flow	1400

Colliery: DAW MILL
 Grade: Washed Smalls (IND) 26080635
 Size: < 25.0 mm
 Quarter/E: 26-DEC-1992
 Seams: 100% - WARWICKSHIRE THICK

As Received Basis	Mean	Min			
Moisture %	10.7	7.0	15.4	1.14	-
Ash %	4.9	4.0	5.7	0.32	0.36
Volatile Matter %	34.7	32.3	35.6	0.64	-
Fixed Carbon %	49.7	-	-	-	-
Sulphur %	1.54	1.34	1.66	0.067	0.064
Chlorine %	0.23	0.21	0.26	0.011	0.012
Calorific Value (KJ/Kg)	28,097	26,463	29,003	414	-
Phosphorus %	0.013	-	-	-	-
Carbon Dioxide %	0.52	-	-	-	-
Mineral Matter %	6.1	-	-	-	-

Coking Properties	
Gray King Coke Type	C
Swelling Index	1.5

Rank	
Reflectance	0.61
Coal Rank Code	802

Ash Fusion Temperature °C (Reducing Atmosphere)	
Initial Def.	1230
Hemisphere	1280
Flow	1340

Appendix B – Fuel Specification for the Experiments on the Industrial Stoker Plant

James Proctor Limited,
PO Box 19,
Hammerton Street,
Burnley,
Lancashire,
BB11 1LJ.

3rd December 1998

CERTIFICATE OF ANALYSIS

CERTIFICATE NUMBER 9166/1
SAMPLE REFERENCE 9166/8
SAMPLE DESCRIPTION COAL
DATE RECEIVED 1ST DECMEBER 1998

Report of Analysis:

Test Method Ref.			As Received	Dry-Basis	Dry-Ash- Free
SM001	Moisture	%	10.6	-	-
SM006	Ash Content	%	8.3	9.3	-
SM005	Volatile Matter	%	30.8	34.5	38.0
SM025	Fixed Carbon	%	50.3	56.2	62.0
SM008	Total Sulphur	%	1.32	1.48	1.63

SM012	Gross Calorific Value	Kcal/Kg	6,389	7,146	7,879
SM012	Gross Calorific Value	KJ/Kg	26,748	29,919	32,987
SM012	Gross Calorific Value	Btu/lb	11,499	12,863	14,182
SM026	Net Calorific Value	Kcal/Kg	6122	-	-
SM026	Net Calorific Value	MJ/Kg	25,630	-	-
SM026	Net Calorific Value	Btu/lb	11019	-	-
SM010	Crucible Swelling No.	-	-	1	-

ASH FUSION TEMPERATURES °C (Test Method Ref. SM017)		
	Reducing Atmosphere	Oxidising Atmosphere
ID	1330	-
HT	>1440	-
FT	>1400	-

Commercial Laboratory: Knight Energy Services Limited,
The Sycamores, Scawthorpe Hall, Great North Road,
Scawthorpe, Doncaster, DN5 7UN.

Appendix C – Grate Ash Analysis to BS1016: Part 104 for Loss on Ignition



MINTON, TREHARNE & DAVIES LIMITED

Consulting Scientists, Mariners & Engineers
Analytical & Testing Laboratories

Our ref: CRM/JW/CF06/R
Certificate/Coal No: C03944:001/98

14th April 1998

We hereby certify that we have analysed the undermentioned samples of Boiler Ash in accordance with BS 1016. The samples were received from you on the 16th March 1998 under your Order No: P50585. Samples identified as:

ASH SAMPLES EX CHAIN GRATE STOKER BOILER

AS RECEIVED BASIS

<u>Sample</u>		<u>Ash Content</u>	<u>Moisture</u>
		%	%
300 kw	Uniform Air	55.8	0.9
300 kw	Thinner Bed	57.7	1.4
400 kw	Opt Air	60.9	1.0
400 kw	High Air	69.4	1.4
400 kw	Low Air	43.7	1.1
400 kw	Uniform Air	55.9	1.1
400 kw	Thinner Bed	37.0	1.0
500 kw	Thinner Bed	55.6	1.2
600 kw	Opt Air	59.6	1.0
600 kw	High Air	72.4	1.1
600 kw	with Neural Controller (burning singles)	53.4	29.7

LTD

MINTON, TREHARNE & DAVIES

C.R. MULLINS

For the attention of Mr Alex Chong (Research Assistant)

School of Design & Advanced Technology
Treforest
Pontypridd
Mid Glam
CF37 1DL

Page 1 of 1

PROXIMATE AND FUEL ANALYSIS

Our sample no. Your Sample ref	8372 500KW OPTIMUM AIR	8373 500KW LOW XS AIR	8374 500KW HIGH XS AIR	8375 300KW OPTIMUM AIR
Free moisture %ar	-	-	-	-
Moisture in the air-dried sample % ad	-	-	-	-
Total moisture % ar	-	-	-	-
Moisture in the analysis sample % ad	1.2	1.4	1.2	1.0
Ash content % ad	67.3	43.4	75.5	58.2
Volatile matter % ad	-	-	-	-
Loss on ignition %db	31.9	56.0	23.6	41.2
Fixed carbon % ad	-	-	-	-
Gross Calorific Value kJ/kg ad	-	-	-	-
kJ/kg db	-	-	-	-
kJ/kg daf	-	-	-	-
Ash Fusibility-Oxidising Deformation temp °C	-	-	-	-
Hemisphere	-	-	-	-
Flow	-	-	-	-
Ash Fusibility-Reducing Deformation temp °C	-	-	-	-
Hemisphere	-	-	-	-
Flow	-	-	-	-
Swelling Number	-	-	-	-
Gray-King Coke Type	-	-	-	-

Comments

- indicates analysis not requested

ad = as analysed (air-dry)

ar = as received

db = dry basis

daf = dry, ash-free basis

PROXIMATE AND FUEL ANALYSIS

Our sample no. Your Sample ref	8376 300KW LOW XS AIR	8377 600KW THINNER FIRE BED	8378 500KW UNIFORM AIR
Free moisture %ar	-	-	-
Moisture in the air-dried sample % ad	-	-	-
Total moisture % ar2	-	-	-
Moisture in the analysis sample % ad	1.4	1.0	1.1
Ash content % ad	33.4	48.2	50.3
Volatile matter % ad	-	-	-
Loss on ignition %db	66.2	51.3	49.2
Fixed carbon % ad	-	-	-
Gross Calorific Value kJ/kg ad	-	-	-
kJ/kg db	-	-	-
kJ/kg daf	-	-	-
Ash Fusibility-Oxidising Deformation temp °C	-	-	-
Hemisphere	-	-	-
Flow	-	-	-
Ash Fusibility-Reducing Deformation temp °C	-	-	-
Hemisphere	-	-	-
Flow	-	-	-
Swelling Number	-	-	-
Gray-King Coke Type	-	-	-

Comments

- indicates analysis not requested

ad = as analysed (air-dry)

ar = as received

db = dry basis

daf = dry, ash-free basis

Appendix D – The NNBC MATLAB™ File for the Stoker Test Facility

% NEURAL CONTROLLER PROGRAM FOR THE ON-LINE CONDITION MONITORING & %
CONTROL OF PB29. - Ver7.0 [20:17 05/06/97]

echo on

% Confining current load(cl) & desired load(dl) to 0.3|0.4|0.5|0.6|0.7MW.

cl=0;

while (floor(10*cl)~=10*cl)|(cl>0.7)|(cl<0.3),cl=input('Current load=');end;

dl=0;

while (floor(10*dl)~=10*dl)|(dl>0.7)|(dl<0.3),dl=input('Desired load=');end;

% Reading in the title elements of TCS feedback file

vnm=['SIC163.SETP';'SIC164.SETP';'FIC153.SETP';'FIC154.SETP';...
'FIC155.SETP';'FIC156.SETP'];

% Staging profile of coal & air.

if dl==cl

disp('Requested load is the current operating load')

break, end;

elseif dl>cl % Stepping up on load.

start1=clock;

delta=dl-cl;

cs=table_p(cl); ns=table_p(dl);

oldair=cs(3:6,:); newair=ns(3:6,:);

extrair=newair-oldair;

steps=(delta/0.1)*5; % Allowing 5 sub-steps for each load level.

dummy1=cl;

for k=1:steps

airstg=oldair+((k/steps).*extrair); % Air setting 1,2,3&4.

nl=dummy1; % nl = next load.

nextstg=table_p(nl);

coalstg=nextstg(1:2,:);

if rem(k+1,5)==0

dummy1=nl+0.1;

disp('Next coal feedrate')

end;

TCSstg=[coalstg; airstg];

fid=fopen('c:\PB291\PB29DOWN.RCP','w');

for n=1:6

fprintf(fid,'%20s %3s %10.4f\r\n',...

vnm(n,:), '=', TCSstg(n,:));

end;

fclose(fid);

while etime(clock,start1)<(k*30); end;

disp('Next linear air increment')

end;

```

elseif dl<cl % Stepping down on load.

    delta=cl-dl; steps=delta/0.1;
    cs=table_p(cl);
    start2=clock;
    for k=1:steps % Bringing the fuelfeed down.
        nl=cl-(k*0.1); % Next load.
        ns=table_p(nl); % Next settings.
        coalstg=ns(1:2,:);
        TCSstg=[coalstg; cs(3:6,:)]; % New coal feed rate but -
                                   % maintaining airfeed rate.
        fid=fopen('c:\PB291\PB29DOWN.RCP','w');
        for n=1:6
            fprintf(fid,'%20s %3s %10.4f\r\n',vnm(n,:),...
                    ' ',TCSstg(n,:));
        end;
        fclose(fid);
        while etime(clock,start2)<(k*30); end;
        disp('Next coal feedrate')
    end;

    start3=clock;
    ns=table_p(dl); % New setting.
    oldair=cs(3:6,:); newair=ns(3:6,:);
    deficit=oldair-newair;
    for m=1:(steps*5) % Bringing the air down.
        airstg=oldair-((m/(steps*5)).*deficit); % Next decrement.
        TCSstg=[coalstg; airstg];
        fid=fopen('c:\PB291\PB29DOWN.RCP','w');
        for n=1:6
            fprintf(fid,'%20s %3s %10.4f\r\n',...
                    vnm(n,:), ' ',TCSstg(n,:));
        end;
        fclose(fid);
        while etime(clock,start3)<(m*30); end;
        disp('Next linear air decrement')
    end;
end;

disp('Staging has been completed for the desired load level')
disp('Do you wish to allow time for transient condition?')
disp(' [Yes-Wait & press any key]/ [No-Ctrl C]')
pause

start5=clock;
disp('Combustion monitoring & control network now initiated!')

% Read in the combustion derivatives recorded by the TCS in D drive -
% once every 30 seconds.

figure(1);
readO2=[]; Oxygenr5=[]; Oxygenr6=[];
readA2=[]; readA3=[]; AD2ref=[]; AD3ref=[];
setair_coal=table_p(dl); % Current setting of air&coal to TCS.
dummyair2_3=setair_coal(4:5,:);

```

for k=1:3000 % Dummy cycles.

```
    fid=-1;
    while fid==-1,
        fid=fopen('c:\PB291\PB29UP.RCP');
        pause(1)
    end;

    [fbv,counts]=fscanf(fid,'%s %s %f');
    fclose(fid);
    aor=fbv(10,:); % Actual Oxygen reading.
    ad2_3=fbv(14:15,:); % Air on duct 2 & 3 for plotting purpose.

    if (aor<5)|(aor>6)
        deltaO2=6 - aor; % Comparing the actual O2 with target.
        deltair=correc_p(deltaO2); % Required % air tuning on duct 2&3.
        chgair=(1+(deltair/200)).*dummyair2_3; % Summation joint.
        dummyair2_3=chgair;

        % Maintain current setting but changing air feed on duct 2 & 3.
        TCSstg1=[setair_coal(1:3,:);chgair;setair_coal(6,:)];

% Updating the primary air setting to TCS.
        fid=fopen('c:\PB291\PB29DOWN.RCP','w');
        for i=1:6
            fprintf(fid,'%20s %3s %10.4f\r\n',vnm(i,:),',',...
                    TCSstg1(i,:));
        end;
        fclose(fid);
    end; % End for "if" block.

% Plotting functions for Oxygen & Airflow duct 2&3.
    readO2=[readO2 aor]; Oxygenr5=[Oxygenr5 5]; Oxygenr6=[Oxygenr6 6];

    readA2=[readA2 ad2_3(1,1)]; readA3=[readA3 ad2_3(2,1)];
    AD2ref=[AD2ref setair_coal(4,1)]; AD3ref=[AD3ref setair_coal(5,1)];

    subplot(2,1,1);
    plot(1:k,readO2,1:k,Oxygenr5,'g--',1:k,Oxygenr6,'g--');
    grid on;
    text(5,5,'Lower limit O2=5'); text(5,6,'Upper limit O2=6');
    ylabel('Oxygen in %v');
    title('Actual Oxygen in flue gas on wet basis');

    subplot(2,1,2);
    plot(1:k,readA2,1:k,readA3,'g',1:k,AD2ref,'r--',1:k,AD3ref,'r--');
    grid on;
    text(5,setair_coal(4,1),'Initial setting of AD2');
    text(5,setair_coal(5,1),'Initial setting of AD3');
    xlabel('Elapsed time in multiple of 110 seconds');
    ylabel('Primary air in l/min');
    title('Primary airfeed to main combustion zone - AD2 & 3');
    drawnow;

    while etime(clock,start5)<(k*120); end;
    disp('Next read')
end;
```

Appendix E – The Setting Network MATLAB™

File for Singles and Smalls Grade Coal

```
% SETTING NETWORK FOR COAL FEED & AIR FLOW FOR PB29 [0.3, 0.4, 0.5, 0.6 &  
% 0.7MW] BURNING SINGLES.  
% STANDARD 3-LAYER PERCEPTRON NETWORK WITH BACKPROPAGATION  
% LEARNING ALGORITHM (ADAPTIVE LEARNING RATE & MOMENTUM).  
% Ver. 5.0 [12:01 22/11/96]
```

```
echo on
```

```
% Desired input in kW.  
input = [300 400 500 600 700];  
P = input./700
```

```
% The corresponding setting for coal & air feed rate.
```

```
target =  
[2.15    2.65    3.30    3.90    4.65;  
 6.2     7.6     9.52   11.25   13.41;  
1200    1200    1300    3000    4200;  
4200    5200    6000    7000    7500;  
3200    4200    5000    7000    7500;  
600     800     1000    1500    3500];
```

```
T = [target(1,:)./nnmaxr(target(1,:));  
     target(2,:)./nnmaxr(target(2,:));  
     target(3,:)./nnmaxr(target(3,:));  
     target(4,:)./nnmaxr(target(4,:));  
     target(5,:)./nnmaxr(target(5,:));  
     target(6,:)./nnmaxr(target(6,:))]
```

```
% Assigning the number of neurons for each layer.  
S1=1; S2=30; S3=6;
```

```
% Initialising the W's and b's for the network using the function "INITFF".  
% MAKE SURE THE ARRANGEMENT OF W & b's ARE PROPERLY DONE.  
% But we must feed in a range of min & max values of input data to "INITFF".  
% Prange = [nnminr(P) nnmaxr(P)]  
% [W1,b1,W2,b2,W3,b3] = initff(Prange,S1,'logsig',S2,'logsig',S3,'logsig');
```

```
% Defining the necessary training parameters for TRAINBPX.
```

```
tp1 = 20; % Frequency of progress display  
tp2 = 500; % Maximum number of epochs  
tp3 = 0.001; % Sum square error goal  
tp4 = 0.6; % Initial learning rate  
tp5 = 1.15; % Learning rate increment factor  
tp6 = 0.85; % Learning rate decrement factor  
tp7 = 0.85; % Momentum constant  
tp8 = 1.15; % Maximum error ratio
```

```
tp = [tp1 tp2 tp3 tp4 tp5 tp6 tp7 tp8];
```

```
load c:\matlab\strategy\setting\table_sg.mat
```

```

[W1,b1,W2,b2,W3,b3,te,tr] = trainbpx(W1,b1,'logsig',W2,b2,'logsig',W3,b3,'logsig',P,T,tp);

A3 = simuff(P,W1,b1,'logsig',W2,b2,'logsig',W3,b3,'logsig');

Output = [ A3(1,:).*4.65; A3(2,:).*13.41; A3(3,:).*4000; A3(4,:).*7500; A3(5,:).*7500;
A3(6,:).*3500]

save c:\matlab\strategy\setting\table_sg.mat W1 W2 W3 b1 b2 b3
% PREDICTION FROM THE SINGLES SETTING NETWORK.

function output=table_sg(input)

% COAL & AIR SETTING FROM THE SETTING NETWORK.
Input_scale=0.7; Output_scale=[13.41;4.65;4200;7500;7500;3500];
P=input/Input_scale;

% Retrieve previously trained weights and biases.
load c:\matlab\strategy\setting\table_sg.mat

% Simulation of network output.
a3=simuff(P,W1,b1,'logsig',W2,b2,'logsig',W3,b3,'logsig');

% Multiplying with scalar.
output=[a3(1,:).*Output_scale(1,:);
        a3(2,:).*Output_scale(2,:);
        a3(3,:).*Output_scale(3,:);
        a3(4,:).*Output_scale(4,:);
        a3(5,:).*Output_scale(5,:);
        a3(6,:).*Output_scale(6,:)];
```

```

% SETTING NETWORK FOR COAL FEED & AIR FLOW FOR PB29 [0.3, 0.4, 0.5, 0.6 &
% 0.7MW] BURNING SMALLS.
% STANDARD 3-LAYER PERCEPTRON NETWORK WITH BACKPROPAGATION
% LEARNING ALGORITHM (ADAPTIVE LEARNING RATE & MOMENTUM).
% Ver. 5.0 [12:01 13/01/98]

echo on

% Desired input in kW.
input = [300 400 500 600];
P = input./600

% The corresponding setting for coal & air feed rate.
target =
[0.93    1.18    1.54    1.81    4.65;
6.2     7.6     9.52   11.25   13.41;
1400    1500    1600    2000    4200;
4300    5400    6000    6500    7500;
3300    4400    5000    6000    7500;
900     1000    1200    1700    3500];

T = [target(1,:)./nnmaxr(target(1,:));
     target(2,:)./nnmaxr(target(2,:));
     target(3,:)./nnmaxr(target(3,:));
     target(4,:)./nnmaxr(target(4,:));
     target(5,:)./nnmaxr(target(5,:));
     target(6,:)./nnmaxr(target(6,:))]
```



```

% Assigning the number of neurons for each layer.
S1=1; S2=30; S3=5;
% Initialising the W's and b's for the network using the function "INITFF".
% MAKE SURE THE ARRANGEMENT OF W & b's ARE PROPERLY DONE.
% But we must feed in a range of min & max values of input data to "INITFF".
% Prange = [nnminr(P) nnmaxr(P)]
% [W1,b1,W2,b2,W3,b3] = initff(Prange,S1,'logsig',S2,'logsig',S3,'logsig');

% Defining the necessary training parameters for TRAINBPX.
tp1 = 20; % Frequency of progress display
tp2 = 500; % Maximum number of epochs
tp3 = 0.001; % Sum square error goal
tp4 = 0.6; % Initial learning rate
tp5 = 1.15; % Learning rate increment factor
tp6 = 0.85; % Learning rate decrement factor
tp7 = 0.85; % Momentum constant
tp8 = 1.15; % Maximum error ratio

tp = [tp1 tp2 tp3 tp4 tp5 tp6 tp7 tp8];

load c:\matlab\strategy\setting\table_sm.mat

[W1,b1,W2,b2,W3,b3,te,tr] = trainbpx(W1,b1,'logsig',W2,b2,'logsig',W3,b3,'logsig',P,T,tp);

A3 = simuff(P,W1,b1,'logsig',W2,b2,'logsig',W3,b3,'logsig');

Output = [A3(1,:).*1.81; A3(2,:).*11.25; A3(3,:).*2000; A3(4,:).*6500; A3(5,:).*6000;
A3(6,:).*1700]

save c:\matlab\strategy\setting\table_sm.mat W1 W2 W3 b1 b2 b3
% PREDICTION FROM THE SMALLS SETTING NETWORK.

function output=table_sm(input)

% COAL & AIR SETTING FROM THE SETTING NETWORK.
Input_scale=0.7; Output_scale=[13.41;4.65;4200;7500;7500;3500];
P=input/Input_scale;

% Retrieve previously trained weights and biases.
load c:\matlab\strategy\setting\table_sm.mat

% Simulation of network output.
a3=simuff(P,W1,b1,'logsig',W2,b2,'logsig',W3,b3,'logsig');

% Multiplying with scalar.
output=[a3(1,:).*Output_scale(1,:);
a3(2,:).*Output_scale(2,:);
a3(3,:).*Output_scale(3,:);
a3(4,:).*Output_scale(4,:);
a3(5,:).*Output_scale(5,:);
a3(6,:).*Output_scale(6,:)];

```

Appendix F – The Corrective Network MATLAB™

File

```
% CORRECTIVE NETWORK CONSTRUCTION WITH THREE LAYER FEEDFORWARD
% NETWORK WITH BACKPROPAGATION.LEARNING ALGORITHM
% Ver. 5.0 [14:12 01/06/97]

echo on

% INTRODUCTION
%*****
% The input to the corrective network is only the Oxygen reading by Zirconia analyser, as
% what a human operator would refer if he is running the plant. Corrective action would be to
% fine tune the air flow delivered to air-duct 2 & 3 only, where the main combustion region
% resides. Please note that no alteration will be performed on the grate speed. Hence the
% boiler behaviour is reflected in three sense by it's Oxygen reading, and these are:
% (i) Optimum airflow, between 5 & 6%,
% (ii) Lower excess air level, lower than 4.9%,
% (iii) Higher excess air level, greater than 6.1%.

% NETWORK CONSTRUCTION
%*****
% Training input vectors for the Corrective Network will have to be derived from the Oxygen
% reading from the Zirconia probe in three possible cases:
% (i) "Optimal Airflow" at O2 between 5.0 to 6.0,
% (ii) "Higher Excess" Air at O2 between 6.1 to 9,
% (iii) "Lower Excess Air" at O2 between 4.9 to 2.
% These data will enable the Corrective Network to detect any sub-optimal boiler behaviour
% based on the difference between the desired target oxygen setting with the actual plant
% response. The target is set to 6. Any alterations on air flow will be done only on DUCT 2 &
% 3. Should the Oxygen be at "optimum", no alteration on airflow will be done. If the Oxygen
% is higher than 6, the airflow in duct 2 & 3 will be reduced by 0.5% for every +0.1 difference
% from 6, from it's initial setting. If the Oxygen is lower than 5, the airflow in duct 2 & 3 will be %
% increased by 0.5% for every -0.1 difference from 5, from it's initial setting.

% Hence the error vectors required for training are:
% Note that the 'green band' is between 5 and 6%.
% (i) Optimum = 6 - (5:0.1:6),
% (ii) Higher excess air = 6 - (6.1:0.1:9),
% (iii) Lower excess air = 6 - (4.9:-0.1:2),

% The corresponding target vectors are:
% (i) Optimum = ones(1,11).*0,
% (ii) Higher excess air = (-1:-1:-30)/2,
% (iii) Lower excess air = (1:1:30)/2,

% TRAINING INPUT & TARGET VECTORS
%*****
Popt = 6-[5:0.1:6]; % Which has a size of 1x11.
Plow = 6-[4.9:-0.1:2]; % Which has a size of 1x30.
Phigh = 6-[6.1:0.1:9]; % Which has a size of 1x30.

Ptotal = [Popt Plow Phigh]; % The complete training input data set.

P = [Ptotal(1,:)./nnmaxr(Ptotal)]
```

```

Topt = ones(2,11).*0; % Which has an exact size to Popt, but with 0 target, i.e. no changes to
% be made on the air on duct 2 & 3.

Tlow = [1:30; 1:30]; % Which has the same number of columns or vectors as Plow, with a
% correction rate of +0.5% for every 0.1 difference from 5 on airflow setting on duct 2 & 3.

Thigh = [(-1:-1:-30)/2; (-1:-1:-30)/2]; % As with Tlow, but with a correction rate of -0.5% for
% every 0.1 difference from 6.

Ttotal = [Topt Tlow Thigh]; % The complete training target data set.

T = [Ttotal(1,:)./nnmaxr(Ttotal(1,:)); Ttotal(2,:)./nnmaxr(Ttotal(2,:))]

% Setting of number of nodes for the three layer.
S1=1; S2=25; S3=2;

% Initialising the W's & b's of the network with function "INITFF"
% Prange=[nnminr(P) nnmaxr(P)]
% [W1,b1,W2,b2,W3,b3]=initff(Prange,S1,'tansig',S2,'tansig',S3,'tansig');

load c:\matlab\strategy\correctn\correct2.mat % Retrieving saved matrices.

% PLEASE NOTE THAT WE ARE USING TANSIG FOR EVERY LAYER BECAUSE WE
% HAVE GOT -VE VALUES IN THE TRAINING DATAS.

% ALWAYS REMEMBER TO ENSURE THAT THE ARRANGEMENT OF W AND b'S ARE
% CORRECT APPROPRIATE FOR THE FUNCTION, e.g. INITFF!!

% Training parameters of Trainlm.
TP(1) = 10; %.....freq. of progress display in epochs.....
TP(2) = 40; %.....max no. of epochs to train.....
TP(3) = 0.0001; %.....sum-squared error goal.....
TP(4) = 0.00001; %.....minimum gradient.....
TP(5) = 0.001; %.....initial value for MV.....
TP(6) = 10; %.....multiplier for increasing MV.....
TP(7) = 0.1; %.....multiplier for decreasing MV.....
TP(8) = 1e10; %.....maximum value for MV.....

tp = [ TP(1) TP(2) TP(3) TP(4) TP(5) TP(6) TP(7) TP(8) ];

[W1,b1,W2,b2,W3,b3,te,tr] = trainlm(W1,b1,'tansig',W2,b2,'tansig',W3,b3,'tansig',P,T,tp);

% Calculating the output of trained network.

A3=simuff(P,W1,b1,'tansig',W2,b2,'tansig',W3,b3,'tansig');

output=[A3(1,:).*nnmaxr(Ttotal(1,:)); A3(2,:).*nnmaxr(Ttotal(2,:))];
net_pred=round(output)

save c:\matlab\strategy\correctn\correct2.mat W1 W2 W3 b1 b2 b3

function output=correc_p(input)

% PREDICTION FROM THE CORRECTIVE NETWORK.
Input_scale=4; Output_scale=15;
P=input/Input_scale;

```

```
% Retrieve previously trained weights and biases.  
load c:\matlab\strategy\correctn\correct2.mat  
  
% Simulation of network output.  
a3=simuff(P,W1,b1,'tansig',W2,b2,'tansig',W3,b3,'tansig');  
  
% Multiplying with scalar and round to nearest integer.  
output=round(Output_scale.*a3);
```

Appendix G – The NNBC MATLAB™ File for the Industrial Stoker Plant

% EXTENSION OF BCURA PROJECT B35(1998/1999); GARTH-NEUCON Ver2 [4/May/99]
% In Collaboration with James Proctor Ltd. & HMP Garth.
%

% IMPORTANT NOTE:

% 1. You can use ctrl C to terminate the program without losing any data.
% 2. Make sure you synchronise the clock time on all PCs BEFORE any tests.
% 3. Make sure you change the mat file name before running this M-file!!!!
% 4. The coal feed (coalfeed.demand.) is the firing rate - as it ranges from 0 to 100% (i.e. 2
% volts to 10 volts, same thing with the airflow!!!!)
% 5. Changing the coal and air set point manually via the Open BSI DataView.
% 6. Parameters to be altered are coalfeed.sp. and airflow.sp.
% 7. If the change in PV is greater than 8 degree C, must allow for 25 minutes waiting time
% before the next FOR loop.
% 8. Data logging of the process variable, water temp, firing rate & airflow must be done with
% another Matlab application! Every 30 seconds! Make sure you change the filename too.
% 9. Make sure you switch the RTU to AUTO before running this M-file.
%

% Must create the communication links to RTU and Testo.

% *****

% Create them in the workspace before you run the programme. You can then be sure that
% the channels are actually established. e.g. RTUChan=ddeinit('Excel','filename.xls'); Since
% you cannot create the Comm link directly with RTU, you'll need to use Excel as the
% intermediate. In the Excel file, type in Bsap|Rtu|parametername.ext.' in the cell and it'll be
% updated continuously. The parameters that needs to be read are hotwater.out.,
% coalfeed.demand. & airflow.demand.. Remember that the parameters that you write to are
% coalfeed.sp. & airflow.sp..

% if RTUChan==0, disp('WARNING! RTUComm channel not established!'), end;
% TESTOChan=ddeinit('winwegde','com2'); % Must use comm. port 2.
% if TESTOChan==0, disp('WARNING! TESTOComm channel not established!'), end;
%

% Defining all arbitrary or dummy constants.

% *****

% Parameters for the firing loop.
sethigh=115; %120; % Highlimit of hotwater temp - alterable.
setlow=112; %115; % Lowlimit of hotwater temp.
K_fr=2.5; % 2.5% of MCR per degree celcius difference - firing rate loop.
maxslope=3; minslope=0.4; % The max and min rate of water temp change.
factorinc=1.15; factordec=0.85; % The adjustment on the gain.

% Parameters for the oxygen tuning loop.

% You will need to set the target depending on the load. i.e. You will need to establish the
% load before setting the target O2/CO2 level. Please refer to log book for further details –
% dated 30/4/99.
K_af=2.5; % 2.5% of the initial setting for every 1% difference in oxygen.

```

o2_maxslope=2; o2_minslope=0.25; % The max and min rate of oxygen change.
o2_factorinc=1.15; o2_factordec=0.85; % The adjustment on the gain.
% Parameters for the plotting functions - defining empty matrices.
figure(1);
pvtemp=[]; hightemp=[]; lowtemp=[]; % pv = hot water temp.
oxygen=[]; higho2=[]; lowo2=[]; % Flue gas oxygen reading.
coal=[]; % Coal feed.
air=[]; % Air feed.
%


---



for k=1:100000; % Dummy cycles. Not too many zeros!!
    looptime=clock; % Recording the initial loop time.

    % Requesting data from RTU via Excel.
    % *****
    RTUdata=ddereq(chanRTU,'r1c1:r3c1');
    % hotwater.out., coalfeed.demand. & airflow.demand.
    if RTUdata==[], disp('WARNING! Failure to read from Excel!'), end;
    hotwater=RTUdata(1,1); coalfeed=RTUdata(2,1); airfeed=RTUdata(3,1);
    %
    

---



    % Requesting data from TESTO. - only one element!!! =oxygen.
    % *****
    o2=ddereq(chanTesto,'Field(1)');
    if o2==[], disp('WARNING! Failure to read from Testo!'), end;
    %
    

---



    % Data logging of all parameters.
    % *****
    totaldata(k,:)= [looptime(1,4:6) o2 RTUdata' k]; % Invert RTUdata!!!
    save c:\alexfile\matlab\april99\050599pv.mat totaldata
    %
    

---



    % Setting of the target oxygen band depending on the firing rate.
    % Remember that the coalfeed IS the firing rate.!!!
    % *****
    firerate=round(coalfeed); % Picking up the coalfeed. i.e. the firing rate, as it ranges
    % from 0 to 100%.
    if firerate<=35, o2sethigh=13; o2setlow=11;
    elseif 65>=firerate>=36, o2sethigh=11; o2setlow=9;
    else 100>=firerate>=66, o2sethigh=9; o2setlow=7;
    end;

    % Firing rate control loop.
    % *****
    if hotwater>sethigh, hwerror=sethigh-hotwater; % Note the -ve sign.
        U_fr=K_fr*hwerror; % Reduction on firing rate.
        newcoalfeed=U_fr+coalfeed;
        newairfeed=U_fr+airfeed;
    elseif hotwater<setlow, hwerror=setlow-hotwater;
        U_fr=K_fr*hwerror;
        newcoalfeed=U_fr+coalfeed;
        newairfeed=U_fr+airfeed;
    else sethigh>=hotwater>=setlow;
        U_fr=0; hwerror=0; newcoalfeed=coalfeed; newairfeed=airfeed;
    end;

```

```

% Setting the loop waiting time.
% *****
if abs(hwerror)>8, waiting=1500; else waiting=180; end;
% 25 minutes fo large load changes, and 3 minutes for small ones.

if abs(U_fr)>=3 & newcoalfeed<coalfeed; % Note the -ve sign on U_fr.
    disp('load step DOWN & staging required');
    delta=round(abs(U_fr)); % The required reduction on load.
    steps=round(delta/2.5); % Steps of 2.5% of MCR each decrement.
    for i=1:steps;
        stgseqcoal=clock;
        % Decrease coal feed first.
        % *****
        newcoalfeed=coalfeed-((i/steps)*delta);
        disp('ATTENTION!coalfeed.sp. is ='); disp(newcoalfeed);
        % Allowing time for each decrement.
        while etime(clock,stgseqcoal)<10; end;

        % Decreasing the air.
        % *****
        stgseqair=clock;
        newairfeed=airfeed-((i/steps)*delta);
        disp('ATTENTION!airflow.sp. is ='); disp(newairfeed);
        infotext=[i steps];
        disp(infotext);
        disp('next load DEcrement');
        % Allowing time for each decrement.
        while etime(clock,stgseqair)<15; end;
    end;

elseif abs(U_fr)>=3 & newcoalfeed>coalfeed
    disp('load step UP & staging required');
    delta=round(abs(U_fr)); % The required increase on load.
    steps=round(delta/2.5); % Size of step=2.5% MCR.
    for i=1:steps;
        stgseqstart=clock;
        newcoalfeed=((i/steps)*delta)+coalfeed;
        newairfeed=((i/steps)*delta)+airfeed;
        disp('ATTENTION!coalfeed.sp. is ='); disp(newcoalfeed);
        disp('ATTENTION!airflow.sp. is ='); disp(newairfeed);
        infotext=[i steps];
        disp(infotext);
        disp('next load INcrement');
        % Allowing time for each load increment.
        while etime(clock,stgseqstart)<20; end;
    end;

elseif abs(U_fr)<3 & newcoalfeed<coalfeed,
    disp('load step DOWN & NO staging required');
    disp('ATTENTION!coalfeed.sp. is ='); disp(newcoalfeed);
    disp('ATTENTION!airflow.sp. is ='); disp(newairfeed);
elseif abs(U_fr)<3 & newcoalfeed>coalfeed,
    disp('load step UP & NO staging required');
    disp('ATTENTION!coalfeed.sp. is ='); disp(newcoalfeed);
    disp('ATTENTION!airflow.sp. is ='); disp(newairfeed);
elseif U_fr==0,
    disp('Boiler Load Providing Desired PV Set Point');
end;

```

```

% Gain tuning for the firing rate control loop.
%*****
if k<3|U_fr==0; disp('No gain change required on firing loop');
else slope=totaldata(k,5)-totaldata(k-1,5); % Calculate change in hot water temp.
    if abs(slope)>maxslope,
        newK_fr=K_fr*factordec; K_fr=newK_fr;
        disp('The Firing Rate Loop Gain Has Been DECREASED!!!');
        disp('New Firing Loop Gain is ='); disp(newK_fr);
    else abs(slope)<minslope
        newK_fr=K_fr*factorinc; K_fr=newK_fr;
        disp('The Firing Rate Loop Gain Has Been INCREASED!!!');
        disp('New Firing Loop Gain is ='); disp(newK_fr);
    end;
end;

% Oxygen tuning loop.
%*****
% 'Timer' for the initiation of the oxygen tuning loop.
% Remember the trick of using historical matrix & not using etime, to check the
% waiting period before activating the o2 tuning loop based on the last load change.

if abs(U_fr)<3, status=0; % You can tune the air as long as the load change is very
    % small!!!!!! Take note!!
elseif abs(U_fr)>=3, status=1;
end;

historymtx(k,:)=[k status];
if k<5, disp('Still Waiting for Oxygen Tuning Loop!');
elseif sum(historymtx(k-4:k,2))==0, % Waiting period=15 mins.
    if o2>o2sethigh, o2error=o2sethigh-o2; % Note the -ve sign.
        U_af=correct_p(o2error)*K_af; % Reduction on the air based on the
            % corrective network gain factor.
        newairfeed=U_af+airfeed;
        disp('less air required');
        disp('ATTENTION!OXYGEN TUNING LOOP - airflow.sp. is =');
        disp(newairfeed);
    elseif o2<o2setlow, o2error=o2setlow-o2;
        U_af= correct_p(o2error)*K_af; % Increase on the air.
        newairfeed=U_af+airfeed;
        disp('more air required');
        disp('ATTENTION!OXYGEN TUNING LOOP - airflow.sp. is =');
        disp(newairfeed);
    else o2sethigh>=o2>=o2setlow;
        U_af=0; newairfeed=airfeed;
        disp('OPTIMUM AIR with boiler load achieving set point');
    end;
end;

% Gain tuning for the oxygen control loop – Corrective network gain tuning.
%*****
if k<6|U_af==0, disp('No gain change required on oxygen loop');
else o2_slope=totaldata(k,4)-totaldata(k-1,4);
    if abs(o2_slope)>o2_maxslope
        newK_af=K_af*o2_factordec; K_af=newK_af;
        disp('The Oxygen Loop Gain Has Been DECREASED!!!');
        disp('New Oxygen Loop Gain is ='); disp(newK_af);
    elseif abs(o2_slope)<o2_minslope
        newK_af=K_af*o2_factorinc; K_af=newK_af;

```



```

        disp('The Oxygen Loop Gain Has Been INCREASED!!');
        disp('New Oxygen Loop Gain is ='); disp(newK_af);
    end;
end;

% Logging of Auxillary Information.
% *****
% Gain for the two loops!!
gain(k,:)= [looptime(1,4:6) K_fr K_af k];
save c:\alexfile\matlab\april99\0505gain.mat gain

% PLOTTING FUNCTIONS: TEMP, OXYGEN & COAL/AIR/FIRING RATE vs TIME.
% *****
pvtemp=[pvtemp hotwater]; hightemp=[hightemp sethigh];
lowtemp=[lowtemp setlow];
oxygen=[oxygen o2]; higho2=[higho2 o2sethigh]; lowo2=[lowo2 o2setlow];
coal=[coal newcoalfeed]; air=[air newairfeed];

% Plotting the hot water temp.
subplot(3,1,1)
plot(1:k,pvtemp,1:k,hightemp,'r--',1:k,lowtemp,'g--');
grid on;
%text(1,(setlow-2),'Lower temp limit = 115');
%text(1,(sethigh-2),'Upper temp limit = 120');
ylabel('Temp in Deg C');
%xlabel('Elapsed Time in Multiple of 3 Minutes');
title('PROCESS VARIABLE WITH TIME');

% Plotting the flue gas oxygen content.
subplot(3,1,2)
plot(1:k,oxygen,1:k,higho2,'r--',1:k,lowo2,'g--');
grid on;
%text(6,5,'Lower O2 Limit = 6%'); text(6,7,'Upper O2 Limit = 8%');
ylabel('Flue Gas O2 %Vol');
%xlabel('Elapsed Time in Multiple of 3 Minutes');
title('EXCESS AIR LEVEL WITH TIME');

% Plotting the coal/air/firing rate.
subplot(3,1,3)
plot(1:k,coal,'y:',1:k,air,'r:');
grid on;
text(3,10,'coal/firing rate=yellow'); text(3,20,'air=red');
ylabel('Firerate/Air in %');
xlabel('Elapsed Time in Multiple of 3 Minutes');
title('FIRERATE/AIR WITH TIME');

while etime(clock,looptime)<waiting, end; % Each loop is 3 minutes long.
disp('next FOR loop!!');

end; % End for the FOR loop.

```

Publications

- [1] Chong, Z.S., Wilcox, S.J., Ward, J. and Butt, A. (1996) The Monitoring and Control of Stoker Fired Boiler Plant by Neural Networks. *Proceedings of the 9th International Conference on Condition Monitoring and Diagnostic Engineering Management*, 289-298, 1996.

- [2] Chong, Z.S., Wilcox, S.J., Ward, J. and Butt, A. (1997) The Development of a Neural Network Controller for Chain Grate Stoker Boiler. *Proceedings of the 4th European Conference on Industrial Furnaces and Boilers: Furnace/Boiler Operation and Design*, 1.

THE MONITORING AND CONTROL OF STOKER-FIRED BOILER PLANT BY NEURAL NETWORKS

Z. S. Chong¹, S. Wilcox¹, J. Ward¹ and A. Butt²

¹Department of Mechanical & Manufacturing Engineering,

University of Glamorgan, Pontypridd, CF37 1DL.

Phone: 44-1443-482565, Fax: 44-1443-482231,

E-mail: czsiong@glam.ac.uk, swilcox1@glam.ac.uk

²Coal Technology Development Division (CTDD),

P.O. Box 199, Stoke Orchard, Cheltenham, GL52 4ZG.

ABSTRACT

Combustion processes are extremely difficult to model effectively with traditional techniques. To achieve a good operating efficiency combined with low Nitrogen Oxides (NO_x) emissions, especially during transient conditions requires careful control of the combustion air flow rate at a particular fuel feed rate. This task is better performed by artificial neural networks which show great potential for adaptive control applications and have several advantages including; the capability to learn about arbitrary non-linear mappings, parallel distributed computation and robustness. This paper describes the initial development of a real-time control system, based on neural networks for the control of a 0.75MW_{th} chain grate coal fired boiler located at the Coal Technology Development Division (CTDD), Tewkesbury, UK.

I. INTRODUCTION

A fossil fuel boiler, or furnace, depends on combustion of the fuel in the presence of oxygen to release heat energy. The efficiency of this process and the resulting emission of pollutants are highly influenced by the combustion airflow(s) and the fuel feed-rate [1]. Non-optimal settings of these governing parameters will lead to significantly higher emissions of, for example, NO_x and Carbon Monoxides (CO) and may result in an increase in the unburned fuel, both in the ash and the hot flue gases. Other consequences may be increased slagging and a larger downtime with a consequent

reduction in the working efficiency. Hence, one would expect that by control of these primary parameters, the optimum working conditions for the boiler would be achieved.

The 1990 Environmental Protection Act (EPA 1990) contains new legislation with respect to combustion plant. Particularly for single or multiple boilers, and furnaces, with a total net rated thermal output of 50MW or more. However, the vast majority of chain grate stoker fired boilers and furnaces in the UK are smaller than this, hence their emissions are subject to the Clean Air Acts of 1956 and 1968, the Dark Smoke (permitted periods) Regulations 1958 and the Clean Air (Emissions of Grit and Dust from Furnaces Regulations) 1972, which unlike the EPA 1990 Act, only consider emissions of smoke and grits and not oxides of nitrogen and sulphur. Future European Union legislation will probably include combustion plant of between 1 and 50 MW net thermal input, although no final decision has yet been made.

Generally there are two approaches that could be taken when attempting to meet the legislative requirements and maintain combustion efficiency; physical modification of the boiler and careful control of the boiler. The first of these approaches is made possible via the current advancement in combustion technology. However, in order to physically modify existing plant a substantial capital outlay is required. The second of these approaches is made possible because the most common cause of a boiler not meeting the legislative requirement is that it is not properly controlled. By careful setting of the controllable parameters on a particular boiler installation it should be possible to allow existing boilers to conform to new legislation at minimal cost [2, 3]. Artificial neural networks (ANN) have been successfully implemented to solve a wide range of practical problems involving the identification of dynamic systems and synthesis of non-linear controllers [4, 5]. All these are possible by virtue of their ability to approximate arbitrary non-linear mappings by learning. By exploiting this property, an ANN can be used in model based control, both as the plant model and also the controller. This paper describes means of developing a controller, that will be able to deliver optimal control settings and tune itself to a particular installation via the use of neural networks.

II. STOKER TEST FACILITY AND CONTROL PROBLEM

A brief description of the 0.75MW_{th} chain grate stoker fired test facility installed at the Coal Technology Development Division (CTDD), Stoke Orchard, Cheltenham, is given in this section. A diagram of the stoker boiler is shown in Figure 1 to further illustrate the test facility. The moving grate carries coal into the combustion chamber or furnace, and the burnt ash and clinker are discharged at the far end. To maintain ignition a refractory arch is installed to radiate heat to the top of the coal bed as it enters the chamber. The principal features of the boiler test facility are a furnace tube fitted with water cooled calorimetric sections, a water cooled reversal chamber and a smoke tube heat exchanger. The stoker was designed as a scaled down version of a commercially available chain grate and can be operated at combustion intensities of up to 1.4 MW/m² which is representative of those found on larger stokers of this type. The coal supply onto the moving grate is controlled using a metered rotary valve, which also acts as a fire break to prevent burn-back. Hot ash and unburned coal is discharged off the end of the grate. The combustion air is supplied in a plenum chamber consisting of eight individual compartments so that the air distribution profile along the length of the fire-bed can be changed to meet the requirements of different coals. The hot gases produced during combustion are cooled by passage through a smoke tube heat exchanger and eventually cleaned by a series of high efficiency cyclones before being discharged into the atmosphere.

The main objective of the work was to investigate the possibility of developing a controller that is able to maintain the production of NO_x at acceptable levels whilst ensuring maximum combustion efficiency. The task of the controller can be defined as, providing the optimum setting of the fuel feed rate and a corresponding flow-rate of combustion air for a particular load. It is common practice for plant operators to provide high levels of excess air to ensure virtually complete combustion, although this can have an adverse effect on efficiency and NO_x formation. A reduction of NO_x emission levels can be achieved by optimising the amount of excess air for combustion. This can reduce both fuel and thermal NO_x formation and may have the added benefit of increasing the boiler thermal efficiency, provided that there is no significant increase in unburned fuel loss. Finally, refractory arch temperature needs to

be monitored to ensure a correct and stable ignition plane to help maintain a good combustion efficiency.

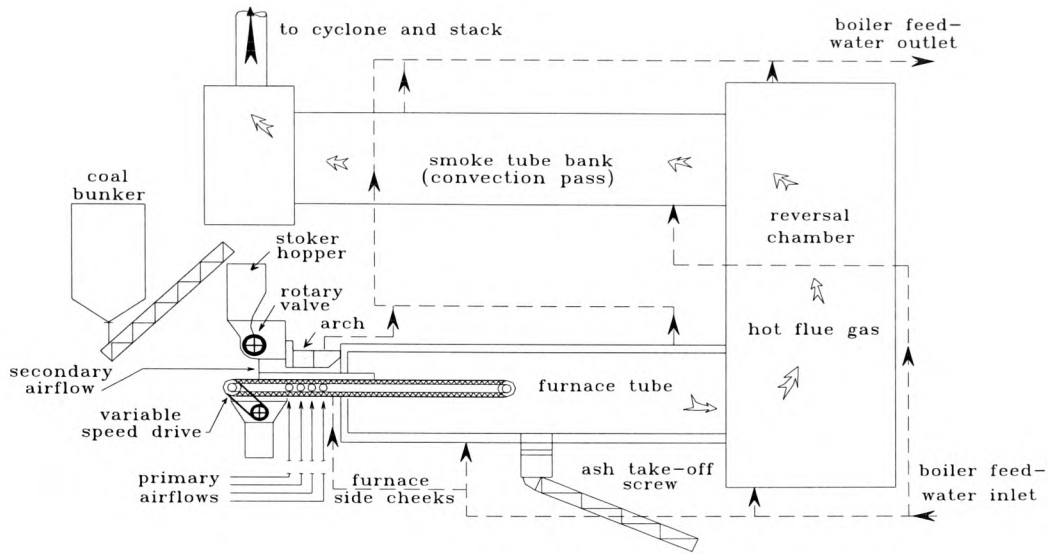


Figure 1: Section View of Chain Grate Coal-Fired Stoker Boiler

III. TRAINING AND TESTING DATA

All the data used in the training and testing of the neural networks were gathered from a series of systematic tests carried out on this 0.75MW_{th} coal fired stoker boiler at CTDD, Stoke Orchard, Cheltenham, UK. The plant was operated at under ‘best practice’ conditions based on operator experience and satisfactory boiler performance was seen throughout the entire duration of the tests. There are 6 controllable input parameters; a) Grate speed (cm/min), b) Rotary valve speed (RPM), c) Primary air flow duct 1 (l/min), d) Primary air flow duct 2 (l/min), e) Primary air flow duct 3 (l/min), f) Primary air flow duct 4 (l/min)

We have also identified 6 major derivatives of combustion that must be measured as a mean of characterising boiler performance. These measured outputs are; a) NO_x emissions (ppm), b) CO emissions (ppm), c) % of Oxygen (O₂) in the dry flue gas, d) Flue gas temperature in the reversal chamber (°C), e) Flue gas temperature in the stack (°C), f) Refractory arch temperature (°C).

1100 data points were gathered from the test run, and the boiler was operated with thermal input from 0.3MW to 0.7MW and back to 0.3MW in 0.1MW step increments. The first half (0.3MW to 0.7MW) of this data was used to train both the plant neural model and the neural controller, with the second half (0.7MW to 0.3MW) being used to test the neural networks.

IV. NEURAL NETWORK PLANT MODEL

A standard three layer feed-forward neural network was developed for the purpose of modelling the relationship between the six controllable input parameters and the six measured plant outputs. The architecture of this network consists of one hidden layer sandwiched between the input and output layer. The building block of these neural networks are simple non-linear processing elements which are essentially, a simplistic model of neurons in a biological brain. These elements are highly interconnected via weighted links. The non-linearity of these artificial neurons arises from a sigmoidal activation function. The output of every artificial neuron is a sigmoid function of the sum of each input to the neuron, multiplied by its weight. The output is scaled to be in the range of 0 to 1. This value determines the activation state of the artificial neuron. By trial and error, the number of artificial neurons for the hidden layer was found to be 30. It appeared that the average learning error increased if the number of hidden neurons was reduced. The learning algorithm adopted for the purpose of training the network was back-propagation with adaptive learning rate and momentum [6]. The best average network error achieved was 0.024 after 1000 training iterations with the first 510 input and output pairs of data described earlier and this error appeared to be the global minimum.

V. NEURAL NETWORK CONTROLLER

The whole idea of a neural network controller design is basically to encapsulate the knowledge of the human operators, and function by trying to mimic the 'teacher'. The basic structure for the neural controller is similar to the neural model, where a standard three layer feed-forward neural network is used. We have employed 15 hidden neurons for this network and applied the same learning algorithm as previously described for the neural model. The only input variable to the controller is the desired

input thermal power (in kW) to the plant. The output elements of the neural controller correspond to all the input elements to the neural model. The resulting average error of the network was found to be 0.0145 after 1000 learning iterations and this appeared to be the global minimum for the network arrangement described. The next section will examine the accuracy of both the developed neural controller and model of the plant when compared to unseen data.

VI. STATIC SIMULATION RESULTS AND DISCUSSIONS

The test data were gathered by operating the boiler between 0.7MW and 0.3MW in 0.1MW steps, as described in Section III.

a) Neural Plant Model

Figures 2(a) and 2(b) compare the outputs from the neural network model against the combustion parameters actually recorded on the boiler. Figure 2(a) illustrates this comparison for NO_x, CO and O₂. It can be seen that the predictions for O₂ are very accurate, whereas those for NO_x and CO are less good, although the neural network correctly follows the trends in both the NO_x and CO levels as the load drops. The maximum error for NO_x is approximately 25% and that of CO, 40% with the mean errors being approximately half of these figures. Although this error is quite large, the CO emission levels for this test facility are very small and will have very little effect on the overall efficiency of the plant. However it is hoped that further training with data collected from more experimental work will help to improve the accuracy of the model.

Figure 2(b) illustrates the differences between the model predictions and the actual flue gas temperatures at the stack inlet and reversal chamber as well as the refractory arch temperature. Again there are errors in the estimation but with a similar prediction of the trends following load changes, apart from the arch temperature prediction for the last step down in load (0.4MW to 0.3MW) where the neural network estimates failed to predict a temperature drop. Despite the coarseness of these results it is expected that this work can be carried forward, with some refinement, to the stage where an optimising controller can be tested on the boiler.

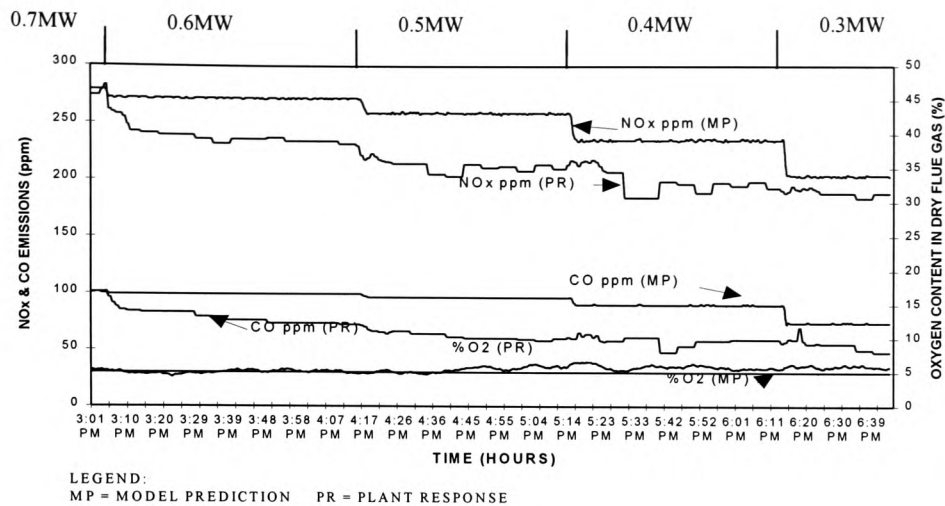


Figure 2(a): Plant Response vs. Model Prediction for Gaseous Emission

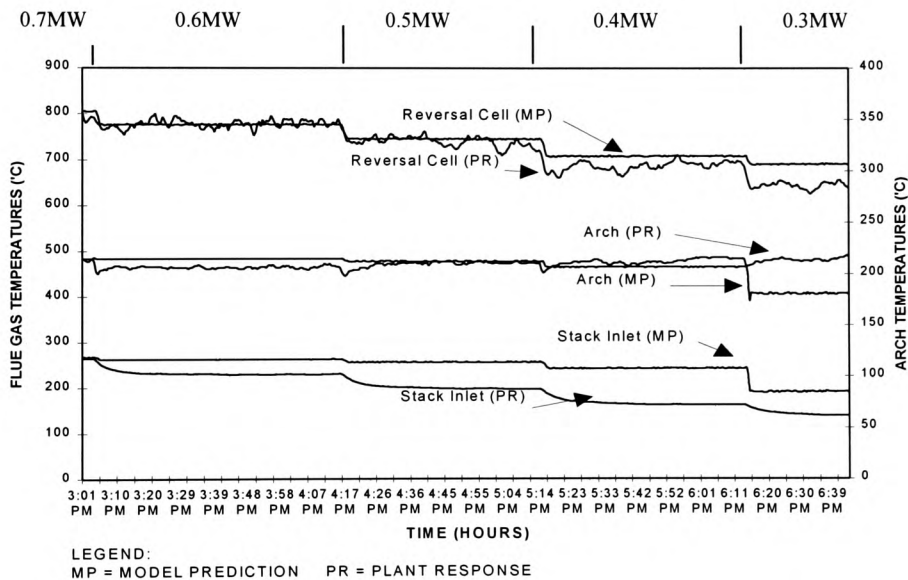


Figure 2(b): Plant Response vs. Model Prediction for Flue Gas & Arch Temperatures

b) Neural Controller

Figures 3(a) and 3(b) illustrate the differences between the settings based on the operators 'best practice' and those estimated by the neural controller. As shown in these figures, the neural controller performs with reasonable accuracy, particularly for the higher boiler loading where the discrepancy is very small. The neural controller is essentially performing the task of looking up the correct values for fuel and air at a

particular load demand as an open loop controller. As the sequence of test loading (full load to turndown) are similar to those used during training, it is not surprising that the network performs well. A scheme whereby any errors that do occur can be further justified will be presented in the next section.

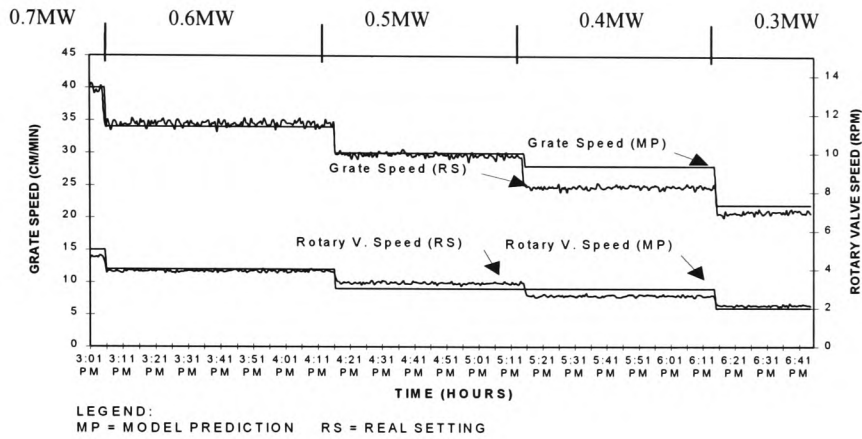


Figure 3(a): Human Operator vs. Controller Settings for Fuel Feed Rate

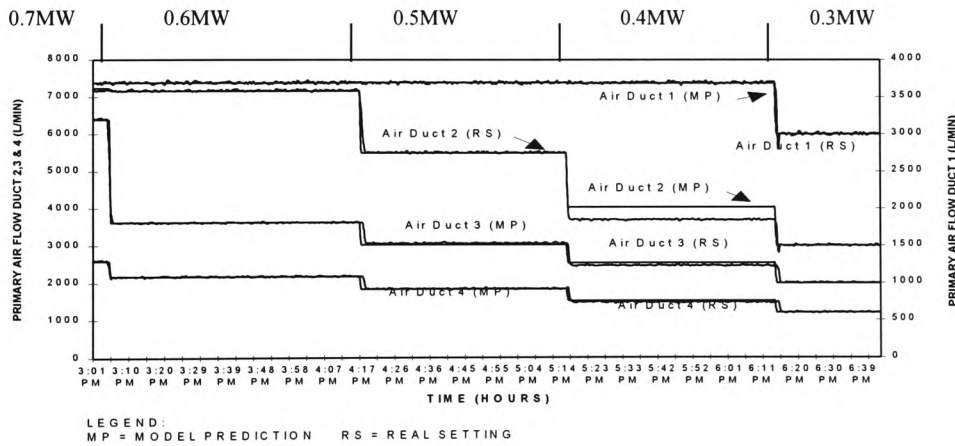


Figure 3(b): Human Operator vs. Controller Settings for Air Flow Rate

VII. OVERALL NEURAL CONTROL STRATEGY

Simple open-loop control of the plant would utilise the trained neural controller to estimate settings for the coal and primary air flow rate to the boiler. Assuming that the boiler was operating at a constant load then this would probably be adequate. If,

however the boiler is operating in a 'load following' manner, a more suitable control structure for on-line process monitoring and control can be obtained by incorporating both the reference model and the neural controller within a closed-loop system. The desired performance of this system is specified through a stable reference neural model and the control system then attempts to ensure that the actual plant output matches the reference model output asymptotically. In this structure the error signal is used to tune the neural controller. This tuning procedure will force the controller to make fine adjustments to the actuator signals (fuel feed rate and combustion air flows), in the sense defined by the reference model. Such a control strategy is currently being developed and will be tested shortly.

VIII. CONCLUSIONS

In this paper, two feed-forward neural networks have been developed for the identification and control of a chain grate coal fired stoker boiler. Both a neural model of the plant and a neural controller have been successfully trained with plant data. The static simulation results demonstrate that both the model and the controller were able to identify the underlying plant dynamics with sufficient accuracy. This model could be used as an off-line advisor to the plant operator. The neural model reference adaptive control strategy presented in this paper should lead to a more robust controller, with both the neural model and controller being combined to provide a novel approach to the control of coal fired boilers under transient, load following conditions.

IX. ACKNOWLEDGEMENT

The authors would like to acknowledge financial support from the British Coal Utilisation Research Association (BCURA) and Energy Technology Support Unit (ETSU) on behalf of DTI. In addition, the assistance from the staff of Coal Technology Development Division in obtaining experimental results was invaluable.

X. REFERENCES

1. Clarke, A.G. and Williams, A., "The Formation and Control of NO_x Emissions", *Chem Ind UK*, Vol.24, pp.917-920, 1991.
2. Livingston, W. R., Birch, M. C. and Chakraborty, R. K., "The Control of NO_x Emissions from Stoker-Fired Boilers", *Proceedings of Second International Conference on Combustion & Emissions Control: Institute of Energy*, pp. 273-283, Dec. 1995.
3. Reinschmidt, K. F. and Ling, B., "Neural Networks with Multiple-State Neurons for Nitrogen Oxide (NO_x) Emissions Modelling and Advisory Control", *Proceedings of IEEE International Conference on Neural Networks: IEEE World Congress on Computational Intelligence*, Vol.6, pp.3834-9, 1994.
4. Narendra, S. and Parthasarathy, K., "Identification and Control of Dynamical Systems Using Neural Networks", *IEEE Transactions on Neural Networks*, Vol.1, No.1, pp.4-27, March 1990.
5. Ribeiro, B., Dourado, A. and Costa, E., "A Neural Network Based Control of a Simulated Industrial Lime Kiln", *Proceedings of International Joint Conference on Neural Networks*, Vol.2, Part.2, pp.2037-40, 1993.
6. Rumelhart, D. E., Hinton, G. E. and Williams, R. J. *Learning Internal Representation by Error Propagation, In Parallel Distributed Processing, 1&2*, MIT Press: Cambridge, MA, USA, 1986.

THE DEVELOPMENT OF A NEURAL NETWORK CONTROLLER FOR CHAIN GRATE STOKER BOILER

Z. S. Chong¹, S. J. Wilcox¹, J. Ward¹ and A. Butt²

¹Department of Mechanical & Manufacturing Engineering,

University of Glamorgan, Pontypridd, CF37 1DL.

Phone: 44-1443-482565, Fax: 44-1443-482231,

E-mail: czsiong@glam.ac.uk, swilcox1@glam.ac.uk

²Coal Technology Development Division (CTDD),

P.O. Box 199, Stoke Orchard, Cheltenham, GL52 4ZG.

ABSTRACT

The development of an integrated on-line condition monitoring and control system for coal fired boiler plant has the potential to maintain longer periods of optimum boiler operation whilst keeping pollutant emissions such as Nitrogen Oxides (NO_x) to acceptable levels. Such effort can also reduce plant down time and improve plant response by regulating a better air/fuel ratio particularly during transient load following conditions which help to prevent fouling and slag formation. This paper describes some of the work undertaken to develop such a symbient system via the use of artificial neural networks for the purpose of on-line monitoring and control of a 0.75MW_{th} chain grate stoker boiler plant located at Coal Technology Development Division (CTDD), at Stoke Orchard, Cheltenham, UK.

KEYWORDS

Neural network modelling; condition monitoring; multivariable non-linear feedback control; chain grate stoker boiler; NO_x emission.

1. INTRODUCTION

Boilers were mostly coal-fired until the 1950's when oil became an affordable alternative. Despite their relatively old technology the essential principles of these coal fired appliances remains the same and is still widely used in many industries, hospitals and schools throughout the UK for hot water and steam. Although new methods of coal firing technique have been developed over the years such as pulverised coal firing and fluidised bed combustion, there is a strong indication that small and medium size conventional coal firing appliances will persist for some time to come.

An important global issue that has received much attention over the past few decades is the effect of greenhouse gases, and with respect to fossil fuel combustion plants in particular, refers to Oxides of Nitrogen and Sulphur [1]. Therefore, increasing pressure has been placed on combustion engineers to develop methods that are able to quantify and enhance the performance of industrial boilers. In particular, the needs to comply with more stringent environmental requirements, by lowering the Nitrogen Oxides emission without having to sacrifice production. Currently the 1990 Environmental Protection Act (EPA 1990) only deals with single or multiple boilers and furnaces with an aggregated total net rated thermal input of 50MW or more, although a related part of the act deals with individual boilers and furnaces of 20 to 50MW net thermal input. However, the European Union is moving towards including small combustion plants of 1 to 50MW thermal input in it's directive, but no final decision has yet been reached.

The work presented in this paper is geared towards improving the combustion efficiency of industrial scale chain grate stoker boilers and also as a step forward in meeting more stringent legislation that could be imposed on them in the near future. The main objective of this research project was to investigate the possibility of developing a controller that is able to maintain the production of NO_x to acceptable levels whilst ensuring maximum combustion efficiency on a $0.75\text{MW}_{\text{th}}$ coal-fired chain grate stoker boiler test facility. Combustion processes exhibit non-linear behaviour and are often difficult to model effectively from a control perspective. Artificial neural networks have been shown to be a very promising technique to overcome this problem by building good models from measured parameters. If a neural network model of a system is available different approaches are then possible when

designing the structure of a control system. One of the many suitable non-linear control schemes is the reference model control structure, which has been adopted and tailored for the purpose of developing the controller for the stoker test facility [2, 3].

2. CHAIN GRATE STOKER & EXPERIMENTAL TEST RUNS

The stoker was designed as a scaled down version of a commercially available chain grate and can be operated at combustion intensities of up to 1.4 MW/m^2 which is common to those found on larger chain grate stokers. Coal is gravity fed onto the chain grate from a mini hopper, the depth of coal is controlled by a rotary valve that also acts as a firebreak system that eliminates the risk of burn-back. The stoker plenum chamber consists of eight individual compartments in total with air being supplied to each of them individually. This enables the air distribution along the length of the fire bed to be altered in order to regulate the position of the ignition plane. As with underfeed combustion, coal is fed beneath an ignited fuel bed and the ignition is maintained by a refractory arch that radiates heat to the top of the coal bed as it enters the furnace tube. The ignition plane travels downward through the bed, reaching the grate at approximately half of its total length. Residual ash is deposited at the rear end of the grate and transported to an ash collection bin situated outside the plant house via a screw feeder. In operation, the ash produced during combustion forms an insulating layer of inert material that protects the downstream part of the grate from the high temperatures prevailing in the furnace tube.

Low ash Dawmill singles grade coal was used to fire the boiler for all the test runs. The speed of the travelling grate was calibrated to that of the rotary valve so as to provide an even bed height of approximately 150mm on the grate. The main parameter regulated being the primary combustion air flow, since this controlled the rate of combustion. It is essential to obtain a correct distribution pattern of the air flow to obtain near optimum combustion rate. A typical arrangement of the primary air flow distribution profile on the grate is as follows:

Table 1: Primary Air Flow Distribution Profile Along the Fire Bed

Plenum Section	Function
1st (front)	The air flow rate to the front section of the plenum chamber is to maintain a desirable ignition plane.
2nd (middle)	To provide sufficient air to burn off the distilled volatiles and residual char.
3rd (middle)	To provide sufficient air to burn off the distilled volatiles and residual char.
4th (rear)	To ensure complete burn out of the remaining char and to provide cooling air to the rear end of the grate.

When the load decreases, initially there can be a deficiency in air flow due to a relatively high combustion intensity on the grate that could lead to smoke emissions. Hence on decreasing load, the coal feed should lead the air flow rates and on increasing load, the air flow rates should lead the coal feed [4]. Even so, these parameters must be properly controlled to ensure a stable ignition plane and to minimise CO emissions particularly when operating the boiler from turn down to full load and vice versa in a single step.

Therefore the main task of the proposed neural network controller would be to regulate the amount of air flow that is required for a particular coal feed for a near optimum combustion rate whilst keeping the NO_x emissions to an acceptable level. It is common practice for plant operators to provide as much excess air as possible to completely burn off the coal. This will inevitably give rise to a higher level of NO_x production due to a higher level of oxygen concentration in the furnace tube. Using the minimum amount of excess air consistent with satisfactory coal burn out will help to minimise NO_x formation [1]. A systematic series of experiments has been conducted to investigate for a “near optimum” air flow profile attainable for each loading stage. The boiler was operated at this “near optimum” air flow and also variation from the optimum level in order to gather information on the boiler operating at sub-optimum conditions. Gathered data were used to teach the individual neural network components off-line, to detect any undesirable boiler behaviour and based on past learning experience, decides on remedy action.

Experimental tests were conducted with the objective of investigating boiler behaviour during transient and steady state conditions with the latter investigating the effect of variations in the excess air level. Knowledge of the flame front movement during transient conditions is essential to ensure correct distribution of air/coal ratio to maintain a stable ignition plane and also acceptable NO_x emissions, particularly when the boiler is operated from turn down to full load and vice versa. The controllable input parameters are the coal feed and the primary combustion air flow rates. Combustion derivatives were continuously monitored throughout the entire duration of the test runs, these being NO_x emissions (ppm), CO emissions (ppm), Oxygen contents in the wet flue gas in percentage and a series of refractory arch temperatures (°C). We would like to point out that an optimum air flow distribution regime has been established for every coal feed-rate in the steady-state operation at optimum air flows, which in effect, is staging the primary combustion air along the fire bed hence providing a means to reduce NO_x emissions. Throughout the entire test run, the amount of NO_x recorded were observed to be within limits whilst satisfying other constraints such as attaining good coal burn out and acceptable CO emissions.

2.1 Steady-state Operations at Optimum, Low & High Level of Excess Air Following Gradual Load Changes.

The boiler was operated from low load at 0.3MW to full load at 0.6MW in 0.1MW step increments and back in three operating conditions. These conditions were at optimum primary air flow and varying the total primary air flow by $\pm 10\%$ for every coal feed rate. The gathered information was then used to train two individual neural network components of the overall control strategy. As such, the knowledge of both the human operator and the past boiler behaviour was encoded in the networks for the purpose of delivering a near optimum setting of the air flow distribution for the load required and also performing the task of fine tuning the air flows for an optimal combustion rate.

2.2 Transient Operation Following A Step Change in Load

The objective of these experiments was to determine the fastest and most stable way to operate the boiler in load following conditions without excessive movement of the ignition plane and the maintenance of acceptable NO_x and CO emissions. Hence it was aimed at providing information of boiler behaviour following abrupt load changes particularly from low load to full load and vice versa by manipulating the coal feed and primary air flow rate. As mentioned in the earlier section, one of the key problems with boiler operation is to maintain a stable ignition plane, particularly in situations where the load demand varies greatly requiring a fast plant response. However further work is still required to establish the actual movement of the flame front with the rate of change of arch temperature readings. This correlation can be found by studying the displacement of the flame front on the point of load change, which we have recorded with a CCD camera during these experiments and determining the rate of arch temperature changes in order to establish the absolute stability of the ignition plane.

3. TEST RESULTS & DISCUSSIONS

3.1 Steady-state Operations at Optimum, Low & High Level of Excess Air Following Gradual Load Changes.

The correct air/fuel stoichiometric ratio of the stoker boiler throughout the entire firing range can be referred to the O₂ content in the flue gas that was maintained to between 5 and 7% for optimum combustion rate. As expected the O₂ level remained mostly within the desired band following gradual load changes at near optimum air flow distribution as shown in Figure 1. The NO_x emissions trend shown in Figure 2 was very similar to the O₂ profile following the load changes. This is due to the fact that both fuel and thermal NO_x, which are the two major constituents of NO_x formation for coal fired boilers are influenced by the amount of excess air available. Since the stoker boiler is inherently a low NO_x burner, the average NO_x emission level for this experiment was approximately 120ppm. As for CO emissions, the average level was 50ppm following gradual load changes at optimum air flow distribution which is highly acceptable. However, deficit in primary air flow distribution had resulted in

excessive CO emissions level in Figure 3, with peaks of up to 6000ppm in the first few load stages when the total primary air was reduced by 20%. This is highly undesirable for safe boiler operation and hence the total air flow was reduced to 10% instead, for the remaining load stages.

This also resulted with the O₂ reading risen to a more appropriate level of between 3 and 5%. Average CO level for this test run following gradual load changes with 10% reduction of total air flow from the optimum is approximately 60ppm. Therefore with a 10% reduction on total primary combustion air flow the average CO emission was increased by 20% from those attainable at optimum conditions. However this reduction on total air flow does not seem to have significant effect on the average NO_x production which is 110ppm. Finally for the case of higher excess air level with 10% increase in total primary air, a higher O₂ trend of between 7 to 9% can be seen in Figure 1. An increase in excess air flow will indefinitely results in lower CO emissions and on this test run, the average CO level was 30ppm which is 60% lower than those attainable at near optimum air flow. Due to this 10% increase in the total primary air flow for combustion, the average NO_x level was brought up to 137ppm which is 13% increment from the optimum.

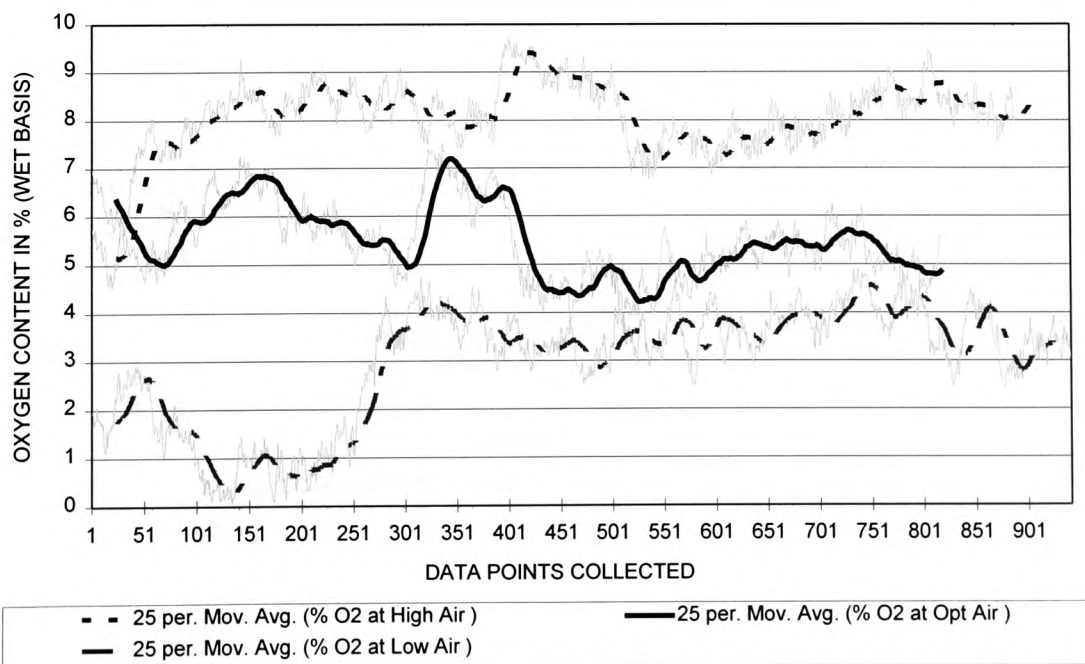


Figure 1: Oxygen Content in Flue Gas on Wet Basis for Optimum, Low & High Level of Excess Air Following Gradual Load Changes

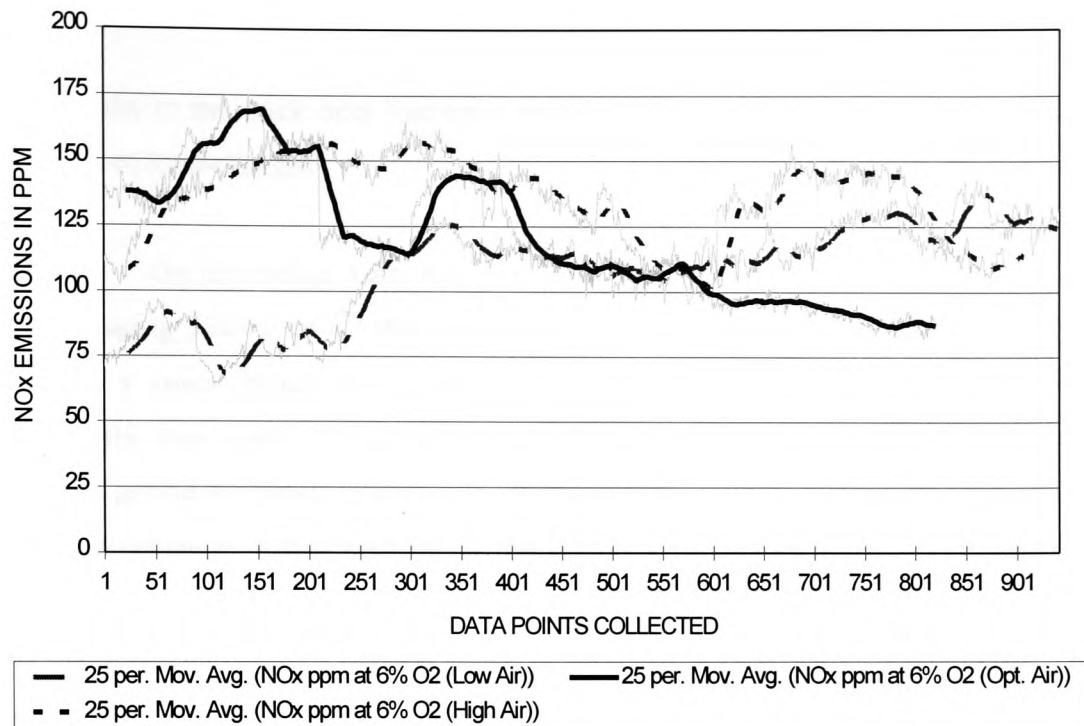


Figure 2: NO_x Emissions at Optimum, Low & High Level of Excess Air Following Gradual Load Changes

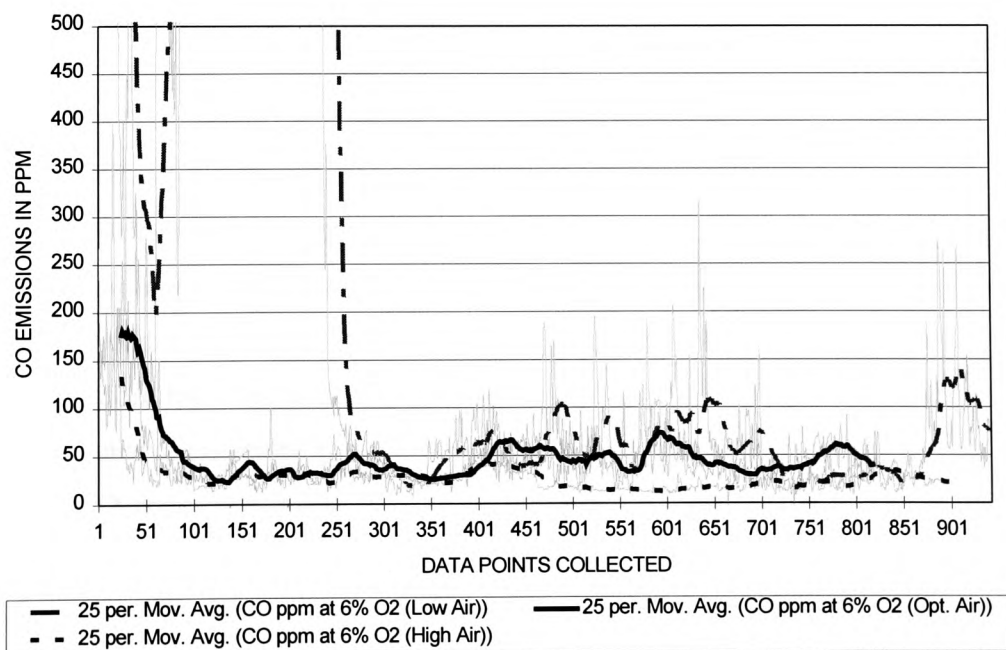


Figure 3: CO Emissions at Optimum, Low & High Level of Excess Air Following Gradual Load Changes

3.2 Transient Operation Following A Step Change in Load

Please refer to the stack inlet flue gas temperature in Figure 4 and 5 as indication on the point of load changes.

Profile 1 - On increasing load, the coal leads the primary combustion air with the whole staging process in 0.1MW steps being completed in 5 minutes. Since the coal feed has a much longer time constant than the primary combustion air flow rates, leading the coal first did not have much effect on the CO emissions during the transient period as shown in Figure 4. The high values of CO before the load change are due to changes in the depth of the fire bed as a result from a previous experiment that was conducted with a thinner bed. However a much different scenario on transient CO emissions can be seen on load decrease with the coal lagging the primary air. This is due to a higher combustion intensity initially prevailing in the furnace tube on decreasing load, where there is a sudden deficit of air flow that resulted in a much higher emission of CO with a peak of 700ppm. A sudden plunge in the O₂ trend from the point of load decrease to 3.5% can also be seen, before gradually creeping up as the combustion intensity moves towards 0.3MW.

Profile 2 - With an understanding of the relationship between coal feed and the required air flow rates in the staging process, the aim of this test run is to demonstrate a desirable transient performance of the boiler following large step changes in load. Therefore on increasing load, primary air flow leads the coal feed and vice versa on decreasing load with the aim of providing a higher combustion intensity initially on the fire bed, before the coal feed is stepped up or down. Again the whole staging process took 5 minutes to complete in 0.1MW steps on both coal and air flow. As expected, the transient CO emissions is less than in profile 1 in both load increase and decrease as shown in Figure 5. This can also be reflected in the O₂ trend, where at load increase the O₂ level climbed to 11% that resulted in a steep descent in the CO profile during transient condition which span over a period of 30 minutes before falling into the optimal range of between 5 to 7%. A relatively less fluctuation in the O₂ readings is observed in the transient period of load decrease that can be attributed to a more intense fire bed on high load with the coal feed leading the air flow.

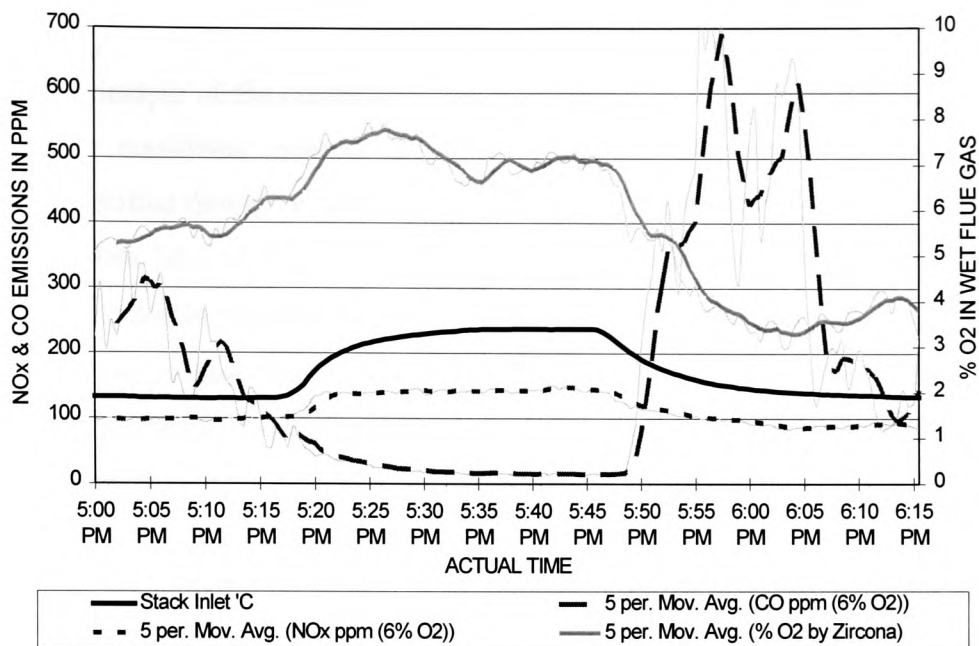


Figure 4: NO_x, CO & O₂ Following A Step Load Change from 0.3 to 0.6MW & Back with Profile 1 - (Undesirable)

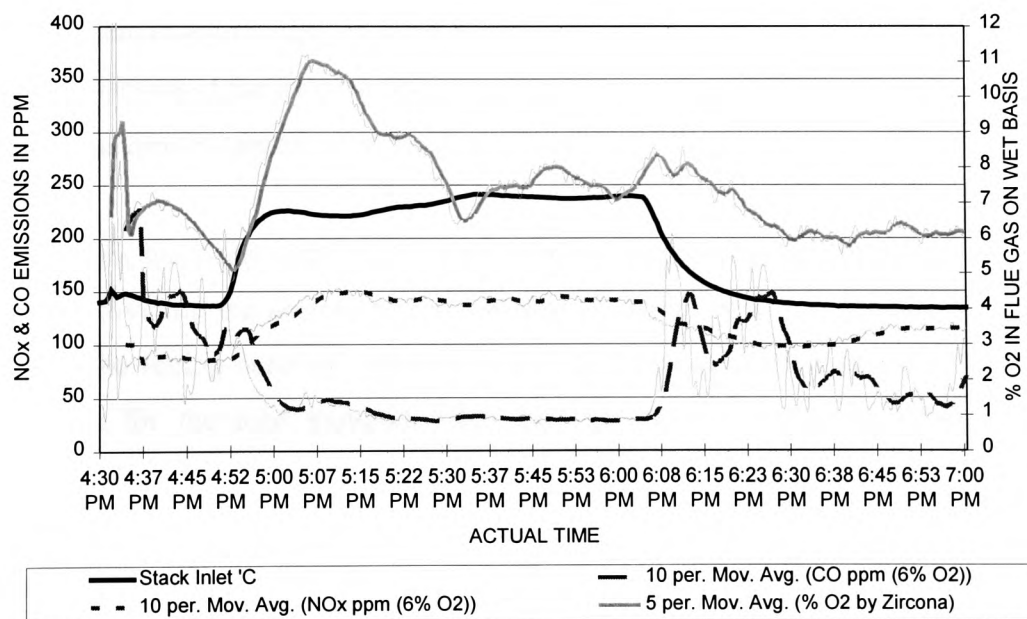


Figure 5: NO_x, CO & O₂ Following A Step Load Change from 0.3 to 0.6MW & Back with Profile 2 - (Desirable)

4. DEVELOPMENT OF NEURAL CONTROLLER STRATEGY

The basic principle of the controller strategy is based on the reference model control structure for non-linear systems [2]. The desired performance of the closed-loop system is specified through a reference model, which is defined by its input-output pair of training data $[r(t), y^r(t)]$. This control scheme attempts to make the actual plant output, $y^p(t)$ to match the reference model output asymptotically, i.e. $\lim_{t \rightarrow \infty} \|y^r(t) - y^p(t)\| \leq \epsilon$ for some specified constant $\epsilon \geq 0$. The primary objective of the neural controller is to ensure a stable ignition plane, before performing the task of fine-tuning the primary air flow rates delivered for a particular coal feed in order to achieve a near optimum combustion rate. Such effort will not only results in a better coal burnout, but also ensures a low emission profile of CO and NO_x during both transient and steady-state operations. With this in mind, the design of the neural controller must seek to satisfy four major constraints on the combustion derivatives of a chain grate stoker-boiler, and these are:

- Minimising movement of the ignition plane
- O₂ content in the flue gas on a wet basis
- CO emissions of the exhaust flue gas
- Grate surface temperature on the stoker front

Earlier work has been carried out to develop the neural reference plant model that is literally providing the desired target response of the boiler at steady-state operations and also the setting network, which provides the necessary coal feed and primary air flow rates for the load required. Both networks were constructed off-line, using gathered test data to train standard three layer feed-forward neural networks with back-propagation algorithm. After training both network outputs were found to be within the desired error goal and when presented with new test data, the trained networks were able to deliver accurate predictions for the load required [5]. The developed setting network will be coupled with a small computer program in order to deliver the optimum staging profile of air/coal for satisfactory transient and steady-state operating conditions. The bench mark of the network is set to achieve the lowest possible NO_x emissions in light of other constraints for the stoker plant under study.

4.1 Corrective Network Construction

The input to the corrective network is the O₂ reading in the flue gas from the Zirconia analyser, and this network functions by mimicking the action of the human operator at steady-state boiler operation. Therefore the corrective action is to fine tune the primary air flow delivered to the two middle sections of the stoker plenum, where the main combustion zone resides on the fire bed for optimum combustion rate. From the test results described in section 3.1, the combustion characteristics of the stoker boiler can be reflected by the O₂ reading in three sense, and these are;

Table 2: Deviation in Total Primary Air Flow Rates with Range of O₂ Readings

Total Primary Air Flow Rates	Range of O ₂ Readings (% by Vol.)
High (+10% from the optimum)	7 to 9
Optimum air flow rates	5 to 7
Low (-10% from the optimum)	3 to 5

Hence the range of training input and target vectors for the corrective network was derived from the O₂ readings from the three possible operating conditions and the required tuning on primary air flow rates (in the middle sections of the plenum). We have co-related the amount of air flow tuning required with the O₂ reading from the gathered data. This is based on the O₂ deviations from the optimal band to changes in the total primary air flow rates and are summarised in Table 3.

Table 3: Input and Target Training Vectors for the Corrective Network

Input Vector (Range of O ₂ Readings)	Target Vector (Range of Air flow Tuning)
Higher air flow rates (7.1 to 9)	-1 to -15% from the Optimum
Optimum air flow rates (5 to 7)	0%
Lower air flow rates (3 to 4.9)	+1 to +15% from the Optimum

A standard three layer feed-forward neural network was used to map the input and target vectors with the tansig non-linearity function being applied to each layer to allow for the negative values within the training vectors. The back-propagation algorithm with adaptive learning rate and momentum was adopted for the training of

the network which consisted of 1 input neuron (error in O_2), 10 hidden neurons and 2 output neurons (tuning for the 2 primary air plenums). After 2000 training iterations, the sum square error of the training envelope was 0.01, which showed sufficient accuracy for the static mapping purpose of the network. Hence the trained network have successfully learned about the possible deviations in the O_2 read out in flue gas during steady-state operations, and based on that error is able to deliver the appropriate air flow tuning.

4.2 Refractory Arch Monitoring Network & Higher Level Decision Maker

Both networks will take in the arch temperature distributions as their inputs. The refractory arch monitoring network will determine the necessary adjustment on the grate speed should the ignition plane is found to be shifting. The higher level decision maker function by classifying the arch temperatures to stable, shifting and unstable regions and is different from the arch monitoring network in its network topology. Subsequent action by the other network within the control structure will rely solely on its decision. As described in section 2.2 more work is still required to determine the absolute stability of the ignition plane to load changes before training of the network can be carried out.

4.3 Control Decision

The neural controller will only be activated after steady-state operation of the boiler is attained from plant start-up. Initial line of command will be given to the ignition plane monitoring network to establish a stable refractory arch before the line of command is passed to the combustion monitoring network that functions to ensure an optimum combustion rate. Even when the combustion monitoring network is at work, the ignition plane monitoring network will be continuously monitoring the arch surface temperature, and should any instability creeps into the ignition plane, the ignition plane monitoring network will regain the line of command and remedy the problem by manipulating the grate speed in order to regain stability. This problem is particularly significant when the boiler is operated from turn down to full load in a huge step, where a sudden intake of freshly supplied coal and primary combustion air flows will

inevitably impose a cooling effect on the arch if these parameters are not properly controlled.

4.4 Overall Neural Controller Structure

The diagram below depicts the overall controller structure that has been devised for on-line control of the stoker boiler. As shown in Figure 6 the higher level decision maker classifies the arch thermocouple readings that are available and has the highest “rank” in the overall strategy. The subsequent control decisions will be based solely on the stability of the ignition plane. Should the decision making network be satisfied with the arch temperature readings, command will be switched over to the combustion monitoring network for fine tuning of the primary air flow rates and conversely the arch monitoring network will be activated to take the necessary measures if the ignition plane is found to be shifting.

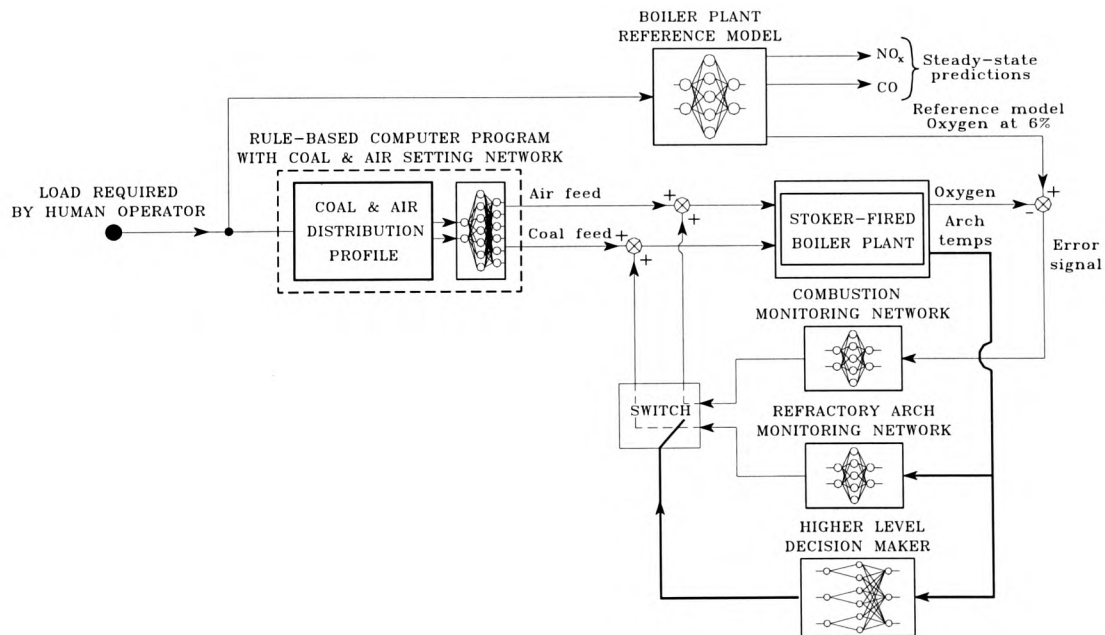


Figure 6: Overall Neural Controller Structure

5. CONCLUSIONS

An optimum steady-state combustion rate can be attained on a 0.75MW_{th} chain grate stoker test facility located at CTDD, Stoke Orchard, by monitoring the O₂ content in the flue gas and performing fine tuning tasks on the primary air flow rates in the main combustion region. Experimental tests were carried out to establish the dependencies between the required primary air flow rates with the fluctuating O₂ levels in the flue gas. This information was successfully encoded in the form of a standard three layer feedforward neural network. Transient emissions of CO can be reduce by regulating a correct air/coal staging profile particularly to large load changes. By virtue of the network static mapping capability, control decisions can be made to regulate within a proposed overall controller scheme that integrates other feedforward networks for the purpose of on-line monitoring and control of the plant.

6. ACKNOWLEDGEMENT

The authors would like to acknowledge financial support from the British Coal Utilisation Research Association (BCURA) and Energy Technology Support Unit (ETSU) on behalf of DTI. In addition the study grant from British High Commissioner's Award Scheme of Malaysia is also gratefully acknowledged. Finally, the assistance from the staff of Coal Technology Development Division in obtaining experimental results was invaluable.

7. REFERENCES

- [1] Clarke, A.G. and Williams, A., "The Formation and Control of NO_x Emissions", *Chem Ind UK*, Vol.24, pp.917-920, 1991.
- [2] Chong, Z.S., Wilcox, S.J., Ward, J. and Butt, A., "The Monitoring and Control of Stoker Fired Boiler Plant by Neural Networks", *Proceedings of the 9th International COMADEM Conference*, pp.289-298, July 1996.
- [3] Gunn, D.C., "Conventional Coal Firing Equipment - 1982", *Private Communication*

- [4] Narendra, S. and Parathasarathy, K., "Identification and Control of Dynamical Systems Using Neural Networks", *IEEE Transactions on Neural Networks*, Vol.1, No.1, pp.4-27, March 1990.
- [5] Narendra, K.S. and Mukhopadhyay, S., "Intelligent Control Using Neural Networks", *IEEE Control Systems Magazine*, Vol. 12, No.2, pp.11-18, April 1992.